TESIS DE LA UNIVERSIDAD DE ZARAGOZA

2024 211

Mario Tovar Calonge

Hacia la erradicación de la tuberculosis: modelización matemática de la enfermedad, vacunas y el impacto de la pandemia de COVID-19

Towards Tuberculosis eradication: mathematical modelling of the disease, vaccines and the impact of the COVID-19 pandemic

Director/es

Moreno Vega, Yamir
Sanz Remón, Joaquín

ISSN 2254-7606

Prensas de la Universidad Universidad Zaragoza

Universidad de Zaragoza
Servicio de Publicaciones

ISSN 2254-7606

Universidad Zaragoza
1542

Tesis Doctoral

HACIA LA ERRADICACIÓN DE LA TUBERCULOSIS: MODELIZACIÓN MATEMÁTICA DE LA ENFERMEDAD, VACUNAS Y EL IMPACTO DE LA PANDEMIA DE COVID-19

TOWARDS TUBERCULOSIS ERADICATION: MATHEMATICAL MODELLING OF THE DISEASE, VACCINES AND THE IMPACT OF THE COVID-19 PANDEMIC

Autor

Mario Tovar Calonge

Director/es

Moreno Vega, Yamir
Sanz Remón, Joaquín

UNIVERSIDAD DE ZARAGOZA
Escuela de Doctorado

Programa de Doctorado en Física

2024

Universidad Zaragoza
1542

Tesis Doctoral

Hacia la erradicación de la tuberculosis: modelización matemática de la enfermedad, vacunas y el impacto de la pandemia de COVID-19

Towards Tuberculosis eradication: mathematical modelling of the disease, vaccines and the impact of the COVID-19 pandemic

Autor

Mario Tovar Calonge

Directores

Yamir Moreno Vega

Joaquín Sanz Remón

FACULTAD DE CIENCIAS/IUI BIFI

2023

Agradecimientos

El camino que he recorrido para llegar a completar esta tesis doctoral ha sido largo, en ocasiones complicado, pero siempre instructivo y también emocionante. Pero llegar al destino no habría sido posible sin la ayuda y el apoyo de mis familiares, seres queridos, amigos y compañeros.

En primer lugar quiero agradecer el apoyo de mis padres, cuyo soporte a todos los niveles ha sido imprescindible para poder cumplir todos mis objetivos personales y académicos. Ellos son los que con su cariño me han impulsado siempre a perseguir mis metas y nunca abandonarlas frente a las adversidades. También quiero agradecer el apoyo que mi hermana, mi cuñado y mi sobrina y sobrino me han brindado, alegrando algunos de los días difíciles, y sabiéndolos siempre cercanos.

Especialmente importante en el proceso ha sido Victoria, quien depositando en mi su cariño, su comprensión, su apoyo incondicional y su paciencia en los días largos antes de una *deadline*, ha sido pieza fundamental del proceso, en lo bueno y en lo malo. Sin ella, este camino habría sido mucho más complicado, pero con ella, "La historia es nuestra y la hacen los pueblos". Por ello, gracias.

He de agradecer, además, la guía de mis tutores, Joaquín y Yamir, gracias a quieres la investigación que se incluye en este documento ha sido posible, ya que decidieron depositar su confianza en mi capacidad para abordar este proyecto.

También quiero agradecer a los compañeros del laboratorio, especialmente a Alfonso, Ariadna, Tiago, Francho, Javier, Alberto, y Felipe, con quienes los comienzos en este camino fueron más agradables. Con Alfonso y Ariadna, de Turín al cielo. Y como no mencionar también a Carlos, quien con sus cafés y sus diatribas nos ha alegrado más de un día. Finalmente, a mis amigos y compañeros en distintas etapas de mi vida, gracias por estar ahí.

Abstract

Since thousands of years ago, the long shadow of Tuberculosis (TB) has tormented humanity, slowly, but constantly, decimating human civilisations. This old disease, caused by the agents of the *Mycobacterium tuberculosis* complex, ravaged all territories around the world while claiming the lives of millions.

So far, mankind's battle against this dreadful disease has been difficult, and not until the discovery of antibiotics and the development of control policies, the results have looked hopeful. Nowadays, although there are effective drugs, and the disease is curable, it persists in all continents, killing an estimated 1.30 million deaths worldwide in 2022. The need to eradicate TB has been a long-lasted goal since the discovery of its causative agent, and the scientific community is putting effort and money into the development of new tools to control the disease.

For its complex characteristics, TB epidemiology benefits from the usage of mathematical models of spreading which can be used as policy-making tools to evaluate the impact of public health interventions. However, describing the spread of TB requires complex models that can close the gap between model and data, whose implementation is not an easy task. Furthermore, the existence of different external perturbations that interact with TB dynamics means that they must be taken into account and included in the models if the impact of the different interventions is to be correctly estimated.

In this thesis, I have focused on the development of modeling approaches to describe the effects of certain external perturbations that are potentially capable to modify TB spreading dynamics. These perturbations may be public health interventions, such as the introduction of novel vaccines, or may be other events, such as the emergence of a new pathogen such as SARS-CoV-2 which compromised the diagnosis and treatment capabilities against TB of healthcare providers worldwide. In this Thesis, the need of removing bias and arbitrariness in the modeling decisions that are implicit in the description of these perturbations is highlighted, towards the production of increasingly better forecasts that may be instrumental to help in the eradication effort.

To contribute to the research effort, first, I have explored how the coupling of new TB vaccines and the mathematical model works, for TB vaccines are nowadays the more promising tool to control and eradicate TB. Our approach is based on the development of new methods that recover suitable descriptions for the vaccine interaction with the natural history that is supported by real data of real clinical trials, something that has largely been ignored in the previous literature. Our results, presented in Chapter 3 and Chapter 4, show that taking our novel approach to measure the impact of new TB

vaccines with mathematical models attending to mechanistic, data-based descriptions of the vaccines reduces the bias in the forecast. developed This allows to compare between vaccine candidates to discriminate those who are more promising.

Moreover, I have explored how the COVID-19 pandemic has influenced the control of TB, as the perturbation of the emergence of this pandemic compromised the TB diagnosis and treatment capabilities of healthcare systems. In this regard, the results in Chapter 5 show that the impact of the COVID-19 pandemic on the transmission dynamics in high-burden settings is non-negligible, and that an excess of mortality associated with the COVID-19 pandemics can be described as a consequence of the healthcare system saturation during the harder times of the pandemic.

Index

Chapter 1

Introduction

> A journey of a thousand miles
> begins with a single step.
>
> Lao Tzu

1.1 The start of the journey

The battle of humanity against the ever-present threat of infectious diseases has, since the very beginning, been one of the most challenging tasks we have faced to conquer the dream of a world free of diseases. Throughout history, epidemics have posed a significant risk to mankind, often reshaping societies, economies, and health outcomes. From ancient plagues that ravaged entire civilisations to more recent pandemics like the Spanish flu, HIV/AIDS, or the COVID-19 pandemic, the world has grappled with a complex interplay of factors that give rise to and perpetuate infectious diseases.

Nowadays, in an age of global connectivity, rapid urbanisation, and climate change, the threat of epidemics continues to loom large. Emerging infectious diseases, and endemic diseases, demonstrate that our vulnerability to these public health crises remains ever-present. Moreover, the impact of epidemics on global populations is not uniform, and the vulnerability of people living in impoverished countries is a stark reminder of the global inequities in healthcare access and resources, where social inequities often force individuals to live in overcrowded and unsanitary conditions, creating fertile ground for disease transmission[1].

Understanding the dynamics of transmission and spreading of communicable diseases is only possible paying attention, at the same time, at the biological properties of the pathogen, its cross-talk with the host, and the conditions that lead to transmission between individuals. By understanding the historical context and the dynamics of epidemics, we have gained valuable insights into the patterns of

transmission, the role of public health interventions, and the factors that influence disease emergence. Moreover, by employing advanced techniques in data collection, analysis, and modelling, we have a better understanding to combat the spread of diseases by combining preventive approaches, early detection, and response.

However, endemic infectious diseases such as tuberculosis (TB) manifest that the battle continues and that the dream of eradicating diseases from the planet needs international cooperation, reducing global inequity and even new and better tools to combat spreading. For these reasons, this thesis is devoted to studying TB, to offer a workable modelling framework designed to provide solutions to some of the challenges in the TB literature. In this book, I compile the novel research produced during the duration of the thesis regarding the analysis of perturbations in the trends of TB, either focusing on public health interventions such as vaccines, which might perturbate the trends for the better, or on negative side effects of other perturbations on TB dynamics, such as the consequences of the COVID-19 pandemic in the TB burden. The idea is to provide workable frameworks that enable a better understanding of the interactions that may bias our predictions, so the models may be used as most reliable tools for policymaking.

This thesis is structured in 6 chapters. In this first chapter, we introduce and contextualise the research topic and the characteristics that make TB one of the top killers worldwide. In Chapter 2, we introduce the methods that have been used in all the research. Then, In Chapter 3, we introduce the problem of understanding the mechanistic effects of vaccines in TB spreading models when addressing the impact of real vaccines evaluated in Randomised controlled trials. In Chapter 4, we present a study of vaccination in a high-burden country to contextualise the additional difficulties that appear when forecasting the impacts of TB vaccines in countries subject to fast demographic ageing processes, such as the case of China. In Chapter 5, we analyse the impact of the COVID-19 pandemic on the TB burden in high-burden settings. Finally, the last chapter is devoted to the global conclusions and achieved goals of the research.

In summary, the research goals are focused around studying the spread of TB, a disease which is currently an endemic epidemic that exists in every part of the world. It has the the dubious honour of being, worldwide, the 13th leading cause of death and the first leading infectious killer, only surpassed recently -and transitorily- by the COVID-19. To understand its impact, the following sections are devoted to contextualise, from a scientific and historic point of view, what are epidemics, what can be done to face them, and what are the challenges that the TB epidemic poses in the complex interconnected world of this century.

1.2 *Epidemia*, Epidemiology and epidemic modelling

The term epidemic came from the combination of the Greek term epi -on- plus the term demos -people-), and the oldest written register of the term appears in the Odyssey, the famous book by Homer. Demos originally meant "the country" (inhabited by its people) before taking the connotation "the people" in classical Greek. Indeed, the word *epidemios* used by Homer, 2 centuries before Hippocrates, meant "who is back home". The word mutated to its medical meaning because of the Hippocrates' *Corpus Hippocraticum*, which contained 7 books titled Epidemics[2]. There, Hippocrates used *epidemios* to mean "which circulates or propagates in a country". This is the origin of the noun in Greek, *epidemia*[3], which is translated to epidemic, in modern English, or to epidemia, in Spanish. The meaning has not changed since Hippocrates, and it is used nowadays to mean "the appearance of a particular disease in a large number of people at the same time", according to the Cambridge Dictionary, becoming a common word to refer to a disease that spreads in a population.

Along the term *Epidemia*, the scientific field that explores the consequences of the spreading of diseases, came into existence. This field was named Epidemiology, and since then, has been a vital area of study in public health which offers a methodical and fact-based approach to studying the prevalence and causes of diseases, and helps in dealing with epidemic outbreaks and prevention. The understanding and control of diseases have always been essential for mankind's survival, and the interest in epidemiology can be traced back to ancient times, although it has evolved unevenly across the ages, always tied to scientific progress. Its roots can be traced back to ancient civilisations that recognized patterns of disease occurrence. In ancient Egypt, for instance, papyrus records documented the recognition and management of diseases like malaria and TB[4, 5], although the causes and reach of those diseases remained unclear at that time. Ancient Greek physicians observed the influence of environmental factors on health and introduced the concept of epidemic diseases, and as stated, gave birth to the noun *epidemia* in the *Corpus Hippocraticum*. Their observations laid the groundwork for the study of disease distribution and causation.

Later, during the Middle Ages and the Renaissance, the interest in epidemiology was shaped by significant events and developments related to disease outbreaks and advancements in medical knowledge. The Middle Ages were marked by devastating epidemics, with the clearest example being the bubonic plague, often referred to at that time as the Black Death. This outbreak spread over more than a century across Europe, causing immense mortality. The massive death toll and fear generated by

the plague led to an increasing interest in understanding the causes and mechanisms of disease transmission, to prevent that this or similar epidemics decimate the population. At that time, the physicians formulated theories to explain the spread of diseases, such as the Miasma theory, which existed since the 5th century BC. This theory attributed diseases to corrupted air and led to the adoption of measures like burning aromatic substances to cleanse the air, sadly ineffective in preventing the spreading.

The progress in medical knowledge produced a shift towards more evidence-based approaches, which emphasised the importance of empirical observation. For instance, in this period, Girolamo Fracastoro, an Italian physician, proposed the concept of contagion as a mode of disease transmission during the 16th century. He theorised that diseases could be transmitted through direct contact, contaminated objects, or even through invisible particles[6]. This theory marked an important conceptual breakthrough in understanding how diseases spread. Additionally, during the Middle Ages and Renaissance, public health measures were put into place in response to disease outbreaks. Quarantine, which involves isolating and controlling the mobility of infected individuals was implemented. Although this approach was frequently motivated by fear and superstition, it shows an early understanding of the importance of limiting disease spreading.

During the Enlightenment periods and the 19th century, significant advancements in scientific thinking happened and had a profound impact on the field of epidemiology. John Graunt, an English statistician, analysed mortality data from the Bills of Mortality, a weekly publication in London that recorded deaths, causes of death, and related data[7]. Graunt's work focused on understanding patterns of disease and mortality and led to the first survival probabilities table that reported survival rates by age. His work helped establish the idea of quantifying and analysing population health data to understand spreading and epidemic risk. In 1796, British physician Edward Jenner showed that infection with the cowpox virus conferred immunity against the smallpox virus[8], which led to the development of the first vaccine against a contagious disease. Later, John Snow identified the source of a cholera outbreak in London by mapping cases and water sources[9], and served as the basis of geographical epidemiology and policy-making to control epidemic outbreaks.

Louis Pasteur's pioneering work on germ theory demonstrated that microorganisms were responsible for infectious diseases. His experiments illustrated that diseases could be prevented by killing germs, supporting the germ theory and its application in clinical medicine[10]. Pasteur's development of vaccines for rabies and anthrax also helped saving thousands of lives, and marked a watershed moment in preventive medicine. Robert Koch established the etiological connection between specific microorganisms

and diseases such as TB, cholera and anthrax. On 24 March 1882 he announced the discovery of the *Mycobacterium tuberculosis*[11]. This discovery was a game-changer, and the 24 March has been established as the "World Tuberculosis Day" since 1982. Moreover, Koch's postulates, introduced in 1884, became a standard for proving causation in epidemiology[12]. For their contributions to the scientific knowledge, Louis Pasteur and Robert Koch are considered as "fathers of microbiology"[13, 14]. Altogether, all the previous scientific advances helped lay the groundwork for modern epidemiology and revolutionised our understanding of infectious diseases, specially given that the Industrial Revolution led to the concentration of people in cities and introduced new health challenges.

Later on, the 20th century saw remarkable advancements in epidemiology and medicine, fundamentally driven by advancements in laboratory techniques, data analysis, and public health infrastructure. Many of those advancements were derived from the suffering of the many wars that humanity witnessed during the century, with World War I (WWI) and World War II (WWII) being representative of how wars shaped scientific progress in medicine and technology. At that time, the Spanish flu spread with ease in the trenches over the battlefields of WWI, which, combined with the major injuries that soldiers suffered led to the introduction of ambulances, antiseptic measures, and generalised use of anaesthesia. Although the advancements in epidemic control were minor, the experience of the Spanish flu in 1918 contributed to the knowledge of epidemics. After the war, Alexander Fleming's discovery of penicillin in 1928 represented a groundbreaking advance, as for the first time humanity had a tool to deal with some bacterial infections[15]. This discovery, along with other control measures, helped enormously in the treatment of infection, contributing to epidemic control and prevention of spreading. WWII saw the expanded use of antibiotics, leading the way for the general usage. Before antibiotics, infectious diseases were the leading cause of death worldwide, and diseases such as meningitis, TB, or pneumonia were very difficult to treat, if even possible, with humanity living under the fear of major epidemics[16]. This fear led the US Army to introduce vaccination campaigns among the troops, an example later followed by other armies around the world, which contributed to reducing the spread of some infectious diseases and avoiding situations like the Spanish flu epidemic in WWI.

The discovery of antibiotics, and the advancements in medicine, and technology, partially due to the war, played crucial roles in combating infectious diseases, as they provided better tools to deal with the agents that cause the diseases and to treat infected individuals. Those were, undoubtedly, the most important advancements that the world witnessed during the first half of the XX century.

Furthermore, it was also in that period that the first stages of the compartmental models were developed, and a discipline called mathematical modelling of infectious diseases emerged, arising a significant step forward regarding epidemiology. In 1927, William Kermack and Anderson McKendrick introduced the first widely recognized mathematical model of infectious diseases, known as the Kermack-McKendrick model or the susceptible-infected-recovered (SIR) model[17]. The development of those models gave, for the first time, a modelling tool to study effectively the spreading of an infectious disease.

In the second half of the 20th century, the global economy underwent significant transformations characterised by the emergence of a more interconnected and interdependent global economic system. The aftermath of World War II saw the establishment of institutions like the International Monetary Fund (IMF) and the World Bank, aimed at promoting stability and development on a global scale. This was a period of globalisation, marked by increased trade and the growth of multinational corporations, which also led to a consolidation of modern societies[18]. This period also led to the consolidation of the healthcare systems worldwide, where there was a shift towards integrated healthcare models[19]. This was possible thanks to the advancements in medical science and technology, where the development of medical techniques and drugs, and the advancements in molecular biology, genetics, and imaging technologies revolutionised diagnostics and treatments. It was in that period that the vaccines against Polio, Measles, Hepatitis B, or Varicella were developed and introduced in the routine vaccination, saving thousands of lives in the long term[20].

Finally, the XXI century led to the creation of modern societies, often considered as "information societies". In this period, with the unstoppable development of computers and other technological and scientific advancements, such as advanced statistical methods, and later, genetic sequencing, humanity witnessed an era of enhanced capabilities to analyse and interpret large datasets of epidemic data and to develop effective tools and policies to safeguard mankind to the deadliest pandemics. On top of that, the development of vaccines, and the robustness of the healthcare systems have improved global health outcomes. However, alongside these successes, we have witnessed the emergence of new and often more complex challenges with the rise of emerging infectious diseases, which continually pose threats to public health on a global scale[21]. Pathogens such as HIV, Zika virus, Zaire ebolavirus, MERS-CoV, Influenza Strains, SARS-CoV-1, and the recent SARS-CoV-2, pose huge threats to public health, being responsible for thousands of deaths worldwide. Moreover, already-known and prevalent diseases have increased their threat through antibiotic resistance. The emergence of Drug-Resistant Tuberculosis strains, Drug-Resistant strains of *M.tb S.*

aureus or *Enterobacter*, among others, are a growing concern in healthcare, for they are harder to treat and more likely to yield a fatal outcome. These pathogens challenge our understanding and response capabilities, highlighting the ongoing need for vigilance, research, and international cooperation to address these evolving health threats effectively.

To this end, in the modern era, epidemiologists aid in the creation of successful policies and programs to safeguard and advance public health by examining patterns, identifying risk factors, and assessing interventions. For such a task, the development of mathematical models of increasing complexity, and the collection of high-quality data capture the effort put into the eradication of infectious diseases, only possible thanks to the parallel development of computation. This shaped epidemic modelling as essential tools for facing the challenges that an interconnected world means for epidemic control.

1.2.1 Mathematical Epidemiology

After this brief introduction to the very concept of epidemiology, and epidemics, we will devote the following lines to contextualise what the history of mathematical descriptions of epidemics has been. Nowadays, there are thousands of academic texts that make use of mathematical models to perform a series of tasks related to epidemic processes that range from estimate the spreading of a given disease, to the usage of statistical models to analyse omic data. This has been possible as both the computing power has increased, and so has done our overall knowledge of the world and the very basic functioning of diseases, but certainly, the idea of mathematical descriptions of diseases came from a past without computers.

First of all, in order to build a mathematical model for the spread of an infectious disease, it is necessary to make some assumptions about the means of spreading infection. The germ theory of disease, which was enhanced by the work of Robert Koch, Joseph Lister, and Louis Pasteur constitute one key aspect of the modern view of disease spreading by contact between individuals. In those contacts, if an infectious individual interact with a susceptible one, an infection through a virus or bacterium vector may happen, and this assumption is in the core of almost any mathematical model of disease spreading nowadays. However, to trace back the origin of the mathematical epidemiology, we need to travel back to 1766, when Daniel Bernoulli published an article where he described the effects of smallpox variolation (a precursor of vaccination) on life expectancy using mathematical life table analysis[22], which does not made direct usage of the idea of spreading through contacts. Nevertheless, once the dynamics of infectious disease's spreading started to be, at least, understood in terms on non-linear dynamics, in the beginning of the XX century, this idea became central.

For instance, the work of Ronald Ross on malaria for which him was awarded the Nobel Prize in Medicine in 1902 demonstrated the dynamics of the transmission of malaria between mosquitoes and humans. Later, in 1906, W.H. Hamer argued that the spread of infection should depend on the number of susceptible and infectious individuals and suggested a mass action law for the rate of new infections that depends upon those quantities, being since them a central idea in mathematical models.

Later, the basic compartmental models to describe the transmission of communicable diseases were introduced. Compartmental models are a kind on mathematical models that classifies individuals according to their health state, and the possible transitions that can happen between those states. They were first introduced in a sequence of three papers by W.O. Kermack and A.G. McKendrick in 1927, 1932, and 1933[23, 24, 25], and they pioneered the concept of a threshold quantity that separates different dynamic regimes. Their works led to the introduction of the SIR model, which may model diseases such as influenza and smallpox. Although it is a simplistic approach nowadays, the impact of this model cannot be overlooked, as it laid the groundwork for subsequent modelling efforts. In this model, individuals are classified as either susceptible, infected or removed according to their health status, and the dynamic describe how the flow of individuals between compartments works over time. A modern formulation of the SIR model would be done as:

$$\begin{aligned} \dot{S}(t) &= -\beta S(t) I(t) \\ \dot{I}(t) &= +\beta S(t) I(t) - \mu I(t) \\ \dot{R}(t) &= +\mu I(t) \end{aligned} \tag{1.1}$$

where it is assumed that individuals interact homogeneously in a sort of mean field of contacts, conforming a well-mixed population. In the previous equations, the susceptible individuals suffer a force of infection β that, upon homogeneous contact with infected individuals, moves them to the infected compartment. From this state, the only way out is driven by the transition governed by μ from infected to removed (either by recovery or death). The threshold quantity that separates the regimes introduced by Kermack and McKendrick can be computed easily. The only two possible regimes in the model are the spread, or not, of the disease. For the disease to spread, we need to have that $\dot{I} > 0$, as the number of individuals should increase over time. This leads to:

$$(\beta S I - \mu I) > 0 \rightarrow 1 < \frac{\beta S}{\mu} \tag{1.2}$$

At the start of an epidemic $S = S_0$, and thus, the infection will only invade the population if the initial proportion of susceptibles $S_0 > \frac{\mu}{\beta}$. This condition can be

rewritten as:

$$S_0 > \frac{1}{R_0} \rightarrow R_0 = \frac{\beta}{\mu} \tag{1.3}$$

where the epidemic will spread if $R_0 > 1$, as in this case the previous condition may be fulfilled. This quantity R_0 is named the basic reproduction number and captures the average new infections that an infected individual produces in a susceptible population. It can be interpreted as the product of the β susceptible individuals infected per day times the average time that the infected individual is infectious μ^{-1}. Then, the different regimes proposed by Kermack and McKendrick arise, as if the basic reproduction number is above the threshold value, then the infectious disease can spread in a susceptible population. This leads to the concept of herd immunity in vaccination, which states that it is not necessary to vaccinate the entire population to eliminate the infectious disease, but only a fraction of them so the epidemic may be pushed out of the spreading regime. The herd immunity idea, and the threshold approach, proved their value during the eradication of smallpox in the 1970s, where a vaccination coverage of around 80% worldwide was sufficient for eradicating the virus.

This simple approach does not work for more complex diseases where there could be more ways to disease, and/or a more complex natural history of the disease whose modelling requires more compartments and/or a different set of assumptions, such as heterogeneity in the exposure, and contacts. This is the case of AIDS, where the well-mixed population assumption needs to be substituted by a heterogeneous network of contacts, which is needed to capture the spreading patterns of a sexually transmitted disease. At the end of the XX century, and the start of the XXI century, mathematical modelling witnessed an increased usage for public health policymaking as modelling approaches were increasingly used to identify the most effective prevention strategies against AIDS pandemic[26, 27]. The development of those models witnessed the interplay between network science and epidemiology and was a significant step forward in the field. On top of that, the need for evaluating intervention strategies for newly emerging and re-emerging diseases such as the already eradicated smallpox virus, or the outbreaks such as the SARS one, contributed to establishing mathematical modelling as a prominent tool to address the spreading and to analyse potential interventions.

The final step in this historic approach to the modelling of infectious diseases was taken when the results of the POLYMOD project were shared[28]. This study provided the first large-scale quantitative approach to contact patterns in the form of contact matrices and allowed, for the first time, to feed the spreading models with an improved parameterisation of the contacts, which, in diseases where infection happens by respiratory or close-contact route, allowed for new modelling approaches. This is the case of TB, a disease in which the modelling requires long periods, and the usage of

the heterogeneity level that networks provided is problematic, whereas the assumption of well-mixed populations is simplistic.

With those matrices, the interaction was shifted towards age groups of individuals rather than individual contacts, and inside each age group the population was considered well-mixed, giving a stratified homogeneous mean field that adds a greater level of detail, and that allows the evaluation of, for instance, age-targeted strategies, such as a targeted vaccination campaign. To analyse the potential impact of such a campaign, the model needs to account for, at least, different age groups, and for the interactions between those groups, which is possible thanks to the contact matrices.

After this long path, one idea that has arisen and that is important when developing mathematical models for describing an infectious process is that there is no unique, correct formulation for a given disease. Instead, the most suitable formulation relates to the precise scientific question that the model needs to address, and to the level of detail of the empirical data that is available to parametrise the model. In this context, as in most other areas of mathematical modelling, there is always a trade-off between model complexity and the wealth of information at hand. When modellers work to address general behaviours, leaning on generic data and a few key epidemiological parameters, the models they use should be simple tools, designed perhaps only to capture the qualitative behaviour of the system to a low level of detail that matches that of the input data. Instead, whenever we intend to use our models to describe the co-evolution of richer data, at a finer scale, with a higher level of detail, model structures must gain complexity to accommodate the description of the richer data at hand, and provide quantitative answers to more nuanced questions, which sometimes is relevant for the models to be used for making policy recommendations for disease control based on quantitative results. However, detailed models are generally impossible to solve analytically and then trust in the computing power to be solved.

In short, the evolution of the mathematical modelling of infectious diseases, the data, and the rise in computation power has yielded the development of models that are useful to give quantitative predictions that are usable for policy making. Nowadays, health organisations such as the WHO, or regional offices for disease control include sections that are focused on the usage of models. In the context of this thesis, the evolution of those models has enabled the possibility of modelling a disease such as TB, whose main characteristics and complexity will be described in the following sections. Thanks to those models, and the available data, it is possible to model the spreading of TB and analyse the effect of the perturbation on the basal trends related to the TB-COVID-19 interaction, and to estimate the effect of public health interventions such as vaccines, which are the main objectives of the whole research endeavour.

1.3 Tuberculosis: an old menace.

1.3.1 An historic approach to the disease

TB has a long-standing history as one of humanity's most devastating infectious diseases. Throughout the centuries, it has afflicted millions of individuals, shaped communities, and influenced medical research and public health strategies. It is an ancient infectious disease, caused by mycobacteria belonging to the *Mycobacterium tuberculosis* complex, which includes *M. tuberculosis*, *M. africanum*, *M. orygis*, *M. bovis*, *M. microti*, *M. canettii*, *M. caprae* and *M. pinnipedii*[29, 30], although the vast majority of cases in humans are caused by *M. tuberculosis*. The origins of this ancient scourge can be traced back thousands of years, with evidence of TB infection found in the skeletal remains of ancient humans. Some of the oldest examples of spinal TB arise in the form of fossil bones, which date back to about 8000 BC [31]. Moreover, findings in certain Egyptian mummies indicate that some form of TB existed around 2400 B.C[32], and evidence of TB in China, around 2000 years B.C. [33] also points out that TB was already disseminated and affecting several parts of the world.

In the Mediterranean Basin, during the late Roman Republic and early Roman Empire, approximately from 200 B.C. to 200 A.D., certain conditions favoured the spread of TB across Italy, within the city of Rome itself, and on the provinces.[34]. During this era, trade and military expansion likely served as conduits for the further dissemination of TB both in the mainland and in the provinces, and even outside the borders of the empire, as the disease could be carried by traders or soldiers. Specifically, there was a significant surge in the number of European archaeological sites and human remains with TB evidence associated with Roman civilisation between around 50 A.D. and 500 A.D[35, 36], and to increased mobility that it introduced[37].

Moreover, the expansion of the Roman Empire brought increased urbanisation across the Mediterranean[38], which, coupled with population growth, may have played a role in TB spreading, as the expansion of the empire also caused the proliferation of small structures, and sometimes, inadequate living conditions. The surge in paleopathological evidence of TB during the Roman era aligns with the notion that the establishment of the Roman Empire disseminated TB along with people and urban culture. However, it's worth noting that there is evidence of TB in places such as Denmark, Russia, or Lithuania[39, 40, 41], which are geographically distant from the borders of Rome, both before and during the roman times. This challenges the theory of TB spread -in the European territory- solely via Roman influence, especially as the archaeological record can be influenced by the extent to which nations invest in

preserving their historical remains.

It is also worth noting that evidence of TB has been found across the world, in distant places, and from different epochs, both pre and post-European expansion, which points heavily towards the presence of the disease in different civilisations, especially in those that reached high levels of urbanisation and/or mobility[42]. In this sense, TB evidence has been found, among others, in pre-Columbian populations[43] dated 800 A.D., in Japan, dating from 454 BC to AD 124, or in China dated 2nd century BC respectively[44]. These pieces of evidence highlight that TB has been present in almost all territories of the world, coexisting with different civilisations.

Back in the European mainland during the Middle Ages, TB persisted as a formidable public health challenge, although it was not as extensively documented as in later centuries. This era witnessed the proliferation of densely populated urban centres, and the consequent increase in the transmission of infectious diseases such as TB, in line with the evidence that Roman urbanisation was responsible for the rise of cases. The crowded living conditions, inadequate sanitation, and limited access to medical care were prevalent during this period and provided fertile ground for the spread of the disease[45].

Records from medieval Europe indicate that TB, commonly known as "consumption" or "the wasting disease," was a well-recognized but poorly comprehended illness. Its symptoms, characterised by coughing, weight loss, and weakness, were frequently noted in historical accounts, although with other names[46]. The true nature of the disease and its microbial cause remained shrouded in mystery until later centuries. Consequently, various remedies and treatments were employed in attempts to alleviate the suffering of the patients, which included herbal remedies, bloodletting, and dietary modifications, yet their efficacy in combating the disease was limited[47].

The lack of a clear understanding of TB hampered the development of effective strategies for prevention and treatment. It wasn't until the emergence of more advanced medical knowledge and technologies in the modern era that significant progress was achieved in combating this ancient scourge. Nevertheless, the historical experiences of TB during the Middle Ages underscore the enduring challenges posed by infectious diseases in pre-modern societies and highlight the importance of ongoing research and public health efforts to combat them[48]. Moreover, the epidemic continued to escalate over the subsequent two centuries and a significant proportion of the Western European population became infected with *M. tuberculosis*, with approximately one in four deaths being due to TB. Consequently, European migrants propagated the disease, to the Americas and other European colonies[49].

The disease gained significant attention during the 19th and early 20th centuries, particularly in industrialised countries that were still experiencing fast urbanisation and overcrowding. During this period, TB became a major public health crisis, especially in densely populated areas, as population density, unsanitary conditions, extreme poverty, and poor hygiene created the ideal environmental conditions for person-to-person transmission[50]. The lack of effective TB treatments exacerbated the problem, leading to high mortality rates. On top of the deaths and rise in prevalence, the impact of TB extended beyond, leading to social and economic consequences. The disease disproportionately affected lower socioeconomic classes[48], perpetuating cycles of poverty and ill health, and whenever the primary earners of families fell ill and were unable to work, they faced financial ruin, while orphanages and institutions struggled to cope with the increasing number of children who had lost parents to TB.

The efforts to control TB started to succeed in the late 19th century and especially, during the 20th century, with scientific discoveries and improved public health measures. In 1882, Robert Koch identified *Mycobacterium tuberculosis*[11], enabling targeted research and diagnostic advancements. Sanatoriums were established in several countries to deal with patients and aid in recovery, emphasising fresh air therapy, rest, and good nutrition. Vaccination also played a crucial role thanks to the development of the Bacillus-Calmette-Guérin (BCG) vaccine in the 1920s[51]. moreover, the introduction of antibiotics, such as streptomycin, in the mid-20th century, revolutionised TB treatment by offering the possibility of a cure[52].

Since then, In Europe, and other developed regions, some key factors and strategies have contributed to the reduction of TB. First, many European countries have well-developed healthcare systems, which provide access to early diagnosis and treatment of TB, which has proven crucial in reducing the spread of the disease. Moreover, in many of those countries, various standarised public health measures to control TB have been implemented, including testing in individuals with compatible symptoms, testing in the contacts of the infected individuals, or patient-centred approaches to ensure adherence to treatment and prevention of drug-resistance emergence[53]. Second, the BCG vaccine was used to protect against TB, although the overall decrease in incidence has led to modifications of BCG policies since the 1960s[54, 55, 56], and BCG vaccination has been limited to children in high-risk populations. Furthermore, the availability of effective antibiotics for TB treatment, such as isoniazid, rifampicin, and others, has contributed heavily towards the control of the disease. Last, comprehensive TB control programs that monitor the disease's prevalence, and implement prevention and treatment strategies, have been established, which, paired with the improvement in living standards, due to the improvement in

socioeconomic conditions have contributed to the reduction of TB transmission.

Despite this situation, TB remains a significant global health challenge in the world, as a consequence of the deep inequality in our societies. The emergence of drug-resistant strains, socioeconomic disparities, and inadequate healthcare systems in many regions have hindered effective control efforts. Moreover, TB is a menace in those places facing conflicts, as in societies characterised by violence, insecurity, and constrained economic prospects the control of TB is compromised heavily. As an example, in the European mainland, TB incidence rose as much as five times the value pre-World War II in some regions as a consequence of WWII[57]. This happens as the population living in conflict areas usually has a hard time accessing healthcare, and is forced to live in bad living conditions, which is a perfect mixture for the spread of TB. This is a concern even in modern societies, with a clear example being the Ruso-Ukranian, as Pre-war Ukraine had the fifth-highest number of confirmed cases of extensively drug-resistant TB[58]. The consequences of the war over TB control are unknown and concerning. In this sense, ongoing research, improved diagnostics, and comprehensive public health strategies are vital to combat the persistent impact of TB on societies worldwide, but so is reducing inequality and putting an end to the ongoing conflicts.

Finally, the cultural impact of TB has been profound and cannot be overlooked, as a disease that has been so long with humanity has rooted deeply in our culture across the world. The disease was for centuries associated with poetic and artistic qualities in its sufferers and was known as “the romantic disease”[59], also depicting the Romantic ideal of a figure embodying creativity and sensitivity. In this sense, TB has played prominent and recurring roles in diverse fields, influencing art, literature, and, cultural perceptions. There are plenty of examples of this influence, such as Thomas Mann’s The Magic Mountain, in literature, Van Morrison’s song ”T.B. Sheets” in music, or Puccini’s La Bohème and Verdi’s La Traviata, in opera. Moreover, Monet’s painting of his first wife Camille on her deathbed captures a tragic death caused by TB. Artists such as Frida Kahlo and Edgar Allan Poe have also captured in their works the suffering caused by TB, and the disease appears even in more modern artistic means, such as films. Throughout history, many important figures have died from TB-related causes. Actors, politicians, writers, or dictators, no one was safe from this threat that has left its mark on multiple societies throughout the centuries.

1.3.2 The dream of eradication

The dream of eradicating TB is an old dream whose consecution, sadly, remains elusive. This dream comprises the complete and permanent elimination of the disease from the global population, with the ultimate goal being having zero new

cases of TB, and halting completely the transmission of TB. Moreover, this policy aims to have zero TB-related deaths, ensuring that no individual succumbs to this disease, even by reactivation of old infections. Achieving eradication is key to ensuring that the global population witnesses a state of zero suffering related to TB, preventing the physical, emotional, and economic burden imposed on individuals and communities. Additionally, it entails ensuring that all populations, regardless of location or socioeconomic status, benefit from these advances in public health, also becoming important to reduce global inequity.

Although difficult, since the XX century, the eradication of the disease started to be formulated, first due to the discovery of the BCG vaccine, and the introduction of effective drugs, and second, due to the substantial commitment of governments. By the 1960s, so many of the components essential to fighting, even eradicating, an infectious disease were in place: tools of diagnosis, therapeutics, and even primary and secondary prevention, and by 10 years, new agents and combinations of drugs were introduced, showing promising results in reducing the burden of TB[60]. The combination of isonicotinic acid hydrazide (INH), rifampin, and pyrazinamide was shown in multiple studies to achieve a cure in just six months, a great step forward.

The availability of effective antibiotic therapy heralded an age of optimism. For instance, in the US, by 1960, the Commissioned Corps of the U.S. Public Health Service (USPHS) announced its goal of “approaching to zero tuberculosis”. In the following 30 years, nearly a 6% per year decline in TB incidence, as a consequence of the introduction of INH, reinforced this sentiment. In 1985, however, a surprising change happened, as TB incidence was increasing. Soon, the same was recognized in other developed nations and, more strikingly, in the developing world, where the annual increase in TB incidence was staggering. One of the key factors that played a substantial role in the resurgence of TB worldwide was the human immunodeficiency virus (HIV) epidemic.

The advent of effective antibiotic treatment marked an era of hope. For example, in the United States, by 1960, the Commissioned Corps of the U.S. Public Health Service (USPHS) set its objective to ”approach to zero tuberculosis”. Over the subsequent three decades, there was a significant annual decrease of approximately 6% in TB cases, primarily due to the introduction of INH, which further boosted this optimistic outlook. However, in 1985, an unexpected shift occurred, with TB cases on the rise. This trend was soon acknowledged in other industrialised countries and, even more alarmingly, in developing nations, where the annual increase in TB cases was particularly concerning. One of the major contributing factors to the resurgence of TB on a global scale was the HIV epidemic. Common risk factors, such as poverty, substance abuse, and

homelessness, contributed to the simultaneous occurrence of TB and HIV infections. As of the mid-1990s, approximately 10% to 15% of TB patients in the United States and over 30% of TB patients in Africa were found to have co-infections with HIV, and it was observed that HIV infection heightened the likelihood of progressing to active disease following a recent infection[61].

Furthermore, the issue of drug resistance played a significant role in the resurgence of TB. The emergence and transmission of multidrug-resistant TB (MDR-TB) in the 1980s were likely the result of suboptimal treatment approaches, including irregular medication intake, inadequate drug regimens, and insufficient treatment duration. These factors may have led to the selection of strains resistant to both INH and rifampin and in some cases, resistance to additional first-line drugs, complicating the treatment process and reducing the chances of successful outcomes for affected patients.

However, a decay has been achieved globally since 1990. This progress in TB control can be attributed to international collaboration, public health measures, and several TB control programs that have been developed around the world, which have played a pivotal role to control TB, but also are insufficient to eradicate TB at the global scale. This is due, in part, to the lack of universal healthcare, inequity, and lack of resources, for which TB control will benefit enormously of increased funding for research, improved healthcare infrastructure, enhanced diagnostics, and better housing with less overcrowding worldwide. In the following lines, we include a summary of some of the most important programs.

In India, the "National TB Programme (NTP)" was introduced by the government in 1962. To combat TB, this program helped increase BCG vaccination rates and gave patients TB treatment. The "Revised National Tuberculosis Control Programme" (RNTCP), based on WHO recommendations, was started in 1997 and had been implemented nationwide by 2006. The government launched "Programmatic Management of Drug Resistant TB" (PMDT) a year later, in 2007, to fight the threat of drug resistance. By 2013, complete geographic coverage had been attained. Despite these efforts, there is still a long way to go before the high incidence and prevalence of TB in India are significantly reduced. The reduction of poverty, undernourishment, and the stigma associated with TB seems to be the key to eradicating the illness, as the lack of resources, stigma, poor infrastructure, drug-resistant infections, and low notification rates offer significant challenges[62].

In China, during the 1990s, the Chinese Center for Disease Control and Prevention (CDC) led the vertical tuberculosis control program. This program focused on TB screening, diagnosis, and outpatient treatment while collaborating closely with community healthcare providers for effective case management. Patients with

complicated cases were referred to general hospitals for care. However, the formidable challenges posed by extensive internal migration, the rise of multi-drug-resistant tuberculosis, and tuberculosis comorbidities (e.g., tuberculosis combined with diabetes) claimed a more comprehensive and integrated approach. To address those concerns, the State Council of China issued a new TB control plan in 2001, lasting 10 years, which expanded the DOTS programme to the entire country. This approach yielded significant results, as TB prevalence in China decreased by 50% between 1990 and 2010, mortality rates dropped by nearly 80%, and incidence rates decreased at a rate of 3.4% per year[63]. Despite these achievements, China is still one of the high-burden countries, ranking among the top 10 countries with the highest number of cases.

In Europe and North America, significant reductions in both the prevalence and incidence of TB have been achieved, thanks to various successful strategies. For instance, in the United States, the early 1980s saw the introduction of Directly Observed Therapy (DOT), following the example set by Karel Styblo of the International Union Against TB & Lung Disease in the 1970s in Tanzania, Malawi, Nicaragua and Mozambique, which involved maintaining close contact with patients throughout their treatment to ensure the completion of the full treatment regimen. This community-based approach allowed the Health Department to provide therapy at a location convenient to the patient, whether it was at home, their workplace, school, or an institutional setting. The adoption of DOT subsequently became the national standard, contributing to the decline in TB incidence in the United States since the mid-1990s. Furthermore, there have been renewed efforts to address TB control. In 1992, the National Action Plan to Combat MDR-TB was introduced, and additionally, a TB screening policy for individuals seeking permanent legal status was implemented. Since then, the Center for Disease Control and Prevention (CDC) has continued to collaborate with international control programs, including those led by the World Health Organization.

In Europe, a TB surveillance network was established in 1996, which covered the WHO European Region. Its primary objectives were to enhance surveillance efforts and to promote the adoption of standardised methodologies for cross-country comparisons. Subsequently, in 2005, the European Centre for Disease Prevention and Control (ECDC) was established, assuming responsibility for coordinating TB control initiatives within the European region. In a collaborative effort between ECDC and the WHO Regional Office for Europe, this organisation validates, analyses, and disseminates TB surveillance data from across Europe. Its primary aim is to uncover epidemiological patterns of TB in the region and monitor progress toward the elimination of TB. Today, the surveillance network comprises experts from 53 countries

within the WHO European Region, which includes the Member States of the European Union and the European Economic Area (EU/EEA). Despite a general decline in TB incidence across the countries in the European region, individuals from the former Soviet Union countries still face an elevated risk of developing TB today, in part due to the economic hardships and resource shortages that followed the dissolution of the Soviet Union in those nations[64].

Besides the necessary control programs inside each country, the World Health Organization, as the leading international authority on health matters, has been actively engaged in eradicating TB through a range of strategies and initiatives[65, 66]. First, the Directly observed treatment, short-course (DOTS) Strategy[67], was introduced by the WHO in 1995 to significantly reduce the TB burden, being a remarkable public health strategy to control TB. This strategy, as the DOT one, was based on the technical strategy developed by Karel Styblo in the African region, which may be consider the first implementation of the strategy. The generalisation of this tactic improved the abilities of national programs to identify and treat TB cases while putting a clear emphasis on those who could spread the infection. Smear-positive cases were given priority for diagnosis and treatment, and short-course chemotherapy schedules were standardised.

The WHO later unveiled the Stop TB Strategy in 2006. This was an extension of the entire DOTS package within a developing framework with ongoing funding. In a patient-centred vision, this technique placed a priority on patient support and was designed to track and assess the effectiveness of interventions. The strategy's new components were measures against MDR-TB and TB/HIV co-infection, the biggest problem in TB control even today. Finally, in 2015, the End TB Strategy targets were introduced. The WHO aimed to reduce TB incidence by 20% and TB-related mortality by 35% globally by 2020. The policy also sought to prevent any TB-affected households from incurring exorbitant fees as a consequence of the disease. Sadly, these goals were not reached; and the global incidence of TB only decreased by 11%, and more than 40% of people suffering from the disease still have to pay expenses that account for a lot of their household income.

In addition to the specific tactics, the WHO is actively involved in promoting more financial and political support for TB programs to ensure that they are appropriately funded. Additionally, it encourages research and innovation to create novel TB diagnostics, therapies, vaccines, and tools, with a focus on teamwork with pharmaceutical companies and academic institutes. Additionally, the WHO provides technical assistance to nations, assisting them in developing the capacity to conduct successful TB control programs, which includes educating healthcare professionals,

bolstering laboratory networks, and enhancing surveillance systems. Finally, to build a strong front against TB, the WHO coordinates with a wide range of partners, including governments, non-governmental organisations, and civil society, to track the development of TB control programs around the world.

Sadly, TB remains a pressing global concern, and the eradication needs the international community to come together with the shared aspiration to eliminate TB and prevent the suffering and death caused by this disease. For instance, the COVID-19 pandemic has led to a shortfall in the global funding of TB programs. On World TB Day 2022, the WHO called for greater investment in TB programs to ensure that all humans witness a future without TB. If the international community does not collaborate and ensure sufficient funding for TB research and control initiatives, the dream of eradicating TB is a noble and essential endeavour for global health but will remain just a distant dream.

1.3.3 TB in the XXI century

During the XXI century, mankind has seen dramatic improvements in public health, treatment, diagnosis, and medical care, not only in developed countries, but all around the world. However, as of TB, the disease remains a big threat, as it has always been since before it was first identified as a pathogen by Koch in 1882. In fact, about a quarter of the global population is estimated to have been infected with *Mycobacterium tuberculosis*[68], even if a majority of them will not develop TB and some will clear the infection obscuring the classical assumption that specific immunoreactivity to mycobacterial antigens always means latent TB infection[69]. Nonetheless, TB is the 13th leading cause of death worldwide, and the second leading infectious killer after COVID-19 (above HIV and AIDS). Nowadays, in humans, the vast majority of cases are caused by infection with *M. tuberculosis*, with *M. bovis*, which was once an important cause of human disease, being responsible for just an estimated 1.4% of incident TB cases nowadays[70].

Although there has been a reduction in the global TB burden since 1990[71], the decay has slowed down in recent years. During 2020 and 2021, and for the first time in decades, the world witnessed a surge in global TB burden levels concerning previous years, which was caused by the COVID-19 pandemic, because of under-diagnosis and under-treatment of TB, paired with the saturation of healthcare systems [72, 73, 74, 75]. In those years alone, the WHO estimated that TB was the cause of death of more than 1.5 and 1.6 million people [72, 76]. To contextualise the global situation, in Figure 1.1, we show the incidence per 100,000 inhabitants, as reported by the WHO data in 2020, just before the COVID-19 pandemic. This data shows that, in more than half of

the world, TB is not a disease of the past, but more of a deadly partner, and this is without considering the impact of the COVID-19 pandemic which has done anything but worsen the situation.

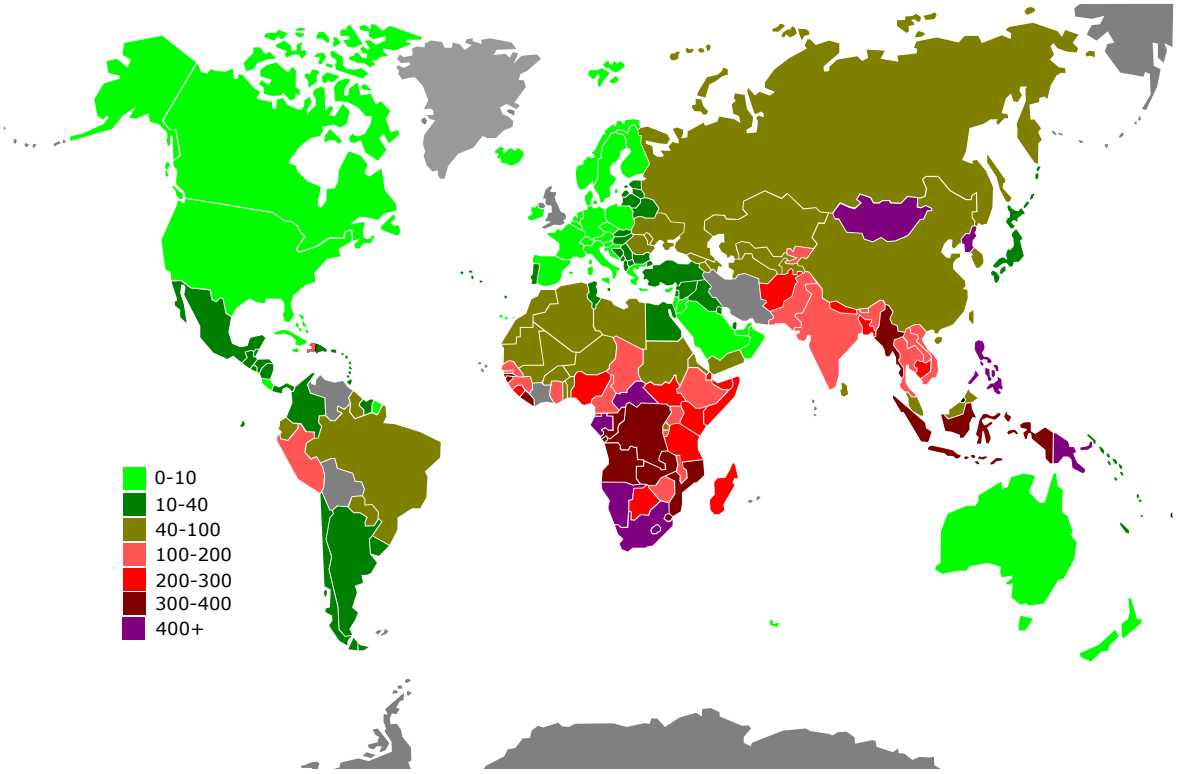

Figure 1.1: Worldwide distribution of TB cases per 100,000 inhabitants in 2020. Elaborated by the author with data from the WHO database and the Stop Partnership interactive charts[76]. In developed countries, the incidence of new TB cases is residual but greater than zero, while in the rest of the world, TB remains a very prevalent infectious disease.

Furthermore, nowadays there is an increasing evidence of the increasing rates of drug resistance [77, 78], which, paired with the great death tool, evidence the necessity of new tools against the disease. Those tools comprise new and better drugs, which guarantee better recovery and more chance of succeeding in curing the disease, as well as improved diagnosis methods, and surveillance systems. Among all these new resources, the development of a new vaccine that either boosts or replaces the current bacillus Calmette-Guerin (BCG) is believed to be the potentially most impactful single intervention that could bend TB transmission. As there is evidence of the limited, and variable efficacy levels observed for BCG against the more transmissible respiratory forms of the disease, especially in young adults [79], which in high-burden countries represent a great share of the new TB infections, the TB eradication dream needs the introduction of a new vaccine. Consequently, the TB vaccine development pipeline is populated by several novel vaccine candidates to follow the dream of eradication, from

which a subset of them are presented in Table 1.1.

Type of vaccine	Vaccines
Targets Infants & neonates	BCG-ZIMP1, MTBVAC, VPM1002
Targets Adolescents & Adults	M72 + ASO1, H107, MIP, GamTBVac, DAR901, H56:IC31 AEC/BC02, TB/Flu04L, CysVac2/Ad
Therapeutic, with treatment	TB/Flu01L, MVA Multiphasic vac, RUTI, ID93/GLA-SE

Table 1.1: Some of the current vaccines in the pipeline at various trial phases, recovered from TBVI webpage[80]. Not all vaccines under development are included in this table, and the ones included are currently at various trial phases. This populated pipeline shows the interest in developing a new TB vaccine, although up to date, any of the vaccines in this table have been introduced to the global population. However, some of them have shown promising results in RCTs. Some of the vaccines in the table are also being tested in other populations, such as MTBVAC in Adolescents and adults. For a complete description of all vaccines under development the reader is referred to[80].

The vaccines in Table 1.1 are undergoing various trial phases, with some of them reaching the phase 3 of the development pipeline. This poses a hopeful horizon, as likely, at leat one of those vaccines will show promising efficacy results. Additionally, the introduction in this century of diagnosis methods like GeneXpert assays have made a big difference. The GeneXpert TB test is made to quickly and precisely identify *Mycobacterium tuberculosis*, the bacteria that causes TB, as well as detect rifampicin resistance on MDR-TB. This method is a game-changer in the attempts to manage TB worldwide, particularly in areas with a high TB burden. Because of that, early detection has been made possible, which contributes to reduce transmission, and improve patient outcome after treatment, ultimately resulting in more successful TB control and prevention efforts.

Despite the previous considerations, which offers some hope, there are still other important factors that condition the spread of TB and put at risk equal access to resources and medical care. TB is a disease that relates very closely with poverty and with low socio-economic levels[81], both in rural and urban spaces. First, especially in developing countries, the lack of access to TB care in rural areas makes more difficult the consecution of TB control programs, as adherence levels might shrink as a consequence of social stigma or lack of resources, among others[82, 83]. Second, in urban areas, poverty correlates with worse housing, overcrowding, and smaller spaces, which might become a worrying scenario for control and prevention[84, 85]. Those inequities have not been addressed in this century, and they are even being exacerbated by the consequences of the COVID-19 pandemic[86]. Moreover, although the disease is preventable and curable, there is still a chronic lack of funding to TB related research, which poses a risk to the development of some of the new vaccines, treatments, or

techniques, that could be crucial to combat TB worldwide[87].

Furthermore, wars and conflicts, either motivated by racial, ethnic, or religious tensions, or by resources, or territorial ambitions, have continued to rage over the first part of the XXI century. Those conflicts have catastrophic repercussions on people's health, and compromise heavily TB care as access to healthcare facilities and treatment becomes more difficult, as, even if the international humanitarian law forbids targeting healthcare facilities during war, this does not stop the destruction of hospitals. As a result, a more peaceful and secure future is also key to proliferating the control programs, and to assure international cooperation to defeat TB. In closing, the currently available tools for TB control might not be sufficient in reaching the 2030 target (a world free of TB), not even in 2035 if the efforts continue at the current pace and no better tool is introduced.

1.4 The characteristics of TB

TB is a disease in which there is a complex interplay of biology, public health, and social dynamics. Understanding the characteristics of TB is necessary, not only to gain knowledge about the disease but also to better understand how the disease should be modelled, as we will be doing along this thesis with the mathematical model of Chapter 2. For this task, in the following lines, we describe briefly how the transmission of the pathogen may occur, the progression within the human host, and how TB is diagnosed and treated.

1.4.1 Transmission

TB is an airborne disease[88], whose causative agent is carried within tiny airborne particles referred to as droplet nuclei, which typically measure between 1 and 5 microns in diameter. These infectious droplet nuclei are produced when individuals with pulmonary or laryngeal TB disease cough, sneeze, shout, or sing, for example. Depending on the surrounding conditions, these minuscule particles can linger in the air for several hours, becoming a risk, especially in poorly ventilated areas, as the transmission of *M. tuberculosis* primarily occurs through the inhalation of these droplet nuclei[88]. The whole process unfolds when an individual breathes in those suspended droplet nuclei containing *M. tuberculosis*, with these particles traveling through the mouth, nasal passages, upper respiratory tract, and bronchi before reaching the alveoli in the lungs. Remarkably, individuals who can spread the disease are those with active pulmonary TB who can cough and expel the droplets into the air, with the LTBI individuals being virtually unable to spread TB, as the bacteria is contained in a

granuloma and thus, unable to reach the respiratory tract.

It's important to note that not everyone exposed to *M. tuberculosis* becomes directly infected or develops active TB disease, as the immune system of the host, along with other environmental factors plays a significant role in determining whether infection will be established, and, if so, whether they will progress to active disease. Generally, the risk of becoming infected relates to:

- Susceptibility: It relates to the immune status of the exposed individual, as, for instance, Immunocompromised individuals are at a higher risk of becoming infected.

- Exposure: the risk of becoming infected relates to the characteristics of the exposure to the bacilli. First, the infectiousness of an infected individual is directly related to the number of bacilli that he or she expels into the air, and persons who expel many bacilli are more infectious than those who expel few or no bacilli. Second, the proximity, frequency, and duration of exposure in the contact between the susceptible and the infected individual, as well as several environmental factors that affect the concentration of *M. tuberculosis* in a space, such as humidity or the ventilation of the space, also relates to the risk of becoming infected.

Taking a closer look at the exposure characteristics, on the one hand, the risk of being infected directly relates to the concentration of droplets in the space in which the exposure happens, as the more droplet nuclei in the air, the more probable that *M. tuberculosis* will be transmitted within this exposure. For this reason, transmission might be enhanced in closed spaces with poor ventilation, or whenever the air circulation does produce recirculation of the same air containing the bacilli, as evidence from studies of TB incidence conducted in prison inmates suggest[89]. Furthermore, overcrowded spaces also might enhance transmission, similar to what happens in other airborne diseases such as measles, although in TB, it is difficult to quantify this increased risk of transmission[90].

On the other hand, if the frequency or duration of exposure is high, so will be the risk of transmission. Something similar happens with the proximity, which increases the risk for transmission, although, in TB, it is also possible that, if droplets stay in the air, they could infect individuals that did not have direct contact with the infected individual[91], especially in the so mentioned closed and bad ventilated spaces which facilitate the concentration of infectious droplets, making transmission more likely. This is especially important for healthcare workers, as they may be at increased risk

of TB exposure, especially when caring for patients with TB, where proper preventive measures, such as wearing masks, are essential to minimise this risk.

Once the droplet nuclei are inhaled, there are also different risk levels depending on the host conditions, such as their immune status, as individuals with weakened immune systems are at a higher risk of developing TB if exposed to the bacteria. Those include patients with HIV, under severe malnutrition, or have other underlying medical conditions such as Diabetes, autoimmune diseases, or cancer. Individuals who abuse drugs and/or alcohol can also have weakened immune systems, making them more susceptible to TB infection. Moreover, children and the elderly are more susceptible to TB infection because their immune systems may not be as robust as those in the prime of their health. A final, obvious risk factor is traveling to areas with a high prevalence of TB, for this increases the risk of exposure to the bacteria no matter what. Considering the rise in drug-resistant strains of TB, such as MDR-TB and extensively drug-resistant TB (XDR-TB) in some high-burden settings, which are harder to treat, the risk is even higher.

1.4.2 The natural history of TB

After initial exposure to *M.tb.* of a susceptible individual, the bacilli may be cleared by the response of the alveoli macrophages, not becoming infected, or may proliferate in the host, until an effective cell-mediated immune (CMI) response develops, usually 2 to 10 weeks following initial infection. After the CMI response, the infection may, or not, be cleared by the effect of the immune system machinery. If it is not cleared after the CMI response, there are two possible outcomes:

- The bacilli are contained in the form of a granuloma by the action of the immune response, and the host enters a latency state. Individuals in this state are referred to as LTBI individuals. This occurs in around the 90% of exposed infected individuals[92, 93, 94], although there is evidence that this number could be lower[95]

- The bacilli proliferate and the immune response is not able to control it. In this case, the host will become infected and progress towards a state of active disease. Those individuals, who typically develop active TB within the first two to three years following infection, will be referred to as fast progressors, and this way to disease is referred to as Primary TB.

If the infection is cleared without the CMI response, it will test negative in interferon-gamma release assays (IGRAs), which are tests conducted to gauge the

immune system's response to interferon gamma release by T lymphocytes after exposure of *M.tb.* antigens (typically ESAT-6/CFP-10). However, if the infection is cleared after the CMI response or the individual is LTBI, the results of the test will be positive. For this reason, a positive result in the IGRA test suggests exposure to the TB bacteria but confirms neither active disease nor present LTBI.

LTBI individuals have no clinical symptoms and are not contagious, but will test positive in IGRA tests. The LTBI state is somehow protective, as it is very unlikely to reactivate in a lifetime as long as the granuloma keeps containing the bacilli. This is why TB is considered a long-cycle disease, as the expected time to reactivate in those individuals is higher than the mean life expectancy. Being in this state also provides some protection against a reinfection event, as one review evaluating 23 paired cohorts (more than 19,000 patients) noted. According to [96], LTBI individuals had a 79% lower risk of progressive TB following reinfection compared with uninfected individuals, although reinfection of LTBI may occur.

However, there is still a small risk for LTBI individuals to progress to active TB disease, especially if the immune system weakens, making it important to follow and manage those individuals in high-risk populations. It is not clear what specific host factors maintain the infection in a latent state and what triggers the latent infection to break containment and become active, but several medical conditions impair innate and acquired immunity and favour the occurrence of endogenous reactivation from LTBI. Arguably, HIV infection is the most significant risk factor, with an annual risk of progression of up to 15% for subjects who are not receiving highly active antiretroviral treatment[97]. Furthermore, there are other immunosuppressive conditions associated with reactivation TB including Chronic and end-stage kidney disease, diabetes mellitus, the diminution in cell-mediated immunity associated with age, being an active cigarette smoker, or the usage of corticosteroids[98, 99, 100, 101, 102, 103, 104].

Whenever the *M. tuberculosis* bacteria become active and multiply within the body, either by Primary TB or by reactivation or reinfection of LTBI individuals, the host becomes infected and is in an active TB state in which it shows clinical symptoms. These three routes to active TB are classically referred to as the "three risks model" [105], a frame coined by Vynnycky and Fine in 1997[106] which we will be using in this thesis, especially in Chapters 3 and 4.

The route to disease constitutes one dimension in the active TB space and allows for a classification of the cases in terms of their origin. A second, perpendicular dimension that should be considered at the same time is that individuals with active TB may also be classified according to the anatomical site where the disease proliferates, leading to having either Pulmonary TB or Extra-pulmonary TB. The former is the most common

form of TB and primarily affects the lungs. It's the primary TB form in around 85% of the infected individuals[72]. The latter is a TB form that affects other parts of the body outside of the lungs, such as the lymph nodes, bones, joints, brain, spine, and other organs, and constitutes the remaining 15% of the TB cases[72]. The symptoms of the latter will vary depending on the affected site.

Pulmonary TB patients can be further broken into having smear-positive TB and smear-negative TB according to their bacteriological results, where the main difference is the presence of the bacilli in the sputum of the patient and their infectiousness. Smear-positive cases are the most infectious and most likely to transmit their disease in their surroundings, and the WHO prioritises them for infection control measures and contact investigations. This is because it signifies a very large bacterial population in the lung lesions whereas several negative smears suggest a smaller bacterial load[107], which leads to more expelled bacilli into the air. In pulmonary TB, bacteria usually grow in the lungs, which may cause symptoms such as:

- A bad cough that lasts 3 weeks or longer, which may involve coughing up blood or sputum.
- Pain in the chest.
- Weakness or fatigue, fever, and/or sweating at night.
- Unexplained weight loss and no appetite.

In nonpulmonary TB, instead, the patients will show, among others, fever, weight loss, night sweats, anorexia, or weakness. As those symptoms are not disease-specific, and nonpulmonary TB is less common and, therefore, less familiar to most clinicians, it is usually harder to detect[108, 109]

One of the problems that arise in diagnosing TB is that only individuals with an active form of the disease show symptoms, which makes it difficult to diagnose and detect cases of past TB infections before they evolve into an active form of the disease. For LTBI, there are typically no symptoms because the *M. tuberculosis* bacteria are contained in the form of a granuloma by the action of the immune response. In those cases, LTBI is diagnosed through screening tests measuring host specific immunoreactivity to mycobacterial antigens (by tuberculin skin tests (TST) or IGRA tests), rather than by the presence of clinical symptoms. Moreover, sometimes it is also difficult to diagnose active TB by the symptoms, as they are not disease-specific to TB, and can appear in other respiratory diseases. Additionally, the severity and combination of symptoms can vary among individuals with TB, with some having

only a few mild symptoms, while others may experience more severe manifestations of the disease. This may produce a delay in the identification of a disease which, if not treated, may result in a fatal outcome in more than 50% of the cases[110]. On top of that, a delay in TB diagnosis also may cause an increased risk of transmission, as the patient has more time to spread the disease among contacts[111]. Nevertheless, in normal circumstances and in high-burden countries, patients are typically diagnosed within a median of 16 days (95% CI 11–20)[112], although there is a great variability depending on the available resources or the socioeconomic factors.

After a confirmed diagnosis of TB, patients should initiate a treatment plan, coupled with preventive measures, especially in patients with pulmonary forms of TB, as they may spread the disease otherwise. Then, once the treatment is started, different outcomes may happen. In a majority of cases, if the drug regime is completed, there is a high probability of recovery, as the treatment is typically effective, except for those cases of drug-resistant tuberculosis[76], which nowadays are a very concerning problem in TB eradication. In those cases, the infection is controlled and TB is cured. In the remaining cases, either by treatment abandon or by failure, the patients will either naturally recover, which is highly unlikely, or die by the action of the disease. Finally, after an individual is treated, there is still another risk that constitutes a fourth route to disease. In a small fraction of cured individuals, the disease becomes active again even after the treatment is completed. This is named TB relapse, and it can only occur when *M.tb.* bacilli persist after treatment completion despite being apparently cured. In that sense, relapse and failure can be seen as different outcomes of the same problem, which is having insufficient bacteriological cure in the treatment of the TB episode[113].

In Figure 1.2, a scheme of the natural history summarising the previous considerations is shown.

To summarise, TB is caused by the bacterium *M. tuberculosis*, and it is an airborne disease that spreads in the form of expelled droplet nuclei by infected individuals. Upon exposure, the infection may be cleared without the intervention of the adaptive immune system, with individuals testing negative on IGRA tests. If not, the infection may be cleared after the CMI response, becoming non-infected but testing positive on IGRA tests. If the infection is not cleared, either the bacilli is encapsulated in a granuloma, and the individual becomes LTBI, or the bacilli proliferates as the immune response is unable to control it, and the individual progresses towards active disease. However, LTBI individuals may progress to active disease too, either by endogenous reactivation or by a reinfection event. In all those cases, the individual progresses towards active disease, and the bacilli tends to affect the respiratory system, although it

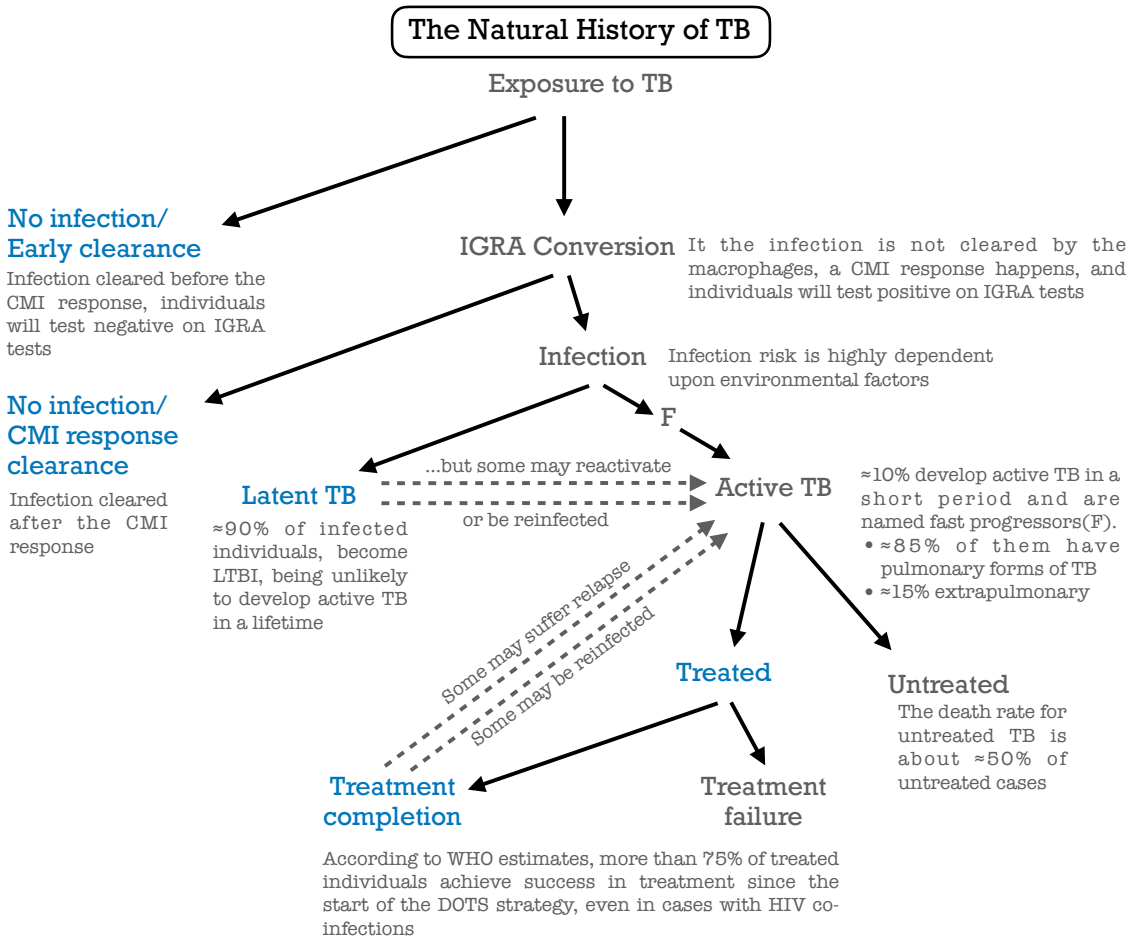

Figure 1.2: Flow chart scheme of the initial stages of the natural history after TB exposure. Treatment completion estimates, death rates, and active disease risk are approximate values commonly used in the literature[76, 93, 94, 110]. Pulmonary TB share is based on WHO data[72]. According to the immune response, only individuals without previous exposure to TB, and individuals who cleared the infection after exposure without the CMI response will show negative results on IGRA tests. Individuals who cleared the infection thanks to the CMI response, or who became infected, either LTBI or nor, will show positive results on the test.

can also manifest in various extra-pulmonary forms, affecting other organs and tissues. Individuals suffering from active TB should then be diagnosed and treated, as untreated individuals have a high risk of death, although there is a small possibility for treated individuals who completed the treatment to suffer relapse and reactivate into an active TB state.

As a consequence of this natural history, mathematical modelling in TB usually requires accounting for the different forms of TB, the different routes to disease, and the possibility of having LTBI individuals that reactivate or that are reinfected after many years, which in turn, makes the scale of the disease comparable with these of the ageing. Those considerations will be dealt with in the next chapter of this thesis when

the mathematical model in use is introduced.

1.4.3 Some considerations on the diagnosis and treatment of TB

The diagnostic process for TB can vary depending on the type of TB (pulmonary or extra-pulmonary) and the availability of resources in different healthcare settings. To diagnose TB, a combination of methods is employed, including the analysis of the patient's medical history, physical examinations, and various diagnostic tests. When a patient exhibits symptoms compatible with TB and is suspected to have a TB infection, a physical examination to assess signs and symptoms of TB should be conducted. Simultaneously, a review of the patient's medical history should also performed to identify potential risk factors for TB such as exposure to individuals with TB, or a history of previous TB infection. Then, a test such as the TST or IGRAs may be performed to determine exposure to the *M.tb.* bacteria. The TST involves injecting a small amount of purified protein derivative (PPD) tuberculin -which is a precipitate of species-nonspecific molecules obtained from filtrates of sterilised, concentrated cultures of *M.tb.*- under the skin and checking for a reaction. In the case of IGRAs, as stated before, the assay works by gauging the immune system's response to interferon gamma release by T lymphocytes after exposure of *M.tb.* antigens. It's important to remark that being IGRA-positive only suggests exposure to the TB bacteria, as the test will also show a positive result in individuals who cleared the disease with the aid of the CMI response. For this reason, this test does cannot confirm active disease or present LTBI.

Subsequently, a chest X-ray can uncover anomalies in the lungs, such as the presence of lung lesions or cavities associated with TB. To definitively diagnose active pulmonary TB, a sputum sample (mucus from the patient's lungs) is collected and subjected to a smear test to detect the presence of TB bacteria. Additionally, as in some TB cases may not be bacteria in the sputum and still may be a case of active pulmonary TB, a culture test can be performed to grow and identify the bacteria, at the cost of taking up to several weeks. The introduction of Nucleic Acid Amplification Tests (NAATs), molecular assays that detect the genetic material of TB bacteria, has reduced the delays in the diagnostic process in comparison to traditional culture methods, so nowadays, NAATs are frequently employed to confirm the diagnosis. Additionally, for cases where extra-pulmonary TB is suspected, further imaging procedures like CT scans or MRIs may be utilised to assess the extent of TB infection and its impact on other organs. In certain situations, confirmation of the diagnosis may necessitate a biopsy of affected tissue, such as lymph nodes.

Following a confirmed diagnosis of TB, it is imperative to initiate a treatment plan, coupled with additional preventive measures. First, during the infectious phase of the disease, patients with pulmonary TB should take precautions to prevent the spread of the infection to others, which may involve wearing masks or isolation. Then, to treat the disease, the identification of antibiotic susceptibility of the TB bacteria is crucial to use effective antibiotics for combating the specific TB strain. Commonly used medications for treating drug-susceptible TB include isoniazid, rifampin, ethambutol, and pyrazinamide, which are typically administered in combination. However, the specific combination and treatment duration can vary, contingent upon factors such as the patient's age, weight, overall health, and the prevalence of drug-resistant TB strains in the local area. Remarkably, TB treatment can be highly effective when administered as prescribed and completed in its entirety. Patients are strongly encouraged to adhere to the entire treatment regimen, even if they begin to feel better before the treatment concludes. Prematurely halting treatment can result in treatment failure and the emergence of drug-resistant TB, which is usually classified as Drug-Resistant TB (DR-TB), MDR-TB, or XDR-TB.

The first one is caused by some strains of *M. tuberculosis* that have developed resistance to one of the drugs commonly used to treat TB. The second one is a more severe form of drug-resistant TB, where the bacterium is resistant to at least two of the most powerful anti-TB drugs. The last one is characterised by strains in which the bacterium is resistant to the standard first-line and second-line anti-TB drugs, making it the most challenging kind of TB to treat. In all cases, the treatment regimen becomes more complex, spanning a longer duration (usually 18-24 months), potentially involving second-line antibiotics, and it is often accompanied by more severe side effects.

For these reasons, patients need to work closely with healthcare providers. In this sense, the introduction of the DOTS strategy of the WHO points towards increasing adherence to the treatment regimen and preventing the development of drug resistance. Under this strategy, a healthcare worker or trained observer watches the patient take their medication. It also involves monitoring regularly the patients to assess their response to treatment, and to identify any adverse effects of the medications or signs of drug resistance.

1.5 TB vaccines and the TB-COVID-19 interaction

1.5.1 Some considerations on new TB vaccines

The BCG vaccine, developed in the early 20th century by French scientists Albert Calmette and Camille Guérin, still stands as a pivotal tool in the global fight against

TB. This vaccine is a live attenuated vaccine derived from *Mycobacterium bovis* and has been widely implemented as a preventive measure against severe forms of TB worldwide. However, as there is evidence of the limited, and variable efficacy levels observed for BCG against the more transmissible respiratory forms of the disease, especially in young adults [79], the development of a new vaccine that either boosts or replaces the BCG is believed to be the potentially most impactful single intervention that could control TB transmission.

Nowadays there are several TB vaccine candidates under development, and some of them were already introduced in Table 1.1. However, those vaccines are based on a variety of immunological principles and vaccine platforms [114], and their targets and protective goals show also diversity. Some of the new vaccines are boosters, others aim to replace BCG, some are therapeutic vaccines whereas others are preventive ones.

On top of this diversity, the lack of reliable correlates of immune protection[115] on TB despite the research effort[116], hinders vaccine development. Because of this lack, efficacy is harder to foresee before phases 2b/3 of the development pipeline than for other diseases, and the RCT outcomes become more crucial. However, the architectures of the clinical trials of vaccine efficacy that are being adopted to test those novel TB vaccine candidates are highly diverse[117, 118], as the vaccines and their protection profiles may be equally diverse.

The consequence of the diversity in vaccines and the trial designs is that the TB vaccine development pipeline is populated by several novel candidates whose efficacy needs to be addressed in RCTs, and whose impact on halting the TB transmission chain in the general population before its introduction needs to be estimated using epidemiological models

Nevertheless, comparing the impacts of those vaccines is highly nontrivial, because of two main reasons. First, for TB there are several routes to disease and the vaccine can confer protection of different parts of the natural history. Given the diversity of vaccines under development, it is unlikely to have all vaccines working in the same way. TB vaccines can protect by preventing the infection, which is referred to as PoI, by preventing the active disease state, which is referred to as PoD, and also by preventing the relapse of already treated individuals, which is referred to as PoR[119]. On top of that, PoD vaccines may confer protection, at least, by three different mechanisms, which relate to halting each one of the possible routes to disease, i.e., primary TB, endogenous reactivation of LTBI, or reinfection. In Figure 1.3, the possible interactions between the vaccines and the natural history of TB are depicted.

As typically in RCTs the vaccine efficacy is assessed globally, and not in each one of the routes to disease, is difficult to fully characterise a new TB vaccine,

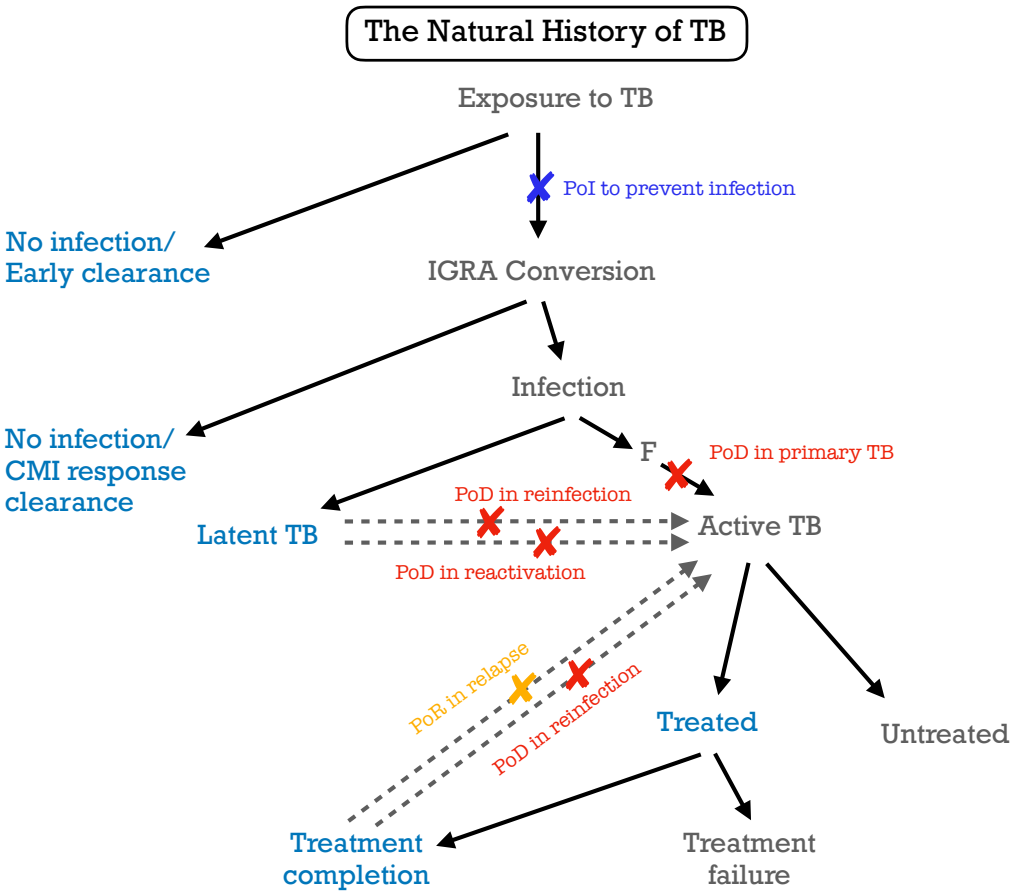

Figure 1.3: Flow chart scheme of the possible vaccine interactions with the natural history of TB. A PoI vaccine may halt the infection process, and a PoR vaccine may halt the recurrence flow. However, a POD vaccine may halt at least three routes to active disease, working either on one route, or in combinations of them.

and, consequently, to model it in terms of the mathematical models, adding a layer of difficulty to the impact comparison exercise. Furthermore, there are two different ways of modelling the protective effect of the vaccine when forecasting the impact of a vaccination campaign. The two common modelling approaches are named all-or-nothing vaccines, or leaky vaccines, and the separation is based on the distribution of the protection across vaccinated individuals. In leaky vaccines, the protection is partial and equal for all vaccinated individuals, whereas in all-or-nothing, the protection is perfect but only unfolds in a fraction of the vaccinated individuals. This problem hinders the vaccine characterization exercises and makes it difficult to compare fairly the expected impacts of the TB vaccine candidates, and solving those difficulties is the core of Chapter 3 of this thesis

1.5.2 The COVID-19 consequences

Starting in December 2019, the irruption of the COVID-19 pandemic, produced a global health crisis that had a profound impact on societies, economies, and healthcare systems around the world. The earliest known cases of COVID-19 were reported in December 2019 in the city of Wuhan, in China, and it was soon discovered that the virus could spread from person to person. Soon after, the virus spread beyond China's borders and reached every continent, and the WHO declared COVID-19 a Public Health Emergency of International Concern. Given the rapid transmission and severity of the disease, it was declared a pandemic on March 11, 2020.

The response of Governments was to introduce measures to contain the spread of the virus, including widespread testing, contact tracing, travel restrictions, lockdowns, social distancing, hand-washing promotion, and mask-wearing[120], although some were more effective, or more widely adopted than others[121, 122]. Nevertheless, the COVID-19 pandemic produced a severe downturn in the global economy[123], and saturated healthcare systems worldwide, leading to shortages of medical supplies, and hospital beds, and affecting healthcare workers[124, 125, 126]. This saturation also had consequences on the care of other diseases such as TB, Cancer, or Malaria. In the middle of the pandemic maelstrom, economic and human resources were redirected to face COVID-19, but at the same time, this led to a great reduction in the diagnosis and resource availability for controlling those other diseases[127, 128]. In this sense, interventions such as long lockdowns and mobility restrictions have exacerbated shortages in resources otherwise destined for the care of patients suffering these, and other pathologies.

Focusing on the main topic of this thesis, TB diagnosis, and patient care were severely disrupted, as reported in the literature[76, 73, 129]. The primary and immediate effect of COVID-19 spreading onto TB transmission dynamics was a reduction in the case notification ratio that was observed during and after lockdowns and in those periods of high COVID-19 incidence that produced the saturation of healthcare facilities[76]. The WHO Global Tuberculosis Report of 2023[130] captures the severity that the interaction with COVID-19 had on TB, as more than half a million people have died as a direct consequence of the measures for controlling the pandemic. In this thesis, we have analysed this interaction in Chapter 5, where we analyse the impact of the diagnosis and treatment reduction on the TB incidence and mortality in high-burden settings, for the long-term consequences of the interaction between the pandemic and TB are still long to be fully understood.

1.6 Challenges in epidemic modelling of TB

The interplay between epidemiology and network science, especially on short-cycle diseases - diseases in which the transmission cycle is shorter than the life expectancy- has produced plenty of knowledge and literature about modelling. Nowadays it is possible to find data, different modelling approaches according to it and to the question that wants to be addressed, and examples of usage of the models for policy making. This development for short-cycle diseases has produced that the state of the art comprises not only the forecast of the disease prevalence, incidence, and/or mortality, but also the evaluation of interventions, integration with complex networks in a shift from population-based models to individual-based ones, metapopulation models, and the introduction of behavioural mechanisms on the population[131, 132, 133, 134], among others.

Instead, in a long-cycle disease such as TB, in which the LTBI presence makes the cycle longer, sometimes higher than the life expectancy, the development has been modest in comparison. TB modelling poses a series of challenges that have hindered scientific progress, and that are discussed in the following lines. First, to model TB spreading, it is always necessary to deal with open systems, for the incubation times of the disease could span for decades as LTBI can reactivate years after the original infection took place. To manage this time scale, models need to include a comprehensive approach to describe the changes in the population due to demographic factors, such as natural death or population growth. For short-cycle diseases, the temporal scale of the disease is typically much faster than the demographic changes, but in TB, those scales are comparable, and as the population does not remain constant in time due to population growth and increased life expectancy, this factor needs to be accounted for. Moreover, including these ingredients in the model also imposes the need to work with, at least, age groups, so the ageing is captured. Moreover, as in TB several key dynamical processes may show dependencies with age, this also imposes the need of using age-dependent parameters[135].

Second, those models need to discard the hypothesis of homogeneous mixing, similar to what was done in short-cycle modelling approaches. However, as the time scale of the disease is longer, and the period that is simulated with models may span decades, it is difficult to make assumptions about the interactions between individuals in different layers, or about mobility. For this reason, TB models typically make use of a coarser grain description of the contact patterns which is based on contact matrices measured on surveys. However, those matrices are measured in a specific demography and a specific year, and, if the population is expected to change, so will be the intensity

and frequency of contact between age groups. Then, the contact matrices need to be adapted to the specific demography and year of the setting that is being simulated. For this task, models need to include methods to describe the evolution of those matrices[136].

Third, TB spreading models need to include a complete description of the natural history of individuals, combining both treated and untreated individuals. As we have seen in the previous section, the natural history of TB is complex, and, in general, dependent on factors such as age, the state of the immune system, and environmental factors. Moreover, as the cycle of TB may span decades, the compartmental model in use needs to couple TB dynamics with ageing and capture in the structure and parametrisation the possible routes to disease that can happen in a lifetime of an infected individual, while considering age-dependent risks to progression to disease, and this only can be done if there is data available.

Finally, if the objective of the model is to serve as a viable policy-making tool, it needs to be able to include, in some way, the effect of interventions that a competent authority may consider, as well as to accommodate descriptions of other external factors that may produce changes in the basal trend of the spreading of the disease. An example of the latter may be the shortage of certain drugs in a high-burden country, which may reduce the rate at which diagnosed individuals complete their treatment, and also may reduce the probability of getting cured. In this sense, there are plenty of external factors that may interplay with the spreading of TB, which the modeller needs to consider and plug into the -already- complex model, as simplest models may not have enough power to include those interplays. Moreover, to address the impact of a proposed public health intervention, the model, again, should be able to include its effect. There are two main types of interventions, pharmaceutical, and non-pharmaceutical interventions (NPIs), which are used to control the spread of infectious diseases. The former is related to the usage of medical treatments to manage the disease, including vaccines or antibiotics, while the latter comprises all interventions that do not make direct use of those elements, such as social distancing or face masks that were introduced in the recent COVID-19 pandemic. TB models for policy-making should be able to incorporate their effects, as, if a vaccine is introduced, the interplay between the vaccine and the disease will modify the natural history of the disease for vaccinated individuals, which is key to addressing the impact. The same applies to the rest of the interventions, as simple models are typically not capable of doing those tasks, for their results are qualitative and not quantitative.

To summarise, modelling TB poses a series of unique conceptual challenges that are essentially different from those of short-cycle diseases, and to address some of the

open questions in the literature, such as the model-based evaluation of public health interventions for policy-making, complex models are needed. In the following lines, we will describe what we need to model to answer the research questions and to minimise the bias in the results when studying vaccines and the interaction of TB and COVID-19.

1.6.1 Addressing the research questions: what needs to be modelled.

Along the next chapters, we are going to work with a spreading model of TB that works at the national level, which is fed with WHO data to capture the burden in the target country and produce a calibration that allows extrapolating, in a data-driven way, the TB burden in the future. The whole idea of the thesis, as we will introduce in the final section of this chapter, is to address: i) the effect of the introduction of a new TB vaccine in the general population, and ii) the effect of the healthcare system saturation during the COVID-19 pandemic over the TB trends in high-burden settings, using for both questions the TB spreading model introduced in Chapter 2[135]. Typically, in the literature, TB spreading models trust in incidence, mortality, and/or prevalence data, to produce a data-driven calibration that captures the overall epidemic situation in the desired setting. Then, with this calibration and the basal trends it produces, it is possible to address the effect of an external perturbation such as those mentioned above. For instance, the models presented in[137, 138, 139, 140, 141, 142, 143], along with our model, make use of this approach.

However, several models lack versatility as they may not be complex enough to address questions they were not designed for. As an example, the model in[139] is used to address the impact of some TB vaccines in high-burden settings, but, as the architecture of the model does not include explicitly the compartment for fast progressors, it is not possible to differentiate the effect of a vaccine that prevents infection from the effect of a vaccine that prevents progression to disease, in those individuals. On the other hand, the model in[137] would be capable of doing so. In this sense, here is when the trade-off between complexity and affordability hits, as the more complex the model, the harder to solve and calibrate, but also the more versatility it has.

In this thesis, to accomplish the research objectives, the TB spreading model in use is complex enough to accomplish the research objectives, given that the structure and architecture allow for the introduction of vaccines, and also to introduce a modulation function on the diagnosis rate, and modify the treatment rate of TB, both consequences of the interaction with the COVID-19. Addressing these questions is interesting in TB because spreading models are, as in the short-cycle case, a powerful tool in

policy-making, giving a solid framework to test the effect of an intervention. At the model level, the objectives mutate into:

1. plugging a vaccine into the model based on how it interacts with the natural history of the disease in vaccinated individuals, which is an example of a pharmaceutical intervention.

2. measuring the effect of the healthcare saturation in the diagnosis and treatment of other diseases, which were the main consequences of the interaction with COVID-19. To this end, I introduce a modulation function to modify the diagnosis rate, and a reduction in the treatment rate based on data.

3. measuring the effect of a diagnosis boost in TB, which is an example of a non-pharmaceutical intervention in the context of the interaction with COVID-19.

In all three cases, the underlying compartments of the model need to capture the natural history of TB and, specifically in the context of vaccines, all possible routes to disease, so vaccines with different combinations of protective mechanisms, that interact differently with the natural history, may be studied. Moreover, the model needs to incorporate ageing and contact patterns that evolve in time, for which the analysed periods are comparable with those needed by demography to evolve and the effect on the long term needs to be addressed. The model in [135], with some modifications that we are going to introduce in the next chapter, is powerful enough to analyse all scenarios.

Focusing on the introduction of a new vaccine, with the model we need to address the impact of a vaccine whose efficacy has been addressed in a Randomised Clinical Trial. These model-based impact forecasts are interesting especially because in TB the introduction of a new vaccine seems to be the promising strategy to control the disease. However, the model may provide a powerful tool to compare and address qualitatively the effect of the vaccine only if it can accommodate the mechanistic effect of the vaccine. As it is explored in Chapter 3 of this thesis, there is no unique way of plugging the efficacy readout of a vaccine in an RCT to a complex TB spreading model, for which the vaccine can halt progression to disease in different parts of the natural history. This imposes the need to give the spreading models the ability to test vaccines that act through different combinations of mechanisms at the model level.

1.7 Objectives and milestones of the thesis

TB is still a cause of concern in the XXI century, and TB epidemiology will be necessary until eradication is achieved, as it is unraveled after having contextualised the state of TB, both historically and contemporarily. However, there are still plenty of challenges in modelling TB, and this thesis is devoted to answering some open questions.

First, the characteristics of TB make that vaccine efficacy harder to address before going to RCTs, and the variability of TB vaccines under development makes it difficult to compare the potential impact they have when analysed using spreading models. Furthermore, forecasting the impact of a vaccine is not a trivial task, as vaccines may halt different routes to disease, or combinations of them, and yet be compatible with the classic efficacy measure that the RCT yielded. To enable comparison, and to provide robust impact forecasts, a better characterisation of the vaccines is needed. Second, the overall impact that the COVID-19 pandemic produced on other diseases is still not fully understood. In TB, the interaction between those diseases arose, at least, in the form of reductions in diagnosis and treatment availability for infected individuals, which in turn was expected to produce new infections, and ultimately, new deaths. Consequently, there are two main objectives in this thesis, which have been anticipated previously, and that are unfolded in the following lines:

- **Obj 1**: produce robust impact forecasts of TB vaccines when analysed using spreading models. To this end, it is necessary to develop a complementary methodology to the classical survival analysis to characterise vaccines that are empirically tested in RCTs undergone on IGRA-negative or IGRA-positive individuals, for the results of the trials are not directly comparable, and also not fully compatible with the typical structures of the mathematical models.

- **Obj 2**: analyse the effect of the interaction between the COVID-19 pandemic in the trends of TB in high burden settings. The ultimate goal is to deal with the main perturbations that arise as a consequence of this interaction, which mainly affected the diagnosis and treatment availability for TB, to provide an estimation of the long-term effect on the incidence and mortality due to TB in high-burden settings.

Several milestones have been accomplished during this thesis to deal with those two objectives, which are the following:

- **Obj.M1**: Develop a new version of the existing spreading model that makes use of a better way of propagating the uncertainty from data to the outcomes, as

the original one was too rigid to allow for some crucial tasks such as explore the uncertainty in differences of vaccination campaign's outcomes. To this end, we capitalise on the original model, which is introduced in the framework section of this thesis, and in the uncertainty section that is explained there.

- **Obj.M2**: Modify extensively the spreading model to estimate the impact of new TB vaccines. We have modified the model to i) enable the possibility of test vaccines that act through different combinations of mechanisms, and ii) estimate the impact using an additional branch that evolves using the modified version of the natural history of TB that vaccinated individuals face.

- **Obj.M3**: Modify the spreading model to introduce the diagnosis perturbations that are explored in this thesis. For this task, we adapted the diagnosis function with a modulation function that acts over the fitted diagnosis rates, as explored in Chapter 5.

Obj.M1 and Obj.M2 were accomplished within the first year of research, while Obj.M3 was accomplished later. In summary, the overall outcome of this thesis is that both objectives have been accomplished. First, two different methodologies to characterise TB vaccines at the mechanistic level have been developed, which enable forecasting their effect using spreading models and reducing the inherited bias in model-based impact evaluations. Second, the impact on incidence and mortality in high-burden countries has been reevaluated after the disruption of the COVID-19 pandemic. To this end, the perturbations on diagnosis and to account for the reductions in diagnosis due to the COVID-19 pandemic, and to accommodate the different vaccine descriptions that emanate from the first objective, to estimate their effect on the TB burden in the long run.

1.7.1 List and summary of works

The contents of this thesis derive from a long Ph.D. journey that yielded 4 complete works, each one having a specific purpose in the research endeavour. In the following lines, a summary of those works, and the references are included by the order of development and publication.

Work 1: In this work, we unravel a problem that has been largely ignored when analysing the outcome of Randomised controlled trials of new TB vaccines. Specifically, a readout of protection against TB disease in a vaccine efficacy trial can be mapped to multiple dynamical mechanisms, and in the case that the recruited population was

IGRA-negative at the start of the trial, this issue appears in the form of two possible mechanistic effects of the vaccine compatible with the same efficacy readout. In this work, we describe this limitation and its effect on model-based evaluations of vaccine impact, and we propose a methodology to analyse efficacy trials that circumvents the problem. Using our approach, we can disentangle the different possible mechanisms of action underlying vaccine protection effects against TB, conditioned to trial design, size, and duration.

Our results unlock a deeper interpretation of the data emanating from efficacy trials of TB vaccines and reveal a problem that could compromise the clarity of impact forecast if not done properly, at least, when the impact is addressed using spreading models. This work is detailed in Chapter 3 of this thesis.

Reference: Tovar, M., Arregui, S., Marinova, D., Martín, C., Sanz, J., & Moreno, Y. (2019). Bridging the gap between efficacy trials and model-based impact evaluation for new tuberculosis vaccines. *Nature communications*, 10(1), 5457.

Work 2: In this work, we studied the potential impact of the COVID-19 pandemic on the TB burden in four high-burden countries. As surely known by the reader, the COVID-19 crisis disrupted daily life and strained global healthcare systems, which threatens the control of diseases like Malaria, Cancer, and, in our case, Tuberculosis. Our study forecasts the surge in Tuberculosis cases and deaths when healthcare systems are saturated, adding an effect on the diagnostic rates that reduce their effectivity, as a consequence of the saturation, using real data of the drops.

Our results indicate that the pandemic may lead to nearly 400,000 extra TB-related deaths in India, Indonesia, Pakistan, and Kenya, but we demonstrate that restoring diagnostic capabilities post-pandemic can mitigate the additional TB deaths caused by the COVID-19 impact. This work is detailed in Chapter 5 of this thesis.

Reference: Tovar, M., Aleta, A., Sanz, J., & Moreno, Y. (2022). modelling the impact of COVID-19 on future tuberculosis burden. *Communications medicine*, 2(1), 77.

Work 3: In this work, we revisit the idea introduced in the first one, which is that in TB vaccine development, multiple factors hinder the design and interpretation of the clinical trials used to estimate vaccine efficacy. As the complex transmission chain of TB includes multiple routes to disease, it's difficult to link the vaccine efficacy observed in a trial to specific protective mechanisms. This problem is even more crucial when dealing with trials such as the analysis of the M72/AS01$_E$ -conducted on IGRA+ individuals-, that we use as a case example. To solve it, we present a Bayesian framework to evaluate the compatibility of different vaccine descriptions with clinical trial outcomes,

unlocking impact forecasting from vaccines whose specific mechanisms of action are unknown. This framework is different from the one used to disentangle the protection in trials that recruit IGRA-negative individuals.

Our results show that the most plausible models for this vaccine needed to include protection against, at least, two of the three possible routes to active TB classically considered in the literature (primary TB, latent TB reactivation, and TB upon re-infection). Moreover, we introduce an approach to reduce the bias in the impact forecast of vaccines characterised using our methodology, which makes use of the Bayesian posterior of each vaccine description. This work is detailed in Chapter 3 of this thesis.

Reference: Tovar, M., Moreno, Y., & Sanz, J. (2023). Addressing mechanism bias in model-based impact forecasts of new tuberculosis vaccines. *Nature Communications*, 14(1), 5312.

Work 4: In this work, we address the bias incurred in the model-based estimation of the impact of a new TB vaccine in China using two descriptions of the coupling between ageing and contact patterns, which governs TB dynamics. In a country like China, there is a fast-ageing process happening, and the eventual impact of vaccines that prevent disease by different mechanisms could correlate with the age of the target but also could depend heavily on the description of the coupling between ageing and contacts. As a consequence, transmission models need to incorporate robust descriptions of the coupling, which unfolds in contact matrices that govern TB transmission across age strata, as well as to be able to accommodate different vaccine descriptions.

Our findings indicate that model-based impact forecasts are affected to an extent that depends on the characteristics of the vaccine and the description of the coupling. Our results also align with previous literature on the convenience of vaccinating elders in China. This work is detailed in Chapter 4 of this thesis.

Reference: Tovar, M., Sanz, J., & Moreno, Y. (2023). Model-based impact evaluation of new tuberculosis vaccines in aging populations under different modelling scenarios: the case of China. *MedArxiv*.

Chapter 2

General methods: The *M.tb.* spreading model

Summary of this chapter: This chapter includes all the relevant features of the tuberculosis (TB) spreading model to ensure reproducibility and to help the reader understand better the results presented in the thesis. This model serves as a mathematical representation of the natural history of TB, where the dynamical evolution is modelled by an ODE system, along with a description of the coupling between age groups, through contact matrices and ageing dynamics. Moreover, we summarise how TB vaccines are introduced into our spreading model, which is key in the results that are presented later, and finally, we remark on some considerations on the statistical methods that are used to obtain some of the results of this thesis.

2.1 The *M.tb.* spreading model: modelling the spread of tuberculosis at the national level

THIS thesis is devoted to the study of the interactions between TB trends and different perturbations, from which the vast majority are vaccines. All the results discussed in the following chapters are directly, or indirectly obtained through the usage of a compartmental model that captures the evolution of TB in high-burden settings, at the national level, which is an adapted version of the model developed by Arregui et al.[135] in previous works.

The adapted version is closely related to the original model, except that it introduces a new way of calculating confidence intervals of the outcomes, which works better than the previous one while preserving all the sources of uncertainties. Moreover, it has been modified to allow the introduction of some model perturbations, which is done according to the coupling between the natural history of TB and the perturbation under study. For instance, to model specific vaccines, we have adapted the spreading model to let vaccines target specific combinations of age groups and transitions between states,

with different descriptions, and to compute the effect of the vaccine when compared to the baseline. In the following lines, we describe the main aspects of the spreading model, including the description of the natural history of the disease, the description of the coupling between the population's ageing and disease dynamics, and the propagation of the uncertainty incurred in the outcome, plus how vaccines may be modelled. With the key elements described here, it is possible to reproduce all the results that are shown in this thesis.

In short, this spreading model is a data-driven, age-structured compartmental model that features 15 different age groups: 14 of them covering 5 years of age up to 70 years old, and the last one containing all individuals older than 70 years old. The age-based structure arises as certain dynamic parameters vary across each age group. Within each age group, we have a class of unexposed individuals –susceptible–, two different latency paths to disease –fast and slow – and six different kinds of disease, depending on its aetiology: -non-pulmonary, pulmonary (smear-positive), and pulmonary (smear-negative)-, and depending on if TB is left untreated or treated. After the disease phase, we consider the treatment outcomes contemplated by the WHO data schemes: treatment completion, default, failure, and death [76].

The temporal evolution is solved using a C-coded version of the Runge-Kutta 4th order algorithm that solves the coupled ODE system, and as the model is data-driven, the goal is to produce a calibration that makes the model-based incidence and mortality reproduce the temporal series that are reported annually by the WHO[76]. With the model calibrated, it is now usable to compute the effect of a vaccine or the COVID-19 interaction in the basal trend by modeling their interactions with the natural history of the disease. Then, it is possible to compute the impact of the TB trends by comparing the perturbed scenario with the base scenario.

2.1.1 Natural history of *M.tb.*

The natural history of TB is modelled with the aid of 19 possible reservoirs for individuals, which depends upon the status of the disease. In Figure 2.1 we schematise the whole model, including the different compartments that relate to the host's status towards the disease, and all the possible transition between those states.

According to the natural history of TB, there are several types of possible transitions between the compartments of the TB natural history, which are explained below along with the parameters that are necessary to account for all phenomena associated to progression through states.

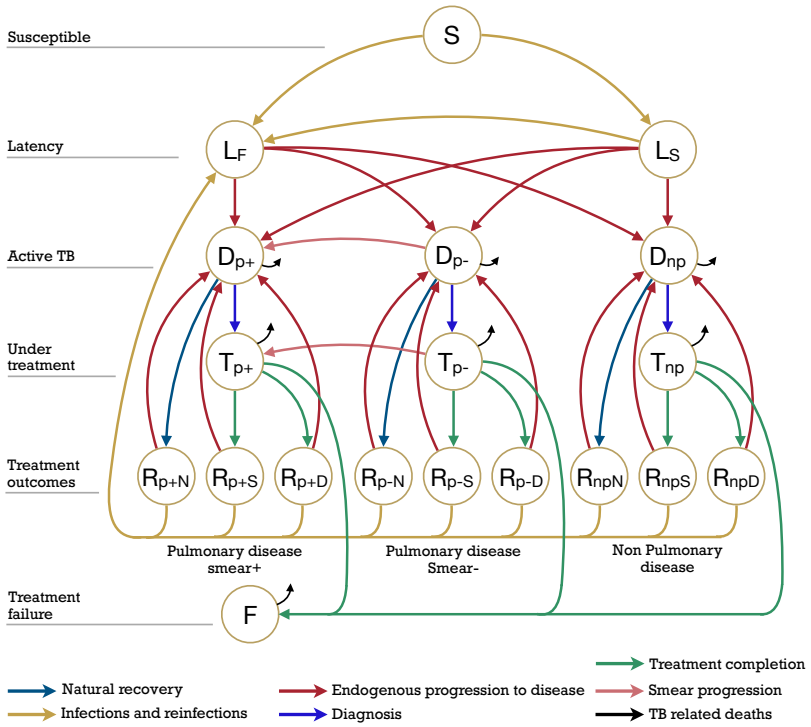

Figure 2.1: Natural history of the disease employed in the mathematical model[135]. Individuals are classified according to their epidemiological status, which can be: S: susceptible. L: latent. D: (untreated) disease, T (treated) disease, R recovered, F: failed recovery . The types of TB considered here are: p+: Pulmonary Smear-Positive, p-: Pulmonary Smear-Negative, and np: Non-pulmonary. Finally, individuals under treatment end it for three different sub-types of recovery, which are: N: Natural, S: Successful, and D: Default (abandon of treatment).

Infection processes: after contact with an infectious individual, susceptible individuals (S) get infected, entering either the fast (L_F), or slow latency states (L_S). In the model, infections occur after contact between susceptible individuals and infectious ones. If $S(a,t)$ represents the number of susceptible subjects in the age group a, at a given time t, the number of new infections that will be observed will be equal to the product of $S(a,t)$ and the force of infection perceived by that sub-population, denoted as $\lambda(a,t)$, and which is proportional to the following sum:

$$\sum_{a'} \xi_c(a,a',t)\Upsilon(a',t) \tag{2.1}$$

where $\Upsilon(a',t)$ is the density of all the infectious individuals within age-group a' at time step t, weighted by their relative infectiousness; and $\xi_c(a,a',t)$ represents the relative contact frequency that an individual of age a has with individuals of age a' at time t, with respect to the overall average of contacts that an individual has per unit time with anyone else. The complete form of the force of infection is a scaled version of Equation 2.1 where the scaled parameter is fitted to capture the temporal

evolution of the previous data on TB incidence and mortality reported by the WHO. Of all the newly infected individuals, a fraction $p(a) \in [0,1]$ will experience a quick development of the disease after a short latency period due to the inability of the host's immune system to restrain mycobacterial growth, and will transit to the L_F latency state. If the individuals' immune system succeeds at containing bacterial proliferation in a host-pathogen dynamic equilibrium, they will transit to an asymptomatic, slow latency state L_s. This situation that can last for the rest of the host's life, or be broken even decades after the infection either by a new infection or by an episode of immunosuppression.

Development of active TB: infected individuals (either L_F or L_S) may develop initially undiagnosed -and thus untreated- TB (D states). Infected individuals can become ill from either fast or slow latency, progressing to one of the three active forms of the disease.The first form, known as non-pulmonary disease D_{np}, is related to the growth of the pathogen in various parts of the host's body that are not related to the lungs, such as bones or the nervous system. Individuals with this form of TB individuals are considered unable to transmit the disease as the bacilli cannot reach the respiratory tract (although it is possible but rare to have pathogens multiplying in the lungs, which will enable transmission). The other two forms are based on the presence of viable bacilli in the sputum: we have either: pulmonary disease, smear-negative D_{p-}, or pulmonary disease smear-positive D_{p+}, with the latter being more contagious than the former.

Then, we parametrise the possible progression to disease with the rates ω_f and ω_s, which capture individuals progression from fast and slow latency respectively, and with $\rho_{p+}(a)$,$\rho_{p-}(a)$ and $\rho_{np}(a)$ that represent the probability to develop each of the three different forms of TB previously described. Those probabilities must fulfil the closure relation $\rho_{p+}(a) + \rho_{p-}(a) + \rho_{np}(a) = 1$.

TB diagnosis: with some delay after the disease onset, TB gets diagnosed and treatment starts (transition from D states to T ones) In the model, individual that belongs to D classes are diagnosed, which moves them to the corresponding treated TB class T. T classes are divided based on the form of TB that the individual had where active TB was developed. The diagnosis rate is denoted $d(t)$, and is country specific, as it depends, among other factors, on the capabilities of Public Health systems. The model also accounts for the varying average time needed for TB diagnosis according to the type of disease. This is due, in part, because the diagnosis criteria for each type are different. Then, at the model level, this variation is taken into account with the η

parameter, which captures the reduction in the diagnosis rate observed for non smear positive TB.

The diagnosis rate is allowed to vary in time, as the capabilities of the Public Health systems may change in time too. It is modelled as a half-sigmoid curve with two parameters, d_0 and d_1, which are involved in the calibration procedure of the model to the TB burden in each country. See the calibration procedure for further details.

Treatment outcomes: (transitions from T states to R ones, or to the F state) different possible outcomes are possible: –either success or failure/default- (failure of treatment moves individuals to F) Right after diagnosis, and supposing that antibiotic treatments are available immediately, sick individuals start their treatment. Those individuals under treatment belong to the T_{np}, T_{p-} or T_{p+} states, depending on the type of disease they had. While being in the T classes individuals are not able to spread the disease. This happens either by the effect of treatment or by the isolation measures that are usually established after a diagnosis of TB.

As the typical antibiotic series last six months, we model the rate at which individuals abandon the T states with the Ψ parameter, that captures rate associated to the inverse of the treatment time. When treatment is completed, different results are possible, and following the WHO classification it is possible to divide individuals according to the treatment outcomes in four main groups:

- Success: the treatment has been completed and bacilli are not present in the sputum.
- Default: the treatment has been abandoned before completion.
- Death.
- Failure: bacilli persist -or appear- in the sputum at the end of the treatment (month five or later).

Therefore, for each possible type of TB there are transitions to the R states or to the F state. This is done by dividing the individuals that abandon the T states based on the probabilities of each one of the treatment outcomes, which will be dependent, again, on the type of TB the individual had. For the smear positive TB individuals that finish the treatment, we denote as f_S^{p+}, f_D^{p+}, f_F^{p+} and f_μ^{p+}, the fraction of them that ends into success, default, failure and death groups. They must fulfil the closure relationship $f_S^{p+} + f_D^{p+} + f_F^{p+} + f_\mu^{p+} = 1$. The fraction f_F^{p+} of the individuals finishing the treatment still show bacilli in the sputum, and therefore move to the F state, in which they have and increased risk of TB mortality and are still infectious. For pulmonary

smear negative and non pulmonary TB cases, the WHO does not differentiate the fractions of treatment outcomes, which means that it is enough to introduce f_S^{p-}, f_D^{p-}, f_F^{p-} and f_μ^{p-} as the fraction of individuals getting each outcome both from pulmonary smear negative and from non pulmonary TB. Again, we have the closure relationship $f_S^{p-}+f_D^{p-}+f_F^{p-}+f_\mu^{p-}=1$, and the fraction f_F^{p-} of the individuals finishing the treatment move to the F state.

Re-infection processes: Individuals in L_S or R could get reinfected, thus increasing the risk of developing active TB. The individuals belonging to classes L_s and R have been previously exposed to TB bacilli, although not being sick while remaining in latency. Those individuals could be exposed again to the pathogen, thus, being re-infected, and a fraction of those individuals will develop TB fast after re-infection. This is modelled as a transition from L_S to L_F, and with transitions from any of the R states ($R_{np,i}$, $R_{p+,i}$, $R_{p-,i}$ with $i \in (S, D, N)$) to the L_F state. In all those transitions, a parameter q is introduced to account for the variation factor of the infection risk of individuals who have been infected in a previous episode.

Natural recovery: Individuals from D states could naturally cure and transit to R. On specific occasions, TB can be cured without medical intervention or treatment[144]. To represent this scenario, three additional classes of naturally recovered individuals are introduced, $R_{npN}(a,t)$, $R_{p-N}(a,t)$, and $R_{p+N}(a,t)$. Individuals that are sick and undiagnosed from each type of TB are assimilated into these new classes at a rate modelled by the ν parameter.

Disease relapse: transitions back from R to D. Some individuals may experience an endogenous reactivation of the disease, if the recovery does not suppose the total elimination of the bacilli from the host organism.[145]. For this reason, in the model there are transitions from the R states to the D states, capturing the effect of a post-cure proliferation of bacilli. This happens for all individuals that enter the R states, with different rates that depends upon the result of the treatment.

This implies that for those individuals that had a successful result, the risk of developing an episode of relapse is lower than those individuals for which the result was default. Moreover, natural cured individuals also show a different risk to relapse when compared to the previous cases, which is captured with the rates r_N for naturally cured individuals, r_S for those whose treatment was successful, and r_D for those that defaulted.

Death: active TB patients, either diagnosed or not, are assigned a TB-specific mortality rate. Individuals in D states could develop disease symptoms, infect other individuals (except the individuals in D_{np}), or die because of the disease. In the model, we model specific mortality rates with four different parameters:

- Deaths of untreated non pulmonary disease: μ_{np}
- Deaths of untreated smear negative pulmonary disease: μ_{p-}
- Deaths of untreated smear positive pulmonary disease: μ_{p+}
- Deaths of treated individuals that do not respond to treatment:

There are few more possible transitions that capture other phenomena like smear progression, where individuals with smear negative pulmonary TB progress to smear positive even after being treated, or mother-child infections that accounts for the possibility of newborns to be infected by their mothers if sick. Those are also introduced in the model and in the ODE system of the next section. the evolution of individuals with time inside the natural history is solved by numerically integrating the ODE system.

2.1.2 Ordinary differential equations system

In the previous section, we included the TB natural history which is used in the model as the compartments of the compartmental model. The evolution of the population in each compartment is given by an ordinal differential equation (ODE) which captures the transitions that either introduce new individuals or withdraw them. The following system of differential equations describes, then, the evolution of the different dynamical states of the model for a given age group a, according to all the possible transitions between states that are described previously.

$$\begin{aligned}
\dot{S}(a,t) &= -\lambda(a,t)S(a,t) - ((1-\delta(a-14))S(a,t) - (1-\delta(a))S(a-1,t))/\tau \\
&+ \delta(a)(1-m_c m_d(t))\Delta_N(a,t) + (1-\delta(a))\Delta_N(a,t)S(a,t)/N(a,t)
\end{aligned} \tag{2.2}$$

$$\begin{aligned}
\dot{L}_s(a,t) &= (1-p(a))\lambda(a,t)S(a,t) - p(a)q\lambda(a,t)L_s(a,t) \\
&- \omega_s L_s(a,t) + \delta(a)m_c m_d(t)(1-p(0))\Delta_N(a,t) - ((1-\delta(a-14))L_s(a,t) \\
&- (1-\delta(a))L_s(a-1,t))/\tau + (1-\delta(a))\Delta_N(a,t)L_s(a,t)/N(a,t)
\end{aligned} \tag{2.3}$$

$$\begin{aligned}
\dot{L}_f(a,t) &= p(a)\lambda(a,t)S(a,t) - \omega_f L_f(a,t) \\
&+ p(a)q\lambda(a,t)(L_s(a,t) + R_{p+N}(a,t) + R_{p-N}(a,t) + R_{npN}(a,t)) \\
&+ p(a)q\lambda(a,t)(R_{p+S}(a,t) + R_{p-S}(a,t) + R_{npS}(a,t)) \\
&+ p(a)q\lambda(a,t)(R_{p+D}(a,t) + R_{p-D}(a,t) + R_{npD}(a,t)) \\
&- ((1-\delta(a-14))L_f(a,t) - (1-\delta(a))L_f(a-1,t))/\tau \\
&+ \delta(a)m_c m_d(t)p(0)\Delta_N(a,t) + (1-\delta(a))\Delta_N(a,t)L_f(a,t)/N(a,t)
\end{aligned} \tag{2.4}$$

$$\begin{aligned}
\dot{D}_{p+}(a,t) &= \omega_f\rho_{p+}(a)L_f(a,t) + \omega_s\rho_{p+}(a)L_s(a,t) - \mu_{p+}D_{p+}(a,t) \\
&- d(t)D_{p+}(a,t) - \nu D_{p+}(a,t) + r_N R_{p+N}(a,t) \\
&+ r_S R_{p+S}(a,t) + r_D R_{p+D}(a,t) + \theta D_{p-}(a,t) \\
&- ((1-\delta(a-14))D_{p+}(a,t) - (1-\delta(a))D_{p+}(a-1,t))/\tau \\
&+ (1-\delta(a))\Delta_N(a,t)D_{p+}(a,t)/N(a,t)
\end{aligned} \tag{2.5}$$

$$\begin{aligned}
\dot{D}_{p-}(a,t) &= \omega_f(1-\rho_{p+}(a)-\rho_{np}(a))L_f(a,t) + \omega_s(1-\rho_{p+}(a)-\rho_{np}(a))L_s(a,t) \\
&- \mu_{p-}D_{p-}(a,t) - \eta d(t)D_{p-}(a,t) - \nu D_{p-}(a,t) + r_N R_{p-N}(a,t) \\
&+ r_S R_{p-S}(a,t) + r_D R_{p-D}(a,t) - \theta D_{p-}(a,t) \\
&- ((1-\delta(a-14))D_{p-}(a,t) - (1-\delta(a))D_{p-}(a-1,t))/\tau \\
&+ (1-\delta(a))\Delta_N(a,t)D_{p-}(a,t)/N(a,t)
\end{aligned} \tag{2.6}$$

$$\begin{aligned}
\dot{D}_{np}(a,t) &= \omega_f\rho_{np}(a)L_f(a,t) + \omega_s\rho_{np}(a)L_s(a,t) - \mu_{np}D_{np}(a,t) - \eta d(t)D_{np}(a,t) \\
&- \nu D_{np}(a,t) + r_N R_{npN}(a,t) + r_S R_{npS}(a,t) + r_D R_{npD}(a,t) \\
&- ((1-\delta(a-14))D_{np}(a,t) - (1-\delta(a))D_{np}(a-1,t))/\tau \\
&+ (1-\delta(a))\Delta_N(a,t)D_{np}(a,t)/N(a,t)
\end{aligned} \tag{2.7}$$

$$\begin{aligned}
\dot{T}_{p+}(a,t) &= d(t)D_{p+}(a,t) - \Psi T_{p+}(a,t) + \theta T_{p-}(a,t) \\
&- ((1-\delta(a-14))T_{p+}(a,t) - (1-\delta(a))T_{p+}(a-1,t))/\tau \\
&+ (1-\delta(a))\Delta_N(a,t)T_{p+}(a,t)/N(a,t)
\end{aligned} \tag{2.8}$$

$$\begin{aligned}
\dot{T}_{p-}(a,t) &= \eta d(t)D_{p-}(a,t) - \Psi T_{p-}(a,t) - \theta T_{p-}(a,t) \\
&- ((1-\delta(a-14))T_{p-}(a,t) - (1-\delta(a))T_{p-}(a-1,t))/\tau \\
&+ (1-\delta(a))\Delta_N(a,t)T_{p-}(a,t)/N(a,t)
\end{aligned} \tag{2.9}$$

$$\begin{aligned}
\dot{T}_{np}(a,t) &= \eta d(t)D_{np}(a,t) - \Psi T_{np}(a,t) \\
&- ((1-\delta(a-14))T_{np}(a,t) - (1-\delta(a))T_{np}(a-1,t))/\tau \\
&+ (1-\delta(a))\Delta_N(a,t)T_{np}(a,t)/N(a,t)
\end{aligned} \tag{2.10}$$

$$\begin{aligned}
\dot{F}(a,t) &= \Psi f_F^{p+}T_{p+}(a,t) + \Psi f_F^{p-}(T_{p-}(a,t) + T_{np}(a,t)) - \mu_{p+}F(a,t) \\
&- ((1-\delta(a-14))F(a,t) - (1-\delta(a))F(a-1,t))/\tau \\
&+ (1-\delta(a))\Delta_N(a,t)F(a,t)/N(a,t)
\end{aligned} \tag{2.11}$$

$$\begin{aligned}
\dot{R}_{p+N}(a,t) &= \nu D_{p+}(a,t) - r_N R_{p+N}(a,t) - p(a)q\lambda(a,t)R_{p+N}(a,t) \\
&- ((1-\delta(a-14))R_{p+N}(a,t) - (1-\delta(a))R_{p+N}(a-1,t))/\tau \\
&+ (1-\delta(a))\Delta_N(a,t)R_{p+N}(a,t)/N(a,t)
\end{aligned} \tag{2.12}$$

$$\begin{aligned}
\dot{R}_{p-N}(a,t) &= \nu D_{p-}(a,t) - r_N R_{p-N}(a,t) - p(a)q\lambda(a,t)R_{p-N}(a,t) \\
&- ((1-\delta(a-14))R_{p-N}(a,t) - (1-\delta(a))R_{p-N}(a-1,t))/\tau \\
&+ (1-\delta(a))\Delta_N(a,t)R_{p-N}(a,t)/N(a,t)
\end{aligned} \tag{2.13}$$

$$\begin{aligned}
\dot{R}_{npN}(a,t) &= \nu D_{np}(a,t) - r_N R_{npN}(a,t) - p(a)q\lambda(a,t)R_{npN}(a,t) \\
&- ((1-\delta(a-14))R_{npN}(a,t) - (1-\delta(a))R_{npN}(a-1,t))/\tau \\
&+ (1-\delta(a))\Delta_N(a,t)R_{npN}(a,t)/N(a,t)
\end{aligned} \tag{2.14}$$

$$\begin{aligned}
\dot{R}_{p+S}(a,t) &= \Psi(1-f_D^{p+}-f_F^{p+}-f_\mu^{p+})T_{p+}(a,t) - r_S R_{p+S}(a,t) - p(a)q\lambda(a,t)R_{p+S}(a,t) \\
&- ((1-\delta(a-14))R_{p+S}(a,t) - (1-\delta(a))R_{p+S}(a-1,t))/\tau \\
&+ (1-\delta(a))\Delta_N(a,t)R_{p+S}(a,t)/N(a,t)
\end{aligned} \tag{2.15}$$

$$\begin{aligned}
\dot{R}_{p-S}(a,t) &= \Psi(1-f_D^{p-}-f_F^{p-}-f_\mu^{p-})T_{p-}(a,t) - r_S R_{p-S}(a,t) - p(a)q\lambda(a,t)R_{p-S}(a,t) \\
&- ((1-\delta(a-14))R_{p-S}(a,t) - (1-\delta(a))R_{p-S}(a-1,t))/\tau \\
&+ (1-\delta(a))\Delta_N(a,t)R_{p-S}(a,t)/N(a,t)
\end{aligned} \tag{2.16}$$

$$\begin{aligned}
\dot{R}_{npS}(a,t) &= \Psi(1-f_D^{p-}-f_F^{p-}-f_\mu^{p-})T_{np}(a,t) - r_S R_{npS}(a,t) - p(a)q\lambda(a,t)R_{npS}(a,t) \\
&- ((1-\delta(a-14))R_{npS}(a,t) - (1-\delta(a))R_{npS}(a-1,t))/\tau \\
&+ (1-\delta(a))\Delta_N(a,t)R_{npS}(a,t)/N(a,t)
\end{aligned} \tag{2.17}$$

$$\begin{aligned}
\dot{R}_{p+D}(a,t) &= \Psi f_D^{p+}T_{p+}(a,t) - r_D R_{p+D}(a,t) - p(a)q\lambda(a,t)R_{p+D}(a,t) \\
&- ((1-\delta(a-14))R_{p+D}(a,t) - (1-\delta(a))R_{p+D}(a-1,t))/\tau \\
&+ (1-\delta(a))\Delta_N(a,t)R_{p+D}(a,t)/N(a,t)
\end{aligned} \tag{2.18}$$

$$\begin{aligned}
\dot{R}_{p-D}(a,t) &= \Psi f_D^{p-}T_{p-}(a,t) - r_D R_{p-D}(a,t) - p(a)q\lambda(a,t)R_{p-D}(a,t) \\
&- ((1-\delta(a-14))R_{p-D}(a,t) - (1-\delta(a))R_{p-D}(a-1,t))/\tau \\
&+ (1-\delta(a))\Delta_N(a,t)R_{p-D}(a,t)/N(a,t)
\end{aligned} \tag{2.19}$$

$$\begin{aligned}
\dot{R}_{npD}(a,t) &= \Psi f_D^{p-}T_{np}(a,t) - r_D R_{npD}(a,t) - p(a)q\lambda(a,t)R_{npD}(a,t) \\
&- ((1-\delta(a-14))R_{npD}(a,t) - (1-\delta(a))R_{npD}(a-1,t))/\tau \\
&+ (1-\delta(a))\Delta_N(a,t)R_{npD}(a,t)/N(a,t)
\end{aligned} \tag{2.20}$$

where $\delta(a)$ stands for the Dirac delta function ($\delta(x=0)=1$ and $\delta(x\neq 0)=0$). There are three quantities that depend on time: the force of infection $\lambda(a,t)$, the diagnosis rate $d(t)$ and the correction terms $\Delta_N(a,t)$, standing for any demographic variation in the population due to causes foreign to TB and ageing. The values and definitions of all parameters appearing in the equations are included in Table 2.1.

The temporal evolution of the system is computed by solving those ODE using the Runge-Kutta 4th order algorithm, coded in C. Using this method, we solve for each age group, in a synchronous way. It is important to notice that, here, the whole 19 ODE's are solved, for each age-group, at the same time. This ODE's are also coupled between age groups according to age, as typically, the spanning time of a TB spreading simulation is large enough to force the inclusion of ageing dynamics and demographic evolution, which will be explained later on in this section.

2.1.3 Literature-based epidemiological parameters.

Table 2.1 shows a summary of the model parameters used in the ODE system governing the evolution of individuals within the TB natural history, and that are based on the literature, i.e., fixed and not calibrated. The table provides a brief description of each

parameter and its assigned value.

Meaning	**Par.**	**Value**	**C.I.**	**Ref.**
Probability of fast progression	$p(a)$	$(a=0)$ 0.187	(0.1474,0.2333)	[146, 135]
		$(a=1)$ 0.0225	(0.0200,0.0250)	
		$(a>1)$ 0.15	(0.10,0.20)	
Rate of fast progression (y^{-1})	ω_f	0.900	(0.765,1.035)	[144]
Rate of slow progression (y^{-1})	ω_s	7.500×10^{-4}	$(6.375,8.625)\times10^{-4}$	[144]
Probability of developing pulmonary smear-positive disease	$\rho_{p+}(a)$	$(a<3)$ 0.100	(0.085,0.115)	[144]
		$(a\geq3)$ 0.500	(0.425,0.575)	
Probability of developing non-pulmonary disease	$\rho_{np}(a)$	$(a<3)$ 0.250	(0.2125,0.2875)	[144]
		$(a\geq3)$ 0.100	(0.085,0.115)	
Mortality rate by pulmonary smear positive TB (y^{-1})	μ_{p+}	0.250	(0.213,0.288)	[144]
Mortality rate by pulmonary smear negative TB (y^{-1})	μ_{p-}	0.100	(0.085,0.115)	[144]
Mortality rate by non-pulmonary TB (y^{-1})	μ_{np}	0.100	(0.085,0.115)	[144]
Reduction of infection risk for previously infected individuals	q	0.650	(0.553,748)	[144]
Treatment completion rate (y^{-1})	Ψ	2.00	(1.70,2.30)	[144]
Smear progression rate (y^{-1})	θ	0.015	(0.007,0.020)	[147]
Relapse rate for individuals who successfully completed treatment (y^{-1})	r_S	9.392×10^{-4}	$(6.364,12.450)\times10^{-4}$	[145, 135]
Relapse rate for individuals who defaulted treatment (y^{-1})	r_D	3.774×10^{-3}	$(1.354,8.620)\times10^{-3}$	[145, 148, 135]
Relapse rate for naturally recovered individuals (y^{-1})	r_N	0.030	(0.020,0.040)	[147]
Natural recovery rate (y^{-1})	ν	0.100	(0.085,0.115)	[147]
Infectiousness reduction coefficient of D_{p-} with respect to D_{p+}	ϕ_{p-}	0.250	(0.213,0.288)	[144]
Infectiousness reduction coefficient of R_{p+D} with respect to D_{p+}	ϕ_D	0.500	(0.250,0.750)	[147]
Proportion of mothers that infect their newborn children	m_c	0.15	(0.10,0.20)	[149]

Table 2.1: Bibliography-based epidemiological parameters used in this thesis.

The probabilities of individuals to end their treatment according the four categories defined by the WHO (success, default, failure or death), defined as:

- $(f_D^{p+}, f_F^{p+}, f_\mu^{p+})$: fraction of default, failure and death outcomes for smear positive pulmonary TB.
- $(f_D^{p-}, f_F^{p-}, f_\mu^{p-})$: fraction of default, failure and death outcomes for smear negative pulmonary and non pulmonary TB.

have been obtained from the WHO Treatment Outcomes database for each country. As for each kind of TB the sum of the 4 treatment outcome probabilities must be equal to 1, it is enough to model just 3 parameters, as the fourth is obtained from the closure relationship.

Population dynamics across age strata: individuals' ageing and demographic evolution.

Our spreading model includes the simultaneous description of the disease dynamics across all age groups in an entire population, using parameters that are, in general, dependent on age. Therefore, it is not enough to describe how the sub-populations associated with the disease states evolve inside each age group, but we also needs to include ageing dynamics that couples the different groups. Moreover, as the span of time that is typically simulated in the thesis is of the order of decades, the demography is expected to change, so it is not enough to describe the ageing but we also need to model this effect.

As stated, the ageing dynamics makes individuals transit across the different age strata as they get older. The model divides the population in 15 different age groups, each one comprising an age interval of $\Delta_t = 5$, except for the last one that includes all individuals older than 70 years. Then, to introduce the ageing dynamics, we need to account for the progression of certain individuals over time from their age group, a, to the following one, $a + 1$. This is by coupling each age strata with a transition defined by:

- ageing of individuals belonging to class $X(a, t)$, transition from $X(a, t)$ to $X(a + 1, t)$: $X(a, t)/\Delta_t$ individuals/unit time.

In those transitions, a fraction $X(a, t)/\Delta_t$ of the individuals in the original group leaves it per unit of time and moves to the $X(a+1, t)$ age group. This is replicated in all age groups except for $X(0, t)$, that receives newborns instead of ageing individuals, and for the last one, $X(14, t)$, for which no further ageing occurs as it already encompasses

all individuals older than 70 years. In any other group, the class $X(a,t)$ receives people from $X(a-1,t)$ and sends out people to $X(a+1,t)$. Next, to account for the evolution of the demographic structure, we need to act over the set of variables defined as:

$$\begin{aligned} N(a,t) = S(a,t) + L_f(a,t) + L_s(a,t) + D_{p+}(a,t) + D_{p-}(a,t) + D_{np}(a,t) + F(a,t) \\ +T_{p+}(a,t) + T_{p-}(a,t) + T_{np}(a,t) + R_{p+N}(a,t) + R_{p-N}(a,t) + R_{npN}(a,t) \\ +R_{p+S}(a,t) + R_{p-S}(a,t) + R_{npS}(a,t) + R_{p+D}(a,t) + R_{p-D}(a,t) + R_{npD}(a,t) \end{aligned} \tag{2.21}$$

where the evolution of $N(a,t)$ -in addition to ageing and death by TB– is subject to other driving forces like births and non-TB deaths, as well as migrations. Our approach to take all this factors into consideration is based on assuming that the temporal evolution of the variables $N(a,t)$ follows the predictions of the United Nations Population Division, available at its on-line databases: $N(a,t) = N_{UN}(a,t)$.[150]

To follow these predictions, we introduce continuous correction terms $\Delta_N(a,t)$ that are added or subtracted from the population within the age stratum a at time t while the simulation unfolds. These terms are calculated dynamically to make the time evolution of the demographic pyramid match the demographic forecasts reported in the United Nations population division database until the end of the simulation. From the UN database, we can trivially fit the projections for each age group to a continuous function $N_{UN}(a,t)$, from which we can derive an analytical derivative $\dot{N}_{UN}(a,t)$ at any moment. In this thesis, a polynomial of degree 10 is used for building that continuous function from the annual data series during the period under study, which does not span more than 2050 in any of the chapters that comprise this thesis.

Taking into account the variation of the population due to TB and ageing in each age group $\dot{N}_o(a,t)$, we can extend this definition by introducing the term $\Delta_N(a,t)$, that forces the total temporal evolution of $N(a,t)$ to follow the function $N_{UN}(a,t)$. This is achieved by defining, at each time step:

$$\Delta_N(a,t) = \dot{N}_{UN}(a,t) - \dot{N}_o(a,t) \tag{2.22}$$

The introduction of those correction terms in the dynamics imposes that:

$$\dot{N}(a,t) = \dot{N}_o(a,t) + \Delta_N(a,t) = \dot{N}_{UN}(a,t) \tag{2.23}$$

which corresponds to the correct behaviour for the demographic structure, i.e., $N(a,t) = N_{UN}(a,t)\ \forall(a,t)$. The computed $\Delta_N(a,t)$ correction terms have to be introduced into the different dynamical states within the same age class preserving their proportions, for all groups with $a > 0$:

$$\Delta_X(a,t) = \Delta_N(a,t)\frac{X(a,t)}{N(a,t)}\ \forall a > 0 \tag{2.24}$$

This way, the correction terms $\Delta_N(a,t)$ are distributed among all disease states proportionally to their relative size. These terms represent changes in the population of each stratum that are unrelated to the dynamics of the disease (TB unrelated mortality and migratory fluxes).

However, this distribution of the correction is debatable in the first age group, $a = 0$, as there, the birth of new individuals is the main cause of population variation. For simplicity, $\Delta_N(a = 0, t)$ is directly associated with the number of newborns, but those individuals are only introduced in the S, L_s, and L_f states. This reflects the fact that a fraction m_c of women who are pregnant and infected can transmit the disease to their children within the first weeks of their lives[149]. The density of infected newborns depends then on the fraction of mothers who have the disease and can transmit it at time step t, considering that women's fertility lies between 15 and 40 years old.

In Figure 2.2 we schematise this phenomenon as the transitions between age strata inside each pyramid and the change in the shape of the demographic pyramid with time. In summary, demographic pyramids in Supplementary Figure 2.2 evolve with

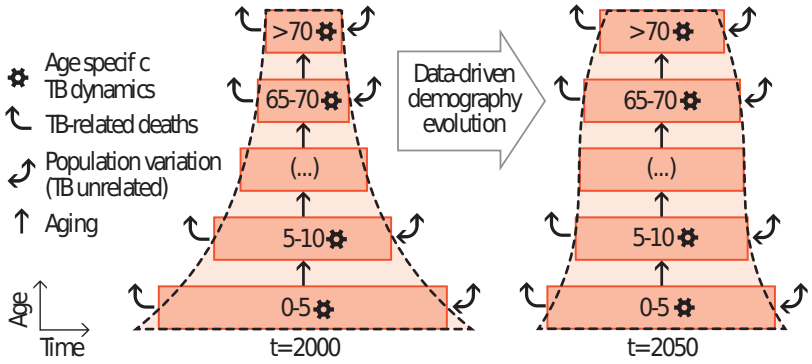

Figure 2.2: Scheme of the coupling between TB dynamics and demographic evolution. The transmission model summarised in A describes the evolution of the disease in each age group, including the removal of individuals due to TB mortality (curved arrows). The evolution of the total volume of each age stratum is corrected (bidirectional arrows: TB-unrelated population variations) to make the demographic pyramid evolve according to UN prospects.

time in such a way that individuals transit inside the pyramid as they age, but also we update the whole population in a data-driven way. That is, we update the number of individuals inside each age stratum according to the prospects of the UN population division, where the correction terms $\Delta_N(a,t)$ are used for this purpose. This assures that both the ageing and the demographic prospects are included in the model, capturing the evolution of the population.

2.1.4 Contact matrices

Contact matrices are mathematical representations of the patterns of contacts between different age groups in a given population. These matrices provide crucial insights into how infectious diseases spread within an age-structured population, as they capture how and with whom the individuals interact, i.e., the likelihood and frequency of interactions between individuals. Contact matrices are based on empirical data collected through surveys, contact tracing studies, or social network analysis.

In this thesis, we use country-wise matrices, denoted as $\xi_c(a, a', t)$. The matrix elements capture the relative contact frequency that an individual of age a has with individuals of age a' at time t, with respect to the overall average of contacts that an individual has per unit time with anyone else. For building the contact matrices used in the model, we have integrated data from different survey studies conducted in several countries. In the case of African countries we combine surveys in Kenya [151], Zimbabwe [152], Uganda [153] and Malawi [154] to obtain a unique matrix broadly representative of contact structures in Africa, as described in [135, 136]. For countries in Asia we combine surveys conducted in China [155], Japan [156], and India [157] to get a matrix usable in the Asian region. The results presented in this thesis make use of those matrices, but the addition of the data from India and Malawi was introduced before the results in[158] were published. This is the reason why the results in Chapter 5 are slightly different in the thesis when compared with the original paper, as the underlying contact matrix used is different, for the matrix used in the thesis integrates more data.

Importantly, we also take into account that, as the demographic structure of the population changes, the contact patterns change too [136], being this the origin of the dependence over time we found in matrices. This is because contact structures among age groups are conditioned not only by cultural and socio-economic differences between countries but also by the underlying demographies of the populations under analysis.

In what follows, we will describe how to build the proper regional matrices. As a first processing step, contact matrices reported in each study are adapted to the age structure of 15 age groups, giving a set of $\xi_s(a, a')$ matrices, where s is the index of each study. The matrices $\xi_s(a, a')$ originally capture the number of contacts that an individual in group a reports towards individuals in group a', during a survey, and per unit of time., The matrices $\xi_s(a, a')$ are not expected to be symmetrical. That is, they could be symmetrical only for a perfectly rectangular demographic pyramid where each age group has the same population, which is not the case here. Nevertheless. they should fulfil the following relationship:

$$\xi_s(a,a')N_s(a) \simeq \xi_s(a',a)N_s(a') \tag{2.25}$$

where $N_s(a)$ is the population of age a in the country s when the survey took place. Since the individuals in each group are not expected to report the same number of contacts, the next step in the computation of the contact matrices is recovering the symmetry exactly, transforming the matrices $\xi_s(a,a')$ as:

$$\xi_s^{\text{sim.}}(a,a') = \frac{1}{N_s(a)} \frac{\xi_c(a,a')N_s(a)n_s(a) + \xi_s(a',a)N_s(a')n_s(a')}{n_s(a) + n_s(a')} \tag{2.26}$$

where $n_s(a)$ is the number of participants of age a recruited for the study s, and $N_s(a)$ the number of individuals of age a in the population of the country s. The total number of contacts between age groups a and a' is an average of the number of contacts that emanates from the reports of both age groups, weighted according to the number of participants in each group. Now, the matrices $\xi_s^{\text{sim.}}(a,a')$ are compatible with the symmetry of Equation 2.25. Then, to enable comparison between studies, we normalise the matrices imposing that the average number of contacts per unit time of an individual (also defined as mean degree) equals 1, regardless of her age or that of her contacts. This way the matrices $\xi_s^{\text{sim.,norm.}}(a,a')$ capture the relative intensity of contacts between age groups a and a' instead of the absolute frequency.

Up to this point, we have normalised and "symmetry-compatible" matrices for each country, but that are representative of the contact patterns only in this specific setting and whenever the demography does not change much. For dealing with this, and obtaining matrices that could be used in this model, i.e., matrices that are suitable for forecasting several decades into the future, we need to take additional steps. First, the matrices $\xi_s^{\text{sim.,norm.}}(a,a')$ could be interpreted as the product of two nuisance factors: the fraction of individuals in a' that exist in the population: $\frac{N_s(a')}{N_{reg}}$, and an auxiliary matrix $\pi_s(a,a')$. The matrix $\pi_s(a,a')$, captures the contact structure of each country s in a rectangular demography, thus, removing the effect of the demography. Those matrices $\pi_s(a,a')$ are obtained as follows:

$$\pi_s(a,a') = \xi_s^{\text{sim.,norm.}}(a,a')\frac{N_s}{N_s(a')} \tag{2.27}$$

where $N_s = \sum_a N_s(a)$. Now, we perform a weighted sum per continent (using the total number of participants in each study as weights) to obtain regional matrices denoted as $\pi_{reg}(a,a')$. We then use the dispersion between studies to define the uncertainty associated with the contact patterns at the intrinsic level. All this procedure means that we have computed an intrinsic regional connectivity matrix that is broadly representative of the contact structures in the African region, or in the Asian region,

and that could be further adapted to any country in those regions via the demography. This is done as follows:

$$\tilde{\xi}_c(a, a', t) = \pi_{reg}(a, a')\frac{N_c(a', t)}{N_c(t)} \tag{2.28}$$

where $N_c(a', t)$ shows dependency over time, as we are dealing with an evolving demography. With this previous approach, we can retrieve a usable contact matrix for a country at any given time, proving that we have demographic data. As a final step, we ensure that the matrices have an average connectivity equal to 1 at every moment, meaning that their entry (a, a') always represents the relative frequency at which individuals of age-group a contact those in age-group a', compared to the overall contact frequency of any individual of the system with anyone else:

$$\xi_c(a, a', t) = \frac{\tilde{\xi}_c(a, a', t)}{< \tilde{k}_c(t) >} = \frac{\pi_{reg}(a, a')N_c(a', t)N_c(t)}{\sum_{a,a'} \pi_{reg}(a, a')N_c(a', t)N_c(a, t)} \tag{2.29}$$

If this is not done, the evolution of the contact structure can produce average connectivities that depart strongly from its initial value. Although considering an evolution of the mean connectivity as demography changes might be reasonable, for some purposes like comparison between infectiousness, which depends upon the contact matrices, could be difficult, and that's something that could be addressed with just this correction.

It is important to notice that, even if we have described here the full procedure to obtain a regional matrix based on an averaged intrinsic connectivity matrix, one does not always follow those steps exactly to get a usable contact matrix. For instance, we have data from studies conducted on Kenya and China separately[151, 155]. If a simulation must be carried out in those countries, it is possible to build just the intrinsic connectivity matrix $\pi_s(a, a')$ of this specific country and work directly with those, as this would be a more exact approach with data coming only from that specific setting, that could be adapted to the evolving demography of the country in the same way as we did with the regional matrices.

2.1.5 Calibration procedure: diagnosis and force of infection and initial conditions

This model is data-driven, and makes use of the past burden of TB to calibrate some parameters that will lead the temporal evolution of the disease. The calibration procedure implies the estimation of 5 parameters per country, which are the initial conditions of the system, represented by the ς parameter, along with the diagnosis rate $d(t)$ and the scaled infectiousness $\beta(t)$, both defined by half-sigmoids dependent upon

2 parameters each. Then, by calibrating those parameters, the goal is to make the model reproduce the TB burden mortality and incidence rates reported by the WHO from $t_o = 2000$ to the end of the training period. This procedure needs to be done for each country in which a simulation is going to be performed, as the training data is country-specific. In the following lines we will explain the calibration procedure and how the initial conditions are derived.

First, regarding initial conditions, this model do not impose that the system must be at stationarity at $t = 0$, unlike previous approaches[147, 144]. A stationary state is reached after freezing the temporal evolution of the time dependent parameters, so they equal their values at the beginning of the training period $t = t_o$. This imposes that $d(t = 0) = d_0$ and $\beta(t = 0) = \beta_0$, and it also imposes that the demographic boundary conditions must be $N(a, t) = N(a, 0)$, where $N(a, t)$. Let us name those stationary levels as $\vec{X}^*(a, d_0, \beta_0, N(a, 0))$,

Instead of directly setting the initial conditions using the stationary levels, we take an alternative approach. First, we calculate the stationary values of all states $\vec{X}^*(a, d_0, \beta_0, \vec{N}(a, 0))$, and then we set up an initial state that can correspond either to higher or lower levels of disease prevalence with respect to the stationary state, via the the ς parameter. In order to map the possible deviations from the stationary levels, we distinguish the unexposed state, $S(a, t)$, from the rest of the states of the natural history, $X(a, t = 0)$, which are comprised by individuals infected with the bacillus at least once. Then, we impose that $\varsigma \in [-1, 1]$. This causes that when $\varsigma < 0$, the initial conditions correspond to a state with lower TB burden than that in the stationary state:

$$S(a, t = 0) = S^*(a, d_0, \beta_0, \vec{N}(a, 0)) \left(1 - \varsigma \textstyle\sum_{X \neq S} X^*(a, d_0, \beta_0, \vec{N}(a, 0))\right) \quad (2.30)$$

$$X(a, t = 0) = (1 + \varsigma) X^*(a, d_0, \beta_0, \vec{N}(a, 0)) \quad (2.31)$$

If the opposite happens, and $\varsigma > 0$, the initial conditions are set to higher burden levels:

$$S(a, t = 0) = S^*(a, d_0, \beta_0, \vec{N}(a, 0))(1 - \varsigma) \quad (2.32)$$

$$X(a, t = 0) = X^*(a, d_0, \beta_0, \vec{N}(a, 0)) \left(1 + \varsigma \frac{S^*(a, d_0, \beta_0, \vec{N}(a, 0))}{\sum_{X \neq S} X^*(a, d_0, \beta_0, \vec{N}(a, 0))}\right) \quad (2.33)$$

Taking it to their extreme values, $\varsigma = -1$ would mean that every individual is at the susceptible state (pathogen-free situation) while $\varsigma = 1$ would mean that all the population is infected with the bacterium.

Second, regarding the diagnosis rate and scaled infectiousness, they are defined by the half -sigmoid-like curves $d(t)$ and $\beta(t)$, as follows:

$$d(t) = \begin{cases} d_0 + (d_{\text{sup}} - d_0)t(t + \frac{1}{d_1})^{-1} & \text{if } d_1 > 0 \\ d_0 & \text{if } d_1 = 0 \\ d_0 - d_0 t(t - \frac{1}{d_1})^{-1} & \text{if } d_1 < 0 \end{cases} \tag{2.34}$$

$$\beta(t) = \begin{cases} \beta_0 + \beta_0 t\left(t + \frac{1}{\beta_1}\right)^{-1} & \beta_1 > 0 \\ \beta_0 & \beta_1 = 0 \\ \beta_0 - \beta_0 t\left(t - \frac{1}{\beta_1}\right)^{-1} & \beta_1 < 0 \end{cases} \tag{2.35}$$

The diagnosis rate and the scaled infectiousness are curves parameterised by two quantities, d_0, d_1 and β_0, β_1. The quantities d_0 and β_0 capture their values at the beginning of the training period, and the other pair, d_1 and β_1, define their temporal evolution. They could evolve either increasing or decreasing with time, which depends on the sign of d_1 and β_1. Both the diagnosis rate and the scaled infectiousness are bounded to be greater than zero. Upper bounds for those quantities are $2 \times \beta_0$ for the scaled infectiousness and $d_{\text{sup}} = 12.17y^{-1}$ for the diagnosis rate. The first bound means that TB infectiousness is not expected to vary much in a span of decades, given the prevalent state in which it is found today. The latter upper bound corresponds to a minimum diagnosis period of one month. Since the main symptom of TB is a continuous cough during three weeks, and there is a diagnostic process which is estimated to last, in a conservative way, at least 10 days[159], we consider this a reasonable bound.

As stated before, the goal of the whole calibration procedure is to capture the temporal evolution given by the WHO data. To do this, we impose the minimisation of the overall error H of the model outcome with respect to the WHO burden data on incidence and mortality rates aggregated across all ages. The error is calculated as follows:

$$H = \sum_{t=t_o}^{t_F} \left(\left(\frac{i(t) - \bar{i}(t)}{\langle \bar{i}(t) \rangle} \right)^2 + \left(\frac{m(t) - \bar{m}(t)}{\langle \bar{m}(t) \rangle} \right)^2 \right) \tag{2.36}$$

where $\bar{i}(t)$ and $\bar{m}(t)$ stand for the annual incidence and mortality rates, corresponding to the national estimations available at the WHO database for TB, and $\langle \bar{i}(t) \rangle$ and $\langle \bar{m}(t) \rangle$ correspond to the averages of incidence and mortality reported by the WHO for the entire training period in each country.

Then, the model could be fitted to reproduce the past data through the iterative evaluation of the model based burden outcome while navigating across the parameter space defined by $(\varsigma, d_0, \beta_0, d_1, \beta_1)$. This parameter space needs to be explored in such a way that minimises the error. For such a task, we use a Levenberg-Marquardt algorithm to solve the multidimensional optimisation problem. In the original model, this was

implemented in C codes, but in the adapted version of the model used in this thesis this procedure has been improved. First, only the core of the code, which solves the evolution of the diseases and all dynamic states is coded in C, while the fitting procedure has been ported to R language through an interface between languages. This way, we can take advantage of the better implementation of the optimisation algorithm in the *minpack.lm* package[160] to improve the model compatibility across operating systems. This also gives better results specially in very ill setups where the temporal series are difficult to fit, as the R version of the algorithm generally finds better sets of values.

2.1.6 Model uncertainty

The uncertainty sources that are propagated to the model outcomes are summarised here:

- Parameters associated with the Natural History of the disease are treated as totally independent uncertainty sources.
- Uncertainties in TB burden estimations provided by the WHO. Based upon a number of case notifications surveilled in each country, the World Health Organization provides estimations for incidence and mortality rates for the countries under analysis, which feature significant uncertainty bands which we propagate to our model outcomes.
- Demographic structures, which are considered as a single uncertainty source. Those demographic structures are reported in the form of demographic pyramids with 15 age groups, first 14 from 0y to 70y each 5y and the last one comprises 70+y. Each group has its own uncertainty, but said uncertainty levels are not independent among them, which we take into account in our analyses.
- Contact matrices, whose uncertainty comes from the variability between studies used for building regional contact matrices.

Those uncertainty sources are managed independently and their contributions to the uncertainty of a certain model outcome x are to be evaluated. On the original version of the model[135] the uncertainty of an outcome was translated by doing a sensibility analysis that accounts for the variation produced in the outcome when the median value of an uncertainty source is changed by its extreme values and the uncertainty is built by grouping individual sensitivities according to the type of input data for building credibility intervals and significance levels for the outcome.

Along this thesis, this procedure is deprecated and has changed radically, as the old procedure was conservative in the sense that for each uncertainty source the worst-case

scenario was assumed *always*, which is not always a realistic approach to spreading. This approach is replaced, and a probabilistic procedure is implemented. The process performed in the new version of the model is described here:

1. Generate a set of **N** new values of the uncertainty sources taking into account the original value and its confidence interval. The generation of new values is not trivial as we cannot treat all the uncertainty sources in the same way. Further details of the generation procedure are explained in the next section.

2. Calibrate the model for each new set of parameters.

3. Run the model for each new set of parameters, thus obtaining a set of N values for a certain outcome.

4. The outcome is obtained as the median value and the credibility interval (CI) that the 95% quantile of the set of model outcomes produces.

Considered these independent uncertainty sources, we propagate them to our model outcomes by generating a set of possible modelling runs where each escalar (i.e. one-dimensional) parameter is independently sampled from a distribution informed by its confidence intervals. In what regards multi-dimensional inputs -that is, TB incidence and mortality series from WHO data, demographic pyramids and contact matrices, the eventual co-dependence of their elements is treated differently in each case, and each case is described in the following section.

2.1.7 Generation of new values for the uncertainty sources

In general, we assume that the reported confidence intervals of each value can be interpreted as coming from a normal distribution, thus being the reported value the mean and building the standard deviation from the CI, so we have $p_i \sim \mathcal{N}(\mu, \sigma)$.

This allows us to generate random numbers under those normal distributions that serve as our new value for the uncertainty source, but caution is needed, as there are several points we must consider. First, some parameters that belong to the interval $\in [0, \infty)$, so their normal distribution must be renormalised in such a way that all the probability lies within the $[0, \infty)$ interval. Other parameters represent probabilities, so not only do they lie in the interval $[0, 1]$ but also are bound to some other parameters. As an example, if we take the treatment success probability and calculate a new value that is higher than the original, then the probability of not succeeding must decrease accordingly. Here, the random number generation procedure trusts in R, as we use the random number generators included in the base package (R 3.4.4).

Uncertainty in contact matrices is estimated from the heterogeneity in the reported results of the different studies used to obtain the aggregated matrices used here. In the case of African countries we combine surveys in Kenya [151], Zimbabwe [152], Uganda [153], and Malawi [154] to obtain a unique matrix broadly representative of contact structures in Africa, as described previously in this text, and also in[135, 136]. For countries in Asia we use surveys conducted in China [155], Japan [156] and India [157] that are combined to get a matrix usable in the Asian region. In this case, the confidence intervals of each field in the matrices are given, and matrices are re-sampled according to them, assuming that matrix fields (corresponding to the results of the surveys on different sub-populations) are mutually independent. To sample a new value from the matrix, and as reported CI might be asymmetrical, we model each field as an asymmetric Gaussian, whose median is the mean reported value for each field, and with two different arms according to the CI. As the number of contacts or the contact rate must lie within the interval $\in [0, \infty)$, they cannot be negative. Then, considering this constraint, a Z-score value is generated from a normal Gaussian distribution, that is used for generating a new value in the asymmetric Gaussian. Given the previous constraint, the values are restricted to lie within the original bounds of the CI.

Moving to the TB burden, two magnitudes need to be addressed: incidence and mortality per million population from the year 2000 to the end of the training period. As our model calibrates both the infection force and the diagnosis rate based on this data, we can modify incidence and mortality separately. Nevertheless, values inside each block must be changed in the same way, so if the new incidence in the year 2000 is higher than the original, then all the incidence values of the other years must be higher than their previous values too, as we are moving towards a high incidence setting.

To capture the co-dependence of the methods used by the WHO to produce the estimates of TB incidence and mortality rates that we use in our model forecasts, we re-sample alternative burden scenarios by drawing numbers from a standard normal distribution, which are later scaled to generate the corresponding incidence i of mortality m series, in each realisation, as follows:

$$i^j_{\text{new}} = i^j_{\text{orig}} + Z \cdot \sigma^j \tag{2.37}$$

$$m^j_{\text{new}} = m^j_{\text{orig}} + Z \cdot \sigma^j_m \tag{2.38}$$

where σ^j_i and σ^j_m are the standard deviations of the incidence and mortality levels, respectively, that are associated with the 95% confidence intervals reported by the WHO at the j-th year.

Then, in order to model uncertainty coming from demographic data, we decided to sample alternative demographic pyramids where random, normally distributed noise

is considered in the proportion of younger vs older individuals, distributed across age strata in a linear way. To do so, in each iteration we draw a single Z score from a standard normal distribution, and generate a new base of the demographic pyramid, $n(a=1)_{\text{new}}$, as follows:

$$n(a=1)_{\text{new}} = n(a=1)_{\text{orig}} + Z \cdot \sigma(a=1) \tag{2.39}$$

Once this is done, we modify the rest of the age groups from the base to the top of the pyramid using age-dependent Z-scores $Z(a)$ that are re-scaled linearly to ensure that, while $Z(1) = Z$, the final $Z(15) = -Z$. This ensures that the individuals added, or removed, at the younger strata are compensated by statistically analogous deviation, in the opposite direction, in the older strata, by applying the following rule:

$$Z(a, Z') = M(Z') \cdot a + K(Z') \tag{2.40}$$

where $M(Z') = -\frac{1}{7}Z'$ and $K(Z') = \frac{8}{7}Z'$. This assures that $Z(1) = Z'$ and $Z(15) = -Z'$, which implies that the excess or lack of population in the base groups balance out by the contrary effect in the top of the pyramid, preserving the total population. Consequently, the new value for any group is given by:

$$n(a)_{\text{new}} = n(a)_{\text{orig}} + Z(a, Z') \cdot \sigma(a) \tag{2.41}$$

This sampling procedure is repeated for all parameters and sources of uncertainty a number $N = 500$ times, after each of which, the model is re-calibrated, the vaccine simulated and the impact forecast registered. Confidence intervals of the final forecast are taken from the obtained distribution.

2.2 Plugging vaccines into the model: the lack of consensus

In chapters 3 and 4, the TB spreading model is used, among others, to compute the impact on the TB burden as a consequence of the introduction of a new TB vaccine in the year 2025. To this end, we make use of two sets of two model runs.

In the first run, the values of all the epidemiological parameters are stochastically drawn from their distribution, as explained in the previous section to propagate the uncertainty. With these parameters, the model is calibrated and the TB burden is computed in a non-vaccine scenario, which we name from now the control run. For this same calibration, the model is run once again but simulating the introduction of the vaccine in 2025, which from now we name the vaccine run. In this second run, the natural history of vaccinated individuals is modified according to the interplay between

the vaccine and the disease. This second run has two separate branches that evolve at the same time. Branch 1 is the normal evolution of the individuals, as done in the control run, whereas Branch 2 is where the protected individuals are moved when vaccinated, and has the modified version of the natural history. This way, we can track at the same time all individuals even if they do not share the same epidemic risks.

Finally, with all those elements together, the impact of the vaccine is estimated by comparing the desired outcome (incidence, mortality, IRR, number of cases, reactivations, etc) in the control run with these in the vaccine run. This procedure is repeated $N = 500$ times, to obtain a distribution of estimated for the vaccine impact, from which the median value along with its CI is computed.

Moving specifically to how to perform this kind of analysis, we need to remark that several factors need to be considered to properly model the vaccine, and to reduce the bias in the forecasts. Those are:

- **The description of the vaccine**: when plugging a vaccine into a spreading model, it is necessary to know which is the interaction between the vaccine and the disease, which in the model is captured in how it is modified the natural history of the disease in the vaccinated individuals. For instance, in our model, where the natural history is captured in Figure 2.1, a vaccine conferring protection against infection (PoI) will modify somehow the transitions between S and L_x states for the vaccinated individuals.

- **How the vaccine confers protection**: there are two main paradigms in vaccine modelling in the current literature and plenty of discussion about their usage. Those comprise how vaccines are referred to and could be classified, being these as all-or-nothing or leaky vaccines. The separation is based on the distribution of the protection across subjects. In leaky vaccines the protection is partial and equal for all vaccinated individuals, whereas in all-or-nothing, the protection is perfect but only unfolds in a fraction of the vaccinated individuals.

- **The target individuals**: when addressing the effect of a vaccine with the model it is necessary to decide whether the vaccine will be introduced in a specific age group and whether the vaccine is designed to protect individuals based on a given state (naive individuals, LTBI, pre-exposed individuals,...). This is because it may be impossible to vaccinate everyone in a population, and there are specific age groups that contribute more towards transmission than others, which are more interesting to vaccinate. Moreover, the vaccines under development are designed to target specific populations with certain characteristics, and to model them this information needs to be preserved.

In a small review exercise, we found that, from 20 different papers that modelled TB vaccines to forecast their impact[161, 162, 139, 140, 141, 163, 164, 165, 166, 167, 138, 168, 137, 169, 170, 171, 172, 173, 174, 143], there were different approaches to deal with the previous factors. First, in the absence of evidence, the modellers often opted for assigning a specific combination of mechanisms to the vaccines without much justification. Only in 3 of them[165, 168, 172], we found an explanation about how the vaccine was introduced into the model, and why it was acting through the mechanisms they proposed. This is not due to the rest of the papers doing poor research, but instead, to the generalised lack of data regarding this particular, which often forces researchers to make unjustified assumptions.

Second, regarding the all-or-nothing vs leaky debate, only 5 of those papers used all-or-nothing descriptions for the vaccine[162, 164, 167, 174, 143], while the rest used leaky ones. Thus, even if the majority of the papers used leaky descriptions, there are still recent works that use an all-or-nothing framework. There is also evidence that the all-or-nothing descriptions provide higher impacts when analysed with spreading models[175], which may be also the root of the literature using the leaky descriptions more often, being more conservative in the absence of empirical evidence for the usage of the alternative description. Nevertheless, the modeller needs to make some assumptions as not much data is available with new TB vaccines in this sense. To understand the difference between the two approaches, first, we need to define each one.

In Figure 2.3 there is a schematic comparison of how all-or-nothing and leaky vaccines work in our spreading model. Let's start with an all-or-nothing vaccine, which is a vaccine typically highly effective at preventing disease in vaccinated individuals and/or transmission of the disease to others, which in the mathematical model, means that the vaccine should confer perfect protection to the vaccinated individuals, halting perfectly any transition between states in which the vaccine may act. However, as the efficacy is not going to be 100%, working in all individuals, the smaller number recorded in efficacy is translated into just a fraction given by that number, among all vaccinated individuals, getting protection from the vaccine. Instead, a leaky vaccine is effective at reducing the severity of disease in vaccinated individuals but does not completely prevent the progression to disease or transmission to others. In terms of the model, this is implemented as a vaccine that modifies the rates at which vaccinated individuals progress to disease, without halting perfectly the transitions, so individuals will still progress but with much less risk. Here, the vaccine is effective in all vaccinated individuals, and the efficacy is linked to the reduction in the progression risk.

In Figure 2.3, in both schemes, a fraction of the target is vaccinated. In the first case, with an all-or-nothing vaccine, only a fraction c of those individuals get protection,

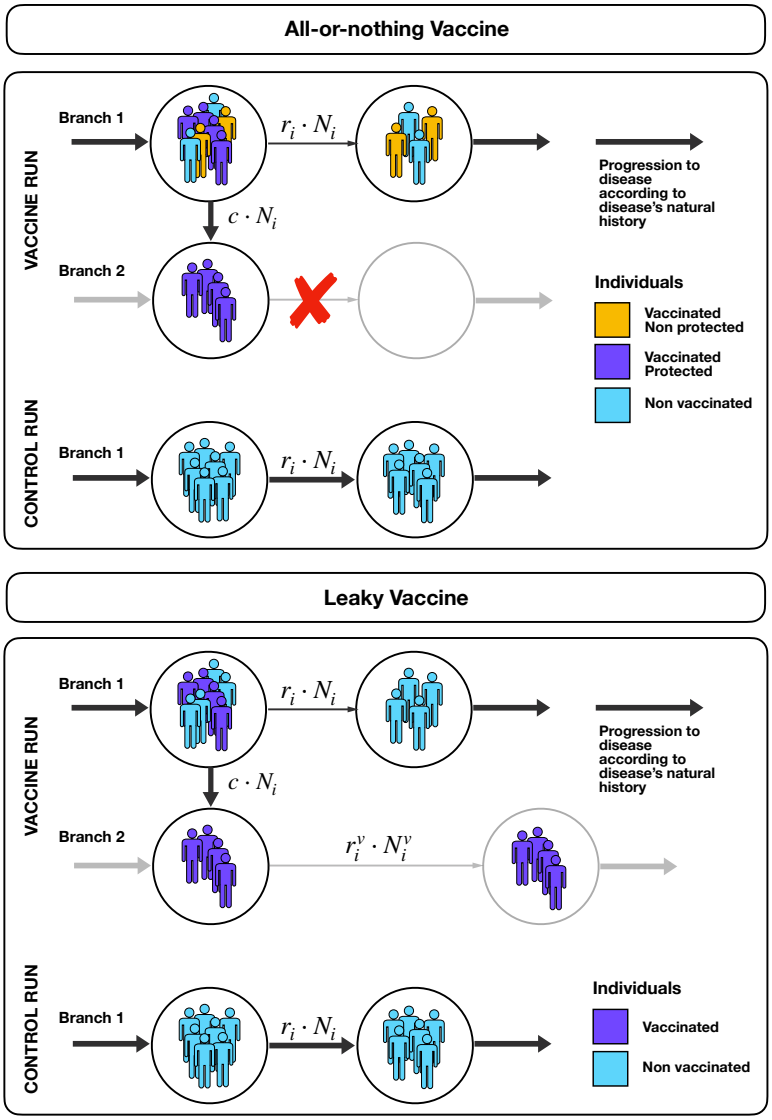

Figure 2.3: Scheme of the interplay between an AoN vaccine and a leaky vaccine with the natural history of TB in our spreading model. In both cases, there are two runs, the control run which comprises the baseline to compare with, and the vaccine run in which the vaccine is implemented. In the vaccine run, we make use of two parallel branches, one for the unvaccinated, or vaccinated but non-protected individuals, and a second branch in which the vaccine alters the progression to disease in some form, in which the vaccinated and protected individuals lie. In the all-or-nothing scheme, from all the vaccinated individuals, only a fraction c of them (the efficacy) get protection, but this protection is perfect. On the other hand, in the leaky vaccine, c captures, again, the efficacy, but this time all vaccinated individuals get protected, at the cost of reducing the overall risk of progression on the parameter r_i^v instead of halting it as in the all-or-nothing case.

but the vaccine perfectly halts progression to disease. In the second case, a fraction c of the population is vaccinated, and all of them are protected to some extent, given by the vaccine efficacy, whose effect is to reduce the risk of progression via r_i^v.

Last, regarding the target, there are also disparities in the literature, but in this case, it is normal since plenty of the vaccines that are currently under development are designed to target specific populations (newborns, adolescents, elders,...). Moreover, it is legit to think that the vaccines won't work equally in populations with different states regarding exposure, as a vaccine designed to stop infection may work fine in naive individuals, but yield a residual impact in pre-exposed individuals. For those reasons, the disparity between studies is normal, and even logical, as shows that in this particular, the TB models usually have the versatility to vaccinate different target populations.

After this review exercise, in the following lines, we are going to explain how we used our spreading model to deal with the previous factors and reduce the bias in impact estimations. Focusing on the description of the vaccine, as we will demonstrate in Chapter 3, it is not easy to capture the mechanistic effect in terms of the interplay the vaccine has with the natural history of the disease if only the efficacy measures of an RCT are taken into account, which also may be on the root of researchers taking one description without much justification. To solve this issue, in this thesis, we developed two methodologies that help distinguish between vaccine descriptions that are compatible with the same RCT results but also are designed to fit our spreading model. This way, we can introduce them into the spreading model using the mechanistic description that has more support from data and produce a more agnostic forecast for the impact of the vaccine. Here, something needs to be noted, as in Chapter 3 we are always working with vaccines that have different values for the intrinsic efficacy -the efficacy parameter that enters into the spreading model- but that is compatible with the efficacy readout that the real vaccine yielded in an RCT. Instead, in Chapter 4, we modelled vaccines with the same intrinsic efficacy -i.e., without having the same efficacy readout in an RCT- but with different mechanistic descriptions, as the vaccines tested there are hypothetical and do not come from real RCTs.

Moving towards how the vaccine works to provide protection, in most of the vaccine-related results of this thesis, the vaccines are being modelled as POD vaccines (designed for pre-exposed individuals without a past of active TB) that work in an all-or-nothing fashion, except for some results in the first methodology presented in Chapter 3. This is a disclaimer that needs to be done, as, in our case, we use generally the all-or-nothing description mainly because we are not trying to estimate quantitatively the impact of just one vaccine but to compare across different vaccination

scenarios, for which the simplicity of the all-or-nothing vaccines works just fine. In this sense, in Chapter 3 we performed two different vaccination exercises, the first one with a leaky description, as the methodology that identifies the mechanistic effect imposes this working mode for the vaccine, and a second one for the second methodology that does not impose this constraint, and that is done with the all-or-nothin description for simplicity, as we do as well in Chapter 4.

Finally, concerning the targeted populations, in Chapter 3, where two vaccines come from two different RCTs (one per methodology), we have performed impact analyses of vaccines showing protection in different populations. In the first case, we targeted naive adolescents or newborns, as the vaccine in the RCT was introduced to individuals who showed negative results on an IGRA test, and without a past of active TB, i.e., susceptible in terms of our model. In the second case, we have targeted adolescents already exposed but without symptoms of active TB, i.e., latent individuals in the model. This was done in this way as adolescents comprised one of the groups recruited in the RCT from which the vaccine came, and the recruited population of this trial was latent without symptoms at the start of the follow-up period. However, in Chapter 4, we opted for a more general approach, and, with a fixed intrinsic efficacy of the vaccine, we explored different mechanistic descriptions, and, in the same philosophy, we targeted different populations (adolescents or elders) and with different epidemic history (naive, pre-exposed with or without a past of active TB, or all together), so the comparison was more complete.

2.3 Some considerations on the statistical methods

The main tool that we use in the thesis is the spreading model of the previous section, but, for clarity's sake, in this section, we introduce how have been managed some methods that are used in the chapters containing results of this thesis. Specifically, in the following lines we are going to describe how we compute median and CI for the measured coming from the sets of model outcomes that the spreading model produces, as this is the standard procedure that we do to obtain almost any model-derived outcome presented in the following chapters. Moreover, we a the usage of the MLE approach to find parameters for a statistical distribution, and the Bayes theorem. Other specific methods are only used in a given chapter, and that will be described in detail there.

2.3.1 Median and CI

For most of this thesis, the spreading model is used to i) get a calibration to the high-risk setting and ii) measure the effect of a given perturbation over the TB trends that the model produces when compared with the baseline scenario without perturbation. However, as explained in the previous sections, to propagate the uncertainty that is inherited from the original data sources -needed to calibrate and to parametrise the model-, there are sets of $N = 500$ outcomes produced, one per each re-calibration done in the uncertainty propagation procedure. Those sets of 500 elements are generated for every outcome that is being measured. For instance, to produce the trends of incidence and mortality, the model yields 500 series of each variable, measured annually. Then, there is still something to do to produce a median result and an appropriate credibility interval, which is to analyse the distribution of outcomes using R software to compute the median and quantiles over the set.

In short, in statistics and probability theory, the median is the value that separates the sample, or the probability distribution, into the higher half and the lower half of the data. In our case, we are dealing with data sets, and in this context, the median may be thought of as "the middle" value. The reason to use it instead of the mean is that it is not skewed by a small proportion of extremely large or small values, which sometimes happens when the uncertainty algorithm tries to calibrate extreme values for the uncertainty sources. As a consequence, the median provides a better representation of the centre.

Similarly, quantiles are the values that divide the observations of a sample, or the range of a probability distribution, into continuous intervals with equal probabilities. It is used to produce the CI of the median value estimated from the model outcomes at a given significance level α, with $\alpha \in [0, 1]$. For a given α, the CI will be given by the interval that captures the $100 \cdot (1 - \alpha)\%$ probability of getting an outcome inside, letting the $100 \cdot \alpha/2\%$ most extreme values at the higher and lower part of the -ordered-set.

Then, with the aid of the *quantile()* function, which is available in base R, we compute the quantiles given by $(\alpha = 0.5, \alpha = 0.025 and \alpha = 0.975]$, which correspond to the median of the empirical distribution, along with the extremes of the 95% CI, for any model outcome that we want to measure. An example of the previous procedure is shown in the scheme in Figure 2.4, for a sample distribution generated using R and the *truncnorm* package.

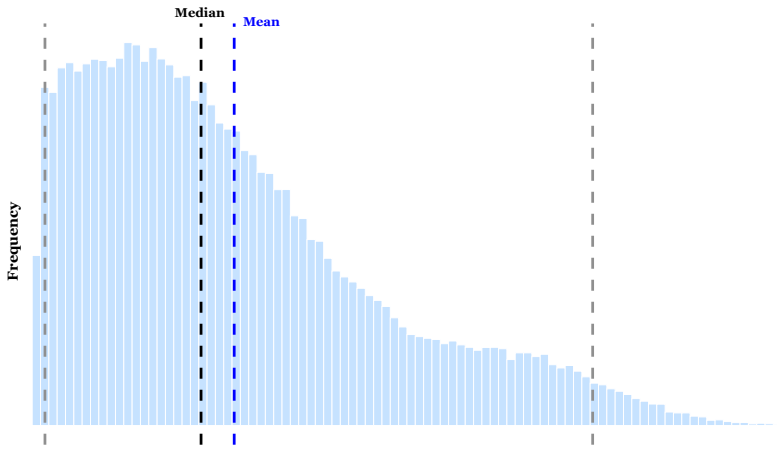

Figure 2.4: Scheme of the statistical mean and 95%CI obtained using R in a sample distribution. The mean (blue) of the sample data is pulled to higher values than the median (black), for which it captures better some sort of centrality in skewed distributions. The vertical dashed lines in grey capture the 95% CI of the data with the plotted distribution.

2.3.2 MLE and the Bayes Rule

Next, in Chapter 3 we introduce two different methodologies to address the mechanistic effect of a vaccine tested in a real RCT. This is done to retrieve a full description of the vaccine at play, so it can be introduced directly into the spreading model without the need to make assumptions that may -or may not- be true by the modeller. The final objective is then to reduce the bias in the impact forecast estimations for TB vaccines. The whole framework is explained in Chapter 3, but to deal with obtaining these mechanistic descriptions, we have trusted two statistical methods. The first methodology makes use of a Maximum Likelihood Estimation (MLE) combined with a statistical model for the effect of a given vaccine in one of the three possible routes to disease that exist in TB. The second methodology trusts the Bayes Theorem to analyse large datasets of outcomes of simulated RCTs and to find the vaccine description, among a proposed set of seven descriptions, that yields the highest Bayesian posterior according to the data. To contextualise the findings over the usage of those statistical methods, in the following lines we introduce the basics about each one about how they are used in the corresponding chapter.

First, MLE is a method used in statistics for estimating the parameters of a statistical model, where the idea is to find the parametrisation of the statistical model that maximises the likelihood function, a measure of how well the model explains the observed data. It is a common approach for estimating model parameters when there is evidence that the statistical model describes the observed data's distribution. This book's objective is not to provide material for a statistical course, and the mathematical

justification and basis of the MLE technique may be found, at a much more detailed level, in [176]. Instead, in the context of this thesis, we will describe a very basic description of the method, and how how the MLE has been implemented.

To this end, let $X_1, ..., X_N$ be a random sample from some distribution which is characterised by a set of parameters $\Theta = (\theta_1, ..., \theta_j)$. Then, if we have a series of observations $[x_1, ..., x_N]$, we can define the likelihood function as the probability of the observed sample, which is a function of Θ:

$$L(x_1, ...x_N, \Theta) = P(X_1 = x_1, X_N = ...x_N, \Theta) \tag{2.42}$$

Then, the MLE method is used to find, among all the parameter space, the values for the parameters that yield the highest likelihood. All computations involving the previous mathematical considerations, but for the specific data and with a suitable likelihood function, have been performed using the computing language R, which is known for its statistical power. Specifically, the package *bbmle* has been used, and the implementation with the original code may be found in Github, in the following link: $https://github.com/NatComIgraMinusCodes$.

Second, the Bayes theorem is a fundamental theorem of the Bayesian statistics corpus, and it is used in Chapter 3 to find the vaccine descriptions that seem to have the highest posterior with the *in-silico* data that is produced. In this second methodology, applying the MLE was more difficult, for some reasons that are stated in Chapter 3, so we needed to swap the algorithm towards other methods, where the Bayes theorem appeared to be the more simple that yet produced the desired information, i.e., an estimator of the relative compatibility of the descriptions of the vaccine with a real result in an RCT.

The Bayes theorem is typically found as:

$$P(A|B) = \frac{P(B|A)P(A)}{P(B)} \tag{2.43}$$

where A and B are events, and $P(B)$ must be non zero, i.e., B must be a possible event. In the formula, $P(A)$ and $P(B)$ capture the probability of each event happening, without any conditions, which are named the prior probabilities, and can be interpreted as the initial belief on each one of the events. The term $P(B|A)$ captures the probability of B happening given that A happened, and it is a conditional probability. The term $P(A|B)$, which is also a conditional probability, is named the posterior probability and captures the probability of the event A happening given that B happened. This posterior probability is what we want to measure when using the Bayes theorem, and it's an updated probability for the event A when there is evidence that the event B happened, and, of course, there is some interplay between A and B.

In this thesis, we are using a frequentist interpretation of the rule, as we are using the proportion of outcomes to define probabilities in this thesis. The implementation of this rule has been made in R language, for the specific events that allow measuring the relative compatibility of the vaccine description from the set of outcomes. In this sense, we are simulating a bunch of *in-silico* RCTs with each vaccine description, and for a range of the interest parameter. Then, we produce an estimation of the posterior of each description which is obtained with the Bayes rule. The implementation with the original code may be found in Github, in the following link: $https://github.com/NatComIgraPlusCodes$.

Chapter 3

Vaccine's efficacy: translating RCT readouts to spreading models.

> Lo peor no es cometer un error, sino tratar de justificarlo, en vez de aprovecharlo como aviso providencial de nuestra ligereza o ignorancia.
>
> Santiago Ramón y Cajal

Summary of this chapter: In tuberculosis (TB) vaccine development, multiple factors hinder the design and interpretation of the clinical trials used to estimate vaccine efficacy. The complex transmission chain of TB includes multiple routes to disease, making it hard to link the vaccine efficacy observed in a trial to specific protective mechanisms. In this chapter, we explore the inherited bias in trial outcomes and vaccine forecasts with transmission models. We identify the two most prominent architectures of clinical trials, being used in two recently completed trials, and propose new complementary algorithms to classical survival analysis to get more complete descriptions of the mechanistic effect of the tested vaccines. We also demonstrate that there are differences in the foreseen impacts of different descriptions of compatible vaccines when forecasted with transmission models, which remarks the importance of our approach.

3.1 A long journey in TB vaccine development.

Since 1990, there has been a worldwide decay in TB incidence and mortality[71], which is key to eradicating this menace. In this direction, the World Health Organization (WHO) introduced the End-TB strategy, which consists of completing a reduction of TB incidence and mortality rates by 90% and 95%, respectively, between 2015 and 2035 [65]. Despite the achieved decay in

burden, the yearly rate of reduction is arguably too slow to meet the goal settled by the WHO. On top of that, starting in 2020, we are witnessing, for the first time in decades, an alarming increase in global TB burden levels concerning previous years. For instance, we accounted for as many as 1.6 million casualties attributable to TB worldwide in 2021, combining HIV negative and positive cases, whereas in 2020 and 2019 the number of accounted deaths was 1.5 and 1.4 million, respectively[76].

This increase was caused by the irruption of the COVID-19 pandemic, which threatens, especially in high-burden countries like India, to raise the TB mortality back to even higher levels in the next few years [177]. In Chapter 5 of this thesis, this interaction is explored and quantified, and the results show that if nothing is done, we can expect more TB-related deaths shortly. This unexpected interaction between TB and COVID-19, as well as the ever-increasing rates of emergence of drug resistance [78], evidence the need for new epidemiological interventions and tools against TB, and in this context, a new and better vaccine than the current bacillus Calmette-Guerin (BCG) [178], whose efficacy against the more transmissible respiratory forms of the disease in young adults is disputed [79], could be key to sustain the gains again the TB pandemic.

But not all that glitters is gold, as TB development and vaccine testing is especially difficult due to several factors. Focusing on the testing part, the slowness of the contagion dynamics forces vaccine developers to consider studies involving larger numbers of participants during longer follow-up periods than for other diseases [179, 180, 181]. Another layer of difficulty is added when defining trial endpoints for a disease where infection status can only be ascertained indirectly, bound together with the lack of immunological correlates of protection[115], which highlights the need for well-designed Randomised Clinical Trials (RCT) to address the efficacy of a tested vaccine, among other important factors such as possible secondary effects. Because of this, designing RCTs for TB vaccines is an extremely challenging and expensive task. Despite all the difficulties, nowadays, several preventive vaccine candidates against TB are being tested in human clinical trials [178, 182].

Some of those vaccine candidates have already completed phases 1, 2, and 2b of their development, and are about to enter into phase 3 to test their efficacy at providing prevention of infection (PoI) and/or prevention of TB disease (PoD) in large cohorts of thousands of participants recruited in high burden settings. The first of the new preventive vaccines against TB that completed the phase 2-2b RCTs was the MVA85A [179], followed by the M72/AS01$_E$[180, 181], and also the H4:IC31 vaccine[183], which was compared to a revaccination protocol with BCG (named BCG-revac). These results of their trials yielded disparate efficacy readouts and were tested within trials of

noticeably diverse designs in some of the several key characteristics such as geographical distribution, participants' age, or their status at the start of the trial, measured as the Interferon-gamma-release-assay (IGRA) status. In this topic, the trial designs typically recruit individuals that are either IGRA-negative (those showing negative results to an Interferon-gamma-release-assay[184]) or IGRA-positive. The characteristics of some ongoing TB vaccine trials are detailed in Table 3.1.

Vaccine	Trial ID (year)	IGRA status	Cohort size	P. Age	Location	Efficacy (95% CI)
MVA85A	NCT00953927 (2009-2011)	Negative	1395 (Placebo) 1399 (MVA85a)	4-6 (m)	S.Africa	PoI: –3.8% CI: (–28.1-15.9) PoD: 17.3% CI: (-31.9-48.2)
M72/AS01E	NCT01755598 (2014-2015)	Positive	1660 (Placebo) 1623 (M72/AS01E)	18-50 (y)	S.Africa Kenya Zambia	PoD: 49.7% CI: (2.1-74.2)
H4:IC31 BCG-revac	NCT02075203 (2014-2015)	Negative	306 (Placebo) 297 (H4:IC31) 312 (BCG)	12-17 (y)	S.Africa	H4:IC31 PoI: 30.5% CI: (-15.8-58.3) BCG PoI: 45.4% CI: (6.4-68.1)

Table 3.1: Phases 2/2b clinical trials for new TB vaccines. The provided years correspond to the recruitment phase. The size of the cohorts corresponds to the final number of individuals included in efficacy analyses. In the MVA85A, the PoD efficacy corresponds to endpoint definition 1, as described in [179]. In the H4:IC31 trial, the POI efficacy is measured against sustained QFT conversion (QFT conversion without reversion within 6 months).

This disparity, summarised in Table 3.1, makes it difficult to compare, and even to analyse, the results in a common, comprehensible way, and that's just involving three pioneer phase 2/2b efficacy trials for novel TB vaccines. Given the diversity of their designs, the question of what is an optimal strategy for testing a preventive vaccine against TB at these stages of vaccine development seems to lack a unique answer. The diversity in trial designs is also expected to do nothing but increase as the rest of the vaccine candidates progress through the development pipeline, as anticipated in [185]. Thus, the field will witness a higher number of trials being explored, and this multiplicity of designs, along with the paucity of resources to allocate for evaluating novel TB vaccine candidates at a global scale [186], makes it absolutely critical to ensure that vaccines with different target product profiles, and, or estimated from trials of different characteristics can be timely compared in their expected ability to halt the global epidemics of TB.

One of the reasons why such a task is difficult is the fact that the PoI or PoD efficacy readouts obtained from an RCT do not offer an unequivocal characterisation of a TB vaccine, since the same risk-reduction readouts observed in a trial can be mapped onto different mechanisms of action in different vaccine candidates[185]. This

is extremely important because some of these compatible mechanisms are impossible to distinguish just by interpreting the trial's results using standard methodologies, and yet, they appear associated with significantly different impacts when forecasted with transmission models in simulated vaccination campaigns, as we will demonstrate in this chapter[117, 118]. Moreover, historically, TB-related research, including vaccine development, has faced challenges in securing sufficient funding compared to other high-profile diseases like HIV/AIDS and malaria. This has always been a concern given the global burden of TB, especially in low- and middle-income countries[187, 188, 87]. This lack of funding forces researchers to get the most out of research, and, given the difficulties in the TB development pipeline, this highlights the necessity of getting usable descriptions of TB vaccines whose impact may eventually addressed with spreading models.

To this end, we settled on one objective of this thesis, which is exploring this problem and developing plausible algorithms and methods that enable a better characterisation of vaccines than merely using classical techniques. Thus, in this chapter, two main types of trial designs are analysed. The first one captures trials such as the one conducted for the MVA85A vaccine [179], which recruited cohorts of naive individuals, IGRA-negative at the start of the trial. The second one captures trials such as the study for the M72/AS01$_E$ vaccine [180, 181], which involved the recruitment of already sensitised subjects. In both cases, we formally describe the issue and characterise its negative impact on our ability to produce unbiased impact evaluations for vaccines. Then, we propose an additional set of analyses that allow us to distinguish among the possible vaccine mechanisms at play and discuss their range of applicability under different epidemiological scenarios, age of participants, and trial dimensions and designs. Our results unlock a deeper interpretation of the data emanating from efficacy trials of TB vaccines, which renders them more interpretable in terms of transmission models and translates into explicit recommendations for vaccine developers.

3.2 Translating outcomes from RCT's based on IGRA- population

3.2.1 The problematic of characterising TB vaccines

The development of TB vaccines is plagued with many conceptual challenges that difficult the evaluation of different candidates across the clinical pipeline[189]. The lack of protection correlates for TB [190, 115] hinders early efficacy evaluations, which forces researchers to wait until late stages (phases 2b and 3 of the clinical pipeline)

to measure vaccine efficacy. Enrolling and observing thousands of individuals in areas with high incidences of TB over multiple years is necessary, and costly, for these trials. In this regard the well-structured phase 2b trial of the MVA85A vaccine offered a robust quantitative basis for determining the necessary minimum group sizes and duration of follow-up periods in contemporary epidemiological settings, even if the trial did not yield substantial evidence of effective protection.[179]. More studies have followed its steps, including different types of phase 2b trials for other vaccines, such as H4:IC31 [183] and the M72/AS01$_E$ [180, 181], which showed 49.7% efficacy (95% CI: 2.1−74.2%) against active TB in adult individuals already exposed to *M.tb*.

Phase 2b clinical trials can be designed to estimate different types of vaccine efficacy, including prevention of infection (POI), prevention of disease (POD), and prevention of recurrence (POR) [188]. Once these effects have been estimated for a given vaccine, its potential impact is estimated through the use of mathematical models of pathogen's transmission [164]. However, trial-derived readouts of vaccine efficacy do not always guarantee an unequivocal interpretation from a TB modelling perspective. This is due to the extreme complexity of the natural history of the disease, which enables different dynamic mechanisms through which a vaccine can provide protection.

After initial infection with *Mycobacterium tuberculosis*, some individuals develop TB within incubation periods of less than $\simeq$2 years [69], (i.e. fast progression). On the other hand, others succeed at containing the infection and become asymptomatic, latent TB-infected individuals (LTBI). LTBI subjects remain so often for the rest of their lives, although they can suffer endogenous reactivation of the disease (slow progressors), even decades after the first infection event. Finally, LTBI individuals can also be re-infected and progress to TB after the secondary infection.

Considering this perspective, a vaccine can protect against TB through various mechanisms. On one hand, it might act by reducing the fraction of individuals who rapidly progress to TB after an infection or reinfection event. On the other hand, the vaccine could delay the onset of active TB, slowing down the dynamics of fast progression instead of preventing it. These dual mechanisms offer distinct interpretations in terms of dynamics and might seem unrelated and not inherently interconnected. Environmental and genetic factors influence an individual's likelihood of following a fast or slow path to disease. However, little is known about whether or how they impact the delay observed between infection and onset of symptoms in TB cases linked with recent transmission [191].

The main focus here is the analysis of an apparently simple interpretation problem: in a POD clinical trial, how does one distinguish between a vaccine that prevents fast progression upon infection, or re-infection, from a vaccine that delays it? This simple

question hinders another important reality: vaccines with the same POD efficacy, acting through different mechanisms do not share the same impacts when introduced in bigger populations. In this section, we describe these limitations and their effect on model-based evaluations of vaccine impact, and we propose a methodology to analyse efficacy that combines compartmental models and stochastic simulations of RCTs. Using our approach, it is possible to disentangle the different possible mechanisms of action underlying vaccine protection effects against TB in trials such as the one conducted for the MVA85A vaccine[179], conducted in cohorts of naive individuals, conditioned to trial size, and duration. Pointing toward the eradication of TB, knowing which vaccines show higher impacts is crucial, and a detailed analysis such as the one proposed here could help in this task.

3.2.2 Methods I: a workable method to analyse IGRA-negative trial results.

3.2.2.1 The basal RCT model

To enlighten the mechanistic effect of a POI-POD vaccine in a trial such as the MVA85A we need a mathematical model of the first stages of the natural history of TB, those that can be observed in an RCT. Within a mathematical description, it is possible to derive analytical relations between the usual efficacy measures (based on survival analyses) that are commonly obtained as the main outcome of an RCT, and the intrinsic efficacies of vaccines that act at the mechanistic level, i.e., modifying, or halting some transitions between states. Moreover, to test the method that we will introduce in the following sections, we need to produce *in-silico* realisations of trials, so we can apply the methodology to estimate the mechanistic effect of the vaccine and address the power of the methodology that we propose.

Then, to fulfil those requirements, we proposed a compartmental model, depicted in Figure 3.1, whose baseline parameters are calibrated to reflect the current epidemic situation in a reference setting. This setting is, in this case, the target cohort of newborns living in Worcester, South Africa, where the MVA85A trial took place from 2009 to 2012 [179]. In this compartmental model, both the control cohort and the vaccine cohort of the trial share a common architecture, which is, that they share the same states, and, if any, the eventual protection conferred by a vaccine will modify the transitions between states only in the vaccine cohort, but not the states.

This architecture capture all three possible routes to disease[144, 164, 135], and arguably reflects one of the most elementary model architectures, among the different options that can be used to describe the initial stages of the transmission chain of *M.tb.*

that include a description of the incubation period of fast progression, which will be a key ingredient for our analyses[192].

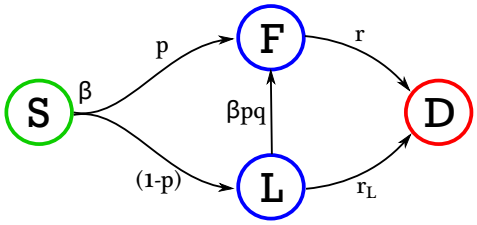

Figure 3.1: Scheme of the elementary *M.tb.* transmission model with states. S: Susceptible, F: Fast-progressors, L: Slow-progressors (LTBI), D: Disease (active TB) of the control cohort in the RCT. The vaccine cohort presents the same architecture, but the epidemiological parameters that model the transitions between states can be modified by the vaccine effects.

According to this architecture, the compartmental model includes 4 different states that capture the first part of the Natural History of TB, which are the only states that recruited participants are expected to visit during the duration of an RCT, for the rest of the natural history will need prohibitive trials sizes and times to be observed. The states are, then S, for susceptible individuals, F and L for fast-progressors and slow-progressors respectively, which capture latent infection, and D, for individuals showing symptoms of active disease. According to the scheme of transitions, the evolution of those states is given, in the control cohort (subindex c), by the following differential equations:

$$\frac{dS_{\mathrm{c}}(t)}{dt} = -\beta S_{\mathrm{c}}(t) \tag{3.1}$$

$$\frac{dF_{\mathrm{c}}(t)}{dt} = \beta p S_{\mathrm{c}}(t) - r F_{\mathrm{c}}(t) + \beta pq L_{\mathrm{c}}(t) \tag{3.2}$$

$$\frac{dL_{\mathrm{c}}(t)}{dt} = \beta(1-p) S_{\mathrm{c}}(t) - r_{\mathrm{L}} L_{\mathrm{c}}(t) - \beta pq L_{\mathrm{c}}(t) \tag{3.3}$$

$$\frac{dD_{\mathrm{c}}(t)}{dt} = r F_{\mathrm{c}}(t) + r_{\mathrm{L}} L_{\mathrm{c}}(t) \tag{3.4}$$

Next, in the vaccine cohort, the previous set of ODEs is modified according to the effect of the vaccine. In this work, we define a vaccine by providing the triad of intrinsic vaccine efficacies, denoted as $\varepsilon_\beta, \varepsilon_{\mathrm{r}}, \varepsilon_{\mathrm{p}}$. Those parameters capture the effects of the vaccine on the infection rate, the transition rate to disease, and the probability of fast progression, respectively. For instance, $\varepsilon_\beta = 0$ means no protection against infection, while $\varepsilon_\beta = 1$ means total protection. Then, with only those parameters we can fully describe the mechanistic effect of the vaccine. Taking this into consideration, for the vaccinated cohort (subindex v), the parameters β, p, and r are modified by the action of the vaccine, which gives the following set of differential equations:

$$\frac{dS_{\mathrm{v}}(t)}{dt} = -(1-\varepsilon_\beta)\beta S_{\mathrm{v}}(t) \tag{3.5}$$

$$\frac{dF_{\mathrm{v}}(t)}{dt} = (1-\varepsilon_\beta)\beta(1-\varepsilon_{\mathrm{p}})pS_{\mathrm{v}}(t) - (1-\varepsilon_{\mathrm{r}})rF_{\mathrm{v}}(t) + (1-\varepsilon_\beta)\beta(1-\varepsilon_{\mathrm{p}})pqL_{\mathrm{v}}(t) \tag{3.6}$$

$$\frac{dL_{\mathrm{v}}(t)}{dt} = (1-\varepsilon_\beta)\beta(1-(1-\varepsilon_{\mathrm{p}})p)S_{\mathrm{v}}(t) - r_{\mathrm{L}}L_{\mathrm{v}}(t) - (1-\varepsilon_\beta)\beta(1-\varepsilon_{\mathrm{p}})pqL_{\mathrm{v}}(t) \tag{3.7}$$

$$\frac{dD_{\mathrm{v}}(t)}{dt} = (1-\varepsilon_{\mathrm{r}})rF_{\mathrm{v}}(t) + r_{\mathrm{L}}L_{\mathrm{v}}(t) \tag{3.8}$$

In both sets, the initial conditions are $S_x = 1$ and $L_x = F_x = D_x = 0$ for $x = c, v$, i.e. all individuals are susceptible at the beginning of the trial, as we are dealing with IGRA-negative population at the start of the trial.

Then, the parameters are calibrated to reflect the epidemic situation in the setting of the trial. The transition rate from LTBI to disease is assumed to be $r_{\mathrm{L}} = 7.5 \times 10^{-4} y^{-1}$, following previous bibliographical estimations [144]. According to [96], we consider that LTBI individuals have a 79% less risk of progressing to TB upon re-infection, which is captured by the parameter $q = 0.21$. Finally, the probability of fast progression has been fixed to $p = 0.375$ which is compatible with previous observations about the high probability of developing fast progression during the first months of life [146]. Once those parameters are fixed, the baseline transmission rate β and the transition rate from fast latency to disease r were estimated to be $\beta = 0.069y^{-1}$ and $r = 0.97y^{-1}$ to reproduce the proportion of infections and TB cases observed in the control cohort of the MVA85A trial (12.8%, and 2.3% after 2 years, respectively). Even though these parameters are representative of epidemiological risks of newborns, the method that we propose in the following sections also works on alternative scenarios, including parameterisations compatible with other age groups.

3.2.2.2 Algorithm to simulate a trial

To simulate the evolution of the individuals in an efficacy trial such as the MVA85A, we solved the previous ODE systems with a stochastic, agent-based approach. That is, we simulate individually the evolution of each enrolled individual across disease states during the trial within a probabilistic scheme, which means that the individuals' fates during the trial are decided according to the epidemiological parameters, through a series of multinomial trials that are conducted at every time point (once a day, here), until the follow-up period of the trial is concluded. The reason behind solving the temporal evolution in this way is that, even if the ODE's system is analytically solvable, we need to preserve the information of all simulated individuals at all times, so they need to be distinguishable. This is due to the proposed method to retrieve the effect of the vaccine that we'll describe in the following sections.

Then, the trial is simulated by solving the set of ODEs for all agents, i.e., recruited individuals, stochastically, which is nothing but a Monte Carlo simulation. As represented in figure 3.1, in both the control and vaccine cohorts we have four states (susceptible S, fast latency F, slow latency L, and active disease D), and five different types of transitions between them ($S->L$, $S->F$, $L->F$, $L->D$ and $F->D$). For the case of the control cohort, the model defines the following set of transition rules for individuals in each state, where all the random numbers ϕ drawn in the context of the multinomial tests proceed from uniform distributions in the interval $[0, 1]$:

Susceptible individuals. On a daily basis, individuals may get infected, with a daily probability equal to β. If they get infected, they can either enter into fast latency with probability p, or slow latency, with probability $(1 - p)$.

- 1. A first random number is drawn to decide if infection occurs: ϕ_1:
  - If $\phi_1 \leq \beta$, the individual gets infected, then:
    - A second random number is drawn to decide if fast progression occurs: ϕ_2:
      - If $\phi_2 \leq p$ individual enters into fast latency: **transition** $S->F$
      - If $\phi_2 > p$: individual develops LTBI: **transition** $S->L$
  - If $\phi > \beta$: individual does not get infected: **No transition**

LTBI individuals. Once an individual is in the LTBI reservoir (slow latency: L), he/she can either undergo endogenous reactivation (with daily probability r_{L}, or TB after a re-infection event (i.e. transition from L to F), with a daily probability equal to the product βpq (i.e. the probability of being infected times the probability of progressing to fast latency after that, modified by q, the protection factor that LTBI confers against progression to disease upon re-infection [96])

- 1. A random number is drawn ϕ_1:
  - If $\phi_1 \leq (\beta pq)$: individual will develop TB fast after exogenous re-infection: **transition** $L->F$
  - If $(\beta pq) < \phi_1 < (\beta pq + r_{\mathrm{L}})$: individual develops TB upon endogenous reactivation: **transition** $L->D$
  - If $(\beta pq + r_{\mathrm{L}}) < \phi_1$: individual remains LTBI: **No transition**

Individuals in F From the reservoir F, we only consider the transition to disease, with daily probability equal to r, as the only possible status change:

- 1. A random number is drawn to decide whether the transition to disease takes place ϕ_1:
  - If $\phi_1 \leq r$: individual develops TB: **transition** $F->D$
  - If $\phi_1 > r$: individual remains in F: **No transition**

The epidemiological parameters ruling the stochastic dynamics of the system ($\beta, p, q, r_{\mathrm{L}}$ and r) are re-scaled from their values to capture daily probabilities. Furthermore, solving for the vaccine cohort is trivial, as, each one of these transitions can, in principle, be modified by a vaccine. Then, to simulate the vaccine cohort, the same procedure described previously is applied to the modified set of transitions. In any case, in this analysis, we only consider vaccines through a reduction of either β, p, or r.

3.2.2.3 Data analysis of trial outcomes

Once that we have developed the basal model for the RCT and the algorithm to solve the temporal evolution of the enrolled individuals, we can focus on the methodology. The idea is that we want to measure the values of the triad of vaccine descriptors $\varepsilon_\beta, \varepsilon_{\mathrm{r}}, \varepsilon_{\mathrm{p}}$ used to capture the effect of a vaccine at the mechanistic level. Using the classical measures based on survival analysis, we only have two quantities, $\mathrm{VE}_{\mathrm{inf}}$ and $\mathrm{VE}_{\mathrm{dis}}$, to estimate the descriptors. We need to derive a complementary method to survival analysis, and, as it is possible to link mathematically all five quantities together, if one of the vaccine descriptors is estimated individually, the rest can be estimated using this link and $\mathrm{VE}_{\mathrm{inf}}$ and $\mathrm{VE}_{\mathrm{dis}}$.

In the following lines, we describe the whole method to do so, in which, using the compartmental description of the RCT, we can derive the relation $\mathrm{VE}_{\mathrm{dis}} = f(\varepsilon_\beta, \varepsilon_{\mathrm{p}}, \varepsilon_{\mathrm{r}})$, and to estimate ε_{r} from the distribution of transition times to active disease of fast progressors. This way, we can recover the effect of the vaccine in two ways, with the survival measures and also through the parameters $\varepsilon_\beta, \varepsilon_{\mathrm{r}}, \varepsilon_{\mathrm{p}}$, which are suitable to be plugged into TB spreading models to forecast the impact of the tested vaccine in bigger settings.

POI and POD efficacy readouts for trials conducted in IGRA-negative populations: $\mathrm{VE}_{\mathrm{inf}}$ and $\mathrm{VE}_{\mathrm{dis}}$ As we want to translate the outcome of the trial to a spreading model, we need to analyse the trial in such a way that enables the

estimation of the set of parameters $(\varepsilon_\beta, \varepsilon_\mathrm{r}, \varepsilon_\mathrm{p})$ used to model the effect of the vaccine at the mechanistic level. When dealing with real RCTs involving fieldwork, the efficacy readouts of POI and POD ($\mathrm{VE_{inf}}$ and $\mathrm{VE_{dis}}$) are estimated using survival analysis (Cox regression [193, 194]). In the case of vaccine POI, the readout of $\mathrm{VE_{inf}}$ obtained this way can be directly associated with a reduction of the risk of infection upon contact with an infectious subject, that is, $\mathrm{VE_{inf}} \equiv \varepsilon_\beta$. Note that $\mathrm{VE_{inf}}$ can only be estimated from a trial based on IGRA-negative subjects[179].

Vaccine-mediated POD can be estimated from trials recruiting IGRA-negative or IGRA-positive individuals, though. However, here is where the main problem arises: the existence of different mechanisms compatible with a single readout of $\mathrm{VE_{dis}}$ poses a series of conceptual challenges to its estimation through classical survival analysis, as ε_r, and ε_p could not be directly derived from just this measure. This supports the adoption of the more elementary approximation $\mathrm{VE_{dis}} = 1 - \rho$, where ρ is the fraction of the total number of individuals with active TB in both cohorts at the end of the trials: $\rho = D_\mathrm{v}(T)/D_\mathrm{c}(T)$. This choice is justified by several reasons. On the one hand, it permits the derivation of an analytic relation between $\mathrm{VE_{dis}}$ and the mechanistic parameters, $(\varepsilon_\beta, \varepsilon_\mathrm{r}, \varepsilon_\mathrm{p})$, which is key to our approach. On the other hand, it produces estimates for $\mathrm{VE_{dis}}$ that deviate residually from the readouts obtained from survival analyses. Finally, using survival analysis to determine $\mathrm{VE_{dis}}$ is problematic at least for some of the possible vaccine mechanisms, as the hypothesis of proportional risks, which is the major conceptual requisite for Cox regression to be applied, is not always respected.

With the aid of Schoenfeld's Residual tests [195], we evaluate the accuracy of the proportional hazards hypothesis for different vaccines with different ε_p and ε_r. We compute sets of 500 *in-silico* trials with the aid of the agent-based model described before. The outcomes of the trials are then analysed, and the results are represented in Figure 3.2. In Figure 3.2A we show the proportion of tests with a p-value lower than 0.05 where the hypothesis of proportional hazards can be rejected (under the null hypothesis the proportion should be precisely 5%). We recover that vaccines that delay the fast progression rates violate more often the hypothesis of Hazards Proportionality, well above 5%. This is also coherent with the observation shown in Figure 3.2B, where we illustrate how the observed efficacies of an ε_r-based vaccine are strongly dependent on the follow-up period of the trial, as whenever the time increases, so do the chance of having active disease individuals that came from other routes.

Also, to test the bias incurred when using our descriptor instead of the Cox-based value, we tested the relative difference between measures in Figure 3.2C, where the quantity $2 \cdot \frac{|\mathrm{VE}_\mathrm{dis}^\mathrm{cox} - \mathrm{VE}_\mathrm{dis}^\mathrm{prop}|}{|\mathrm{VE}_\mathrm{dis}^\mathrm{cox} + \mathrm{VE}_\mathrm{dis}^\mathrm{prop}|}$ is computed and shown for different combinations of $(\varepsilon_\mathrm{r}, \varepsilon_\mathrm{p})$.

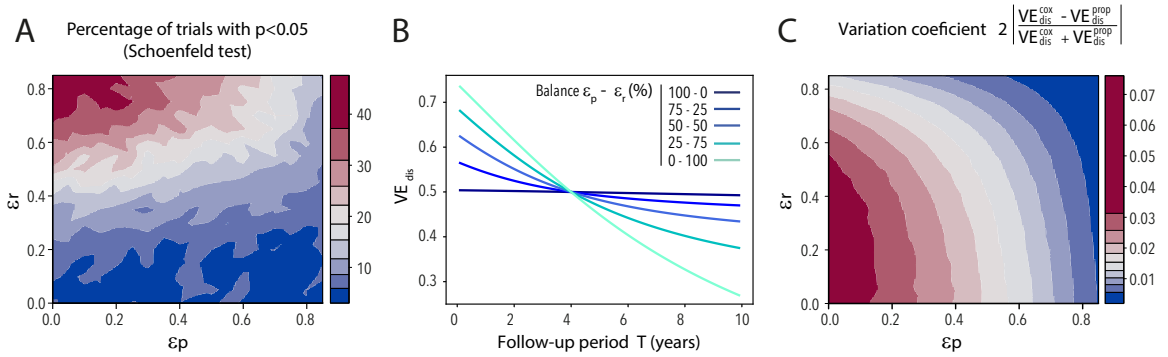

Figure 3.2: **A**. Proportion of Schoenfeld's Residual tests with a p-value below 5% as a function of ε_{p} and ε_{r}. Simulations have been performed with a Cohort Size of 3000 individuals, a follow-up period of 4 years, and 500 iterations. **B**. Evolution of measured $\mathrm{VE}_{\mathrm{dis}}$ as a function of the follow-up period for five different vaccines that are compatible with a common readout from a $T = 4$ years trial but lean on different ratios $(\varepsilon_{\mathrm{p}}, \varepsilon_{\mathrm{r}})$ in their mechanisms of action. Unlike vaccines that are based on reducing the probability of fast TB (whose $\mathrm{VE}_{\mathrm{dis}}$ readouts are essentially independent of follow-up periods), the readout of $\mathrm{VE}_{\mathrm{dis}}$ for vaccines that delay incubation periods is strongly dependent on trial duration. **C**. Coefficients of variation. Simulations have been performed with a Cohort Size of 3000 individuals and a follow-up period of 4 years.

We observe that the relative differences remain below 8% of the mean of the efficacies estimated from both methods, so the incurred bias is low enough to allow the usage of the proportional descriptor of $\mathrm{VE}_{\mathrm{dis}}$

Derivation of the relation $\mathrm{VE}_{\mathrm{dis}} = f(\varepsilon_\beta, \varepsilon_{\mathrm{p}}, \varepsilon_{\mathrm{r}})$ The ODE systems 3.4 and 3.8 model the temporal evolution of individuals in an RCT that recruits IGRA-negative individuals at the start of the trial. Using this equations, and the elementary measure of $\mathrm{VE}_{\mathrm{dis}} = 1 - \rho$ it is possible to derive a link between the parameters ε_x and $\mathrm{VE}_{\mathrm{dis}}$, as $\rho = \frac{D_c(T)}{D_v(T)}$ with T being the end of the trial. The idea here is that, if we can independently obtain either ε_{p} or ε_{r}, we can use the link to get the other, as the rest of the parameters will be known. Then, solving the system of differential equations 3.4 and 3.8, we obtain the proportion for every state at each cohort. We have considered that the initial conditions are $S_x = 1$ and $L_x = F_x = D_x = 0$ for $x = c, v$, i.e. all individuals are susceptible at the beginning of the trial, which is the real situation. For the susceptible states we get:

$$S_{\mathrm{c}}(t) = \exp(-\beta t) \tag{3.9}$$
$$S_{\mathrm{v}}(t) = \exp(-(1-\varepsilon_\beta)\beta t) \tag{3.10}$$

Then, for the F reservoirs, solving the ODE's yields:

$$F_{\mathrm{c}}(t) = K\exp(-rt) + \frac{\beta p}{r-\beta}\exp(-\beta t) + \frac{\beta^2 pq(1-p)}{r_{\mathrm{L}}+\beta pq-\beta}\left[\frac{\exp(-\beta t)}{r-\beta} - \frac{\exp(-(r_{\mathrm{L}}+\beta pq)t)}{r-r_{\mathrm{L}}-\beta pq}\right] \tag{3.11}$$

$$\begin{aligned} F_{\mathrm{v}}(t) = {} & K'\exp(-(1-\varepsilon_{\mathrm{r}})rt) + \frac{(1-\varepsilon_\beta)\beta(1-\varepsilon_{\mathrm{p}})p}{(1-\varepsilon_{\mathrm{r}})r-(1-\varepsilon_\beta)\beta}\exp(-(1-\varepsilon_\beta)\beta t) \\ & + \frac{((1-\varepsilon_\beta)\beta)^2(1-\varepsilon_{\mathrm{p}})pq(1-(1-\varepsilon_{\mathrm{p}})p)}{r_{\mathrm{L}}+(1-\varepsilon_\beta)\beta(1-\varepsilon_{\mathrm{p}})pq-(1-\varepsilon_\beta)\beta}\left[\frac{\exp(-(1-\varepsilon_\beta)\beta t)}{(1-\varepsilon_{\mathrm{r}})r-(1-\varepsilon_\beta)\beta}\right. \\ & \left. - \frac{\exp(-(r_{\mathrm{L}}+(1-\varepsilon_\beta)\beta(1-\varepsilon_{\mathrm{p}})pq)t)}{(1-\varepsilon_{\mathrm{r}})r-r_{\mathrm{L}}-(1-\varepsilon_\beta)\beta(1-\varepsilon_{\mathrm{p}})pq}\right] \end{aligned} \tag{3.12}$$

where:

$$K = -\beta p\left[\frac{r-r_{\mathrm{L}}-q\beta}{(r-\beta)(r-r_{\mathrm{L}}-\beta pq)}\right] \tag{3.13}$$

$$K' = -(1-\varepsilon_\beta)\beta(1-\varepsilon_{\mathrm{p}})p\left[\frac{(1-\varepsilon_{\mathrm{r}})r-r_{\mathrm{L}}-(1-\varepsilon_\beta)\beta(1-\varepsilon_{\mathrm{p}})pq-q(1-\varepsilon_\beta)\beta(1-(1-\varepsilon_{\mathrm{p}})p)}{((1-\varepsilon_{\mathrm{r}})r-(1-\varepsilon_\beta)\beta)((1-\varepsilon_{\mathrm{r}})r-r_{\mathrm{L}}-(1-\varepsilon_\beta)\beta(1-\varepsilon_{\mathrm{p}})pq)}\right] \tag{3.14}$$

For the L states we get:

$$L_{\mathrm{c}}(t) = \frac{\beta(1-p)}{r_{\mathrm{L}}+\beta pq-\beta}\left[\exp(-\beta t) - \exp(-(r_{\mathrm{L}}+\beta pq)t)\right] \tag{3.15}$$

$$\begin{aligned} L_{\mathrm{v}}(t) = {} & \frac{(1-\varepsilon_\beta)\beta(1-(1-\varepsilon_{\mathrm{p}})p)}{r_{\mathrm{L}}+(1-\varepsilon_\beta)\beta(1-\varepsilon_{\mathrm{p}})pq-(1-\varepsilon_\beta)\beta}\left[\exp(-(1-\varepsilon_\beta)\beta t)\right. \\ & \left. - \exp(-(r_{\mathrm{L}}+(1-\varepsilon_\beta)\beta(1-\varepsilon_{\mathrm{p}})pq)t)\right] \end{aligned} \tag{3.16}$$

And finally, noticing that $D_x(t) = 1 - S_x(t) - L_x(t) - F_x(t)$ we recover the following results for the active disease states:

$$D_{\mathrm{c}}(t) = 1 - \alpha\exp(-\beta t) + \Omega\exp(-rt) + \gamma\exp(-(r_{\mathrm{L}}+\beta pq)t) \tag{3.17}$$

$$\begin{aligned} D_{\mathrm{v}}(t) = {} & 1 - \alpha'\exp(-(1-\varepsilon_\beta)\beta t) + \Omega'\exp(-(1-\varepsilon_{\mathrm{r}})rt) \\ & + \gamma'\exp(-(r_{\mathrm{L}}+(1-\varepsilon_\beta)\beta(1-\varepsilon_{\mathrm{p}})pq)t) \end{aligned} \tag{3.18}$$

where:

$$\alpha = rr_{\mathrm{L}} + \beta pqr - \beta r_{\mathrm{L}} - \beta pr + \beta pr_{\mathrm{L}} \tag{3.19}$$

$$\Omega = \beta p\frac{r-r_{\mathrm{L}}-q\beta}{(r-\beta)(r-r_{\mathrm{L}}-\beta pq)} \tag{3.20}$$

$$\gamma = \beta r - \beta r_{\mathrm{L}} - \beta pr + \beta pr_{\mathrm{L}} \tag{3.21}$$

$$\alpha' = (1-\varepsilon_{\mathrm{r}})rr_{\mathrm{L}} + (1-\varepsilon_\beta)\beta[(1-\varepsilon_{\mathrm{p}})pq(1-\varepsilon_{\mathrm{r}})r - r_{\mathrm{L}} - (1-\varepsilon_{\mathrm{p}})p(1-\varepsilon_{\mathrm{r}})r + (1-\varepsilon_{\mathrm{p}})pr_{\mathrm{L}}] \tag{3.22}$$

$$\Omega' = (1-\varepsilon_\beta)\beta p\frac{(1-\varepsilon_{\mathrm{r}})r-r_{\mathrm{L}}-q(1-\varepsilon_\beta)\beta}{((1-\varepsilon_{\mathrm{r}})r-(1-\varepsilon_\beta)\beta)((1-\varepsilon_{\mathrm{r}})r-r_{\mathrm{L}}-(1-\varepsilon_\beta)\beta(1-\varepsilon_{\mathrm{p}})pq)} \tag{3.23}$$

$$\gamma' = \beta[(1-\varepsilon_{\mathrm{r}})r - r_{\mathrm{L}} - (1-\varepsilon_{\mathrm{p}})p(1-\varepsilon_{\mathrm{r}})r + (1-\varepsilon_{\mathrm{p}})pr_{\mathrm{L}}] \tag{3.24}$$

Then, we can combine those final equations in order to obtain the disease-ratio at the end of the trial as follows:

$$\rho(T) = \frac{D_{\mathrm{v}}(T)}{D_{\mathrm{c}}(T)} = \frac{[1-\alpha'e^{-(1-\varepsilon_\beta)\beta T} + \Omega'e^{-(1-\varepsilon_{\mathrm{r}})rT} + \gamma'e^{-(r_{\mathrm{L}}+(1-\varepsilon_\beta)\beta(1-\varepsilon_{\mathrm{p}})pq)T}]}{[1-\alpha e^{-\beta T} + \Omega e^{-rT} + \gamma e^{-(r_{\mathrm{L}}+\beta pq)T}]} \tag{3.25}$$

This ratio will depend not only on the parameters of the vaccine (ε_β, ε_{p} and ε_{r}) but also on the natural parameters of the disease (β, p, q, r and r_{L}) and on the trial

follow-up period T. This expression for the disease ratio ρ as a function of ε_β, ε_p and ε_r captures in itself the relation that we looked for, namely, $\mathrm{VE}_\mathrm{dis} = f(\varepsilon_\beta, \varepsilon_\mathrm{p}, \varepsilon_\mathrm{r})$, since VE_dis is estimated as $1 - \rho$.

The disease ratio ρ defines by itself our estimate of VE_dis, since $\mathrm{VE}_\mathrm{dis} = 1 - \rho$. For this reason, the functional relationship $\rho(t = T, \varepsilon_\beta, \varepsilon_\mathrm{p}, \varepsilon_\mathrm{r})$ can be also expressed as $\mathrm{VE}_\mathrm{dis}(\varepsilon_\beta, \varepsilon_\mathrm{p}, \varepsilon_\mathrm{r})$, or, in the specific case where ε_β is assumed to be known (after survival analysis), as $\mathrm{VE}_\mathrm{dis}(\varepsilon_\mathrm{p}, \varepsilon_\mathrm{r})$.

Cracking the trial outcomes: estimation of ε_r In trials conducted on IGRA-negative cohorts, ε_r can be estimated from a truncated fit of uncensored sub-cohorts' transition rates. In this case, a vast majority of all TB cases can be expected to correspond to fast progression after a first infection event. We used our agent-based model to test the validity of this key assumption by tracking the particular paths to disease followed by each individual and seeing how often the disease has been reached by fast progression, slow progression, or after a reinfection event.

To do that, we perform 500 simulations of each cohort solving the agent-based model, and using the probabilistic parameters that are compatible with the reference case of the MVA85A study cohorts[179], that we use as a case example. Then, we record the weight that every possible route has in each cohort, and average across realisations, as the whole process is stochastic. For the vaccine cohort, we propose two POD vaccine descriptions in terms of the parameters ε_p and ε_r that are compatible with the $\mathrm{VE}_\mathrm{dis} = 50\%$ observed in the MVA85A trial.

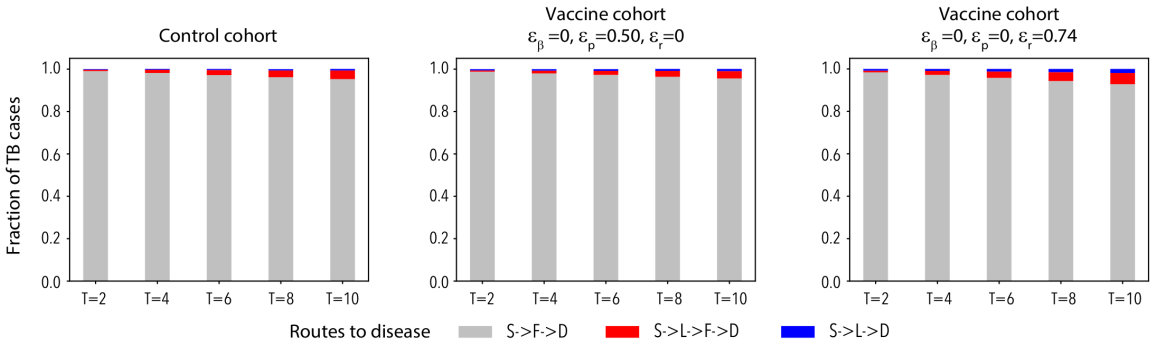

Figure 3.3: Fraction of TB cases that correspond to the three different paths to disease, for different trial durations, in a control cohort (left), a vaccine cohort based on the reduction of the probability of fast progression upon infection (centre, $\varepsilon_\beta = \varepsilon_\mathrm{r} = 0, \varepsilon_\mathrm{p} = 0.5$) and a vaccine cohort based on the reduction of fast progression rates (right, $\varepsilon_\beta = \varepsilon_\mathrm{p} = 0, \varepsilon_\mathrm{r} = 0.74$). Grey fraction corresponds to fast progression, red to reinfection evens and blue to slow progression.

The results of this exercise are represented in Figure 3.3, in a control cohort (left), or in the intervention cohort of the two vaccines, all observed in a 4 years trial, as in

the MVA85A trial. The centre panel corresponds to a vaccine conferring POD through a reduction in the probability of fast progression upon infection ($\varepsilon_{\mathrm{p}} = 0.5$), while the right panel corresponds to its counterpart based on reducing the fast progression rate to TB ($\varepsilon_{\mathrm{r}} = 0.74$). In all the cases explored in Figure 3.3, for different trial sizes and active mechanisms, a minimum of 93% of the individuals that develop active TB came from fast-progression, and less than 2% and 5% made its way through slow progression and reinfection, respectively.

With this assumption working well, we can now derive an independent way of estimating ε_{r}. If we assume that transition from active disease upon infection is a Poisson process, -as it is assumed in the TB modelling literature [196, 144, 197]-, the theoretical probability distribution function (PDF) of the time $t = t_{\mathrm{dis.}} - t_{\mathrm{inf.}}$ between infection and disease of an individual in the control cohort corresponds to an exponential curve $f(t|r) = re^{-rt}$, from which the average transition time $\langle t \rangle = 1/r$ and its associated variance $\sigma_t = \langle t^2 \rangle - \langle t \rangle^2 = 1/r^2$ can be obtained by integrating the moments of the PDF.

However, in a clinical trial, the period of measure cannot be arbitrarily extended, which implies that the maximum transition time that can be observed for a subject who was initially infected at t_{inf} is truncated at $t_{max} = T - t_{\mathrm{inf}}$, where T stands for the follow-up period of the trial. This situation implies that the integrals needed to obtain the expected value of the transition time must be truncated as well, which ultimately makes $\langle t \rangle$ depend on t_{inf}:

$$\langle t \rangle(t_{\mathrm{inf}}) = \frac{\int_0^{T-t_{\mathrm{inf}}} t f(t|r)dt}{\int_0^{T-t_{\mathrm{inf}}} f(t|r)dt} = \frac{1}{r} - \frac{e^{-r(T-t_{\mathrm{inf}})}\,(T - t_{\mathrm{inf}})}{1 - e^{-r(T-t_{\mathrm{inf}})}} \tag{3.26}$$

Similarly, by truncating the integrals of the second moment of the distribution, we can obtain its dependence with time at infection, $\langle t^2 \rangle(t_{\mathrm{inf}})$), and ultimately derive the corresponding expression for the variance of observed transition times as a function of t_{inf}:

$$\begin{aligned} \sigma_t^2(t_{\mathrm{inf}}) \;=\; & \frac{-e^{-r(T-t_{\mathrm{inf}})}\left(1 + (r(T - t_{\mathrm{inf}}) + 1)^2\right) + 2\left(1 + r(T - t_{\mathrm{inf}})e^{-r(T-t_{\mathrm{inf}})}\right)}{r^2\left(1 - e^{-r(T-t_{\mathrm{inf}})}\right)} \\ & -\frac{1}{r^2} - \frac{(T - t_{\mathrm{inf}})^2 e^{-2r(T-t_{\mathrm{inf}})}}{\left(1 - e^{-r(T-t_{\mathrm{inf}})}\right)^2} \end{aligned} \tag{3.27}$$

Equations 3.26 and 3.27 describe how observed transition times from infection to disease and their variance are expected to be biased towards lower values as the infections occur later during the trial. This is simply because the later the infection takes place, the less time available to observe a transition to disease is left. These expressions allow us to isolate the effect of that bias, and to infer, using only data from individuals developing active TB during the trial, the transition rate r within the

control cohort, using a Maximum Likelihood approach (R package *bbmle* [198]) along with its confidence intervals. Then, the exercise is repeated in the vaccine cohort, whose transition rate r^{v}, in terms of our transmission model would be expressed as the product $r(1-\varepsilon_{\mathrm{r}})$, which yields the following expression for the vaccine effect on the fast progression rate ε_{r}:

$$\varepsilon_{\mathrm{r}} = 1 - \frac{r^{\mathrm{v}}}{r} \tag{3.28}$$

Our ability to estimate the vaccine-mediated effects on the incubation rates that are captured by ε_{r} depends, by construction, being able to observe those times in the context of a trial, implying registering the moment when individuals undergo IGRA-conversion, and then, fall sick. Once again, this obviously implies that observing this effect is only possible if we recruit IGRA-negative individuals. In a trial conducted on already infected subjects, the eventual effects that a vaccine might have on incubation rates could never be isolated.

Cracking the trial outcomes: estimation of ε_{p} Once ε_{r} is obtained from the method described above, the next step consists of inferring the last unknown vaccine mechanism ε_{p}, as the effect of the vaccine on the infection rate is captured by $\varepsilon_\beta \equiv \mathrm{VE}_{\mathrm{inf}}$, and, as such, can be inferred using Cox-regression (R package OIsurv [194]). Furthermore, ε_{r} has been independently estimated by analysing times of progression from infection to disease, as described above.

To infer the third vaccine effect -reduction of fast progression probability ε_{p}-, we capitalise on the analytical relationship $\rho = \rho(t, \varepsilon_\beta, \varepsilon_{\mathrm{p}}, \varepsilon_{\mathrm{r}})$ derived on Equation 3.25, that will allow us to solve for ε_{p} once the other parameters, including $\mathrm{VE}_{\mathrm{dis}} = 1-\rho$, have already been estimated. Then, we evaluate $\rho(t = T, \varepsilon_\beta, \varepsilon_{\mathrm{p}}, \varepsilon_{\mathrm{r}})$ at the end of the trial, along with its uncertainty, which is propagated assuming that both D_{v} and D_{c} come from two independent binomial distributions (total number of tests equal to cohort size). Finally, using the independent estimators of ε_β and ε_{r} as well as their uncertainty estimates, we can get our final estimate of ε_{p} solving numerically the Equation 3.25, for which we use the classical Brent method.

To estimate the confidence interval for ε_{p}, we propagate standard error from ε_β (Cox regression), ε_{r} (from Maximum likelihood-based inference of fast-progression rates at control cohort and at vaccine cohort, as explained in the main text) and ρ. Regarding the last source of uncertainty, we obtain the variance associated with the disease fraction as follows:

$$s^2 = \frac{1 - D_{\rm c}(T)}{D_{\rm c}(T)N} + \frac{1 - D_{\rm v}(T)}{D_{\rm v}(T)N} \tag{3.29}$$

which yields the following confidence interval:

$$\mathrm{CI} = 1 - \exp\left(\ln\left(\frac{D_{\rm v}(T)}{D_{\rm c}(T)}\right) \mp z_{1-\frac{\alpha}{2}} s\right) \tag{3.30}$$

where $D_{\rm c}(T)$ and $D_{\rm v}(T)$ are the fraction of cases observed at both cohorts during the follow-up period, and $z_{1-\frac{\alpha}{2}}$ is the standard score for the chosen level of significance α (95%).

Once the estimates of the three parameters ρ, $\mathrm{VE_{inf}} \equiv \varepsilon_\beta$ and $\varepsilon_{\rm r}$ and their uncertainties are available, we use series of N=1000 realisations in which we obtain estimates for each of the three known parameters that are drawn for normal distributions that are coherent with mean and CI of each parameter. Doing this independently for the three parameters, and solving in each set using the Brent method on Equation 3.25, we obtain a distribution of corresponding values for $\varepsilon_{\rm p}$, from which we derive the CI.

Some considerations on the methodology. After following the previous steps, and applying our methodology to the results of a trial, it is expected that the intrinsic efficacies of the vaccine are comprised between 0 and 1, where 1 would mean total efficacy and 0 no effect at all. However, a vaccine can have a negative effect. In the case of efficacies affecting rates (i.e., ε_β and $\varepsilon_{\rm r}$) there is no formal lower limit and a rate equals to ∞ (associated with $\varepsilon = -\infty$) would mean an instantaneous process, although a conservative enough limit of -300 is implemented to avoid numerical instabilities in the codes. On the contrary, $\varepsilon_{\rm p}$ works as a modifier of a probability, which implies that $(1-\varepsilon_{\rm p})p$ has to be comprised between 0 and 1, introducing a lower limit for $\varepsilon_{\rm p}$ that is $\varepsilon_{p,\min} = 1 - \frac{1}{p}$. Furthermore, the existence of such lower bound in $\varepsilon_{\rm p}$ generates, in turn, an upper bound for $\varepsilon_{\rm r}$, since these two parameters are bound through the relationship $\mathrm{VE_{dis}}(\varepsilon_\beta, \varepsilon_{\rm p}, \varepsilon_{\rm r})$. Notwithstanding this, the inference of $\varepsilon_{\rm r}$ is agnostic to the value of ρ or $\varepsilon_{\rm p}$, and, as a consequence, for poor statistical settings –most often in the case of vaccines delaying fast-progression– some individual trial realisations lead to vaccine descriptor estimates that lie beyond these epidemiologically meaningful intervals for parameters $\varepsilon_{\rm p}$ and $\varepsilon_{\rm r}$, and are considered to be failed realisations.

It is important to notice that, if our methodology is applied to real data coming from a real trial, it is equivalent to estimating the vaccine descriptors along with their CIs just from one realisation, so no further calculations are necessary, as there are no more realisations of that particular trial. But, in what follows, we produced *in-silico*

trials of different vaccines to test the accuracy and power of our methodology, so the individual outcomes of each trial should be combined to obtain global estimates and confidence intervals for the vaccine descriptors. To do so, we follow a 3-step approach.

First, we generate a set of 500 synthetic clinical trials for each vaccine analysed. Second, for each of these simulated trials, we infer the values of the vaccine descriptors $\varepsilon_\beta, \varepsilon_{\rm p}$ and $\varepsilon_{\rm r}$ along with their confidence intervals: that of ε_β from Cox-regression, that of $\varepsilon_{\rm r}$, propagated from the maximum-likelihood estimates of $r^{\rm c}$ and $r^{\rm v}$, and, finally, that of $\varepsilon_{\rm p}$ propagated from the other two, and from the CI of the disease ratio ρ. Finally, we assume that the true values of these parameters come from an unweighted mixture of normal distributions each of which is associated with the log transform of one minus the outcome of each simulated trial. The final value and CI of each of the three vaccine descriptors are associated with the median and 95% CI of such distribution mixture, back in the linear scale.

3.2.2.4 Impact evaluations of TB vaccines

Once we have discussed how to characterise a given vaccine from the outcomes of different types of trials, we need a way to evaluate and compare the potential impact of these hypothetical vaccines when applied to larger populations, or in different settings, as the whole point of the complex analyses is to enable the possibility of producing robust impact forecast of new TB vaccines, in a better way than just blindly extrapolating efficacy readouts to other models.

To do so, we take advantage of the *M.tb.* transmission model described in [135], and in Chapter 2 of this thesis, which serves as a tool for the description of *M.tb.* transmission in trans-national settings characterised by different TB burden levels, different demographic trends and mixing patterns across age-groups. Conceptually, the model used to simulate the RCT, depicted in Figure 3.1 is a simplification of the *M.tb.* transmission model that keeps the same dynamics in progressing to active disease, at least, in the first steps before treatment. The most important difference between both formulations is that, while the elementary transmission model described in this work is suited to capture the time evolution of the fraction of susceptible, infected, and sick individuals only within the trials' cohorts and only during the development of the study, the more complex version developed in [135] describes the situation in entire populations, during larger periods (decades).

Nonetheless, introducing a vaccine to the model is simple following our approach. Once the values for the parameters ε_x, which governs the effect of the vaccine either in POI or in POD, are obtained using our methodology, they can be interpreted as the reduction of the transition rates between states that exist in both the reduced and the

M.tb. transmission model. Then, they can be directly used in the big model, to halt the corresponding transitions in the same way that it is done in the reduced version. Here, *M.tb.* transmission model is calibrated to reproduce TB incidence and mortality rates in Ethiopia and, once the model is calibrated, we use it to produce forecasts until 2050 under two different scenarios: one scenario of no-intervention, and another one where a vaccine is introduced by the end of 2025. Then, we obtain impact estimates of the different vaccines analysed in this study as the difference in total TB cases between those two scenarios. In the latter scenario, the spreading model has two branches that evolve at the same time, one for the vaccinated individuals, and another one for the unvaccinated ones.

In the forecasted impacts presented in the following sections, two types of vaccination campaigns are considered, either focused on newborns or adolescents. Newborn vaccination acts on the flux of new births, which, from the moment the vaccination campaign starts is directly introduced within the vaccinated branch instead of the non-vaccinated. Therefore, we are not describing possible delays between birth and vaccination, no matter whether the new vaccine is applied instead of BCG, or in addition to it, where these delays might thus be larger. In regards to vaccines introduced to adolescents, we progressively vaccinate individuals without a history of past TB as they turn fifteen years old from the beginning of the campaign. In both types of vaccination campaigns, the vaccine remains active until the end of 2050, always acting on the same population targets (newborns or fifteen-years-old individuals, who are vaccinated as they turn that age). For simplicity, we have assumed 100% vaccine coverage. Regarding vaccine protection, in the general case, we have assumed a stable, non-decaying profile. We have also conducted simulations where the diverse vaccine parameters ε decay at rates of 1% and 5% per year, modelled through the introduction of decaying protection levels across age groups within the vaccinated cohort.

3.2.3 Testing the first method: results

3.2.3.1 Mapping prevention readouts onto multiple vaccine mechanisms

In the elementary version of *M.tb.* transmission models used to model the first stages of the natural history of TB in an RCT (Figure 3.4A), susceptible individuals (S) are defined by their absence of immunoreactivity to TB, and get infected at a rate β. Upon infection, they split between two classes of infected individuals: F -fast progression to disease-, with probability p, or L, associated with LTBI, with the remaining probability $1-p$. Individuals in groups F and L are latent, unable to spread the disease, but differ in their risk of developing active TB per unit of time. While fast progressors develop

the disease (D) at a rate r associated with typical transition times lower than two years [69], LTBI individuals can remain in latency for decades [199], eventually falling sick, at a rate $r_{\mathrm{L}} << r$. Furthermore, LTBI individuals can suffer a re-infection event, after which a fraction of them will progress rapidly to disease. This event occurs at a rate that is proportional to the product of the basal infection rate times the probability of fast progression upon infection (βp), modulated by a coefficient q that accounts for the protection against fast progression to TB upon re-infection that LTBI confers [96]. For vaccinated subjects, parameters β, p and r may be reduced to $(1-\varepsilon_\beta)\beta$, $(1-\varepsilon_{\mathrm{p}})p$ and $(1-\varepsilon_{\mathrm{r}})r$ respectively, as a consequence of the action of the vaccine (in all three cases $\varepsilon < 1$). Typically, trial duration is too short, and cohort size too small, to observe protective effects related to the rate of progression to disease from LTBI, as the results of Figure 3.3 demonstrate, where the vast majority of all the active disease cases at the end of the trial came from fast progression, even with cohorts of 3000 individuals each.

When a clinical trial is conducted in cohorts of susceptible individuals (IGRA-negative), the entire dynamical process represented in Figure 3.4A can be observed within the context of the study. The infection end-point is usually addressed by IGRA conversion, while the disease is defined upon standard TB diagnosis criteria [179]. The classical approach to interpreting the results of these studies is based on survival analyses and works by analysing the times elapsed until requirements of infection and disease end-points are verified (Figure 3.4, panels B, C). This way, it is possible to infer two efficacy parameters: efficacy against infection $\mathrm{VE_{inf}}$ and against disease $\mathrm{VE_{dis}}$, (i.e. POI and POD [188]). However, in terms of the mathematical model, these two vaccine efficacy observations can arise from at least three independent mechanisms: reduction of susceptibility to infection (via $\varepsilon_\beta > 0$), reduction of the probability of fast progression ($\varepsilon_{\mathrm{p}} > 0$), and reduction of the rate of fast progression to disease ($\varepsilon_{\mathrm{r}} > 0$).

Then, *the problem* arises: how to estimate three independent vaccine mechanisms $(\varepsilon_\beta, \varepsilon_{\mathrm{p}}, \varepsilon_{\mathrm{r}})$ from only two measurements of vaccine efficacy $(\mathrm{VE_{inf}}, \mathrm{VE_{dis}})$? The efficacy measured to a reduction in the probability of getting infected upon contact with an infectious individual is easily matched to POI, as no further processes can occur, which yields $\mathrm{VE_{inf}} \equiv \varepsilon_\beta$. POD, on the other hand, is more complex, and a single readout of $\mathrm{VE_{dis}}$ is compatible with different combinations of effects on fast progression probabilities and transition rates to disease. This can be demonstrated mathematically using the derived Equation 3.25, in which $\mathrm{VE_{dis}} = f(\varepsilon_{\mathrm{p}}, \varepsilon_{\mathrm{r}}, \varepsilon_\beta)$. This equation bounds all the parameters together, and, when a given POI and POD is measured, the quantities $\mathrm{VE_{inf}} \equiv \varepsilon_\beta$ and $\mathrm{VE_{dis}}$ are fixed, giving a whole curve of possible pairs of

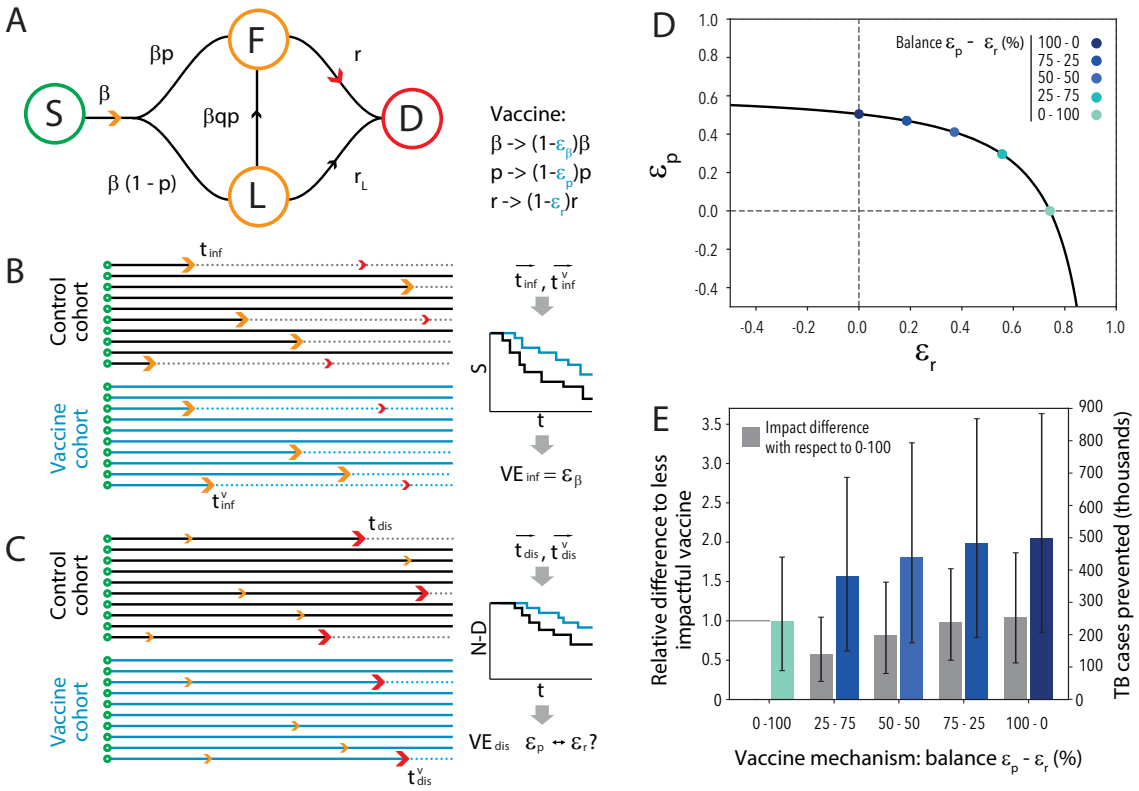

Figure 3.4: Equal prevention readouts from vaccine efficacy trials can map to multiple vaccine mechanisms and expected vaccine impacts. **A**. Elementary *M.tb.* transmission model. S=susceptible, F=Infected, fast progression to disease, L-Infected, slow progression to disease (LTBI), D=active TB. The epidemiological parameters (black) can be modified by the vaccine effects (blue). **B**. From the distributions of transition times between the beginning of the trial (green dots) until end-point infection (orange arrows), survival curves are built for the control and vaccine cohorts, and, from their analysis, VE_{inf} is estimated. **C**. Equivalent schematics for the estimation of VE_{dis} from survival analysis of transition times from trial's beginning (green) to the end-point associated with active TB (red arrows). **D**. Curve of values of (ε_p,ε_r) compatible with a measurement of POD of $VE_{dis} = 0.5$ after 4 years of follow-up (assuming no POI, that is $\varepsilon_\beta = 0$). We have marked 5 different points in this curve, with different balances between ε_p and ε_r, to be used in the next examples. **E**. Foreseen impacts obtained after introducing the vaccines highlighted in Figure 3.4D in Ethiopia, at the end of 2025. Blue bars: vaccines impact. Grey bars: difference in impact estimated between each vaccine and the least impactful case of a vaccine acting entirely through ε_r (lightest blue). Impacts are estimated using a large-scale transmission model as the number of TB cases prevented in the country by the vaccine during the period 2026-2050. Error bars (black bars) represent the 95% confidence interval.

values for $\varepsilon_r, \varepsilon_p$. In Figure 3.4D this relation is depicted for a case with $VE_{dis} = 50\%$ and $\varepsilon_\beta = 0$.

Importantly, this issue is an unavoidable consequence of incubation periods of fast progression to TB being of the same order as the maximum follow-up periods affordable in this type of trial. This makes it possible to confound an eventual delay in incubation

(i.e. ε_r) with genuine vaccine-mediated prevention of fast progression to TB (i.e. ε_p). In this sense, this is not an artefact of the modelling architecture chosen, and the same ambiguity can be easily recovered by choosing other possible architectures, as long as these include a description of the time of incubation of fast progression to TB [192].

Now, that the anticipated problem has appeared, a second question arises: do vaccines with a common value of VE_{dis}, but acting through different combinations of $(\varepsilon_p, \varepsilon_r)$ produce equivalent impacts when applied on large populations?

To answer this question, we capitalised on the *M.tb.* transmission model for trans-national settings described in Chapter 2 of this thesis. Using this model, we simulated the introduction of different types of vaccines at the end of 2025, in a high-burden country such as Ethiopia, and estimated their impact, measured as the total number of TB cases prevented until 2050, upon an immunisation campaign that targets newborns. We assume an ideal scenario of 100% vaccine coverage, with long-lasting vaccine effects. The results of this exercise are shown in Figure 3.4E for five vaccines with the combinations of parameters marked in Figure 3.4D, all sharing a common value of VE_{dis}. For this particular case, a vaccine preventing fast progression to disease (via ε_p) is expected to prevent as many as 256000 more TB cases (95% CI: 104-466 $x10^3$) than a vaccine based on delaying it (via ε_r), even if the values of these parameters in either case ($\varepsilon_p = 0.5$ vs. $\varepsilon_r = 0.74$) are compatible with the same efficacy readout $VE_{dis} = 50\%$ obtained from a 4 year-trial. This amounts to a relative difference of 104% (82-144 95% CI) concerning the least favourable case.

In a more realistic scenario where the vaccine has waned over time, such deviation is also significant. In Figure 3.5, we show the results of forecasting the impact of the same previous 5 vaccines but with decaying protection levels across age groups within the vaccinated cohort. The decay happens at rates of 1% and 5% per year, and we recover the same observation as before, yielding 120% (CI 93-161%) relative difference, concerning the least favourable case, for 1% immunity waning per year, and 176% (CI 139-224%) for 5%. That is, these patterns of immunity waning do not interfere with the observation that impacts associated with vaccines that lean on different dynamical mechanisms to provide analogous readouts of VE_{dis} are significantly different when evaluated at larger demographic and temporal scales.

3.2.3.2 Testing the methodology to gauge vaccine mechanisms from trials data

As shown before, a given measure of VE_{dis} is compatible with several combinations of ε_r and ε_p, and vaccines acting through different mechanisms show different impacts when forecasted in bigger populations. In the following lines, we test the proposed

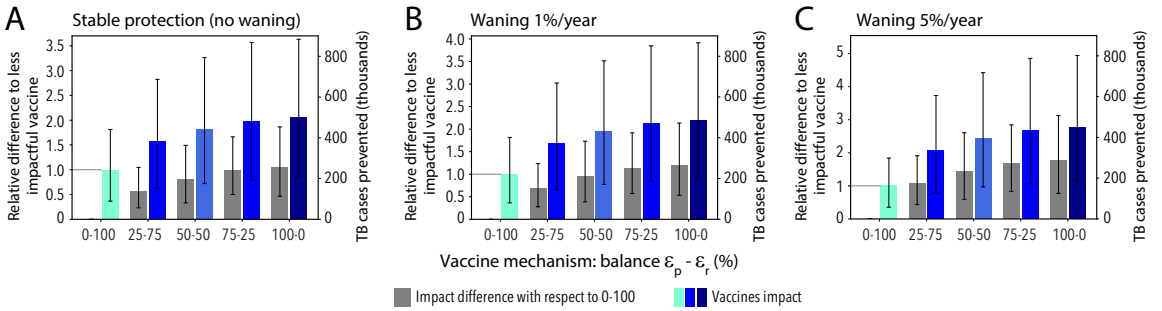

Figure 3.5: Impact foreseen for several POD vaccines characterised by different combinations of the initial values of their parameters ε_{p}-ε_{r}, under different scenarios regarding protection waning after vaccination. **A**. Reference scenario: persistent protection. **B**. Moderate waning: ε_{p} and ε_{r} decay at a rate of 1% per year. **C**. Strong waning: they decay a 5% every year. Error bars (black bars) represent the 95% confidence interval.

methodology that makes use of an analytical approach to estimate independently the different mechanistic contributions to vaccine POD (ε_{r} and ε_{p}). The summary of the situation is that ε_β is directly equivalent to the POI readout ($\varepsilon_\beta \equiv \mathrm{VE}_{\mathrm{inf}}$), and can be estimated through Cox regression, but ε_{r} and ε_{p} cannot, since multiple combinations of them are compatible with a single efficacy readout (Figure 3.4D).

To break this degeneracy, we perform another independent statistical analysis to estimate ε_{r} in addition to the estimation of $\mathrm{VE}_{\mathrm{inf}}$ and $\mathrm{VE}_{\mathrm{dis}}$. This complementary analysis trusts in the comparison of the transition times between end-point infection and end-point disease across cohorts (Figure 3.6A). To do so, we assume that all TB cases observed in a trial correspond exclusively to fast progressors, which is not far from the reality as Figure 3.3 shows.

Within this assumption, we derived an analytical expression for the expected distribution of transition times observed between IGRA conversion and TB diagnosis $t = t_{\mathrm{dis}} - t_{\mathrm{inf}}$. This distribution $t = \Psi(r_{\mathrm{cohort}}, t_{\mathrm{inf}})$ depends only on the transition rate to disease of the cohort under analysis (r for the control cohort, or $r(1-\varepsilon_{\mathrm{r}})$ for the vaccine one). Using a maximum-likelihood approach it is possible to infer these two parameters from the transition times's data in both cohorts and use them to estimate ε_{r} (see Figure 3.6B, and Methods).

Finally, with an independent estimation of ε_{r}, plus the measures of both $\mathrm{VE}_{\mathrm{inf}}$ and $\mathrm{VE}_{\mathrm{dis}}$, the analytical relationship $\mathrm{VE}_{\mathrm{dis}} = f(\varepsilon_\beta, \varepsilon_{\mathrm{r}}, \varepsilon_{\mathrm{p}})$ previously derived (in Methods I, Equation 3.25 and Figure 3.4D), can be solved for the only parameter that remains unknown: ε_{p}. The result of the whole exercise is a full description of the vaccine through $(\varepsilon_\beta, \varepsilon_{\mathrm{r}}, \varepsilon_{\mathrm{p}})$.

To test the performance of our approach we use Monte Carlo methods, simulating

clinical trials of different dimensions for different vaccines (Figure 3.6C) [200]. The procedure is as follows: for a cohort size N and follow-up period T, we define as inputs the ground truth values of the vaccine parameters $(\varepsilon_\beta, \varepsilon_\mathrm{r}, \varepsilon_\mathrm{p})$, and we apply our approach to calibrate how well the method captures those values. To do so, we simulate the stochastic development of possible realisations of the trial using an agent-based implementation of the model represented in Figure 3.4A. From these synthetic trials, we recover two vectors of transition times to infection and TB across participants. Using this data, we apply our method to characterise the vaccine and evaluate its goodness comparing the results to the a-priori-known ground-truth values. Since the model is stochastic, we iterate to obtain a set of simulated trials that yield a distribution of most likely outcomes conditioned both by trial dimensions and vaccine characteristics.

The first metric to quantify our method's performance captures if the estimates produced lie within epidemiologically meaningful ranges often enough. To test that, we defined meaningful intervals for the vaccine-mediated reduction of fast transition rates (ε_r) and probability of fast progression (ε_p) by imposing a series of basic requisites (see Methods I: a vaccine cannot delay fast-progression to disease to make it slower than slow progression, or modify probabilities of fast progression that go beyond the interval $[0, 1]$). Then, we label as failed attempts the simulations that, due to insufficient statistics, derive parameter estimates that go beyond those intervals. In Figure 3.6D we represent the fraction of simulations yielding valid inferences of vaccine descriptors, for the five vaccines marked in Figure 3.4D (0-100 to 100-0). For a trial such as the MVA85A, with a cohort size of $N = 3000$ and a follow-up period of $T = 4$ years, only a vaccine acting exclusively through ε_r yields a probability of observing a failed trial that surpasses 1%, which enhances the usability of our methodology.

For the comparison between the distribution of inferred estimates and ground-truth values used to produce the *in-silico* trials, our method succeeds at producing median estimators that closely resemble the ground truth for different vaccines, as shown in Figure 3.6E. The maximum deviation between median estimates and ground truth values is equal to 0.03 standard deviations, although with a vast uncertainty which is caused by the low sample size.

Hence, uncertainty might undermine the workability of our method, particularly if the cohort's size is small or the trial is too short to guarantee enough statistical data. To gain insight into this matter, we conducted simulations involving varying trial sizes and durations for the two vaccines illustrated in Figure 3.6E. In each scenario, we assessed the probability of achieving a successful simulation that produces a reliable inferred parameter for the driving mechanism, that is, one that is both valid (excluding unsuccessful trial runs) and statistically significant (with a 95% non-crossing zero

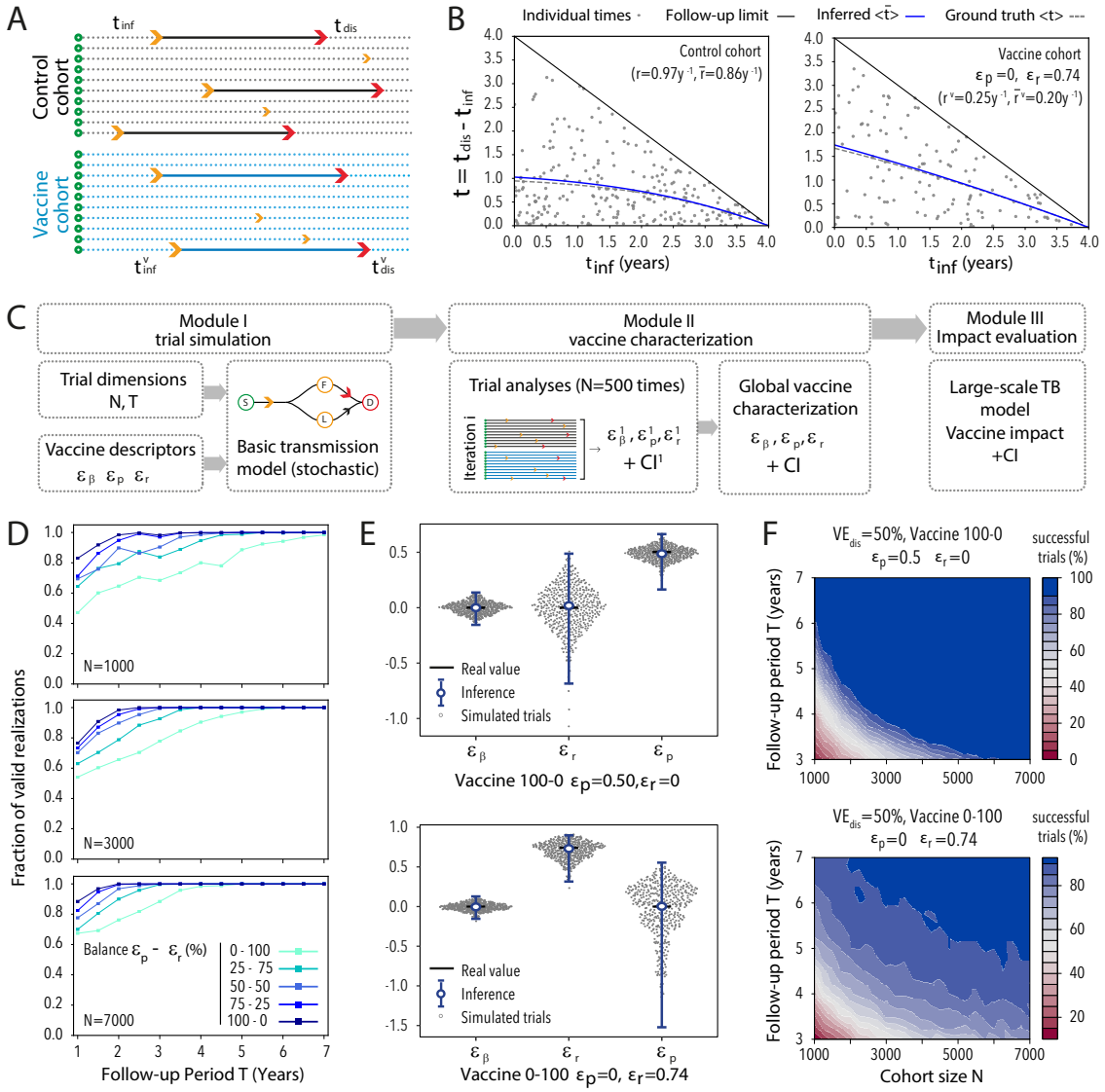

Figure 3.6: Testing of the methodology to measure vaccine mechanisms in clinical trials with naive cohorts. **A**. Inference of ε_{r}. From the clinical trial data we get the distribution of times from infection (orange) to disease (red). **B**. Using mle and the transition times, we infer the transmission rates to disease, r^{c} in control cohort (left) and r^{v} in vaccine cohort(right: vaccine acting through ε_{r}), that are associated with expected values for the transition times (blue, continuous lines) that closely resemble the a priori known analytical predictions (dashed lines). From these estimates, ε_{r} is estimated as $1 - r^{\mathrm{v}}/r^{\mathrm{c}}$. **C**. Schematic representation of the computational pipeline for the analysis of clinical trials conducted on IGRA-negative cohorts. Module I: trial simulation: From a given vaccine $(\varepsilon_\beta, \varepsilon_{\mathrm{r}}, \varepsilon_{\mathrm{p}})$ and trial dimensions (N, T) we simulate 500 equivalent trials. Module II: vaccine characterisation and estimation of ε_β, ε_{r} and ε_{p} with our methodology. Module III: impact evaluation. Forecast of characterised vaccines's impact with a transmission model. **D**: Fraction of valid realisations of a trial yielding epidemiologically plausible vaccine parameterisations, (excluding failed attempts). **E**. Vaccine characterisation of $\varepsilon_\beta, \varepsilon_{\mathrm{r}}, \varepsilon_{\mathrm{p}}$. Error bars represent the 95% confidence interval of the median value. **F**. Estimated probability of obtaining a trial result leading to a successful characterisation of ε_{p} (up) or ε_{r} (bottom) (CI not crossing 0 at a 95% confidence level for parameters with non-zero ground-truth values).

confidence interval). The results of this exercise are shown in Figure 3.6F, where a vaccine that reduced the probability of fast progression (ε_{p}, top) is easier to characterise than a vaccine that delays it (ε_{r}, bottom). For a trial of $N = 3000$ and $T = 4$ years, the first vaccine will be successfully characterised with $p = 0.95$, while, for the second vaccine, that probability of success goes down to $p = 0.75$.

All the results presented in Figure 3.6 correspond to a vaccine that provides POD, but not POI (that is: $\varepsilon_\beta = 0$). In Figure 3.7 we show that, for vaccines conferring at the same time significant levels of POI and POD, the methods presented here can be equally applied, even if, in this scenario, the mechanistic variability underlying POD becomes quantitatively less important.

In Figure 3.7A we recover the same behaviour of the balance curve between $\varepsilon_{\mathrm{p}}, \varepsilon_{\mathrm{p}}$ for a single readout of $\mathrm{VE}_{\mathrm{dis}}$, as in the case without POI, which yields also different expected impacts for the five marked vaccines, as shown in Figure 3.7B. Here, the relative difference between the first vaccine ($\varepsilon_\beta = 0.25, \varepsilon_{\mathrm{p}} = 0.35, \varepsilon_{\mathrm{r}} = 0$) and the last one ($\varepsilon_\beta = 0.25, \varepsilon_{\mathrm{p}} = 0, \varepsilon_{\mathrm{r}} = 0.62$) is 41% (35-49, 95% CI), less than in the case without POI, but still yielding differential impacts. Moreover, in Figure 3.7C, we also recover the same qualitative dependency in the value of $\mathrm{VE}_{\mathrm{dis}}$ with the follow-up period of the trial.

Then, concerning the method to measure ε_β, ε_{p} and ε_{p}, in Figure 3.7D, E, and F we presented the results of the characterisation of the vaccines $100 - 0$ and $0 - 100$, with a fixed $\varepsilon_\beta = 0.25$. The results of this additional analysis ensure that, even in cases in which the tested vaccine acts through combinations of POD and POI-related mechanisms, it is robust enough to provide a more complete characterisation of its mechanistic effect.

3.2.3.3 Impact evaluation of empirically characterised vaccines

Summarising, up to this point we have described and tested the applicability of our method to estimate the different mechanistic contributions to vaccine POD from the analysis of IGRA-negative trials data. One of the main drivers of the development of the method is illustrated in Figure 3.4E and in Figure 3.5, which is the fact that the impacts of vaccines leaning on different combinations of these mechanisms are highly dependent upon the driver mechanism giving protection. However, in those previous analysis, the uncertainty of impact estimates does not come from vaccine descriptions, which were considered error-free, but was only derived from the transmission model. Therefore, it remains pending to address the role of the additional uncertainty introduced in impact forecasts that are due to our limited resolution when estimating vaccine parameters.

To address this question, we turn back to the transmission model used to estimate

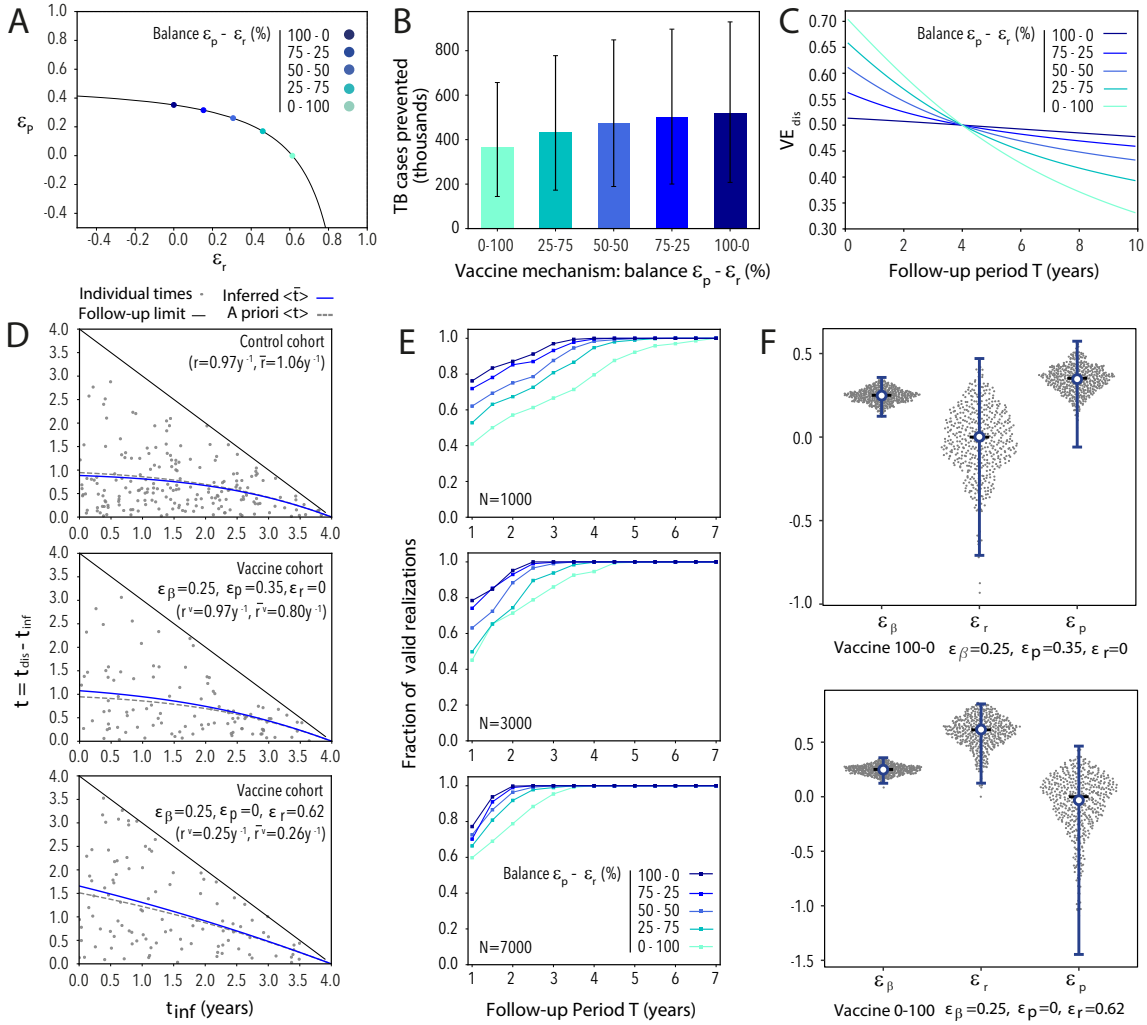

Figure 3.7: characterisation of vaccines conferring simultaneously POI and POD. These vaccines are compatible with the same measurements of efficacy against disease (same $\mathrm{VE}_{\mathrm{dis}}$ after 4 years), but having also efficacy against infection. **A**. Curve of values of (ε_{p},ε_{r}) compatible with a measurement of $\mathrm{VE}_{\mathrm{dis}} = 0.5$ after 4 years of follow-up (assuming $\varepsilon_\beta = 0.25$). We have marked 5 different points in this curve to be used in next panels. **B**. Predicted impacts after introducing the 5 highlighted vaccines in Ethiopia during the period 2025-2050. **C**. Evolution of measurement of $\mathrm{VE}_{\mathrm{dis}}$ for the 5 highlighted vaccines as a function of the follow-up period. **D**. Transition times for the control cohort, and the vaccine cohort for the two vaccines considered (balance 0-100 and 100-0). These vaccines have a smaller effect on the pathways against disease, so the number of transitions remains, approximately, the same; and our method is able to extract the rates of fast-progression. **E**. Probability density of the inferred parameters of the vaccines ($\varepsilon_\beta, \varepsilon_{\mathrm{r}}, \varepsilon_{\mathrm{p}}$), alongside the inferred parameters (with their respective CI) for two different vaccines: ε_{p}-based (top) and ε_{r}-based (bottom) (additionally to the protection against infection $\varepsilon_\beta = 0.25$). **F**. Fraction of correct realisations of a trial (i.e. with an epidemiologically plausible parametrisation) as a function of the follow-up period, for three different cohort sizes and 5 different vaccines. Error bars (black bars in B and blue bars in F) represent the 95% confidence interval.

impacts and we study how the uncertainty in vaccine characterisation propagates into impact evaluations. First, we simulate sets of trials for vaccines of efficacy against disease (VE_{dis}) of 25%, 50% and 75%, leaning on different values for ε_r and ε_p. Then, we use our methodology to infer the values of these parameters, along with their corresponding uncertainty intervals. With the median values and the CI, we feed the transmission model to estimate vaccine impact in Ethiopia for a hypothetical vaccination strategy implemented on newborns between the end of 2025 and 2050, as done in the previous impact forecasts. Now, we also use the CI knowledge to compute the impact using the extreme values, and those results are propagated to estimate the final CI of the impact forecast.

The results of these analyses are shown in Figure 3.8. In all cases, both the reference one with $VE_{dis} = 50\%$, and for efficacy equal to 25% and 75%, we observe significant differences in impact when comparing vaccines that depend on the two mechanisms studied (relative difference between a ε_p-based vaccine and a ε_r vaccine equal to 165% (CI 127-224%) for $VE_{dis} = 0.25$, and 48% (CI 37-66%) for $VE_{dis} = 0.75$, concerning the vaccine acting through ε_r).

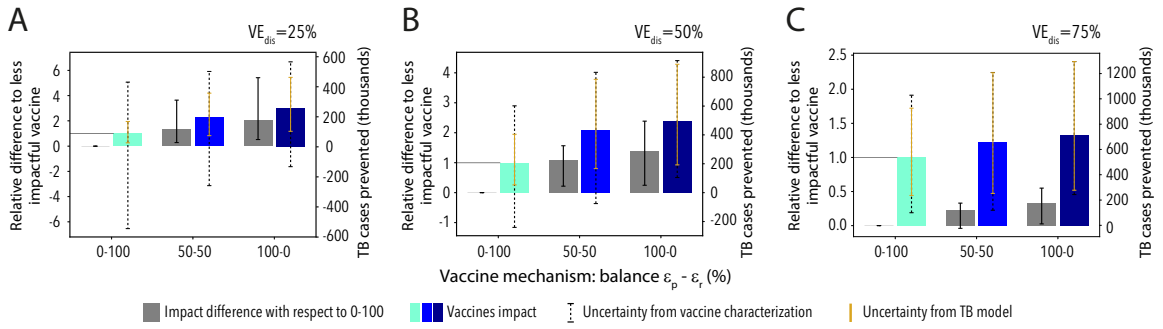

Figure 3.8: Impact evaluation of empirically characterised vaccines with associated uncertainty. **A**. Vaccines characterised from an efficacy readout of $VE_{dis} = 25\%$. **B**. Vaccines characterised from an efficacy readout of $VE_{dis} = 50\%$. **C**. Vaccines characterised from an efficacy readout of $VE_{dis} = 75\%$. In all panels, blue bars represent the impact estimates for each vaccine. There are two different contributions to overall impact uncertainty. Gold bars capture the intrinsic contribution coming just from the transmission model. Black-dashed bars capture the extra contribution that came from uncertain vaccine characterisations. In all three panels, grey bars compute the differences in impact between each vaccine and the least impactful case of a vaccine acting 100% through ε_p. All error bars represent the 95% confidence interval.

Under the light of the results of Figure 3.8, the uncertainty of vaccine characterisation adds to the rest of the uncertainty sources of the transmission model, contributing to total impact C.I.'s with a fraction that varies from 3.3% to 85.3%, depending on vaccine efficacy levels and mechanisms.

In our calculations, this big uncertainty prevents us from rejecting the null impact in more than one-half of the cases explored as the intervals cross zero. The vaccines that are based exclusively on ε_r and/or those characterised by low VE_{dis} (25%), as well as for the mixed vaccine with $VE_{dis} = 50\%$ suffer from this more than the others. Nonetheless, the results of Figure 3.8 show that the differences between the impacts estimated by vaccines leaning on different combinations of ε_r-ε_p for the same values of VE_{dis} (grey bars) are still significant regardless how uncertain vaccine characterisation is, which remarks the importance of our -or similar- approaches.

3.2.4 Evidence of the same problem in other architectures

The problem presented in previous sections warns us against plugging directly the outcome of clinical trials conducted on cohorts of IGRA-negative individuals to spreading models without first analysing the mechanistic effect of the vaccine at play. It would be legit to think that this is just a problem that arises as a consequence of the very basic architecture of the trial, but this is not true. Given the complexity of the transmission chain in TB, specifically when dealing with POD vaccines, the protective effect of a vaccine is difficult to map to one specific mechanism of action using only the classical measures, and this is independent of the architecture that models the initial steps of the progression to disease in recently infected individuals, as long as they include a separate description of fast and slow progressors.

For instance, the results from the candidate M72/AS01E [180] have shifted the focus to an alternative design, conducted among TB-, IGRA+ individuals without a past of active TB. In this kind of trial, the episodes of incident TB to be observed during the study can be divided into three different groups or routes to disease. First, some of the individuals whose IGRA conversion had occurred relatively recently will be expected to progress to primary TB during the first 12-24 months after exposure to the pathogen, which will typically overlap with the follow-up period. This happens at a fast progression rate denoted here as r. Second, enrolled individuals whose IGRA+ status is associated with a latent TB infection (LTBI, linked to an exposure that occurred, typically, > 2 years before the beginning of the study) would be at a much lower risk of experimenting endogenous reactivation during the trial, mapped to a slow transition rate denoted as r_L in Figure 3.9, with $r_L << r$. Third, enrolled individuals may undergo primary TB followed upon re-exposure to the pathogen during the study, which happens at a rate proportional to $\beta \cdot q \cdot p$, where β means the basal force of Infection, and q is a reduction coefficient capturing the relative risk of infection of previously infected (IGRA+) concerning unsensitised individuals (IGRA-). These three possible routes to active TB, sketched in the compartmental model diagram in Figure 3.9, are

classically referred to as the "three risks model" [105], a frame coined by Vynnycky and Fine in 1997[106].

In Figure 3.9A we distinguish each of them according to one of the most commonly assumed model structures found in TB modelling literature[192]. In this case, we could expect to find two different sub-populations of individuals in each of the cohorts. First, a group of subjects who were infected on average a long time ago, and are assumed to be LTBI carriers (slow latency reservoir, L), and those infected more recently and who would be progressing through the sub-clinical TB spectrum [201] (fast latency reservoir F). The system of equations that describe this situation, and the model depicted in Figure 3.9A, would be:

$$\frac{dF(t)}{dt} = -(1-\varepsilon_{\mathrm{r}})rF(t) + (1-\hat{\varepsilon}_{\mathrm{p}})\beta pqL(t) \tag{3.31}$$

$$\frac{dL(t)}{dt} = -r_{\mathrm{L}}L(t) - (1-\hat{\varepsilon}_{\mathrm{p}})\beta pqL(t) \tag{3.32}$$

$$\frac{dD(t)}{dt} = (1-\varepsilon_{\mathrm{r}})rF(t) + r_{\mathrm{L}}L(t) \tag{3.33}$$

One crucial difference between this case and the previous one is that, in the former case, all N individuals recruited begin the trial within the state S, but now, they should be distributed between states. If, ideally, the cohorts have the same size, and the number of fast progressors is the same in both cohorts -which is extremely unlikely-, the recruited individuals would be distributed between F and L as follows: $F_x(t=0) = F_0$, and $L_x(t=0) = N - F_0$ for $x = c, v$. This introduces one additional unknown parameter, namely, the number of individuals F_0 that begin the trial within the state F in each cohort.

In this case, the same kind of multiple-interpretation issue that we described above is equally pertinent, as the vaccine might be delaying the progression to disease of F individuals (through ε_{r}), or it might protect the LBTI individuals against disease progression after a secondary infection event registered during the trial. This effect is parametrised as $\hat{\varepsilon}_p$, and would relate the parametrisation of the IGRA-negative case through the relation $(1-\hat{\varepsilon}_{\mathrm{p}}) \equiv (1-\varepsilon_\beta)(1-\varepsilon_{\mathrm{p}})$. Moreover, an eventual effect of a vaccine on r_{L}, could possibly be observed, but only with arguably prohibitive cohort size and/or trial duration, and with a negligible contribution of fast progressors and re-infections, which is only possible in low burden settings. Since these conditions are not met in the type of studies that the community is currently engaged in [179, 180], the observation of these effects in the trials here analysed would be unlikely, and, therefore, we do not consider it. Using these parameters to model the mechanistic effect of the vaccine, the resolution of the ODEs in this case yields the following evolution of the latency compartments:

$$F_{\mathrm{c}}(t) = F_0 \exp(-rt) + \frac{\beta pq L_0}{r - r_{\mathrm{L}} - \beta pq} \left[\exp(-(r_{\mathrm{L}} + \beta pq)t) - \exp(-rt)\right] \tag{3.34}$$

$$F_{\mathrm{v}}(t) = F_0 \exp(-(1-\varepsilon_{\mathrm{r}})rt) + \frac{(1-\varepsilon)\beta pq L_0}{(1-\varepsilon_{\mathrm{r}})r - r_{\mathrm{L}} - (1-\varepsilon)\beta pq} \left[\exp(-(r_{\mathrm{L}} + (1-\varepsilon)\beta pq)t) - \exp(-(1-\varepsilon_{\mathrm{r}})rt)\right] \tag{3.35}$$

$$L_{\mathrm{c}}(t) = L_0 \exp(-(r_{\mathrm{L}} + \beta pq)t) \tag{3.36}$$

$$L_{\mathrm{v}}(t) = L_0 \exp(-(r_{\mathrm{L}} + (1-\varepsilon)\beta pq)t) \tag{3.37}$$

Then, as the population is conservative, the rule $N_x = F_x(t) + L_x(t) + D_x(t)$ allows to compute the evolution of the active disease reservoirs.

$$D_{\mathrm{c}}(t) = N_0 - L_0 \exp(-(r_{\mathrm{L}} + \beta pq)t) - F_0 \exp(-rt) + \frac{\beta pq L_0}{r - r_{\mathrm{L}} - \beta pq} \left[\exp(-(r_{\mathrm{L}} + \beta pq)t) - \exp(-rt)\right] \tag{3.38}$$

$$D_{\mathrm{v}}(t) = N_0 - L_0 \exp(-(r_{\mathrm{L}} + (1-\varepsilon)\beta pq)t) - F_0 \exp(-(1-\varepsilon_{\mathrm{r}})rt) + \frac{(1-\varepsilon)\beta pq L_0}{(1-\varepsilon_{\mathrm{r}})r - r_{\mathrm{L}} - (1-\varepsilon)\beta pq} \left[\exp(-(r_{\mathrm{L}} + (1-\varepsilon)\beta pq)t) - \exp(-(1-\varepsilon_{\mathrm{r}})rt)\right] \tag{3.39}$$

From these expressions, we obtain the disease-ratio at the end of the trial as follows:

$$\rho(T) = \frac{D_{\mathrm{v}}(T)}{D_{\mathrm{c}}(T)} \tag{3.40}$$

This time, Equation 3.40 defines a functional relation $\rho = f(F_0, \varepsilon_{\mathrm{r}}, \hat{\varepsilon}_{\mathrm{p}})$ that does not allow to solve for $\hat{\varepsilon}_{\mathrm{p}}$, as the initial fraction of fast progressors F_0 can not be easily determined during trial recruitment. This parameter introduces an unknown degree of freedom in the functional relationship between $\mathrm{VE}_{\mathrm{dis}}$ and the vaccine parameters, but also turns the curve of values $\hat{\varepsilon}_{\mathrm{p}}$ - ε_{r} compatible with a given efficacy readout of $\mathrm{VE}_{\mathrm{dis}}$, and an estimation of ε_β, into the envelope of a whole family of curves. As a result, we can only derive, using numerical solvers (Brent method from Scipy v1.3.0, in Python), the relation that is established between ε_{r} and $\hat{\varepsilon}_p$, for different levels of F_0, and different observations of $\mathrm{VE}_{\mathrm{dis}} = 1 - \rho$. For $\varepsilon_\beta = 0$, we have now the envelope of a parametric family of curves (as shown in Figure 3.9B).

This exacerbates, by construction, the multiplicity of different combinations of vaccine mechanisms that could underlie the readout of a trial. But, even if we knew how many of the individuals begin the trial in the F vs L reservoirs, we would not have enough information to estimate independently the eventual vaccine-mediated delay of incubation periods of fast progressors ε_{r}, since we do not know the IGRA-conversion times, and therefore we cannot observe the times between infection and disease.

As a consequence, the interpretation of the outcomes of a trial such as the one of M72/AS01E [180] is hindered by the very study design. The uncertainty of any vaccine impact evaluation that does not obviate the possibility of observing different vaccine

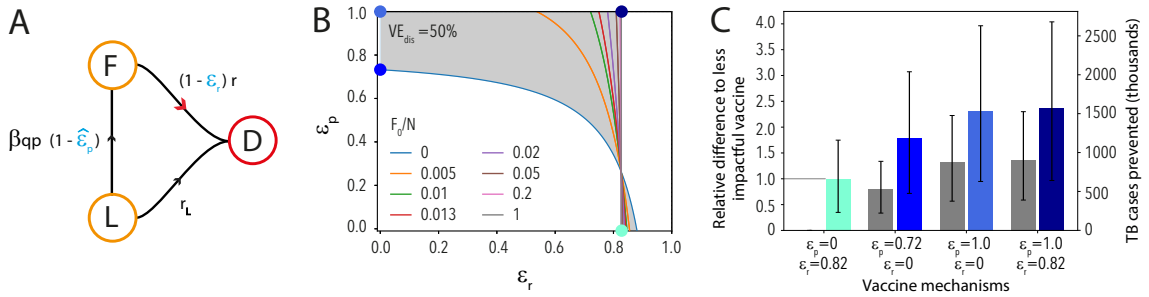

Figure 3.9: Vaccine characterisation from clinical trials conducted on IGRA-positive individuals. **A**. Section of the transmission chain that is observed during a trial conducted on cohorts of IGRA-positive individuals. Recruiting IGRA-positive participants turns possible to observe a vaccine-mediated protection against fast progression to TB upon re-infection during the trial (i.e. $\hat{\varepsilon_p}$), in addition to a delay in the transition rate to disease (ε_r). **B**. Family of curves that bound VE_{dis}, $\hat{\varepsilon_p}$ and ε_r for different levels of the fraction of individuals recruited within the reservoir F: $F/(L+F)$. The shaded area represent the whole set of points ($\hat{\varepsilon_p}$,ε_r) that are compatible with a single readout $VE_{dis} = 50\%$, when the basal epidemiological parameters of the population are the same used in previous sections. The dots represent four extreme vaccine examples whose impacts are to be estimated later **C**. Different impacts foreseen from the four extreme vaccines highlighted in panel B (blue bars), and differences with respect to the least favourable interpretation (grey bars). Error bars (black bars) represent the 95% confidence interval.

mechanisms of action gets compromised. In Figure 3.9 we forecast the impact of a vaccine showing $VE_{dis} = 50\%$, analysed on a trial conducted on adolescent population (15 years old individuals), for several combinations of the vaccine parameters. The epidemiological parameters in the trial are the same as before, but the probability of fast progression upon infection is fixed at $p = 0.15$ to capture the situation of adolescents/adults, as this type of design is more commonly considered within the context of studies conducted on adolescents and/or adults.

The results show that the differential effects of vaccine mechanisms on impact estimates also appear beyond the context of vaccines applied to newborns. As shown in Figure 3.9C these differences translate into a wide variety of possible impacts, (maximum impact is 136% higher than the minimum one (CI: $114 - 180\%$). This difficulty in characterising the mechanistic effect of the vaccine, again, adds up to the uncertainty that is intrinsic to the production of model-based forecasts themselves, reinforcing the pertinence of more powerful approaches to analyse trial outcomes.

3.2.5 Some considerations on the first method and results

In trials trusting in the recruitment of IGRA-negative individuals without a past of TB, we have uncovered an interesting problem that bias the characterisation of new TB vaccines when using only classical analysis of clinical trials's outcome, specifically, in TB vaccines conferring POD. In those cases, vaccine protection can be attributed to several dynamic mechanisms, as a vaccine can protect by either slowing down the fast progression to disease or by preventing it. But as we have seen before, those mechanisms cannot be disentangled by classical survival analysis alone.

This reality makes trial readouts hard to mix with transmission model architectures, which constitutes a relevant issue. That's because vaccines that differ in the mechanisms through which POD takes place are expected to cause significantly different impacts, even when they appear equally effective in the context of a clinical trial. Moreover, our results indicate that prevention of fast progression to TB upon infection should be recognized as a preferred product characteristic for TB vaccines instead of the delay of incubation periods[202]. Vaccines that are based on delaying the incubation period are comparatively less impactful and harder to characterise successfully than their counterparts. This observation is equally valid regardless of the age group to target, for they are robust under a series of alternative epidemiological assumptions, including values of the basal parameters characteristic of both infants and adults.

Our conclusions are not exempt from other limitations, though. First, the possible vaccine mechanisms of action analysed here are not the only possible. In principle, a vaccine can disrupt the dynamics of the natural history of the disease at any point[203], and yet these effects would be virtually impossible to observe in trials within phases 2b/3 with the discussed architectures and characteristics. Furthermore, it is important to highlight that model-based impact evaluation of vaccines is always a daunting task, especially in TB. The importance of aspects such as the uneven quality of the empiric evidence behind the many parameters these models rely on, or the assumption that all IGRA-positive readouts can be interpreted as real latent infection cases cannot be overstated[69]. Also, heterogeneities in clinical outcomes due to either host, pathogen, or environmental variability impose an additional layer of complexity that goes beyond the phenomena discussed here, whose interaction with vaccine function needs to be assessed too. Concerning the impact estimates that we provide in this study, they have been obtained from vaccine assumptions that are to a great extent an idealisation, such as the 100% coverage levels, long-lasting duration of protection, and immediate acquisition of immunity upon vaccination. However, the differences between the cases associated with different mechanisms are robust under different vaccine scenarios, such

as different basal efficacy levels, different levels of protection waning, and combinations of POI/POD effects.

There are two additional limitations to highlight in the case of IGRA-negative designs. First, our approach can only be of use if sufficient statistics are available. This means high levels of basal TB incidence, and trials of enough follow-up period and cohort size are mandatory. Second, there is a maximum duration of trials for which our method would still be sensible. This limitation arises because our ability to estimate ε_{r} relies on the assumption that all individuals who develop active TB during the trial are fast progressors. This assumption becomes less valid as the follow-up period increases. Furthermore, both infection and disease risks in TB are known to be strongly age-dependent. Then, the usage of a single set of epidemiological parameters (mainly β and p) in the basal model may not be accurate and introduce bias. That's because this parametrisation would be valid for individuals of a given age, but not if the study is too long. Regarding this, the methods here described could be granted with age structure to estimate vaccine effects conditioned to the variation of basal epidemiological parameters with age and to estimate how vaccine effects change with time since vaccination, provided that enough statistics are available.

In any case, the method proposed in this section narrows the gap between trial-derived efficacy estimations and model-based impact evaluations. Our results have shown that the combination of Monte-Carlo methods and compartmental models constitutes a powerful resource to make substantial progress in that direction. It also may serve to advise trial designers about the differential advantages of different possible trial dimensions and designs, along with other practical implications. As demonstrated in this work, it is necessary to reconcile the interpretation of trial results with the formulation of the mathematical models used to evaluate vaccine impact, as it is key to reducing uncertainty in impact evaluations. This improvement of the impact evaluation could serve to help with the evaluation of candidate vaccines and reduce risk in the decision-making processes of funding agencies and public health authorities.

3.3 A workable algorithm to analyse RCT's based on IGRA+ population

3.3.1 A bit of context

The lack of data about the IGRA conversion times in trials such as the M72/AS01$_E$ vaccine prevents us from trusting in time-based algorithms to measure independently the effect of the vaccine over the fast progression to disease, as we did for breaking the

degeneracy in the simpler case of having IGRA-negative population at the start of the trial. In this section, thus, we propose a Bayesian modelling approach to explore those kinds of trials, which differs substantially from the analyses performed before.

The objective for the rest of the chapter will be, then, to introduce and test this methodology using the M72/AS01$_E$ as a case example. The pertinence of such an approach is linked to the need to understand better the mechanistic effect of the vaccines at play in the trials, but also points towards getting a reduction in the bias when the impact of those vaccines is addressed using transmission models. Typically, in the lack of mechanistic descriptions of the vaccines at play, modellers tend to either introduce vaccines that can stop all possible routes to disease, or lie in a specific combination of mechanisms without justification. To relax such kind of assumptions, in our framework, we define a family of possible compartmental vaccine models characterised by different vaccine mechanisms from each of which we can estimate the likelihood associated with a particular RCT outcome. Using those likelihoods combined with uniform, non-informative priors for each of the possible models in the family, we can estimate the posterior probabilities of each model, providing in this way a means to evaluate the compatibility of each of the possible models with the RCT outcomes observed.

To illustrate this approach, we analyse the case of the multi-centric clinical trial of the candidate vaccine M72/AS01$_E$, conducted on IGRA-positive individuals from settings in three different high-burden countries: Kenya, Zambia, and South Africa, which led to a promising PoD readout of $\text{VE}_{\text{dis}} = 49.7\%$ (95% C.I. 2.1-74.2). Specifically, we apply our formalism to evaluate the a posteriori plausibility of the different vaccine descriptions that can be built as all-or-nothing vaccine models[204, 205, 206] by incorporating in their parameterisations different combinations of protective effects. Furthermore, we identify the specific combinations of protection mechanisms that generate more plausible model descriptions, under the light of the observed trial outcome. This offers a rationale for selecting the most adequate vaccine model structures, and weighing them to produce mechanism-agnostic impact forecast averages.

Finally, the method that we propose to analyse this king of trials also features an approach to reduce the uncertainty, not only in vaccine characterisation but also in the forecasted impacts. Different from the previous method, where we only were able to characterise the mechanistic effect of the vaccine over the main routes to disease, here we also recovered the relative compatibility of each description with the real outcome of the trial. Then, the Bayesian posteriors that capture the compatibility can be used as natural weights for producing a Bayesian average of each model's impact forecasts.

This Bayesian average is -at least within the family of models considered- independent of mechanistic assumptions.

3.3.2 Methods II: a bayesian approach to analyse IGRA-positive trials.

3.3.2.1 The basal RCT model

Similarly to what we did in the previous sections with the IGRA-negative case, we capitalise on compartmental models to describe the first stages of progression to disease of recruited IGRA-positive participants during the trial. This architecture, which captures all three possible routes to disease[144, 164, 135], is depicted in Figure 3.10. We have inherited the same architecture used in the previous section to demonstrate that the uncertainty in vaccine characterisation is not derived from the selected architecture, but also appears in other trial designs as long as they treat fast progression explicitly.

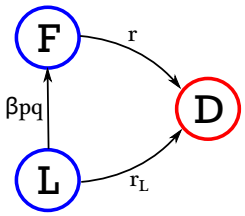

Figure 3.10: Scheme of the control cohort's states. F: Fast-progressors, L: Slow-progressors (LTBI), D: Disease (active TB) of the control cohort in the RCT.

Within this model, TB acquisition of participants in the placebo arm during the trial can be expressed through the following system of ordinary differential equations:

$$\begin{aligned} \dot{L}_c &= -r_L L_c - \beta p q L_c \\ \dot{F}_c &= -r F_c + \beta p q L_c \\ \dot{D}_c &= r F_c + r_L L_c \end{aligned} \tag{3.41}$$

which is formally identical to the one presented in the IGRA-positive analysis of the previous section. In this model, there are three states (fast latency F, slow latency L and active disease D), five epidemiological parameters (infection rate β, fast (slow) progression to disease rates r (r_L), probability of fast progression upon infection p, and risk reduction for fast progression upon re-infection q), and three different types of transitions between them (events): reinfections ($L- > F$), slow progression to disease ($L- > D$) and fast progression to disease ($F- > D$).

The method that we propose for analysing the outcome of a trial with IGRA-positive recruited individuals trusts in an all-or-nothing description of the effect of the vaccine. A vaccine modelled in this way is supposed to block perfectly the route to disease to

which its protection is associated, and the intrinsic efficacy is not related to a reduction in the progression to disease, but to the fraction of the vaccinated individuals that get that perfect protection.

Then, to simulate the vaccine arm, we first need to describe the temporal evolution of the vaccinated individuals who get protection from the vaccine. We have considered vaccines featuring three basic mechanisms of action, either alone or combined, which gives a total of 7 possible models that describe the effect of the vaccine. These mechanisms correspond to the ability of the vaccine to effectively block, independently, each of the transition types ($L- > F- > D$, $L- > D$, or $F- > D$) in a fraction equal to ε of all vaccinated individuals, according to the all-or-nothing vaccine description. Therefore, in each of the models, a parallel compartmental model can be derived, not for all the vaccinated individuals, but only for the fraction ε of them who are effectively protected.

In what follows we describe all these compartmental models for the vaccinated individuals that experience protection, as the remaining fraction of unprotected vaccinated individuals will obey the same temporal rules introduced in Equations 3.41.

Model 1 In this vaccine model, the transition $F- > D$ of individuals who already were in F at the beginning of the study is halted. This is modelled by shifting the protected individuals from F to L right after their vaccination, therefore assuming that vaccine protection implies that the risk of fast progression is substituted with the much lower risk of slow progression after endogenous reactivation. This way, the dynamical rules for the time evolution of this arm remain unchanged with respect to those described above in Equations 3.41, and the difference between arms comes from the fact that the fast progression reservoir is emptied right after vaccination in the intervention arm.

Model 2 In this model the vaccine is able to completely stop the reinfections from **L** to **F**, which is described by the subsequent ODEs for the ε fraction of vaccinated individuals:

$$\begin{aligned} \dot{L} &= -r_L L \\ \dot{F} &= -rF \\ \dot{D} &= rF + r_L L \end{aligned} \tag{3.42}$$

Model 3 In this model the vaccine has the ability to interrupt the endogenous reactivation process, thus preventing **L** individuals to progress to disease. This

situation is described by the following system of ODEs for the ε fraction of vaccinated individuals that is protected:

$$\begin{aligned} \dot{L} &= \beta pqL \\ \dot{F} &= -rF + \beta pqL \\ \dot{D} &= rF \end{aligned} \tag{3.43}$$

Model 4 Here we assume that the vaccine can completely stop the reinfections from **L** to **F**, which is described by the same ODEs of the second model, as well as another effect that mimics model 1. We have then a shift in the initial distribution of participants from **F** to **L** in the protection cohort, combined with perfect protection versus reinfections.

Model 5 Here we consider that the vaccine can completely stop the endogenous reactivations, which is described by the same ODEs of the third model, combined with the effect of model 1. That means that we have then a shift in the initial distribution of participants from **F** to **L** in the protection cohort combined with perfect protection against disease for **L** individuals.

Model 6 This model combines the effect of models 2 and 3, acting at the same time over endogenous and exogenous reactivation. This situation is described with ODEs as follows:

$$\begin{aligned} \dot{L} &= 0 \\ \dot{F} &= -rF \\ \dot{D} &= rF \end{aligned} \tag{3.44}$$

Model 7 In this model we are considering that the vaccine holds a combination of all the three basic effects depicted in models 1 to 3, thus being the most powerful vaccine among all the models, for the same intrinsic efficacy ε. The dynamical behaviour is the same that we have in model 6 combined with the fact that several **F** individuals are moved towards **L** at the start of the trial.

3.3.2.2 Gillespie Algorithm

The sequence of events of each type during the follow up of the study is modelled stochastically, using an implementation of the Gillespie algorithm where the daily probabilities (propensities) of each type of transition are: $a_{L\to F} = \beta pqL$, $a_{L\to D} = r_L \cdot L$, and $a_F = r \cdot F$, respectively. In our implementation, the reservoir F is duplicated: one instance contains only the individuals already in F at the beginning of the study, while the second one starts empty, and receives the eventual cases of reinfections that will

undergo fast progression. In this way we can keep track of all three different routes to disease independently without altering the dynamics.

The algorithm works, by iterating, at each time step t, the following operations:

1. Calculate the probabilities a_j of each type of event happening at t.
2. Generate an exponentially distributed random variable $dt = -\frac{log(r_n)}{R}$, where r_n is a random number uniformly distributed in the interval $(0, 1)$ and R is the sum of the probabilities of all events at time t. The next event will occur at $t' = t + dt$.
3. Determine the event to occur by stochastically drawing a process from all possible processes according to their respective probabilities a_j.
4. Update the population according to the event that has taken place.
   - If a reinfection takes place, then $L(t+dt) = L(t)-1$ and $F(t+dt) = F(t)+1$
   - If an endogenous reactivation occurs, then $L(t + dt) = L(t) - 1$ and $D(t + dt) = D(t) + 1$.
   - If a fast transition to disease happens, then $F(t + dt) = F(t) - 1$ and $D(t + dt) = D(t) + 1$.
5. Move to the next time step, $t = t + dt$.

For the vaccine cohort, in those cases in which the dynamic rules are modified under the effect of the vaccine, the algorithm presented above for the control cohort needs to be modified accordingly. This is done, for each vaccine model, as follows:

1. **Model 1**: The algorithm remains the same.
2. **Model 2**: Within this model, the ε fraction of individuals that are protected by the vaccine is simulated using a variant of the Gillespie algorithm where the reinfection event is not considered. Each time that a new time is selected by the algorithm, the event that takes place is selected only between endogenous reactivation and fast progression.
3. **Model 3**: Within this model, endogenous reactivation to disease is blocked. Each time that a new time is selected by the Gillespie algorithm, the event that takes place is selected only between reinfection and fast progression.
4. **Model 4**: In this model, the Gillespie algorithm works as in model 2, and it is combined with a shift in the share of latent individuals that do not change the evolution rules.

5. **Model 5**: Within this model, the Gillespie algorithm works as in model 3, combined with a shift in the share of latent individuals that do not change the evolution rules.

6. **Model 6**: In this model, the Gillespie algorithm is the most simple one we can have, as only an event can take place. Now, each new time that an event occurs, a fast progression event happens.

7. **Model 7**: Within this model, the algorithm is the same as in model 6, combined with a shift in the share of latent individuals that do not change the evolution rules.

3.3.2.3 Parametrising the model and simulating a trial.

In a subsequent step, we need to get estimations of all the parameters involved in the compartmental model, to solve it using the Gillespie algorithm. Thus, we need two main ingredients: the epidemiological parameters r, r_L, q, and p governing the transitions, as well as the expected initial prevalence of fast (F) vs. slow progressors (L), and the forces of infection $\beta(a)$ in the population sampled during the recruitment phase of the clinical trial. The epidemiological parameters are assumed to have the same values in all countries and age groups analysed, and are extracted from previous literature. In Table 3.2, we gather together all literature-based parameters, along with the reported values and the original references from which they were obtained.

Parameter	Value	Reference
p	0.150 (0.100-0.200)	[92, 207, 106]
q	0.210 (0.140-0.300)	[96]
r	0.900 (0.765-1.035)	[144]
r_l	$7.5 \cdot 10^{-4}$ ($6.4 \cdot 10^{-4}$-$8.6 \cdot 10^{-4}$)	[144]

Table 3.2: Literature related parameters that are used in Gillespie algorithm. Along with the median value and the CI of the parameters, we include the references from which they were taken.

Here, we consider an endogenous LTBI reactivation rate centered around $r_L = 7.5 \cdot 10^{-4}\ \mathrm{y}^{-1}$ whereas fast progression rate to TB is centered in $r = 0.9\ \mathrm{y}^{-1}$. These values are widely adopted in the modelling literature[144, 208, 209], and are broadly compatible with empirical estimates[192, 210]. Moreover, we consider that LTBI individuals have a 79% less risk of progressing to TB upon reinfection, and a probability of fast progression centred around $p = 0.15$, broadly compatible with the observed share of individuals that undergo fast progression to disease in young adults.

Then, to estimate the force of infection β in each country and age group, we capitalise on the comprehensive spreading model described in Chapter 2, designed not to provide a description of the disease transitions within the context of a trial, but to provide an exhaustive description of TB transmission dynamics on the whole population of an entire country during several decades.

Calibrating the force of infection and the diagnosis rates, this model reproduces TB incidence and mortality trends reported in the WHO Database in the three countries of the M72/AS01$_E$ study (South Africa, Kenya, and Zambia) during the period 2000-2018. The results of this calibration are shown in Figure 3.11, panels A, B. From this calibration procedure we then obtain a complete model-based description of the dynamical evolution of TB epidemics in each country.

From the outcomes of this model, it is possible to record the calibrated force of infection, as, within this model, infections may occur after contact between susceptible individuals and infectious ones. Let $S(a,t)$ represent the number of susceptible subjects in age group a, at a given time t, the number of new infections that will be observed will be equal to the product of $S(a,t)$ and the force of infection perceived by that sub-population, $\lambda(a,t)$, which represents the fraction of susceptible individuals who get infected per year, defined in Equation 3.45.

$$\lambda(a,t) = \tilde{\beta(t)} \sum_{a'} \xi_c(a,a',t)\Upsilon(a',t) \tag{3.45}$$

In Equation 3.45, $\Upsilon(a',t)$ is the density of all the infectious individuals within age-group a' at time step t, weighted by their relative infectiousness, and $\xi_c(a,a',t)$ represents the relative contact frequency that an individual of age a has with individuals of age a' at time t, with respect to the overall average of contacts that an individual has per unit time with anyone else. Furthermore, $\tilde{\beta(t)}$ captures the scale factor for the infectiousness, which is calibrated to a sigmoid curve that depends on time, for all age groups alike, as described in Chapter 2. From there, we can obtain the value of $\lambda(a,t)$ at any time, for all age groups, and for all countries involved in the study. Then, as the M72/AS01$_E$ trial lasted for 3 years (from 2015 to 2018), we get our estimates for the force of infection by averaging $\lambda(a,t)$ in this period, as done in Equation 3.46.

$$\beta(a) = \int_{t=2015}^{t=2018} \frac{1}{T}\lambda(a,t)dt \tag{3.46}$$

In Equation 3.46, T captures the duration of the M72/ASO1E trial. As stated, this procedure is done per age group, and country, and yields a distribution for the force of infection during the years of the trial that can be used later, in the Gillespie algorithm, to pro. Estimated distributions of β across countries and age groups are shown in Figure 3.11C, for the age groups that compose the recruited population of

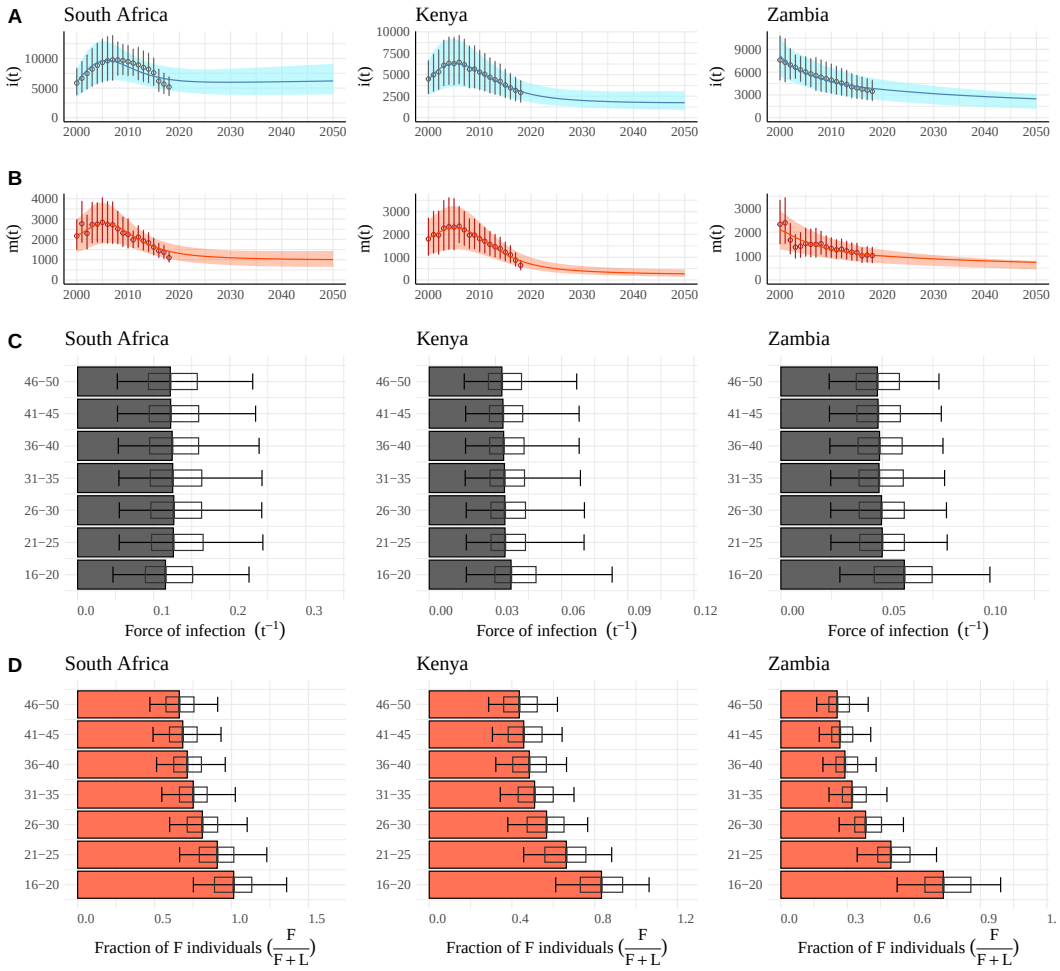

Figure 3.11: Estimation of the force of infection and the fraction of fast progressors per country and age group. **A, B**. The country-level transmission model described in Chapter 2 is calibrated to reproduce TB incidence and mortality in each country involved in the trial. The error bars represent the reported uncertainty of incidence estimates in the WHO tuberculosis database, which is used to fit the model, and shaded areas capture the 95% CI in all the trajectories forecasted by the model in the calibration procedure for $N = 500$ realisations (see Chapter 2). **C**. From the calibrated simulations conducted country-wise, we obtain estimates of the force of infection per country and age group (fraction of susceptible individuals infected per year and age group), which is needed to calibrate the basal model of the RCT. **D**. From the same simulations, we retrieve estimates for the relative fraction of fast progressors over the total population of IGRA+ individuals without a past of active TB $\frac{F}{F+L}$ that is expected in each country in the year of the trial, which are needed to set the initial conditions of the RCT. In all panels, bars represent the median, boxes capture the inter-quartile range, and error bars represent the 95% CI from a set of $N = 500$ simulations.

the original M72/AS01$_E$ study.

Finally, we also used the model to obtain estimates of the relative fraction of latent individuals without a past of active TB who show a high risk of progressing to active TB in the next 12-24 months (fast progressors) and those for whom that risk is much lower (slow progressors). This is done similarly to what we did with the force of infection. First, we compute the size of the reservoirs F and L, and their evolution in time. Those reservoirs capture all the population undergoing latency for a TB-related cause. Then, we compute the fraction of fast progressors, as $\frac{F}{F+L}$ in the year 2015, which is the first year of the original study. The results of this exercise, for each country and age group, are represented in Figure 3.11D.

With those ingredients at hand, we are still unable to produce *in-silico* realisations of trials such as the M72/AS01$_E$. To achieve this end, and realising that we need to simulate a multicentric trial, i.e., a trial that was performed in more than one country, we needed to gather some more data. From the original study[180, 181] we recover the age distribution of the participants enrolled in the study, in each cohort (placebo and vaccine). We also record the total number of individuals in each cohort, as well as the share of participants in the trial that came from each country, which is included in Table 3.3.

Original Age Group	Control Cohort	Vaccine Cohort
15-24	724	706
25-29	321	339
30-49	594	581
Country	Share in Control Cohort	Share in Vaccine Cohort
South Africa	80.81%	80.38%
Kenya	14.91%	15.07%
Zambia	4.27%	4.55%

Table 3.3: Distribution of participants in the original M72/AS01$_E$[180] according to their age and origin. In this trial, participants where recruited from three age groups with uneven representation and different spans. The overall number of participants were similar between both cohorts, with a total of $N^c = 1639$ participants in the control cohort and $N^v = 1626$ participants in the vaccine cohort. Those participants where recruited in three countries, South Africa, Kenya and Zambia. The representation of each country was also uneven, with South Africa accounting approximately for the 80% of the participants, and Kenya and Zambia accounting for the 15% and 5%, respectively.

Now, the approach to simulate a trial is based on the following steps:

1. Select a country, vaccine model and age group to simulate.

2. Break down the original age distribution into age groups spanning 5 years, so we

can make use of the distributions for the force of infection and the share of fast progressors. We use the relative share of the individuals in the whole demography of the selected country as a proxy to separate the bigger age groups into groups spanning 5 years each.

3. Drawn stochastically a set of parameters from their distributions, for the specific values in the country.

4. Set the initial conditions using the estimated distribution of fast progressors.

5. Use the Gillespie algorithm to simulate the fate of all the participants in each cohort using the previous parametrisation, and a given value of the intrinsic efficacy of the vaccine ε, which captures the efficacy of the vaccine the mechanistic level.

6. Measure $\mathrm{VE}_{\mathrm{dis}}(a, C)$ at the end of the trial, which depends upon the reduction of cases in the vaccine cohort with respect the control one, in each age group a and country C.

Then, we repeat these steps $N = 10000$ times to account for the uncertainty in the parameters, and we do the same task for all age groups in all countries. To recover a single value of efficacy in the trial, we combine the results for $\mathrm{VE}_{\mathrm{dis}}(a, C)$ using the age distribution of participants, and the share of participants that came from each country, as weights of a weighted summation. At the end of this calculation, we end with a set of $N = 10000$ values of $\mathrm{VE}_{\mathrm{dis}}$, which captures the efficacy of a vaccine described according to the selected model, for an intrinsic efficacy of ε, in the whole trial. The previous steps are, finally, repeated once per vaccine model, and for a range of values of $\varepsilon \in [0, 1]$.

The result of this exercise is a could of $\mathrm{VE}_{\mathrm{dis}}$ values, distributed along the axis defined by ε. We simulated $N = 10000$ trials for each model and value of the intrinsic efficacy, with 200 values of the intrinsic efficacy ε uniformly distributed in the range $[0, 1]$, and each one of these instances involves the simulation of the dynamics in both cohorts in three countries and within seven age-groups, this yields a total number of trials simulated equal to $4.2 \cdot 10^7$ (200 intrinsic efficacies x 10.000 instances x 7 age groups x 3 countries). This yields clouds of $N = 2 \cdot 10^6$ points, after the combination procedure, and the results can be analysed using the methodology that we propose in the next section.

3.3.2.4 Cracking the trial outcomes: Bayesian analyses

With the outcomes of the myriad of trials simulated according to previous sections, it is possible to derive, using the Bayes Rule, a method that yields a Bayesian posterior to each vaccine model when confronted with the real $\mathrm{VE}_{\mathrm{dis}}$ measured in a trial. In the following lines, we introduce the whole derivation. Let us consider the likelihood $P(\mathrm{VE}_{\mathrm{dis}} = 49.7\%|i,\varepsilon)$ that each one of the possible vaccine models, defined by the combination of parameters i,ε generates a PoD efficacy estimate compatible with the one observed for $\mathrm{M72/AS01}_E$. The integer index $i \in 1,2,...,7$ determines the specific vaccine mechanisms at play (i.e., the vaccine model), and the continuous parameter $\varepsilon \in [0,1]$ captures the intrinsic efficacy. Using this likelihood term, we may apply the Bayes rule to define the posterior probability associated with each particular model:

$$P(i,\varepsilon|\mathrm{VE}_{\mathrm{dis}} = 49.7\%) = \frac{P(\mathrm{VE}_{\mathrm{dis}} = 49.7\%|i,\varepsilon)\cdot P(i,\varepsilon)}{\sum_{i'}\int_{\varepsilon'} P(\mathrm{VE}_{\mathrm{dis}} = 49.7\%|i',\varepsilon')\cdot P(i',\varepsilon')\cdot d\varepsilon'} \tag{3.47}$$

And derive a model-type posterior probability, by integrating over all possible intrinsic efficacy values as follows:

$$\begin{aligned} P(i|\mathrm{VE}_{\mathrm{dis}} = 49.7\%) &= \int_{\varepsilon} P(i,\varepsilon|\mathrm{VE}_{\mathrm{dis}} = 49.7\%)d\varepsilon \\ &= \frac{\int_{\varepsilon} P(\mathrm{VE}_{\mathrm{dis}} = 49.7\%|i,\varepsilon)\cdot P(i,\varepsilon)\cdot d\varepsilon}{\sum_{i'}\int_{\varepsilon'} P(\mathrm{VE}_{\mathrm{dis}} = 49.7\%|i',\varepsilon')\cdot P(i',\varepsilon')\cdot d\varepsilon'} \end{aligned} \tag{3.48}$$

If we consider uniform non-informative priors in Equation 3.48 (that is $P(i,\varepsilon) = P(i',\varepsilon')\forall(i,i',\varepsilon,\varepsilon')$), the model-type posterior can be obtained from the marginalised likelihoods as follows:

$$P(\mathrm{VE}_{\mathrm{dis}} = 49.7\%|i) = \int_{\varepsilon} P(\mathrm{VE}_{\mathrm{dis}} = 49.7\%|i,\varepsilon)\cdot P(i,\varepsilon)\cdot d\varepsilon \tag{3.49}$$

which we estimate from the density distributions of the PoD efficacy readouts $\mathrm{VE}_{\mathrm{dis}}$ obtained from each model using the value of Kernel density estimators (R package KerSmooth) of the frequency of trials evaluated at $\mathrm{VE}_{\mathrm{dis}} = 49.7\%$. Plugging the numerical estimates of $P(\mathrm{VE}_{\mathrm{dis}} = 49.7\%|i)$ into Equation 3.48 allows us to quantify the relative support in the data for the seven different vaccine descriptions provided. Confidence intervals for these model posterior estimates are computed by bootstrapping the calculations $N = 5000$ times, each of which is obtained by sampling with replacement $N = 1000000$ trial simulations.

Then, we also estimate the intrinsic efficacy values ε that are most compatible with the given observed efficacy-against-disease readout $\mathrm{VE}_{\mathrm{dis}} = 49.7\%$ under each of the model type descriptions, this time applying the Bayes rule over each model type independently:

$$P(\varepsilon|\mathrm{VE}_{\mathrm{dis}} = 49.7\%,i) = \frac{P(\mathrm{VE}_{\mathrm{dis}} = 49.7\%|i,\varepsilon)\cdot P(i,\varepsilon)}{\int_{\varepsilon'} P(\mathrm{VE}_{\mathrm{dis}} = 49.7\%|i,\varepsilon')\cdot P(i,\varepsilon')\cdot d\varepsilon'} \tag{3.50}$$

Where likelihood terms $P(\text{VE}_{\text{dis}} = 49.7\%|i, \varepsilon)$ are estimated from the simulations using Kernel density estimates obtained for each of the $N = 200$ values of ε covered. The first momentum of these posterior distributions corresponds to the expected values of the intrinsic efficacy parameter under each model type, that is:

$$\langle \varepsilon \rangle_i = \int_\varepsilon P(\varepsilon|\text{VE}_{\text{dis}} = 49.7\%, i) \cdot \varepsilon \cdot d\varepsilon = \frac{\int_\varepsilon P(\text{VE}_{\text{dis}} = 49.7\%|i, \varepsilon) \cdot P(i, \varepsilon) \cdot \varepsilon \cdot d\varepsilon}{\int_{\varepsilon'} P(\text{VE}_{\text{dis}} = 49.7\%|i, \varepsilon') \cdot P(i, \varepsilon') \cdot d\varepsilon'} \tag{3.51}$$

3.3.2.5 Impact evaluations of TB vaccines: bayesian estimates

After performing the Bayesian analysis we recover different results. On the one hand, we got a value, along with its CI, for each one of the intrinsic efficacies that capture the effect of the vaccine in all vaccine descriptions explored. On the other hand, we also recover a Bayesian posterior that captures the relative compatibility of the vaccine description with the real measure of VE_{dis} of a real trial. With those ingredients at hand, it is possible to go even further in our quest to reduce the bias in impact evaluation, for which we need to address the impact of those vaccines in some settings using transmission models. Capitalising again on the spreading model of Chapter 2, which we used to get an estimate of both the force of infection and the share of fast progressors in the overall pool of latent individuals, we can forecast the impact of each one of the seven vaccines proposed here, in three different countries: India, Indonesia, and Ethiopia.

To do so, we make use of two runs of the model. In the first one, we draw a set of parameters for the model from their distributions, as it is explained in the first chapter, and using them, we calibrate the model and estimate normally the spread of TB, computing the relevant measures of TB burden. This is labeled as the control run and serves to set the baseline without the introduction of the vaccine. Then, we run, for the same calibration, the model again, but this time introducing the desired vaccine in 2025, targeting the adolescent population. Vaccine-mediated protection is described, within the framework of our model, in a parallel branch where the dynamics of protected individuals unfold, as it is depicted in Figure 3.12. The protection induced by any of the seven vaccines is described according to an all-or-nothing scheme, meaning that an ε fraction of the vaccinated individuals is fully protected against the routes to disease blocked by the vaccine (and only against them), while the rest remains susceptible. For the sake of our analyses, vaccine coverage is ideally assumed to be 100%, and no efficacy waning has been modelled. In turn, the vaccine only protects IGRA+ subjects to avoid extrapolating its efficacy estimates to unexposed individuals, where efficacy evidence has not yet been gathered for this vaccine.

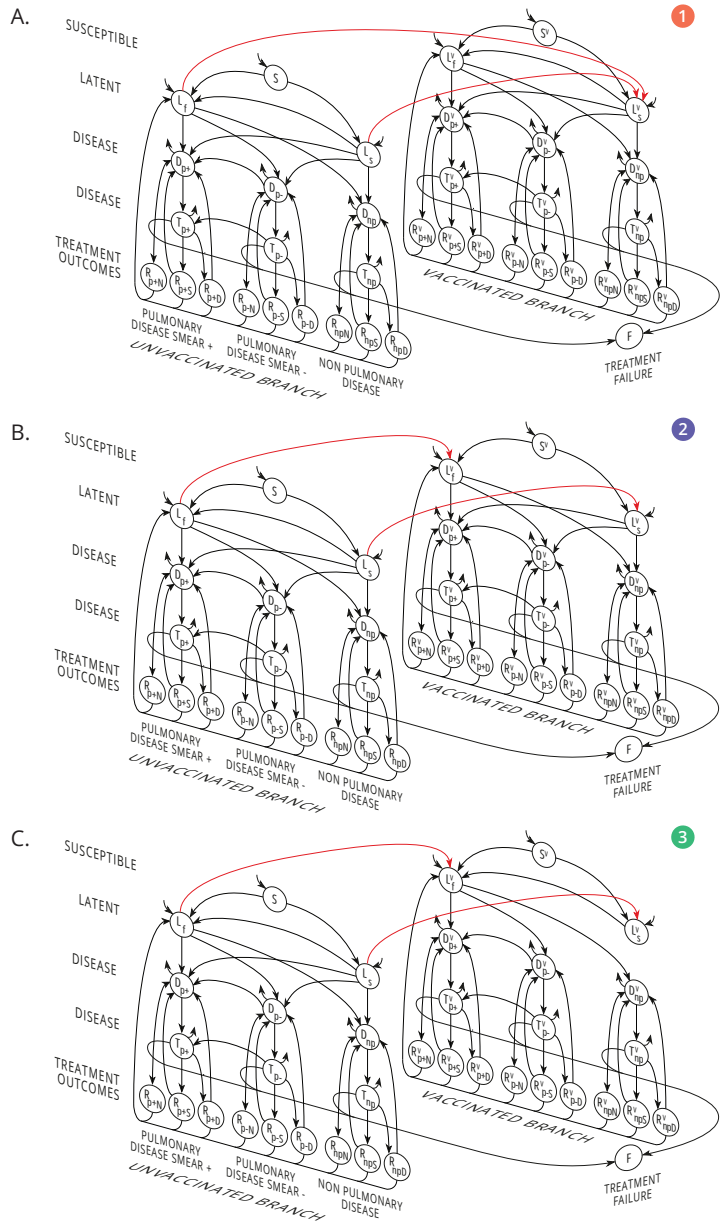

Figure 3.12: Natural History schemes of the transmission model for control and vaccine runs. Two branches are modelled: the placebo arm (i.e. non-vaccinated, or vaccinated but non-protected), and a parallel branch for individuals protected by the the vaccine. Vaccination transitions between cohorts are therefore included (i.e. red arrow transitions), and each panel features a vaccine arm corresponding to the first three vaccine descriptions. **A**. Model structure 1: the vaccine protects against primary TB upon first infection. This is implemented as in the Gillespie algorithm, by shifting individuals from L_F to L_S^v when they reach the target age-group ($15-19$ years old) of the vaccination campaign. **B**. Model structure 2: the vaccine protects against re-infection, which is implemented by blocking the transition L_S^v to L_F^v for all age strata from the target group onward **C**. Model structure 3: the vaccine protects against endogenous reactivation of LTBI, achieved by blocking the direct transitions from L_S^v to the active disease reservoirs D^v for all age strata from the target group onward. Model structures 4 to 7 can be trivially obtained by combining these three.

Then, at the end of this second run of the model, we measure again the relevant measures of TB burden that allow us to estimate the eventual impact of the tested vaccine, which, in what remains of this chapter will be the Incidence Rate Reduction (IRR), a measure of the relative reduction in the overall incidence between both runs, measured at the end of the simulation. Repeating this $N = 500$ times for each vaccine, we end with seven sets of dimension N of impact measures, one set for each of the vaccines tested. In each realisation, we are drawing intrinsic efficacy values (ε) from the parameter CI to account for the uncertainty inherited in the characterisation of ε. From those results, we can obtain the median, along with the CI, for the individual impacts of each vaccine.

Finally, to reduce bias in the impacts, we build model-based Bayesian estimates of vaccine impact as a weighted linear combination of the IRRs foreseen by each type of vaccine. If we are considering vaccine type $i \in [1, 7]$, and model-run $v \in [1, 500]$, we will denote the corresponding impact as $IRR(i, \langle\epsilon\rangle_i, v)$, where $\langle\epsilon\rangle_i$ is the expected value of the efficacy parameter for model i, that we have derived using the bayesian framework. In a final step, we combine the results of all models in a weighted sum performed for each realisation that uses Bayesian posteriors as weights to obtain an overall estimate of impact $\langle IRR(v)\rangle$, with $v \in [1, 500]$, that is, in each case, agnostic to the vaccine mechanism. These Bayesian averages are obtained as follows:

$$\langle IRR(v)\rangle = \frac{\sum_{i=1}^{7} I(i,v)P(i,v|VE_{\text{dis}} = 49.7\%)}{\sum_{i=1}^{7} P(i,v|VE_{\text{dis}} = 49.7\%)} \tag{3.52}$$

where the posteriors $P(i, v|VE_{\text{dis}} = 49.7\%)$ used in each case are drawn stochastically from the marginal posterior distributions in each realisation $v \in [1, 500]$. This yields a set of $N = 500$ averaged impacts, that does not depend upon the vaccine model used. From this set, the median value and the 95% confidence interval for the average impact can be calculated. When comparing impacts derived from two vaccine models, it is important to highlight that the differences are paired, in such a way that the differences in impact between two given vaccine models are evaluated $N = 500$ times, in each of which both vaccines are compared against the same baseline trend.

3.3.3 Testing our method: results

Leaning on this basic model description of disease dynamics sketched in the section 3.3.2, and in Figure 3.10, our first goal is to implement computational simulations to estimate the relative weight of each route to disease in the incidence observed in

the placebo arm of a clinical trial such as the M72/AS01$_E$ study. We then perform a first set of *in-silico* trial simulations stratified per age group in each of these three countries, wherein participants´ fates are simulated stochastically, according to an implementation of the Gillespie algorithm that allows tracking the three routes to disease independently. Through these simulations, we quantify the fraction of total TB cases associated with each route to disease in the placebo arms enrolled in each country, stratified per age group. In Figure 3.13, we show the final distribution of TB cases in the relevant age groups.

Then, as we are dealing with a multi-centric trial, participants between 18 and 50 years old were enrolled in South Africa, Kenya, and Zambia[180]. Considering the distribution across ages and countries (see Table 3.3 and methods), we produce a global estimate of the contribution of each route to disease to the incidence observed in the placebo arm of the entire study in the M72/AS01$_E$ trial, as an average of the results of the age groups and countries involved in the study, weighted by their relative frequencies, whose result are included in Figure 3.13.

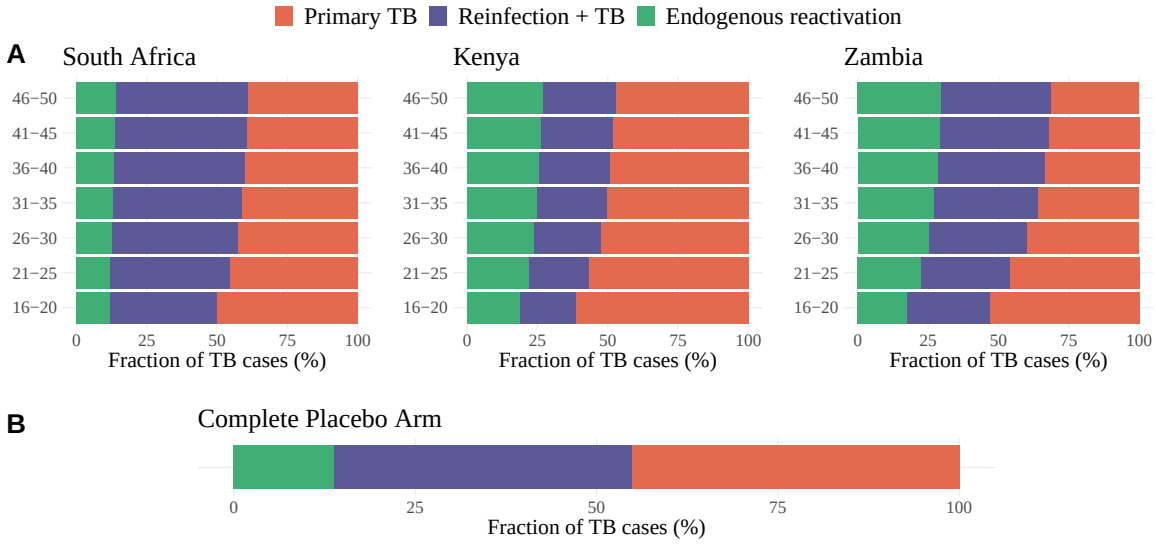

Figure 3.13: Distribution of active TB cases in the placebo arm of the trial across the three possible routes to disease. **A**. Using the estimates of the force of infection, the share of fast progressors in the latency states, and literature-based estimates for the epidemiological parameters r, r_L, q, and p, the placebo arm of the M72/ASO1$_E$ study can be simulated *in-silico*. From this simulations, we can estimate the expected fraction of incident TB cases associated to each of the routes to disease. **B**. Weighting the contributions estimated for country and age group, according to the age and country-wise distributions of participants in the M72/AS01$_E$ trial, we obtain an overall estimate of the relative contribution of each route to disease to the total incidence observed in the global placebo arm of the trial.

Now, within the framework of the "three risks model", it is conceptually possible that vaccines may provide PoD by reducing only the disease risk associated with some of

these three routes to disease. The estimates of the relative share of total incidence that can be attributed to each route to disease give us very useful information about what are the precise mechanisms that may be more interesting to target in a given population. However, the immunological components of host responses against *Mycobacterium tuberculosis* (*M.tb.*, the causative agent of TB) that are involved in protecting against primary TB upon recent infection, endogenous reactivation, or re-infection are complex and neither homogeneous nor linear; and could be boosted to different extents by a vaccine in a way that is difficult to predict a priori.

To accommodate modelling decisions to this uncertainty, we consider a set of vaccines that provide PoD by reducing each of the three individual risks, either alone or combined, as shown in Figure 3.14. This yields seven vaccine models that can be denoted as $M(i, \varepsilon)$, where we have each model being defined by the integer index $i \in [1, 2, ..., 7]$, determining the specific protection mechanism(s) present in the vaccine (Figure 3.14A) and the continuous parameter $\varepsilon \in [0, 1]$, which captures the intrinsic efficacy, modelled as the fraction of individuals protected within an all-or-nothing modelling framework, considered identical for all the vaccine effects present in each case. This way, while in models 1-3 only one of the three routes to TB is disrupted by the vaccine, models 4-7 incorporate several mechanisms simultaneously (see Figure 3.14). For instance, model 5 describes a vaccine that protects against primary TB and LTBI endogenous reactivation at the same time, and model 7 represents a vaccine tackling all three routes alike. Crucially, as represented in Figure 3.14B, the maximum fraction of total TB cases that a vaccine behaving according to each of these models can prevent is variable, spanning from 13.8% of cases that would be prevented by a vaccine with a 100% efficacy against LTBI reactivation only, to the obvious 100% of cases, that would be prevented by a perfect vaccine with 100% efficacy against all routes of TB alike.

Therefore, the set of vaccine descriptions $M(i, \varepsilon)$ will constitute a space of possible models, within which we will look after the one(s) whose assumptions are most compatible with a trial's PoD readout of vaccine efficacy, that is, with the largest Bayesian posteriors, instead of blindly assuming that a vaccine acts through a given specific mechanism, or, for example, that it reduces all risks alike. To accomplish that task, we expand the Gillespie stochastic simulations mentioned before to include the simulation of vaccine arms each of them coherent with the seven types of vaccine models described, as it is explained in the methods. Specifically, we assume a uniform non-informative prior on the efficacy parameter and register the observed efficacy against disease $\mathrm{VE}_{\mathrm{dis}}$ (that is, the PoD readout) that is associated with each trial simulation. As explained before, this procedure yields a cloud of $\mathrm{VE}_{\mathrm{dis}}$ distributed

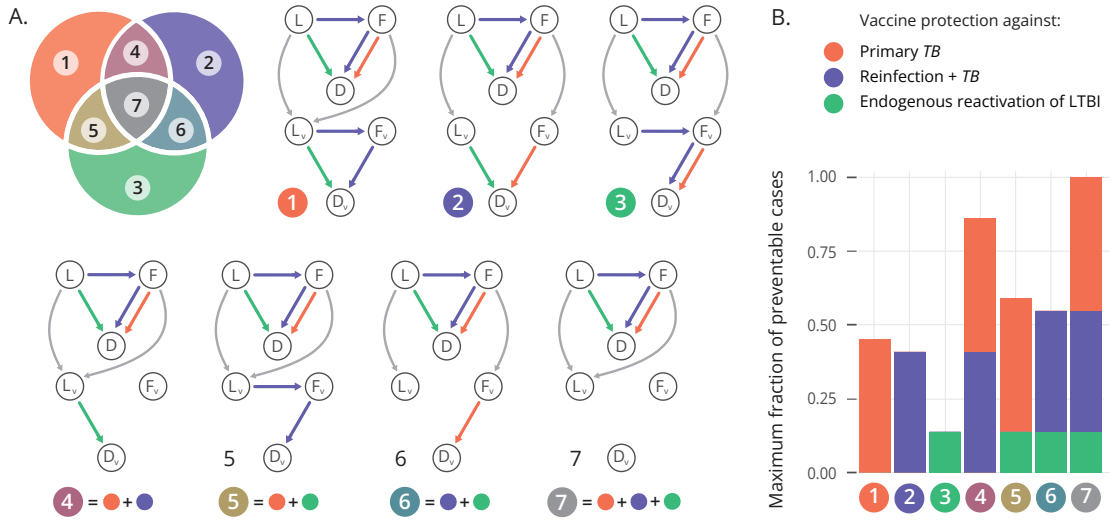

Figure 3.14: Compartmental models to accommodate the description of vaccines providing PoD by acting on specific routes to disease. **A**. (Top left): Venn diagram sketching the seven vaccine types contemplated in the study, as a function of the routes to disease they are assumed to protect against: primary TB (model 1), TB upon reinfection (model 2) or endogenous reactivation of LTBI (model 3). Combinations of these mechanisms yield models 4-7, which describe vaccines that are able to halt two (models 4,5 and 6), or all three routes to disease at once. Each region of the Venn diagram corresponds to a value of the discrete index $i \in [1, 2, \ldots, 7]$. Beside the diagram, we show the compartmental descriptions of each vaccine type. In each of the seven models, a vaccine arm is included in parallel to the placebo arm, that defines the disease dynamics of the vaccinated individuals who are protected against developing disease through the corresponding routes. **B**. Maximum fraction of preventable cases by each vaccine, considering the mechanisms of protection present in each case.

along the intrinsic efficacy parameter, and the results are included in Figure 3.15A. After we conduct a total amount of two million simulations for each model type (one million per trial arm), we consider the likelihood $P(\text{VE}_{\text{dis}} = 49.7\%|i, \varepsilon)$, associated to each possible model defined by the combination of parameters $[i, \varepsilon]$. Integrating these likelihoods over all possible values of ε for each vaccine type we retrieve the marginalised likelihood curves $P(\text{VE}_{\text{dis}} = 49.7\%|i)$ represented along with the simulation clouds in Figure 3.15A. Red dashed lines on top of these marginalised likelihoods capture the probability that a trial with the specifications of the one described in[180, 181], conducted on a given vaccine behaving according to the i-th vaccine model, will lead to a PoD efficacy readout VE_{dis} that is compatible with the observations made in the real trial:$\text{VE}_{\text{dis}} = 49.7\%$[181].

Using this marginalised likelihood, we can apply the Bayes rule to define the marginal posterior probability associated with each particular model, $P(i|\text{VE}_{\text{dis}} = 49.7\%)$. These marginal posteriors, represented in Figure 3.15B, provide means to

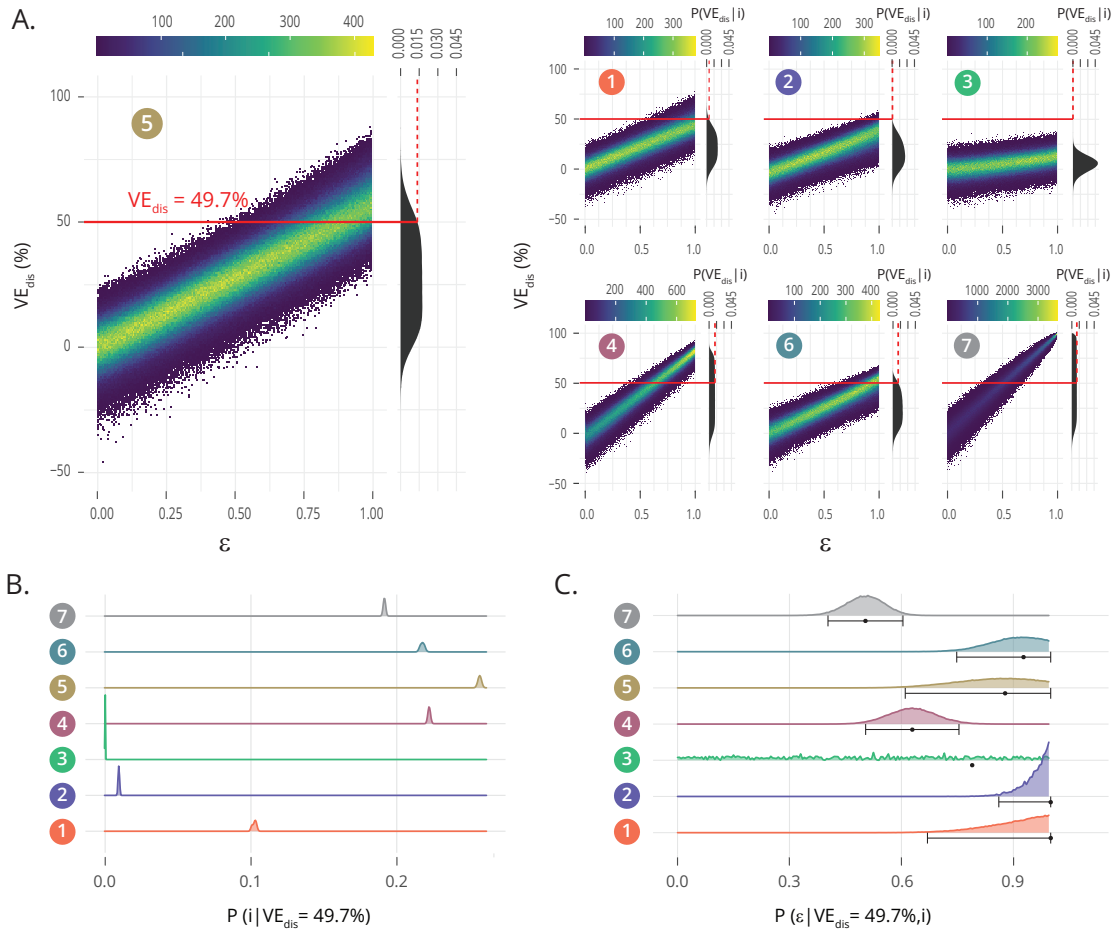

Figure 3.15: Bayesian analysis of possible modelling architectures underlying a trial-derived observation of vaccine efficacy. **A**. Absolute frequency density distributions of efficacy values $\mathrm{VE}_{\mathrm{dis}}$ obtained in sets of $N = 2 \cdot 10^6$ clinical trial simulations per model, uniformly distributed across the intrinsic vaccine efficacy parameter ε (efficacy resolution: 0.005, with 10000 realisations for each value of ε). Red horizontal lines mark the PoD efficacy observed in the M72/AS01$_E$ trial $\mathrm{VE}_{\mathrm{dis}} = 49.7\%$. Along with each bi-dimensional density cloud, we represent its marginalised frequencies over the vertical axis, obtained upon adding simulation results over all possible values of ε for each model. These density curves capture the marginalised likelihoods $P(\mathrm{VE}_{\mathrm{dis}}|i)$. Red dashed lines capture their value at the observed efficacy, that is $P(\mathrm{VE}_{\mathrm{dis}} = 49.7\%|i)$. **B**. Marginal posteriors $P(i|\mathrm{VE}_{\mathrm{dis}} = 49.7\%)$, capturing the relative compatibility of each model with respect to the efficacy observed in the M72AS01$_E$ trial. **C**. Distribution $P(\varepsilon|\mathrm{VE}_{\mathrm{dis}} = 49.7\%)$ of the intrinsic vaccine efficacy parameter ε in each model type, given the observed efficacy $\mathrm{VE}_{\mathrm{dis}} = 49.7\%$, along with mean and 95% confidence intervals associated to them. For M3, the CI was omitted, for it spans the entire range $\varepsilon \in [0, 1]$, as the model fails systematically to produce simulation instances compatible with the observed $\mathrm{VE}_{\mathrm{dis}} = 49.7\%$.

quantify the relative support in a given trial's outcome for each one of the seven different vaccine descriptions provided. In our case, the observed PoD efficacy readout reported for the vaccine M72/AS01$_E$[181] appears more compatible with models 4, 5, 6, or 7, each featuring a combination of several vaccine mechanisms, than with models where vaccine effects are associated to a unique mechanism of action. The reason behind this emerging hierarchy between vaccine models is the relation between the observed $\mathrm{VE_{dis}}$ and the maximum fraction of events that are preventable by each type of vaccine (shown in Figure 3.14B). Posteriors of models whose maximum fraction of preventable cases is smaller than the observed $\mathrm{VE_{dis}}$ are in turn smaller, meaning that the protection mechanisms present in these vaccines are likely insufficient to explain the observed trial result (models 1, 2 and 3: see Figure 3.14B, and 3.15A).

In what regards the remaining vaccine models (4 to 7), all of them protect several routes to disease, featuring maximum fractions of preventable cases that are well above the $\mathrm{VE_{dis}}$ value observed in the trial (see Figure 3.14B). Their different posteriors can then be understood by comparing the relative frequency at which each model is expected to generate simulated values for $\mathrm{VE_{dis}}$ that are compatible with the trial observation, when all simulations for all possible values of ε, distributed around the uniform, non-informative prior, are considered (marginal density curves over the $\mathrm{VE_{dis}}$ axis in Figure 3.15A). Observing those curves, -the marginalised likelihoods, integrated over ε for each model as defined in Equation 3.49 (see Methods)- we see that models 4-6 show marginalised densities with a tighter spread around intermediate values of $\mathrm{VE_{dis}}$ than model 7, showing higher values around the observed $\mathrm{VE_{dis}} = 49.7\%$, and therefore higher model posteriors than model 7. Maximum fractions of preventable cases for models 4, 5, and 6 are smaller than that of model 7, which is equal to 1 since the latter can potentially prevent all TB cases by blocking all routes to disease. This translates into a cloud of simulated data for model 7 with a steeper slope in Figure 3.15A, which in turn causes the flatter marginal density curve for model 7 than for models 4-6. Taken together, these results lead to the slightly lower marginal posterior probability observed for model 7 than for models 4-6, evaluated at $\mathrm{VE_{dis}} = 49.7\%$, as shown in Figure 3.15B)

Finishing with the analysis of the cloud plots, our approach can also be used to estimate the intrinsic efficacy values ε that are most compatible with the observed PoD efficacy readout $\mathrm{VE_{dis}} = 49.7\%$ under each vaccine model, by applying the Bayes rule over each of the seven types of models independently to obtain the conditional posteriors $P(\varepsilon|\mathrm{VE_{dis}} = 49.7\%, i))$. The first momentum of these conditional posteriors corresponds to the expected values of the intrinsic efficacy parameter under each model type, that is $\langle\varepsilon\rangle_i$, which is computed and included in Figure 3.15C, along with its

confidence intervals obtained from the conditional posterior distribution itself. These efficacy estimates illustrate a sensible feature of our model approach, namely, that a given PoD readout VE_{dis} must be mapped to lower intrinsic efficacy ε values when the vaccine can halt progression to disease through all possible routes than when it acts on a subset of them.

Once we have described our Bayesian approach to inform vaccine characterisation by combining trials' results with *in-silico* simulations, we illustrate how it can be used to reduce arbitrariness from impact evaluations based on transmission models. A typical line of action for prospective impact evaluation of a vaccine consists of three steps: 1) implementing a transmission model accommodating a sensible vaccine description defined a priori. 2) Infer the vaccine parameter(s) conditional on the model structure that provides an optimal agreement with trial data, and 3) produce model-based forecasts of vaccine impact. A potential problem with this approach is, of course, that there exist many vaccine descriptions that can be adopted in the second step, and that they may lead to substantially different impact forecasts. To illustrate this problem and quantify its importance, we capitalise on the same transmission model used above to infer forces of infection and fractions of fast vs. slow progressors. This model was able to capture the description of the effects of the introduction of new vaccines compatible with each of the seven models under analysis (see Methods).

In Figure 3.16A, we show the incidence reduction rate (IRR), evaluated in 2050, achieved by the introduction of a vaccine in 2025 on a vaccination campaign targeting adolescents (16-20 years old), under each of the seven types of models analysed in this study, forecasted in three high burden countries: India, Indonesia, and Ethiopia. Here, the intrinsic efficacy modelled in each case corresponds to the expected value $\langle\varepsilon\rangle_i$ conditional to the model architecture and the vaccine trial PoD readout VE_{dis} observed in the trial. In this exercise, vaccine coverage is ideally assumed to be 100%, and no efficacy waning has been modelled. Moreover, the vaccine only protects IGRA+ subjects to avoid extrapolating its efficacy estimates to unexposed individuals, where efficacy evidence has not yet been gathered for this vaccine. According to each model description (see Figures 3.14 and 3.12), only PoD effects (no PoI or PoR) are included in our models. These impacts range from 2.2% of IRR in 2050 (95% CI: 1.2-4.0, as foreseen by model model 2 in Ethiopia), to 10.6% of IRR (95% CI: 8.0-13.8) foreseen by model 6 in Indonesia.

Then, we observed that many of the differences in vaccine impact that emanate from different vaccine models within the same country are also statistically significant. In Figure 3.16B, we compute the relative differences in IRR that arise in each country when comparing each vaccine model and the model with the highest posterior

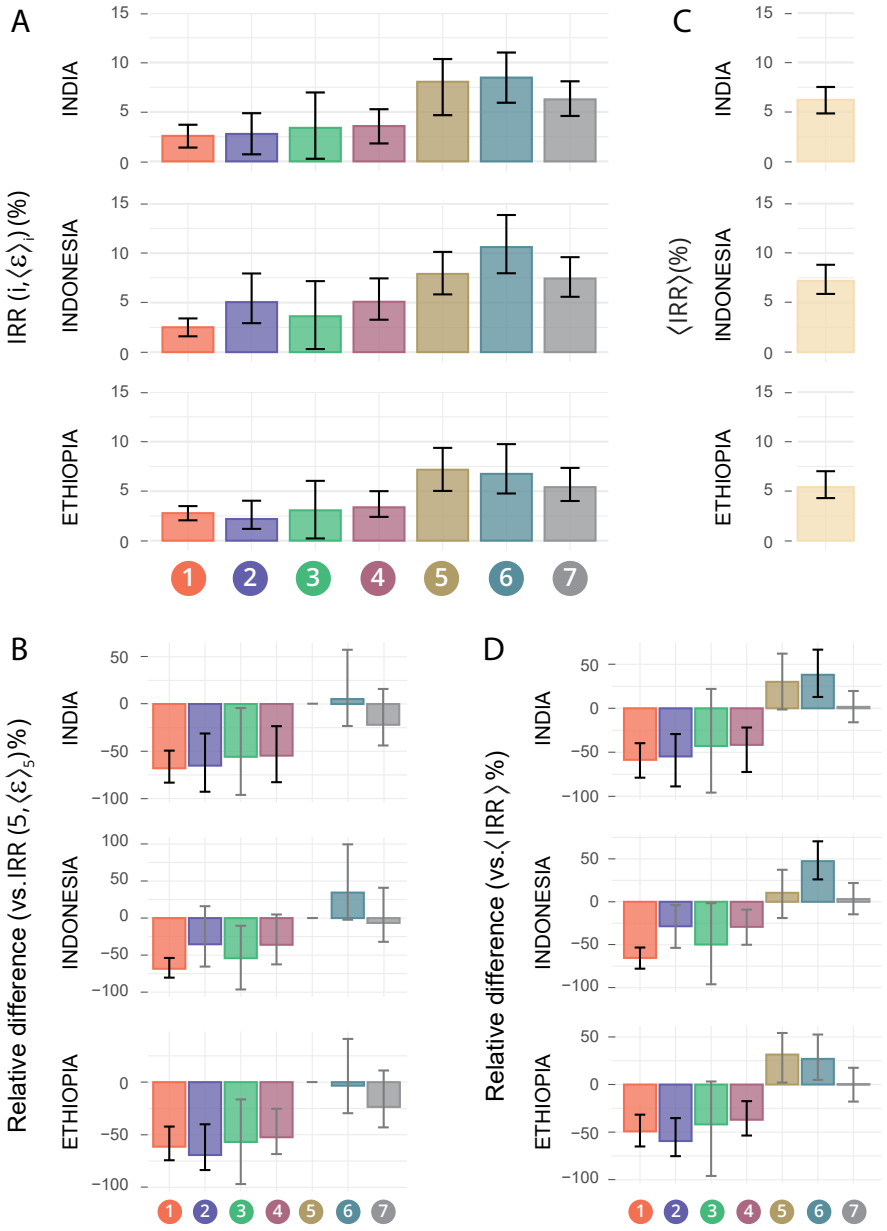

Figure 3.16: Impact forecasts variation across model structures vs mechanism agnostic Bayesian estimates of impact. **A**. Vaccine impact forecasts obtained through the comprehensive transmission model introduced in Chapter 2, when the vaccine is modelled according to the each of the seven descriptions here discussed. **B**. Relative differences between the impacts foreseen by each model and the model with maximum Bayesian posteriors (model 5). **C**. Combined, mechanism-agnostic ⟨IRR⟩ estimates for the same impacts, in the same countries, where each of the seven models contributes proportionally to its Bayesian posterior. **D**. Relative differences between ⟨IRR⟩ and impacts foreseen by each individual model. In all panels, bars capture the median impact, and error bars represent the 95% CI from sets of $N = 500$ impact simulations. P-values are obtained as the fraction of simulations yielding to impact estimates crossing zero, over the total set (one-tailed empiric test). P-values are adjusted for multiple testing using Bonferroni correction with $N = 63$ tests. Black error-bars correspond to significant statistics (Bonferroni-adjusted-$p < 0.05$).

probability (model 5), which describes a vaccine that protects against endogenous reactivation of LTBI and primary TB at once. These differences are statistically significant in 6 out of 18 cases (Bonferroni-adjusted p-values ¡0.05), and account for as much as 69.3% of the impact foreseen by model 5 in the most extreme case (IRR$(2, \langle\varepsilon\rangle_2)$ impact compared to IRR$(5, \langle\varepsilon\rangle_5)$, in Ethiopia). These significant differences evidence the importance of removing arbitrariness from modelling choices of vaccine descriptions.

This can be achieved within the family of models under analysis by using, again, our Bayesian approach. To reduce arbitrariness, we propose the computation of Bayesian estimates of expected vaccine impact $\langle$IRR$\rangle$ as a mean of the impacts foreseen by each type of vaccine IRR$(i, \langle\varepsilon\rangle_i)$, weighted by the marginal posteriors $P(i|\text{VE}_{\text{dis}} = 49.7\%)$. The results of this exercise are presented in Figure 3.16C for India, Indonesia, and Ethiopia. In the impact forecasted in Figure 3.16C, IRRs range from 13.35% in Ethiopia vs 1.99% in India, in line with results provided in other recent modelling studies for vaccines of comparable profiles, in comparable vaccination strategies[162, 139].

As with comparisons across models, deviations of individual vaccine descriptions concerning $\langle$IRR$\rangle$ range between +47.3% IRR$(6, \langle\varepsilon\rangle_6)$ above $\langle$IRR$\rangle$ in Indonesia) and -65.4% (IRR$(1, \langle\varepsilon\rangle_1)$ below $\langle$IRR$\rangle$ in Indonesia), and are statistically significant in 9 over 21 occasions (Bonferroni-adjusted p-values < 0.05, Figure 3.16D). This highlights again the risk of adopting a priori a given dynamical structure for vaccine descriptions in transmission models, and the convenience of adopting a Bayesian approach to this problem.

3.3.4 Some considerations on the second method and results

Using our method, we were able to assign different posterior probabilities to each of the seven vaccine models proposed that could be responsible for protection in terms of the mathematical models. The magnitude of the posterior of each model essentially depends on whether the maximum amount of TB cases preventable by each vaccine model is enough to explain the protection level observed in the trial, and, when we compare models with large enough maximum preventable fractions, on how frequently each model can produce simulated trials compatible with the observed vaccine efficacy.

Our analyses showed that models 1,2, and 3, each of which tackles a single route to disease, show lower posterior probabilities than models acting on either two (models 4, 5, and 6) or all three routes to disease (model 7), suggesting that, for this particular case, a simple vaccine acting only in one of the routes to disease does not seem compatible with data. Furthermore, the vaccine model offering the highest posterior probabilities given the trial result is model 5, where vaccine PoD leans on protection against endogenous reactivation of LTBI and primary TB, even though models 4, 6,

and 7 show similarly high posterior probabilities. Regarding this, the potential of our approach to disentangle specific vaccine mechanisms with better specificity that yields greater differences in Bayesian posteriors could be further exploited if applied in multi-centric RCTs conducted on sites with divergent TB burden distributions across age strata and routes to disease, and including participants distributed more homogeneously across settings. For context, in the case example of the M72/ASO1$_E$, the estimated distribution of TB cases across routes to disease is very similar in the three countries in the study, but a majority of recruited participants came from South Africa (¿80%), which discourages disaggregating the analysis per site. If further data is collected, for this or another vaccine, that enables disaggregating the analysis, our Bayesian approach could be stratified per site or age cohort, to integrate more than just one efficacy observation. This, in turn, would unlock the estimation of more decisive Bayesian posteriors for the different vaccine models proposed.

Despite these precautions, the entire set of model posteriors constitutes a meaningful resource that unlocks producing vaccine impact forecasts that are mechanism-agnostic. Using the derived posteriors as weights of the impact forecasts produced from each of the seven proposed models we can compute a Bayesian impact estimate that does not lean on any vaccine mechanism assumption. Importantly enough, our Bayesian estimates for the M72/ASO1$_E$ vaccine impact are broadly compatible with those produced by model 7 alone, which is an architecture that has recently been used to produce the first impact forecasts for vaccines similar to M72/ASO1$_E$[162, 139]. This suggests that the analyses presented in these references would not be incurring relevant bias in this particular case due to the implicit mechanistic assumptions made in their vaccine modelling choices. However, it is equally important to highlight that this does not guarantee that model 7 could be generally considered, for the situation could be different for other vaccines, or even for this same vaccine after more evidence becomes available.

Nonetheless, our approach also fosters important limitations. On the one hand, the implementation of the clinical trials simulations requires estimating a series of epidemiological parameters a priori, including the fraction of individuals in the fast vs. slow progression reservoirs, rates of re-infection, and fast progression to disease; conditioned by age stratum and epidemic setting to combine them, at a later stage, to describe the global study population.

First, we have been forced to adapt the coarse granularity of participants' age groups reported in the trial to smaller age groups used in the model assuming unbiased representation of the smaller age groups in each country in the wider cohorts reported in the trial, which could not be the real scenario. Second, we assumed that the overall

epidemic risk in the countries of the trial was representative of the overall situation in each specific setting in the year of the trial, which is also a hard assumption, as the forces of infection used here might underestimate the actual values observed in the trial since trial settings are chosen by their typically high transmission levels. Although it would be very valuable to count with empiric estimates for the force of infection in the trial sites, the estimates that we obtained, ranging between 4% and 11% depending on the country and the age group, are broadly compatible with expected values of the annual rate of infection in high TB burden settings, according to a recent study by Dowdy and Behr[211]. This study concludes that, unlike classical estimates for this parameter, adult populations in contemporary high-burden settings may present annual rates of infection between 5% and 10%, or even higher; a range that is compatible with the parametrisation that we are using here.

Last, IGRA+ clinical trial designers should include strategies to explicitly quantify the fraction of the participants who underwent recent vs. remote IGRA conversion before the beginning of the trial, which would remove the need to estimate fast vs. slow progression reservoirs from transmission models. This could be done directly (i.e. by including an IGRA screening phase lasting circa one year before the trial starts, where individuals who are initially testing negative are re-evaluated to capture a fraction of recent IGRA conversions before the beginning of the study), or, perhaps more feasibly, by using bio-markers of time since IGRA-conversion[212]. All of those are factors that may alter the relative weight of different routes to disease in our analysis, biasing our conclusions, and suggest that whenever exact age distributions of the participants and more relevant information on incidence levels at the specific settings are available, they should be used to refine quantitative conclusions.

On the other hand, it is important to highlight that our method, as implemented here, only permits vaccine descriptions where mechanisms are either absent, or present to the same extent, but does not accommodate more general situations where all vaccine mechanisms may be present with different intrinsic efficacies. generalising the formalism to deal with leaky vaccines -where different efficacy values are permitted, associated with different routes to disease, in the same model-, would unlock descriptions of more general vaccine behaviours. However, it is key to acknowledge that the amount and quality of efficacy data needed for generalising our method in that direction is currently unavailable, for example, for the M72/AS01$_E$ vaccine case. Again, it would be necessary to count with enough participants distributed across locations in multicentric studies, and/or age groups, where baseline distributions of estimated cases associated with each of the TB routes were divergent enough. Using that information, vaccine efficacy could be analysed independently in different subgroups

of data, producing more decisive posterior estimates of the mechanisms in place and their relative efficacy, also in a leaky vaccine scenario[205, 206].

3.4 Discussion

In a disease with a complex transmission chain, such as TB, vaccine mechanisms can be modelled in many different ways, some of which can be rendered compatible with clinical trial observations and yet produce divergent results when plugged into transmission models for their prospective evaluation. The fact that we only recover partial knowledge of the myriad of possible effects that a vaccine can confer protection by, exacerbates the uncertainty in vaccine characterisation. This, in TB, is far more problematic than in other diseases, as a result of RCTs being crucial in addressing vaccine efficacy in a disease in which the lack of correlates of protection difficult the development of new vaccines.

The problem of identifying the vaccine mechanism at play is not universally solvable at the date of this thesis development and depends heavily upon the type of trial design. In this chapter, we have explored two main architectures that have been used in two real trials of TB vaccine candidates, which were the phase 2b trial of the MVA85A vaccine, which failed to show efficacy, and the more recent M72/AS01$_E$ [180, 181], which showed 49.7% efficacy (95% CI: $2.1 - 74.2\%$) against active TB in adult individuals. The trial of the MVA85A vaccine was designed to recruit IGRA-negative individuals at the start of the trial, whereas the M72/AS01$_E$ recruited already exposed individuals, IGRA-positive at the start of the trial, but without a past of active TB (i.e. individuals with latent TB). On top of that, several vaccines under development are expected to enter phase 2b of the development pipeline, which may expand even further the disparity in trial designs.

The discussion addressed here, then, is pertinent within the context of TB vaccine development, since vaccines activating certain immune pathways and responses may exert different effects on the risk of developing TB associated with different routes to disease. First, we identified this problem when analysing the MVA85A trial, in which we demonstrate that compatible vaccine with the same VE_{dis}, but acting through different mechanisms, yielded different impacts in the long run (see Figure 3.8). Moreover, when dealing with the second trial architecture, the phase 2b efficacy trial of the promising vaccine candidate M72/AS01E, and even with a different way of modelling vaccines, we recovered the same problem of having different vaccines yielding significantly different impacts in the general population.

To address these concerns, and to reduce uncertainty in vaccine characterisation,

in this chapter we have proposed two different methodologies, one per explored trial's architecture, that enable getting more complete descriptions of the mechanistic effects at play, which in turn, is later on needed to produce robust impact forecast using transmission models.

For trials conducted on IGRA-negative cohorts, it is possible to identify the vaccine mechanisms at play using our first methodology, which consists of independently estimating one of the mechanistic effects, from a complementary measure, and then, through a mathematical link, derive the other one. This is only doable in those trials, as the method trusts in using the distribution of times between IGRA conversion and active disease. Sadly, in a trial design based on the recruitment of IGRA-positive subjects, there are additional intrinsic limitations that make it harder to distinguish between the mechanisms underlying vaccine protection using the first method. Specifically, the fraction of recruited participants who are on their way to the active disease by fast progression at the beginning of the trial, and the times when they were first infected, are missing, which means that we cannot estimate independently an eventual effect of the vaccine over the fast progression to disease. Without access to these data, the POD readouts obtained from these designs are harder to interpret in terms of transmission models. Furthermore, there is an additional, and obvious limitation of IGRA-positive designs, which is that they do not allow estimating possible POI effects.

Being aware of those limitations, in the second part of the chapter we proposed a different methodology that works with IGRA-positive trials. In short, we introduced a method that combines *in-silico* simulations, model estimation of the missing parameters, and actual trial results, to quantify the relative compatibility of different vaccine descriptions with trial-derived observations. These model-to-data compatibility metrics are nothing but Bayesian posteriors which we use as weights to retrieve expected vaccine impact forecasts where models that are more compatible with trial observations contribute more than those in conflict with data. By doing this, we have provided a rationale that helps circumvent the need to make arbitrary modelling decisions concerning vaccine mechanisms, which may bias their quantitative conclusions.

This second method can be used for interpreting RCTs for vaccine efficacy against active TB (PoD) conducted on IGRA+ individuals, and it can be extended to other trial designs, even for diseases obeying different transmission dynamics structures. For example, it could be extended to the study of trials conducted with IGRA-negative individuals, where PoD mediated by PoI would emerge as an additional vaccine mechanism to integrate within the framework. It can furthermore be used coupled with any transmission model of choice (see[204] for an exhaustive review of the most recent

modelling tools described in recent literature for TB), as long as it accommodates the description of the different routes to disease and mechanisms of action here described. It will be possible, in principle, to adapt our method to these situations, and produce less arbitrary model-based impact forecasts based on vaccine descriptions where the knowledge about the vaccine behaviour is incomplete. Moreover, it also can be extended to work with the architecture based on IGRA-negative participants, although in that case, the first method will be easier to use.

It is also important to notice that, even when we modelled all-or-nothing vaccines, in the case of the M72/AS01$_E$ trial, the forecasted impacts are modest. This is remarkable, as all-or-nothing vaccines are expected to yield higher impacts than their leaky counterparts, and yet they do not seem to be powerful enough. When analysing the results of the simulated vaccination campaigns for the vaccine, the weighted averages for the impact of a vaccine derived from the M72/AS01$_E$ trial foreseen an IRR of 6.22%, CI (4.85-7.52), 7.20% CI (5.88-8.82) and 5.44%, CI (4.30-7.02) when evaluated in 2050 in India, Indonesia and Ethiopia, respectively. This is done for a vaccine applied to adolescents starting in 2025, assuming perfect coverage and no efficacy waning, and assuming that previous exposure is needed for protection. Even with these unrealistic assumptions, the small impact yielded suggests that wider vaccination campaigns would be necessary to meet the End-TB strategy goals if the efficacy profile of this vaccine is consolidated in further, phase 3 studies and no better tool is at hand.

In summary, the methods presented in this chapter go one step further in trying to characterise specific profiles of mechanistic protection for real vaccines, which is very much needed in a disease such as TB, for the impact of vaccines should be addressed with transmission models, and our approach reduces the uncertainty in those steps. Although there are plenty of limitations, both in the methods and the model-based estimation of impact, our methodology provides a workable framework that could be exported to future trials and vaccines, adapted, and expanded, and help in the quest of eradicating TB in the near future.

Chapter 4

Modelling bias in vaccine's impact forecasting: the case of China.

Summary of this chapter: In this chapter we analyse the bias incurred when estimating the potential impact of a new tuberculosis (TB) vaccine in China, a country with a fast ageing demography. We target adolescents (15-19 y.o.) or elder people (60-64 y.o.) according to reasonable varying vaccine descriptions at the mechanistic level that yield prevention of disease (PoD), or prevention of recurrence (PoR). We also explored two approaches to describe the evolution of the contact matrices through which *Mycobacterium tuberculosis* spreads among individuals belonging to different age strata. Then, we use those results to measure the influence of the description of the coupling between transmission dynamics and ageing in TB transmission models. Our findings indicate that the extent to which model-based impact forecast are affected largely hinges on the characteristics of the vaccine, as well as the specific modelling methodology employed to depict the changes in contact patterns over time.

4.1 Forecasting TB vaccine impact: the importance of the setting and modelling decisions.

In a disease such as TB, the interactions between demography and the spreading of the disease are, by far, more important than in most other diseases, as the incubation times of some individuals are long enough for a demographic structure to change. This is the case in a country like China, which is a high burden setting that, as of 2021, represented the 7.4% of the total number of TB cases world-wide[72]. Here, addressing the potential impact of a new vaccine must consider age of the targeted individuals as a factor leading to some levels of impact, but also needs to address how the age distribution of risk and cases is expected to change, as in a changing demography some groups could be more important than others when trying to halt transmission. In this chapter we devote our time to study how we can

take advantage of our TB spreading model to forecast the impact of a new TB vaccine in China. To perform this task properly, we need to take into account the potential biases in which a modeller may incur when introducing vaccines into spreading models, as we described profusely in Chapter 2. Moreover, we also need to consider the influence of other external factors that, in TB, could risk the results of such a modelling exercise, such as the mentioned influence of the demography over the vaccination campaigns.

We focused our efforts in simulating the introduction of a new TB vaccine, as, arguably, vaccines and vaccination campaigns are the most efficient tool that we can deploy to eradicate TB and to meet the goal of the WHO End TB strategy, which consists of completing a reduction of TB incidence and mortality rates by 90% and 95%, between 2015 and 2035 [65]. This is true even if a decay in incidence and mortality was achieved worldwide since 1990 [71], as the recent increase in TB burden observed in 2020-2022 due to the irruption of the COVID-19 pandemic, threatens, specially in high-burden countries like India or Indonesia, to raise the TB burden back to even higher levels than before[177, 158], and to turn the End TB strategy unrealisable. Moreover, the ever-increasing rates of emergence of drug resistance [78] evidences the necessity of new tools against the disease, including new and better drugs, improved diagnosis methods, and, potentially, a new vaccine that either boosts or replaces the current bacillus Calmette-Guerin (BCG), as it provides limited and variable efficacy levels against the more transmissible respiratory forms of the disease in young adults [79].

Consequently, the TB vaccine development pipeline is populated by a number of novel candidates of different types, based on a variety of immunological principles and vaccine platforms [114]. For estimating and comparing the potential impact of each of these candidates on halting the TB transmission chain, the development of epidemiological models arises as a powerful tool. Refining these models and addressing the main sources of uncertainty and bias in their architecture constitutes an important step towards the development of new TB vaccines. The impact of these vaccines on the general population needs to be addressed using disease-transmission models, and, in a country like China, where high TB burden levels hit a population undergoing a fast process of demographic ageing, it is important to ensure that mathematical models used to estimate the impact of TB vaccines in China offer robust descriptions of the coupling between TB dynamics and demographic evolution. According to the UN population division estimates, among the top-8 countries with highest number of incident TB cases in 2021 (China, India, Indonesia, Philippines, Pakistan, Nigeria, Bangladesh and Democratic Republic of Congo), China is the one where population ageing in the years to come will be more pronounced, going from a median age of 39.0

in 2023 to 50.7 years in 2050. In fact, in Figure 4.1, the demographic pyramid in China, and its projection in 2050, are represented, and capture this fast ageing process that is undergoing in this country.

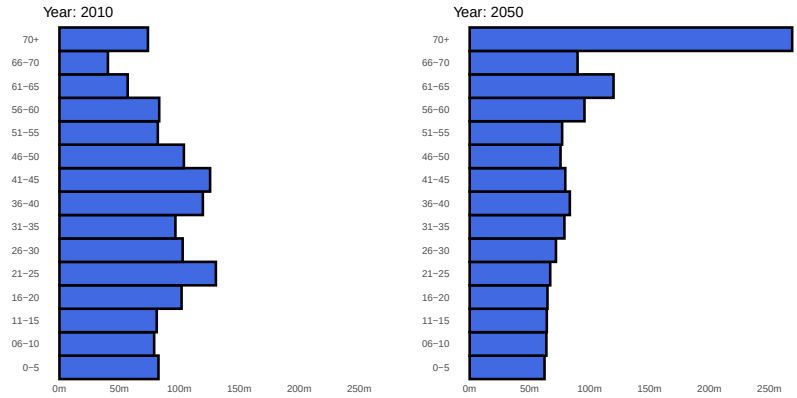

Figure 4.1: Demography pyramid in China in 2010 and projection in 2050. Population ageing increases the share of individuals between 60-64 years old, and decreases the share of adolescents (15-19 years old), in the total population. Overall, the population is expected to undergo a scenario of fast ageing, populating more the elder strata of the pyramids.

The projections in Figure 4.1 highlight the importance of considering ageing as a key demographic determinant to produce robust estimates for vaccine impact in China, which differs from the majority of high-burden countries in TB. There, the impact of TB vaccination campaigns may correlate differently with the age of targeted populations than in other high TB burden countries featuring younger demographic structures. Moreover, it is also important to have a model that is able to accommodate different mechanistic descriptions of TB vaccine protection as it could, again, correlate differently with the age of vaccinated individuals. Considering this reality, recent modelling studies have suggested that targeting elder population groups in a vaccination campaign may produce greater impact than targeting children or young adults [162].

The consequence of having this demographic changes is that, in order to estimate the impact of a vaccine, several technical aspects must be considered. First, from a modelling perspective, demographic ageing couples with TB transmission dynamics in the contact matrices[135]. Age-mixing contact matrices capture the relative frequency of social and/or physical contacts between individuals of different age-strata, and constitute a great tool for representing contact patterns within epidemic models, as the whole network of contacts is usually unobtainable. In TB, the time scales are comparable to those of demographic evolution, which forces models to incorporate sensible heuristics to describe the evolution of those matrices over time. Arregui et

al.[136] identified different methods that can be used to adapt the contact matrices, that were measured in a given population, as the population ages over time. Two of these methods are often found in modelling studies of TB [135, 117, 162]. First, contact matrices can be adapted to ensure that the symmetry of the encoded information is preserved, namely, the number of contacts per unit time between two age groups, i and j, should be the same, when calculated from the number of contacts per capita, from i to j and from j to i. This method is commonly referred to as the pairwise correction method. Furthermore, these matrices can be also corrected to ensure that not only the symmetry, but also the average connectivity of the networks is preserved across time while underlying populations are ageing. This second method is referred in this chapter as the intrinsic connectivity method. The adoption of each of these methods to describe the evolution of contacts within TB transmission models may affect model outcomes regarding the impact of a new vaccine, and its influence remains to be addressed, specially in ageing settings like China.

Second, another relevant aspect in which populations' ageing and vaccine impact forecasts may couple is in the vaccine mechanisms of action, combined with its protection profiles, and that's something difficult to predict a priori. A successful TB vaccine may confer either POD or POR through a variety of mechanisms, including halting fast progression towards primary TB upon a recent, first infection event, diminishing the endogenous reactivation rates upon latent infection, diminishing the risk of reinfection and/or preventing recurrence after recovery of a previous disease episode. Furthermore, the ability of a vaccine to confer protection through each of these mechanisms may depend upon the previous exposure of vaccine recipients to *Mycobacterium tuberculosis*, ascertained by an interferon-gamma release assay (IGRA). Since the fraction of individuals who have been previously exposed to the pathogen varies across age, and, in an ageing population, that changes across time, exploring the effects of vaccine protection profiles and mechanisms of action at once is crucial to compare different vaccination strategies targeting different age groups in China.

The goal of this chapter is, then, to investigate the impact of these aspects on the vaccine impact foreseen from two vaccination campaigns targeting adolescents (15-19 y.o) and elder individuals (60-64 y.o.) in China, starting in 2025. In Figure 4.2 we summarise those goals. Briefly, capitalising on our TB transmission model we produced *in-silico* impact evaluations of a series of vaccines with different protection profiles, acting through different mechanisms, evaluated in different simulations where contact patterns evolve according to different methods. In what concerns the distribution of vaccine-mediated protection across vaccinated individuals, we modelled vaccines as all-or-nothing (AON) as it is widely used in the modelling literature [204, 205, 206].

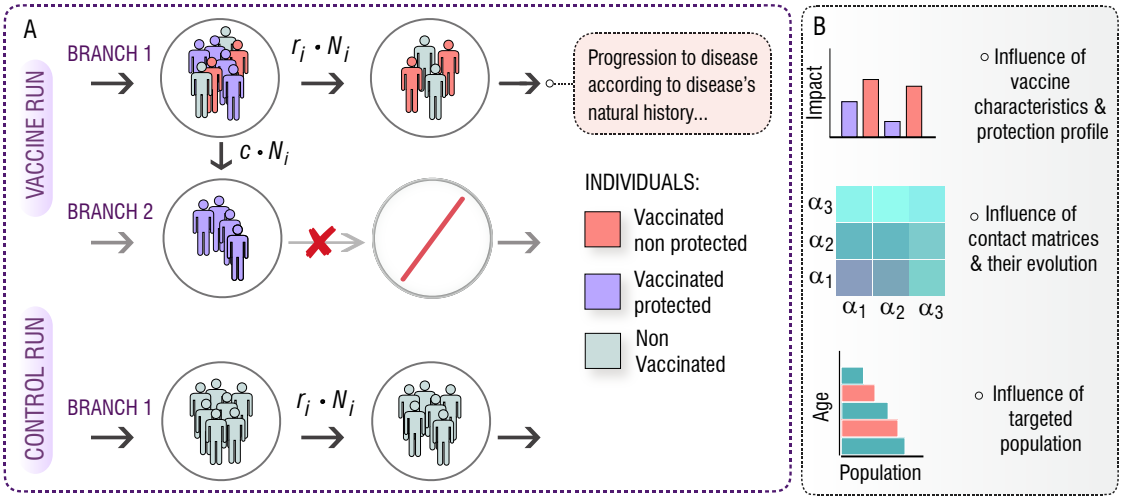

Figure 4.2: **A**. *in-silico* simulations for the introduction of an AON vaccine in a mathematical model of TB transmission. The model is run twice, one as a control run and the second time with the introduction of the vaccine. In the **control run** (bottom) the natural history of the disease remains unaltered, and every transition between states of the model is present. In the **vaccine run**, there are two different branches that evolve in parallel. On **branch 1**, the natural history of the disease remains unaltered, but a c fraction of the individuals that receive the vaccine is moved towards **branch 2**, in which the natural history is modified according to the effect of the vaccine, thus, neglecting some transitions and conferring protection. This way, a fraction c of the vaccinated individuals becomes protected. **B**. Implementing this general approach for different vaccine characteristics and protection profiles, under different descriptions of contact matrices evolution, we aim to study the effect of these aspects on the impact foreseen by our computational model for a vaccine applied either in adolescents (15-19 years old), or in older individuals (60-64 years old).

AON vaccines confer perfect protection to a fraction of the vaccinated individuals but are ineffective for the remaining fraction of vaccinated individuals. The share between those fractions is related to the overall efficacy of the vaccine. To estimate the impact, we make use of two runs of the mathematical model (control and vaccine), and we analyse the results in terms of the targeted population, the protection profile of the vaccine, and the method used for updating the contact matrix.

Our results show that the magnitude of model-based impact estimates substantially depends upon the vaccine profile, and it is also strongly related with the modelling approach chosen to describe the time evolution of contact matrices. In spite of these sources of uncertainty, our results also show, in line with previous modelling works, that elder vaccination is a suitable option in China to reduce the incidence of TB, specially when vaccines offer protection to individuals previously infected from progressing to active TB.

4.2 Methods

4.2.1 modelling the effect of the vaccine

The efficacy estimates obtained for a given vaccine in a clinical trial can be mapped onto mechanistic descriptions within a transmission model in a number of different ways. Elucidating what are the specific mechanisms at place that are most likely compatible with trials' results for a given vaccine is not a trivial task, and the architecture of the model, as well as the characteristics of the population enrolled and detailed data analysis of the results are needed for extrapolating the efficacy levels observed in a trial into transmission models describing TB dynamics in entire populations we demonstrate in Chapter 2 of this thesis (see also[117, 118]). In a disease such as TB, a vaccine conferring POD or POR effects may base its protective effects on interfering with different processes throughout the natural history of the disease, preventing Individuals' progression to TB by halting specific routes to disease. In the lack of direct evidence concerning the specific dynamic mechanisms at place in a given vaccine, modellers often implement vaccine descriptions where all the main routes to disease putatively affected by the vaccine are equally impacted. Instead, in this chapter, we aim at comparing the impact of different vaccines whose protection acts through different dynamical mechanisms. Formally, we assume that a vaccine can reduce the risk of progressing further from a given state toward disease, thus conferring protection to vaccinated individuals at different stages in the natural history of the disease. Capitalising on our transmission model, we selected four different basic vaccine mechanisms that can act either alone, or combined, at different parts of the natural history of TB. Those are:

- E_p**:** Protection against primary TB: The vaccine confers protection against fast progression to disease upon a recent first infection event. This mechanism is present in a POD vaccine that prevents fast latency toward active disease (see Figure 4.3)

- E_{rl}**:** Protection against endogenous reactivation of LTBI: Vaccine confers protection against endogenous reactivation. of bacilli in individuals with latent TB infection (LTBI). This mechanism is present in a POD vaccine that prevents slow latency towards active disease.

- E_q**:** Protection against TB upon reinfection: Vaccine confers protection against exogenous reactivation caused by a secondary infection event i n subjects who had been previously infected. This mechanism is present in a POD vaccine that prevents progression towards active disease upon reinfection, for individuals

who had already been exposed to the pathogen before (either LTBI or recovered individuals).

– E_{relapse}**:** Protection against TB relapse: This mechanism is present in a POR vaccine that prevents endogenous reactivation in individuals who had a past episode of active TB.

– All: Every vaccine's mechanism acts at the same time.

The interaction between vaccines conferring protection at any of the previous mechanisms, and the natural history of the disease, first introduced in Figure 2.1, is sketched in Figure 4.3. In short, the fraction of the vaccinated individuals that get protection from the vaccine will face a modified version of the natural history according to the effect of the vaccine, where some key transitions are halted.

4.2.2 Model-based impact evaluations of TB vaccines

Once the vaccines's descriptions are fixes, we ten aim to estimate their impact when introduced in the general population. As we did in Chapter 3, for this task we can use an adapted version of the transmission model depicted in Chapter 2 of this thesis (see also [135]), which is a deterministic, age-structured model based on ordinary differential equations, where individuals belonging to different age strata are considered to experiment different levels of epidemiological risk. The model also includes ageing dynamics, as explained in this Chapter, and in Figure 2.2, which is key in countries undergoing fast demographic changes, as it happens to be the case of China.

Regarding the impact evaluation, we use two different runs of the model that ultimately lead to an estimate of the incidence rate reduction due to the vaccine. In the first run, specific values of all the epidemiologic parameters are stochastically drawn from suitable distributions. Using the specific set of parameters obtained, the model is calibrated and the spreading of the disease is forecast in a non-intervention scenario, referred here as the control run. Then, the model is run again, using the same calibration, but introducing the vaccine in 2025. This vaccine run does not follow qualitatively the same Natural History as in the control run, as the vaccine alters it by reducing the progression risk of protected individuals in certain transitions that depend on the characteristics of the vaccine (see Figure 4.3). Finally, the impact of the vaccine is estimated by comparing those two runs through the obtention of the incidence rate reduction (IRR) at the end of 2050, as follows:

$$\text{IRR}(t = 2050)(\%) = \frac{i_{\text{control run}}(t = 2050) - i_{\text{vaccine run}}(2050)}{i_{\text{control run}}(t = 2050)} \cdot 100 \qquad (4.1)$$

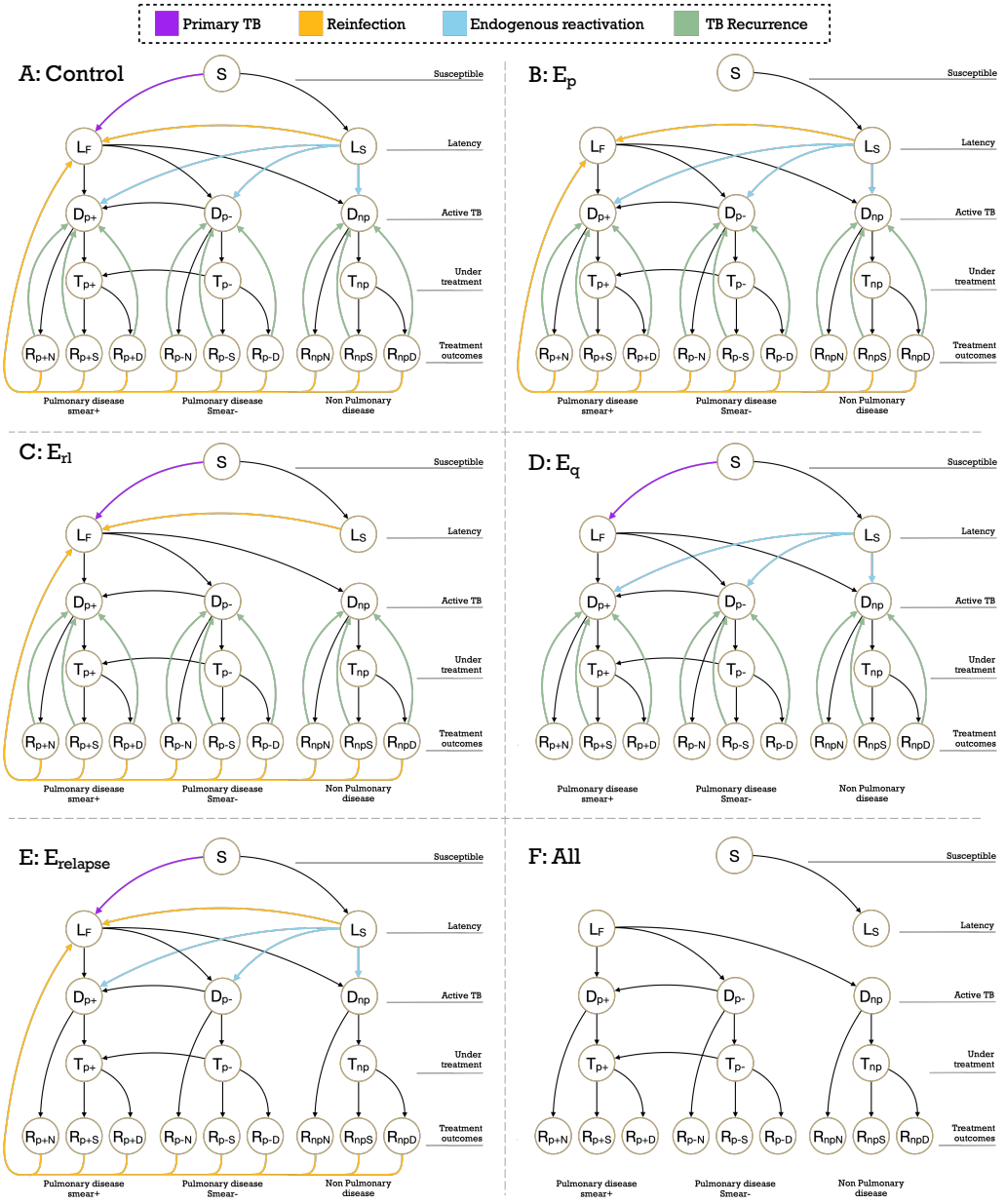

Figure 4.3: Scheme of the coupling between the vaccines and TB natural history. All vaccines are modelled as all-or-nothing, and can act by halting one or more transitions between compartments. **A**. Possible transitions between compartments for unprotected individuals in the control and vaccine runs. Vaccinated and protected individuals will face a modified version of the natural history according to the mechanistic action of the vaccine. **B**. Modified natural history for an E_p vaccine conferring protection against fast progression to disease upon a recent first infection event. **C**. Modified natural history for an E_{rl} vaccine conferring protection against endogenous reactivation of LTBI individuals. **D**. Modified natural history for an E_q vaccine conferring protection against reinfections. This vaccine prevents secondary events of infection in subjects who had been previously infected. **E**. Modified natural history for an E_{relapse} vaccine conferring protection against TB recurrence. This prevents endogenous reactivation in individuals who had a past episode of active TB. **F**. Modified natural history for a vaccine conferring protection in all previous mechanisms at the same time.

Repeating this procedure a number of $N = 500$ times, we obtain a distribution of forecast vaccine impacts, which allows us to build suitable expected values and confidence intervals that propagate uncertainty from model inputs to vaccine impacts.

All vaccines are introduced into the model according to an AON scheme, which means they only show efficacy in a fraction c of the vaccinated individuals, which in this context represent the vaccine efficacy under a scenario of perfect coverage. Those individuals comprised in the c fraction will then face a modified version of the Natural History according to the effect of the vaccine, where some of the transitions listed in the previous section are halted. In turn, the remaining $1 - c$ fraction of vaccinated individuals do not benefit from these effects and preserve the same dynamics as the unvaccinated individuals. Formally, this is modelled by displacing a fraction c of vaccinated individuals from a control branch to a vaccine-protection branch, where the dynamics is modified to reflect these changes.

The vaccines considered in this chapter feature different levels of waning. As vaccinated individuals progress from their age at vaccination a_v to $a > a_v$, the vaccine efficacy is expected to decay, eventually becoming inefficient some years after vaccination, captured by the waning level w. To implement waning in an AON vaccine, we need to introduce in the model a series of return fluxes that move individuals in the age group $a > a_v$ back from the protected to the non-protected branch of the model. The intensity of those fluxes is given by Equation 4.3.

$$w_i(a, a_v) = 1 - e^{-\ln(2)\cdot\frac{5(a-a_v)}{w}} \tag{4.2}$$

where a is the age group that suffers the waning, a_v is the age group that is being vaccinated, and w captures the waning, in years. This formula ensures that, after w years, the vaccinated individuals will suffer a waning intensity of 50%. Moreover, for any $a \leq a_v$, the waning intensity is set to zero, constituting a viable approach to implement vaccination campaigns targetting one specific age stratum. Then, the waning flux is calculated as:

$$W_f(a, a_v, t) = w_i(a, a_v) \cdot X(a, t) \tag{4.3}$$

where $X(a)$ is the population in the age group a, in the reservoir X at time t.

Besides the alterations in epidemiological risks experienced by the individuals protected by the vaccine, another important vaccine characteristic concerns the immunological status that individuals may need to fulfil before vaccination for the vaccine to confer protection to them. Depending on the immunological principles of the vaccine considered, its protection may unfold contingent to the previous exposure of the vaccinated subject to the pathogen, and, as such, it is possible that new vaccines

may confer protection only to susceptible, immunologically naive individuals, or to individuals who have been previously infected with *M.tuberculosis*. To illustrate the effect of the dependency between recipient's status and vaccine efficacy, we reproduce vaccine impact simulations where the protective effect of the vaccine, described through the displacement of a fraction c of individuals towards the protected branch, only takes place from different source reservoirs. This way, we explore four possible scenarios where only a fraction c of individuals in the following reservoirs get protection:

- Only Susceptible individuals, without a previous exposure to the disease.
- Only LTBI individuals.
- Only previously exposed individuals, which includes LTBI and also recovered subjects.
- All previous groups all together.

Finally, the vaccination is implemented in two ways. First, a mass vaccination campaign, similar to the one proposed in[162] takes places, vaccinating annually a third of the population in the reservoirs affected by the vaccine, and for the age targeted population (15-19 or 60-64). Then, after this campaign vanishes, the vaccination continues routinely coupled to the ageing.

4.2.3 Updating contact matrices with evolving demography

The complete knowledge of the network of contacts at play in the setting that wants to be introduced the vaccine into is usually unreachable or impossible to implement. Thus, for modelling purposes, age-mixing contact matrices play a key role in epidemic spreading [213, 214, 215], as they capture study age-group interactions and how age-strata mix between them. Commonly, empirical contact matrices are obtained through statistical surveys where participants are asked how many contacts they have during the day and with whom. This allows us to obtain the (average) number of contacts that an individual of a particular age i has with individuals of age group j. The resulting matrix is not symmetric due to the different number of individuals in each age group. However, it is precisely the demographic structure that imposes constraints in the entries of this matrix, as reciprocity of contacts should be fulfilled at any time (i.e., the total number of contacts reported by age-group i with age-group j should be equal in the opposite direction). Therefore, an empirical contact matrix, that has been measured on a specific population, should not be used directly without adapting it to the demographic structure of a different population under study.

This issue has important consequences in the field of disease modelling. As contact matrices play a key role in disease forecast, it is essential to assure that the matrices implemented are adapted to the demographic structure of the population considered to avoid biased estimations. For some short-cycle diseases like influenza, the time scale of the epidemic is much shorter than the typical times needed for a demographic structure to evolve [216]. The previous considerations are more troublesome for the case of persistent diseases that need long-term simulations, for which the hypothesis of constant demographic structures does not hold anymore[135]. Particularly, in the case of TB modelling, time scales are typically long, as the presence of latent individuals may lead to TB cases decades after primary infection [217]. This ultimately leads to the urge to adapt the contact matrices measured in a specific demography in such a way that they evolve accordingly to the demography of that setting. To this end, we capitalise on the methods proposed by Arregui et al. [136], which are briefly described below. We selected the methods labelled in the original article as M1 (Pairwise corrections) and M3 (Intrinsic connectivity) as the first one is typically used in the literature, also for modelling TB e.g. [162]), and is the simplest one for short-lives diseases, whereas the second one (M3) allows projecting contact matrices along with demography, which fits our needs in TB forecasting.

Pairwise correction The magnitude usually reported when measuring contact patterns is the mean number of contacts that an individual in age group i has with individuals in age group j during a measured period of time. Calling $M_{i,j}$ this quantity, we observe that, in order to fulfil reciprocity, $M_{i,j}$ should equal $M_{j,i}$, which is not the case with direct measured data. An immediate correction is to average those numbers, so the excess of contacts measured in one direction is transferred to the reciprocal. Then, the matrix entry in a new demography is computed as:

$$M'_{i,j} = \frac{1}{N'_i}\frac{1}{2}(M_{i,j}N'_i + M_{j,i}N'_j) \tag{4.4}$$

where $M'_{i,j}$ corresponds to the new demography under study.

Intrinsic connectivity matrix An alternative method that preserve the mean connectivity of the contact network makes use of the density matrix, or intrinsic connectivity matrix. Using the original data the density matrix Γ is extracted as:

$$\Gamma_{i,j} = M_{i,j}\frac{N}{N_j} \tag{4.5}$$

Γ matrix corresponds, except for a global factor, to the contact pattern in a "rectangular" demography (a population structure where all age groups have the same

density). Then, introducing a new demography, the contact matrix is obtained as:

$$M'_{i,j} = \frac{\Gamma_{i,j} N'_j N'}{\sum_{i,j} \Gamma_{i,j} N'_i N'_j} \tag{4.6}$$

An example of the evolution of the contact matrix that we are using to produce the results of this chapter is included in Figure 4.4, where we present the matrices in 2010 and 2050 using the same base matrix reported in[155], but updating it according to each one of the two methods. In panels A and B the results for the pairwise method are included, while in panels C and D we present the matrix when using the intrinsic connectivity method.

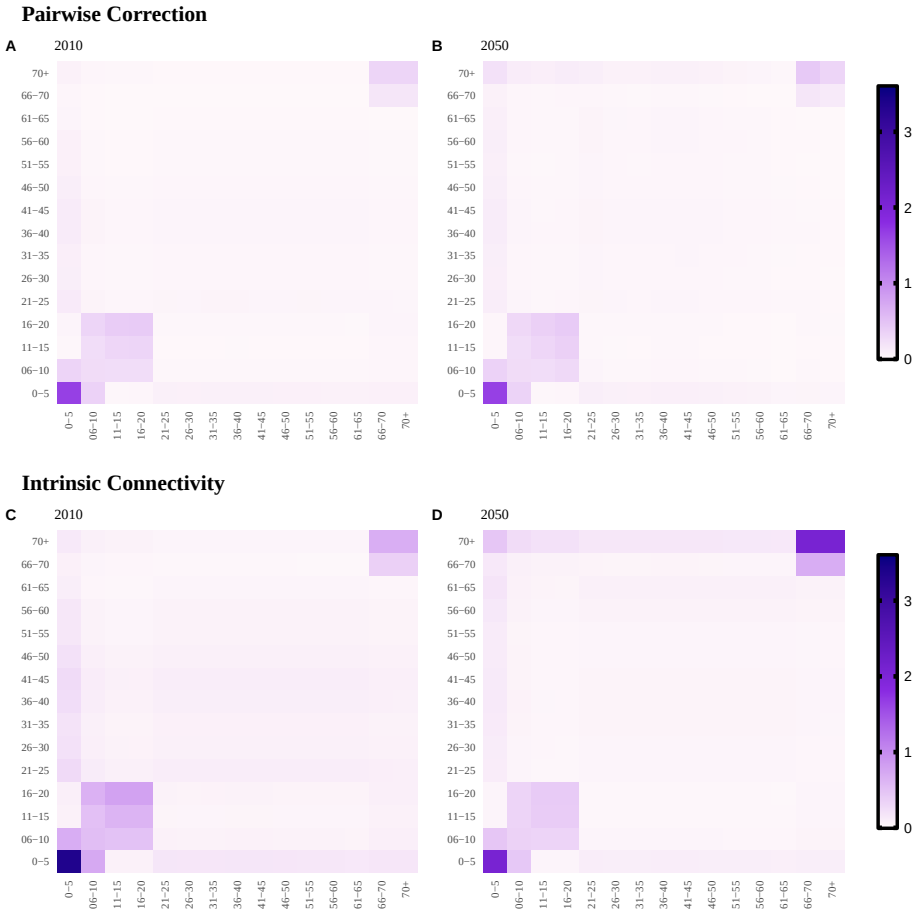

Figure 4.4: Contact matrices in 2010 and projection in 2050 under two methods: Pairwise correction and Intrinsic Connectivity. All cells capture the mean number of contacts that individuals of age i have with individuals of age j, during a day, after the correction of the selected method is applied. When evolution of demography is captured in the contact matrix using the intrinsic connectivity method, elder population tends to contact more than when using the pairwise correction, whereas adolescents tend to contact less.

4.2.4 Breaking down incidence contribution according to different routes to disease

In this chapter, in order to contextualise the findings in the following sections, we need to estimate the distribution of TB cases across the different routes to disease that are classically described in TB. Those routes are: fast progression to primary TB upon recent infection, TB upon exogenous reinfection, TB after endogenous reactivation from LTBI, or TB recurrence, after a previous disease event. In the following lines, we summarise how each contribution is estimated using the outcomes of the spreading model. In this model, the fluxes between compartments that end in the reservoir D_a capture the number of new incident cases, during a year, that progress from the initial state of the individuals to active TB in the age group a, added in all three TB classes (non pulmonary, pulmonary smear-positive and pulmonary smear-negative). The sum of all those cases in all age groups capture the global incidence. Then, we need to break down this global incidence in the different contributions that each possible route to disease gives.

The cases corresponding to TB after endogenous reactivation from LTBI can be estimated easily, as they map directly to the fluxes between the reservoir L_S, and the reservoirs D_{p+}, D_{p-} and D_{np}, as showed in Figure 2.1. This way, the contribution at any time t to the overall pool of TB cases will be calculated as:

$$C_{\text{endogenous}}(t) = \sum_i f_{L \to D_i}(t) \tag{4.7}$$

where $i \in$

Similarly, the cases corresponding to TB recurrence are also directly mappable to specific transitions between reservoirs, being those the ones between R_x reservoirs and D_i ones. The contribution at any time t to the overall pool of TB cases will be calculated as:

$$C_{\text{recurrence}}(t) = \sum_i , x f_{R_x \to D_i}(t) \tag{4.8}$$

However, for primary TB and exogenous reactivation cases it is not possible to get a 1 to 1 correspondence in terms of the transitions in the model, as all individuals ends in L_F reservoir as a middle step in its way to disease, effectively mixing all the individuals together, which make them indistinguishable. To solve this, we approximate the contribution to disease using the fluxes between the corresponding origin and the fast latency reservoir L_F, times the rate of fast progression to disease r, as the individuals are not expected to stay for a large amount of time in this reservoir, and they will abandon it precisely at this rate r.

Then, the contribution of primary TB is estimated as:

$$C_{\text{primary}}(t) = r \cdot f_{S \to L_F}(t) \tag{4.9}$$

whereas the contribution of exogenous reinfection can have two origins, a reinfection while in latency or a reinfection after treatment, so the final estimator is build as:

$$C_{\text{exogenous}}(t) = r \cdot \left[f_{L_S \to L_F}(t) + \sum_x f_{R_x \to L_F}(t) \right] \tag{4.10}$$

Now, with each one of those contributions calculated independently, it is possible to build the distribution of cases at any time t.

4.3 Results

4.3.1 Vaccine impact forecast in China

To evaluate the bias incurred when forecasting the impact of a TB vaccine in China, we took advantage of our transmission model to implement several vaccines of varying characteristics, that were simulated using models where contact matrices are updated using different methods, in either adolescents (15-19 years old), or elder individuals (60-64 years old). In Figure 4.5 and Figure 4.6 we represent the forecast impact of each vaccine using our model. As discussed in the methods section, all vaccines are modelled according to an all-or-nothing scheme, conferring different types of protection (E_p, E_q, E_{r_l}, $E_{relapse}$, or all at once) to a fraction c of vaccinated individuals in certain disease reservoirs (susceptible, latent and/or recovered individuals, or all). The efficacy of the vaccine in all scenarios is set to $c = 56\%$, as a reference value compatible with applying a highly protective vaccine with a 70% efficacy through a high-coverage campaign reaching 80% of the target population, similar to one among the most optimistic scenarios explored in previous modelling studies undertaken in China[162]. The vaccination campaign in the simulation starts in 2025, and we forecast the impact of the vaccine measuring the IRR in 2050, as explained in the previous methods section. Individuals of the targeted age group, are vaccinated when they first enter the corresponding age group, and following an initial catch up campaign lasting three years that vaccinate yearly a third of the population in the reservoir. Furthermore, we implement vaccines that experience waning levels of 10 years, as described previously.

In Figure 4.5, we show the IRRs achieved, by each one of the vaccines considered in this chapter, when applied on the elder population. In this case, we found that, when vaccines are able to confer protection to immunologically naive individuals, either

alone (Susceptible only) or along with the rest of individuals in the population, (whole population), vaccines featuring the largest impact are those that are able to prevent fast progression to primary TB upon recent infection (E_p). Instead, if vaccine protection depends on individuals having been previously infected by the time of vaccination (protection active to either latent, or latent plus recovered individuals only), the most impactful vaccines are those that are able to protect individuals from developing active TB upon endogenous reactivation of dormant bacilli. Furthermore, it is important to notice that, the impact tends to be higher when updating the contact matrix according to the intrinsic connectivity approach.

Then, in Figure 4.6, we gather the analogous results, but associated with a vaccination campaign targeting the population between 15 and 19 years old. Although vaccines protecting against primary TB are still more impactful as long as susceptible individuals are protected, and vaccines halting endogenous reactivation of latent bacilli are more impactful if protection takes place after infection, in this case the impact associated with vaccines in the latter case is comparatively lower than what is found in elders. In what concerns the influence of contact matrices on forecast impacts, interestingly, we observe that highest impacts were associated with the pairwise-corrections method, unlike what is observed in the older age group.

Comparing the impacts from both campaigns targeting elders (Figure 4.5) and adolescents (Figure 4.6), we see that the question of what is the optimal age group to target in an immunisation campaign for a new TB vaccine finds different answers depending on the combination of vaccine characteristics, protection profiles, and modelling assumptions. More specifically, what we recover is that in those cases where previous infection is required for vaccines to show their protective effects, i.e., vaccines conferring protection against endogenous reactivation (E_{rl}) or against relapse ($E_{relapse}$), then targeting the older age group always appears as a superior choice according to our simulations. This result is somehow logical, as the older an individual is, the more time it has to get infected and progress to disease via a reactivation event, which is the main reason for which the adolescent group show smaller impacts in those vaccines.

However, as soon as protection against primary TB is granted to susceptible individuals as one among the possible protective mechanisms of the vaccines, the quantitative description of contagion dynamics implemented within our model becomes more crucial, and, consequently, model forecasts are more sensitive to the adoption of either one of the two modelling approaches explored for describing contact matrices evolution: pairwise corrections vs. intrinsic connectivity. As a result, only in some occasions when the over-simplified pairwise correction method is adopted, the impacts foreseen for an adolescent focused campaign can overcome the impacts found for an

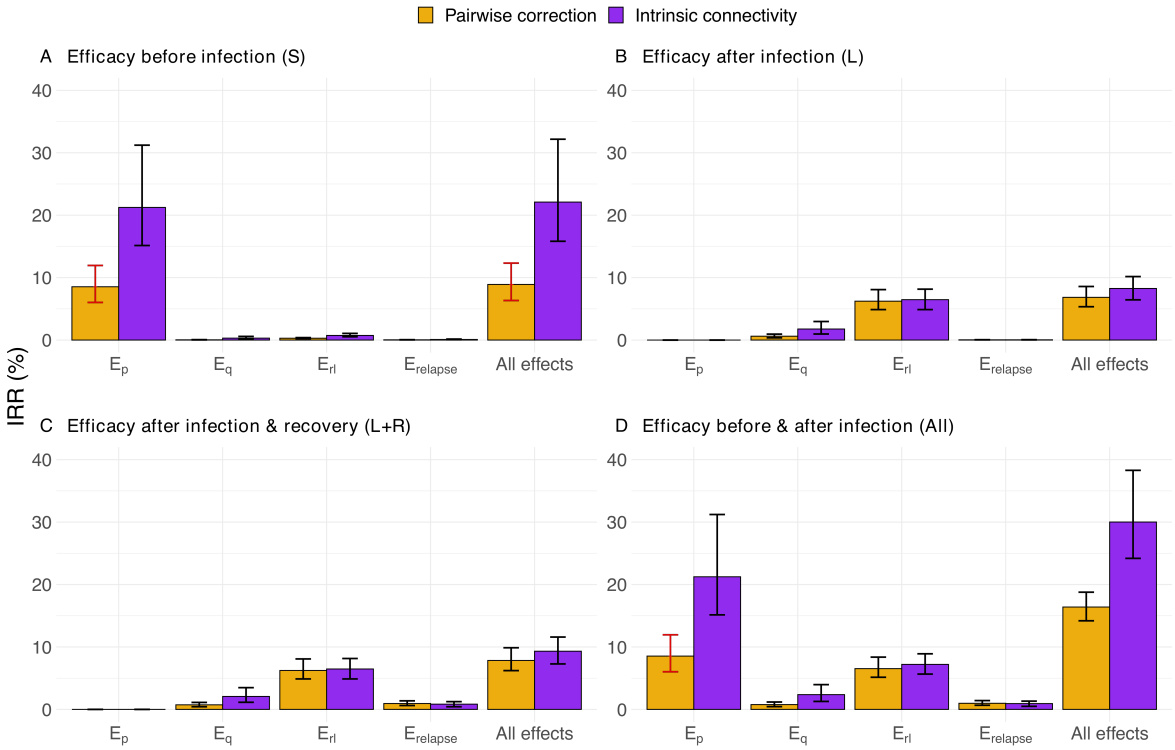

Figure 4.5: Impact of different vaccines in China applied to individuals between 60-64 years old. In all panels, tested vaccines act in different parts of the natural history of TB, halting progression to disease in one or more of the possible routes to disease, as described in the methods: E_p: protection against primary TB, E_q protection against reinfection, E_{rl}: protection against endogenous progression to TB after LTBI, $E_{relapse}$: prevention of recurrence. We analyse independently the impact of vaccines whose protective effects unfold when applied to individuals belonging to different compartments of the natural history. **A**. Susceptible subjects (efficacy observed before infection). **B**. Latently infected individuals (efficacy observed after infection). **C**. Latently infected and recovered individuals. **D**. Entire population. In each case, the impact of each vaccine is evaluated for a waning level of 10 years. In all panels, golden bars correspond to estimates obtained through the pairwise correction method for modelling the time evolution of contact matrices. Magenta bars, in turn, correspond to forecasts obtained using contact matrices derived from the intrinsic connectivity method. Bars represent median values for the IRR measured in 2050, associated with the introduction of the vaccine in 2025. Errorbars capture 95% confidence intervals from a set of $N = 500$ model outcomes in each case.

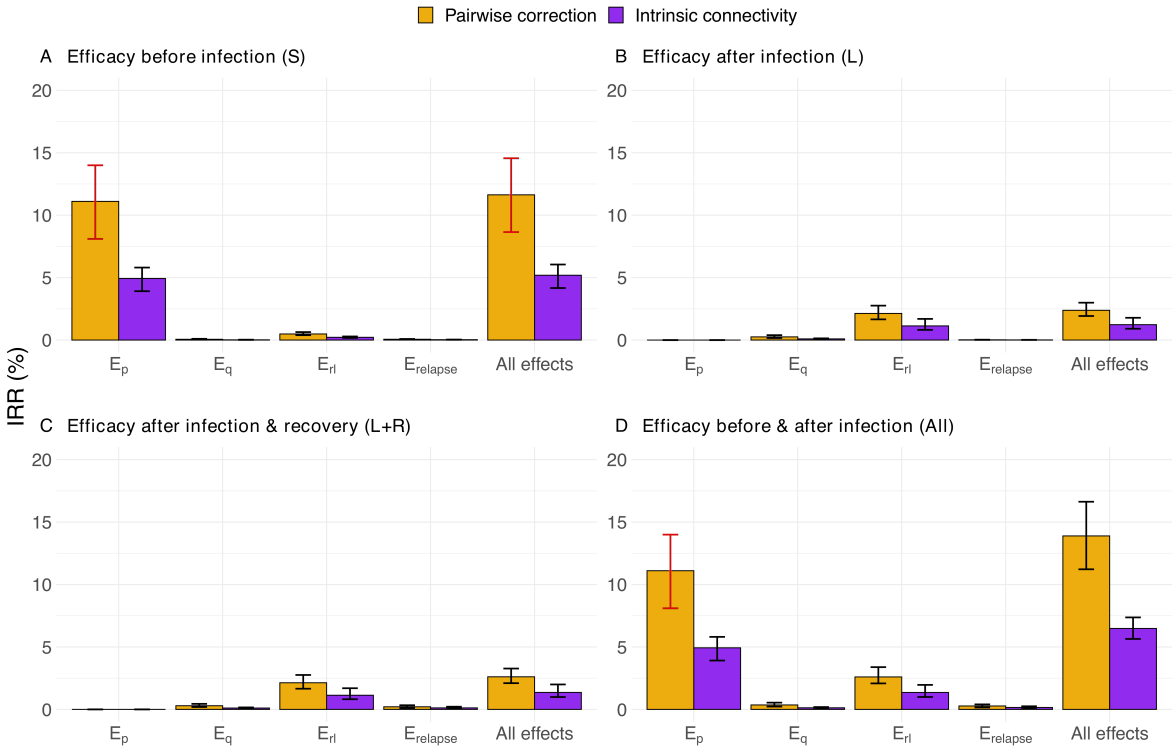

Figure 4.6: Impact of different vaccines applied in China to adolescents, with ages between 15-19 years old. Analogous to Figure 4.5, in all panels, tested vaccines act in different parts of the natural history of TB, halting progression to disease in one or more of the possible routes to disease: E_p: protection against primary TB, E_q protection against reinfection, E_{rl}: protection against endogenous progression to TB after LTBI, $E_{relapse}$: prevention of recurrence. We analyse independently the impact of vaccines whose protective effects unfold when applied to individuals belonging to different compartments of the natural history, **A**. Susceptible subjects (efficacy observed before infection). **B**. Latently infected individuals (efficacy observed after infection). **C**. Latently infected and recovered individuals. **D**. Entire population. In each case, the impact of each vaccine is evaluated for a waning level of 10 years. In all panels, golden bars correspond to estimates obtained through the pairwise correction method for modelling the time evolution of contact matrices. Magenta bars, in turn, correspond to forecasts obtained using contact matrices derived from the intrinsic connectivity method. Bars represent median values for the IRR measured in 2050, associated with the introduction of the vaccine in 2025. Errorbars capture 95% confidence intervals from a set of $N = 500$ model outcomes in each case.

elder vaccination campaign (Bars marked in red) for these vaccines. In those scenarios, both adolescent and elder represent a suitable option for a vaccination campaign, but the dependence upon the modelling choices could hinder the forecasting exercise if this possible bias is not taken into consideration.

Importantly, none of these observations are affected by the level of vaccine waning: while Figures 4.5 and 4.6 capture impacts associated with vaccines which protection lasts ten years, largely comparable results are obtained for longer lasting vaccines. In Figure 4.7, the same simulations performed before are repeated for a waning level of $w = 20$ years, and the results reproduce the same qualitative scenario as before in terms of the impact's hierarchy.

4.3.2 Understanding the impact hierarchy.

In order to understand the influence of the vaccine mechanisms on their respective impacts, we measure the time evolution of the distribution of TB cases across the different routes to disease classically described in TB, aggregated across age groups, as we represent in Figures 4.8A and 4.8B. These routes include fast progression to primary TB upon a first, recent infection event; TB after endogenous reactivation from LTBI; TB upon exogenous reinfection and, last, TB recurrence after a previous disease event (see Methods of this chapter). Importantly, each one of the four vaccine mechanisms explored in this work tackles specifically one of these routes, and do not include posterior effects in other routes. As seen in Figures 4.8A and 4.8B, primary TB upon recent infection is the prominent cause of TB cases during the simulated period, which makes protection against primary TB the most impactful vaccine mechanism, as long as the susceptible individuals (who are those under a higher risk of developing primary TB upon infection[96]), can be protected by the vaccine (see Figures 4.5 and 4.6, panels **A,D**). Furthermore, we also observe that endogenous reactivation of LTBI individuals is the second more prominent type of event responsible of new active TB cases. This explains why vaccines protecting LTBI individuals are most impactful when they protect against endogenous reactivation (see Figures 4.5 and 4.6, panels **B,C**), and why those vaccines halting re-infection or relapse are comparatively less impactful, even when applied on older age groups where prevalence of infected and recovered subjects is higher.

This previous breakdown of cases does not explain, though, the technical influence of the modelling assumptions concerning the evolution of contacts when comparing impact forecasts from analogous immunisation campaigns. In this sense, in order to understand the behaviour, it is important to highlight that this influence manifests more strongly when comparing forecasts for vaccines targeting TB upon recent infection

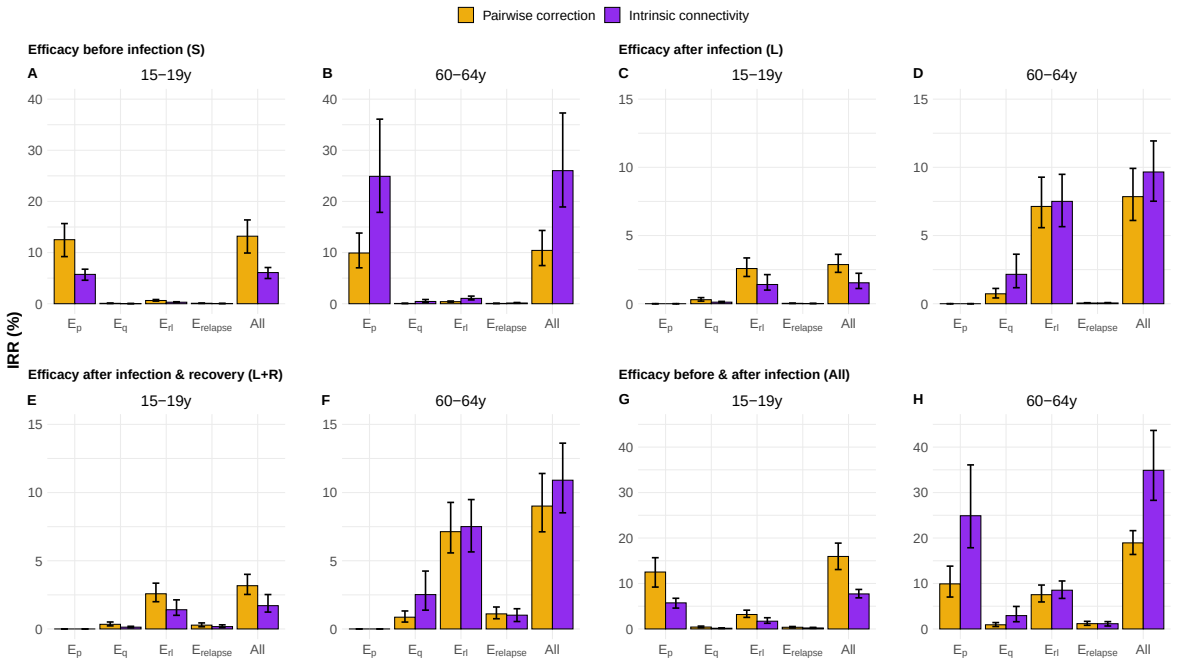

Figure 4.7: Comparison between the IRR achieved when vaccinating individuals of the 15-19 or 60-64 strata with a waning level of 20 years. In all panels, the simulated vaccines act in different parts of the natural history of TB, halting progression to disease in one or more of the possible routes to disease: E_p: protection against primary TB, E_q protection against reinfection, E_{r_l}: protection against endogenous progression to TB after LTBI, $E_{relapse}$: prevention of recurrence. In each case, the impact of each vaccine is evaluated for a waning level of 10 years. We analyse independently the impact of vaccines whose protective effects unfold when applied to individuals belonging to different compartments of the natural history, **A,B**. Susceptible subjects (efficacy observed before infection). **C,D**. Latently infected individuals (efficacy observed after infection). **E,F**. Latently infected and recovered individuals. **G,H**. Entire population. In all cases, the impacts are evaluated for a waning level of 20 years. In all panels, golden bars correspond to estimates obtained through the pairwise correction method for modelling the time evolution of contact matrices. Magenta bars, in turn, correspond to forecasts obtained using contact matrices derived from the intrinsic connectivity method. Bars represent median values for the IRR measured in 2050, associated with the introduction of the vaccine in 2025. Errorbars capture 95% confidence intervals from a set of $N = 500$ model outcomes in each case.

(E_p vaccines) or reinfection (E_q vaccines), which is to say, when the vaccine targets transmission, as in terms of the model, the contact matrices couple with the force of infection, which is key to modulate the transmission of the disease. In such cases, the adoption of the method providing intrinsic connectivity control appears systematically associated to larger impacts when we analyse elder-focused campaigns, as well as to lower impacts, when we focus on campaigns targeting adolescents. This can be further contextualised by observing the evolution of the force of infection, which is defined as the fraction of susceptible individuals in a given group that gets infected per year. Thus, we compute this observable for the individuals in each of the two age strata, according to our each of the two models explored to describe the evolution of contact matrices. As seen in Figures 4.8C and 4.8D, using the pairwise model to model appears associated with an underestimation of the force of infection suffered by individuals in the older age group, and an overestimation of it among adolescents, with respect to the adoption of the more rigorous correction method based on preserving the intrinsic connectivity of contact matrices. This explain why, no matter the age of the targets, the IRR's measured in adolescents are higher with the pairwise correction, and why in elders this happens the other way around.

Finally, we still need to contextualise the differences in impact found between elder and adolescents-focused campaigns. In order to understand those differences, in Figure 4.8E, we present a simultaneous break-down of TB cases predicted by 2050, in each of the age groups, associated with each of the routes to disease, according to each of the contact matrices models. In this figure, we see how both modelling approaches for contact matrices concur in assigning a higher incidence for TB cases related with LTBI reactivation, reinfection, or relapses, which can be interpreted as the main cause why, in Figures 4.5 and 4.6, we observe that E_{rl}, E_q and $E_{relapse}$ vaccines are systematically more impactful in elder individuals than in adolescents. However, in Figure 4.8E, we can also observe how the number of cases associated with primary TB is either higher, or lower in adolescents than it is in the older age group, depending on whether we adopt the pairwise correction method, or the intrinsic connectivity method, respectively.

4.4 A brief discussion on the topic

Mathematical disease-transmission models are a powerful tool for estimating the impact of new TB vaccines, which, if done properly, may be instrumental to compare the potential of different vaccine candidates and immunisation campaigns. This is true, especially in TB, where vaccine development must face two simultaneous hindrances. First, vaccine efficacy is harder to foresee before phases 2b/3 of the development

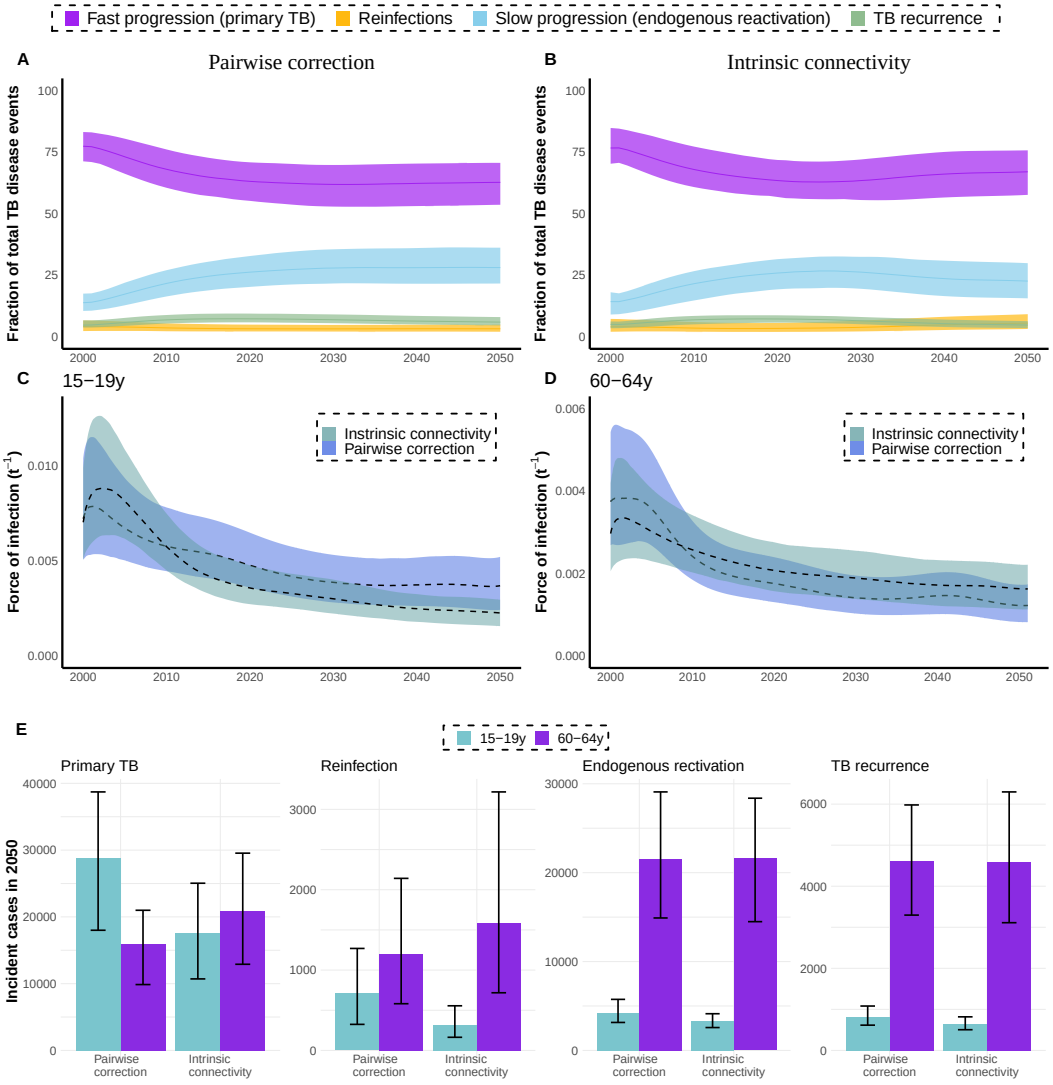

Figure 4.8: Complementary observables to disentangle impact's hierarchy. **A,B**. Evolution of the Percent of TB cases associated with rapid progression upon recent infection (primary TB), endogenous reactivation of LTBI, TB upon reinfection, or TB relapse; each of them foreseen from the indicated method for describing contact matrices evolution (pairwise correction or intrinsic connectivity). Primary TB upon recent infection, followed by endogenous reactivation of LTBI individuals are the two most common types of events. Central lines are medians and shadowed area represent the 95% CI from $N = 500$ model realisations. **C,D**. Evolution of the force of infection associated with individuals in age groups 15-19 and 60-64 in the period 2000-2050, as foreseen by the model when using the two frameworks for describing the time evolution of contact matrices. The simpler pairwise correction method yields a lower estimate of the force of infection in the older age group, and an overestimation in the younger stratum. Central lines are medians and shadowed area represent the 95% CI from $N = 500$ model realisations. **E**. Break down of the different contributions to the overall TB incidence pool in 2050, distributed across the routes to disease protected by the vaccines. The number of cases in the routes associated with already exposed individuals are systematically higher in elders than adolescents, no matter which correction for the contact matrices is at play. Bars represent median values measured in 2050. Errorbars capture 95% CI from $N = 500$ model realisations.

pipeline than for other diseases, given the lack of reliable correlates of immune protection[115]. Second, the architectures of the clinical trials of vaccine efficacy that are being adopted to test novel TB vaccine candidates are highly diverse [117, 118], and the protection profiles of the tested vaccines may be equally diverse. Taken together, these issues claim for the development of rigorous computational models to produce impact comparisons for different vaccines tested in trials of different characteristics, and implemented through assorted immunisation campaigns. These constitute extremely non-trivial tasks, which enhances the need of ensuring that current TB models can handle them while minimising bias and uncertainty.

In accomplishing this goal, an aspect that demands for an especial attention is the description of the coupling between demographic ageing and the evolution of TB epidemiology in a given population. This is especially true in a country such as China, where two simultaneous aspects concur, namely: an intense process of demographic ageing -already ongoing, and expected to continue in the next few decades-, concomitant with a high burden of TB incidence and prevalence levels. While previous works pointed to the observation that immunisation campaigns targeting older age groups (paradigmatically individuals above 60 years old) are expected to cause a stronger reduction in global TB incidence levels than campaigns targeting adolescents (16-20 years old) [162], the robustness of these results under different modelling scenarios, including different vaccine characteristics and modelling decisions concerning the evolution of contact matrices among different age-groups remained to be proven.

Capitalising on a mathematical model previously developed by the team [135, 117, 118], in this work we reproduce the general observation that, in China, immunisation campaigns targeting older individuals, in the age group between 60 and 64 years old, are associated with promising levels of reduction in the incidence rates expected by 2050, with varying forecast impacts depending on vaccine characteristics and modelling assumptions, specially if the vaccine is able to protect already exposed individuals. This observation can be interpreted under the light of the demographic shift expected in the country, where older age strata are expected to accumulate a higher fraction of total TB cases in the years to come. However, by using our model, we were able to address, for the first time in this study, how this observation may depend, in turn, on vaccine characteristics (the combination of its mechanisms of action and protection profile), as well as on modelling assumptions (the description of contact matrices over time).

On the one hand, when modelling TB vaccines, it is important to acknowledge the multiplicity of possible mechanisms of action a vaccine may confer protection through [117, 118]. This aspect, in turn, must be considered simultaneously to the fact that the

initial immunological profile of vaccinated individuals (i.e. their IGRA status) may in turn influence the ability of the vaccine to provide its protective effects. [162]. In this work, we describe how these two aspects are coupled, generating strong interactions between the vaccine mechanisms at place and the sub-population reservoirs that may gain their protective effects upon vaccination. Specifically, we observed that vaccines protecting susceptible, immunologically naive individuals are more impactful when their mechanism of action is based upon the prevention of primary TB after infection. This result can be understood by observing that progression to primary TB upon recent infection represents not just the main epidemiological risk for susceptible individuals, but the most common route to disease in the whole population, as sketched in Figures 4.8A and 4.8B. Importantly, our simulations indicate that tackling primary TB is the most promising intervention, not only when the immunisation campaign targets adolescents, but also when it targets older individuals, as long as vaccine protection unfolds for susceptible individuals at least. Furthermore, when a vaccine precises that vaccinated individuals have previously been infected, the most impactful vaccine mechanism of action is based on preventing endogenous reactivation of LTBI. This indicates that, for LTBI subjects, endogenous progression to TB represents the highest epidemiological risk, which is shown in Figures 4.8A and 4.8B, where endogenous reactivation in the second most common route to disease. These couplings between vaccine mechanisms and protection profiles should be carefully taken into account when testing and comparing vaccine candidates with different profiles and immunisation strategies.

On the other hand, in a country such as China, it is key to produce model-based descriptions of TB dynamics that are robust under the scenario of fast demographic ageing. Under these circumstances, the adoption of plausible description frameworks to describe the evolution of contact matrices is key. The reason for this is that these matrices capture the relative frequency of contacts that may lead to new infections among individuals of different ages, and these are bound to evolve with time in an ageing population. While relatively naive descriptions of contact matrices based on symmetry preservation through pairwise corrections is enough when modelling infectious diseases during short periods of time, TB demands for more sophisticated approaches that preserve not only the symmetry, but also the overall connectivity of the entire contact networks [136]. The reason for this is that during the extended time windows that TB modelling requires, demographic structures are expected to vary significantly, and, with them, the frequencies of social contacts among age strata, and the entire connectivity, measured as the average number of contacts per individual, of the system.

In this chapter we showed that more sophisticated modelling approaches based on imposing the preservation of the intrinsic connectivity of contact networks (instead of simpler methods based on pairwise corrections aiming only at preserving symmetry) is linked to higher vaccine impacts when immunisation campaigns target transmission among elder individuals. In turn, for campaigns targeting transmission among adolescents, it is the simpler methods, based on pairwise corrections, the one yielding higher impacts. In short, our simulations indicate that vaccines whose protection mechanisms take place after infection (e.g. E_{rl}, E_q and $E_{relapse}$ on L, L+R or All population), are expected to elicit higher population impacts if applied in elder individuals, as well as vaccines protecting susceptible individuals against primary TB, providing that an adequate modelling approach is used to describe the evolution of their contact matrices, ensuring intrinsic connectivity control.

We also need to mention that our approach is not exempt from limitations that affect TB transmission models. The outcomes of our model depend on a series of epidemiological parameters and initial burden estimates that are subject to strong sources of uncertainty, thus propagating this uncertainty to the results. This means that future improvements in measuring the input data are expected to impact the quantitative outcomes of our mathematical model, in the same way it would affect any other model that leans on them. Always bearing in mind the strong uncertainties that the forecasts inherit, our results highlight the importance of acknowledging the complexity of TB transmission dynamics when modelling the effects of an age-focused intervention such the introduction of a new vaccine on a specific age group.

In closing, our results emphasise the idea that immunisation campaigns for the introduction of new TB vaccines in different countries can be, and must be tailored using mathematical models that integrate information of vaccines' profiles, population demography and basal TB epidemiology.

Chapter 5

The interaction between Tuberculosis and COVID-19

Summary of this chapter: The COVID-19 pandemic has disrupted everyday life and put public health services and healthcare systems worldwide under stress. This has compromised the ability to control other diseases such as Malaria, Cancer, and Tuberculosis (TB). In this chapter, we predict the rise in TB occurrence and mortality when healthcare systems are impacted and diagnosis capabilities are blocked in India, Indonesia, Pakistan, and Kenya, countries where TB is prevalent. Our calculations show that an increase in new TB cases due to the COVID-19 pandemic could result in almost 400,000 additional deaths in those countries. We also show that increased diagnosis capabilities after the pandemic could reduce the additional deaths from TB resulting from the COVID-19 pandemic impact, suggesting that the far-reaching effects on TB mortality could be halted.

5.1 COVID-19 and Tuberculosis: an introduction.

From December 2019, and for the following years, the world witnessed the surge of a menace long time foreseen, the irruption of a pandemic caused by a virus that spread fast and was difficult to detect, and to treat, which led to high levels of mortality across the world. This was the COVID-19 pandemic. Caused by the coronavirus SARS-CoV-2, the pandemic was a global health crisis that had a profound impact on societies, economies, and healthcare systems around the world. The earliest known cases of COVID-19 were reported in December 2019 in the city of Wuhan, in China. Initially, the cases were linked to a seafood market, suggesting an animal-to-human transmission. However, it was soon discovered that the virus spread from person to person through respiratory droplets. The virus quickly spread beyond China's borders, with cases appearing in neighbouring countries and eventually reaching every continent. As a consequence, on January 2020, the World Health Organization declared COVID-19 a Public Health Emergency of International

Concern on January 30. Then, the rapid transmission and severity of the disease led the WHO to declare COVID-19 a pandemic on March 11, 2020.

Governments worldwide implemented a range of measures to contain the spread of the virus and mitigate its impact. These measures included widespread testing, contact tracing, travel restrictions, lockdowns, social distancing, and the promotion of good hygiene practices such as frequent hand-washing and mask-wearing[120], although some were more effective, or more widely adopted than others due to different responses among the population[121, 122]. The COVID-19 pandemic has had far-reaching consequences on multiple fronts. The global economy suffered a severe downturn, with businesses closing, supply chains disrupted, and millions of people losing their jobs[123]. The pandemic also strained healthcare systems, particularly in areas with high infection rates, leading to shortages of medical supplies, hospital beds, and healthcare workers. Specifically, the impact on public health has been immense, with millions of people contracting the virus and suffering from a range of symptoms, from mild respiratory issues to severe pneumonia and acute respiratory distress syndrome. The elderly and those with underlying health conditions have been particularly vulnerable.

During the hardest years of the pandemic, as stated, plenty of countermeasures were deployed to face the ongoing pandemic, as it was a deadly threat. But at the same time, other diseases continued to pose a menace to public health, whose severity was even higher than before as the healthcare systems saturated. In the middle of this maelstrom, TB, the main topic of this thesis, remained one of the greatest threats to public health worldwide, being the deadliest single-agent persistent infectious disease nowadays. According to the 2021 Global TB Report by the World Health Organisation (WHO)[76], 10 million people developed TB and nearly 1.5 million people died because of TB infection in 2020, during the first year of the COVID-19 pandemic. And, as a consequence of the global situation, for the first time in a decade, there was an increase in TB-caused deaths. It's important to notice that, in the last decades, the WHO deployed a series of global strategies that have since been the backbone of the global fight against TB. In 1995, the Directed Observed Treatment Strategy (DOTS) was introduced, which significantly strengthened the capacity of national programs to diagnose and treat TB cases. Later, the Stop TB Strategy, announced in 2006, was the first of such plans to set a TB elimination horizon, defined as a reduction of incidence levels under 1 case per million and year by 2050. A redefinition of the eradication goal took place in 2014 when the previous objective was moved forward to 2035 within the End TB Strategy.

With this in mind, and being elimination target set by the End TB strategy already an ambitious goal[218], the emergence of the COVID-19 pandemic caused by the

new coronavirus SARS-CoV-2 sheds significant concerns on whether these goals are still reachable. During the acute stages of the COVID-19 pandemic, economic and human resources were redirected to control and mitigate the emergency caused by the pandemic, which led to a great reduction in the diagnosis of new cases of other diseases, as already documented for cancer, or malaria[127, 128]. Interventions such as long lockdowns and mobility restrictions have exacerbated shortages in resources otherwise destined for the care of patients suffering these, and other pathologies. Moreover, COVID-19 has greatly affected healthcare workers[124, 125, 126], thus creating additional pressure on healthcare systems. TB diagnosis and patient care were no exceptions, as reported in previous literature[76, 73, 129]. As a primary and immediate effect of COVID-19 spreading onto TB transmission dynamics, a reduction in the case notification ratio was observed during and immediately after lockdowns and periods of high COVID-19 incidence and saturation of healthcare facilities [76].

The objectives of this chapter are, then, to study the interaction created by COVID-19 and TB, at the burden level of the latter. We hypothesise that this disruption alone will lead to a surge in TB burden in the years that have to come, even before the more complex, and less predictable effects of the COVID-19 pandemic on TB management and transmission dynamics can be properly characterised. For example, drastic drops in laboratory capacity needed to support TB diagnosis are expected along with interruptions in the supply of drugs, which could result in shortages of medications and could delay the start of treatments until the supply chain is reestablished[219, 220, 74]. Moreover, as suggested by Cilloni et al. [177], even temporary stoppages might cause long-term increases in TB incidence and mortality, and a peak in TB burden is to be observed as a consequence of the healthcare system disruption.

Taking all the previous considerations together, in this chapter, we assess the impact of COVID-19 on the expected TB burden until the year 2035, which marks the target horizon of the End TB Strategy. Specifically, we incorporate the observed drop in TB diagnosis and treatment compliance rates caused by COVID-19 into a mathematical model that produces long-term forecasts of TB burden [135]. This allows us to: i) quantify the effect of the COVID-19 stoppage about a baseline scenario in which no pandemic happened, and ii) compute the effect of a rapid response to the uprising TB burden in the following years, in the form of a compensatory intervention aiming at boosting TB diagnosis rates as soon as the COVID-19 pandemic ends, has over long-term TB goals. Our results show that an effort focused on increasing TB diagnosis capabilities once the pandemic is over could revert the effect of the pandemic in the long term.

5.2 Methods

5.2.1 Model calibration and diagnosis rate

In this chapter, we have capitalized on the detailed *M.tb.* transmission model developed by Arregui et al. [135, 221] (see Chapter 2) that it is used along the thesis. Conceptually, this model is an age-stratified compartmental model that describes TB dynamics within a whole, closed population, stratified into 15 age groups during periods of the order of several decades. The model is detailed enough to include demographic evolution and ageing, along with heterogeneous contact patterns among age groups that have been adapted from empirical survey studies.

Here, the model is calibrated to reproduce TB incidence and mortality rates in each country under study for the period 2000–2019, using the burden estimates provided by the WHO. The calibration process gives the diagnosis rate $d(t)$ and the scaled infectiousness $\beta(t)$, which are modelled as half-sigmoid-like curves, and, among other parameters, are country-specific. This allows the model to reproduce different epidemiological scenarios. Specifically, the diagnosis rate is defined as:

$$d(t) = \begin{cases} d_0 + (d_{\text{sup}} - d_0)t(t + \frac{1}{d_1})^{-1} & \text{if} \quad d_1 > 0 \\ d_0 & \text{if} \quad d_1 = 0 \\ d_0 - d_0 t(t - \frac{1}{d_1})^{-1} & \text{if} \quad d_1 < 0 \end{cases} \tag{5.1}$$

Therefore, the diagnosis rate is parameterised by two quantities (d_0, d_1), where d_0 is the value at the beginning of the calibrating window (i.e. year 2000 in this study), and d_1 defines its evolution, either increasing or decreasing with time depending on d_1's sign. In the case of a decreasing evolution, the diagnosis rate is bound to be greater than zero, while in the case of increasing evolution, the upper bound is $d_{\text{sup}} = 12.17(\text{y}^{-1})$[135]. This latter upper bound corresponds to a minimum diagnosis period of one month, assuming that, with a conservative lower boundary, the main symptom of TB is a continuous cough lasting for three weeks, followed by a diagnosis time estimated to last at least 10 days [222]. For further details regarding the specific values of epidemiological parameters, calibration processes, and uncertainty estimates, the reader is referred to Chapter 2 of this thesis and to the original source[135].

In this chapter, an additional ingredient is needed on top of the spreading model and its calibration. This is, as explained in the second objective of the thesis, and the defined milestones, it is necessary to modify the diagnosis curves to capture the disruptions due to the pandemic, and thus, to be able to produce forecasts until 2035 under two different scenarios: the baseline scenario, namely, a scenario in which there is no COVID-19 pandemic and thus, no disruption in healthcare systems is introduced,

and another one in which a disruption is introduced at the start of 2020 up to the end of 2021, which is the pandemic scenario. During the duration of the pandemic, the diagnosis rate dropped according to the reduction observed in the notifications of TB cases that were reported by WHO online, in the last global TB report, and also by the Nikshay program in India. Therefore, the drops in diagnosis rates are country-specific. These drops in TB notifications are fitted to a bump-like asymmetric function, as described through $d_{red}(t)$ in Equation 5.2. This function reproduces the real data and is then applied to the model-calibrated diagnosis rate to produce the diagnosis function under the pandemic scenario. The fitting procedure is a Levenberg-Marquardt Nonlinear Least-Squares using *minpack.lm* R's package [223], where Equation 5.2 is applied to the data after being normalised by the 2019 mean for each country.

$$d_{red}(t) = \begin{cases} 1 & t \leq t_0 \\ 1 - h \cdot \exp \frac{-k_1(t-t_1)^2}{(t_1-t_0)^2-(t-t_1)^2} & t_0 < t \leq t_1 \\ 1 - h \cdot \exp \frac{-k_2(t-t_1)^2}{(t_2-t_1)^2-(t-t_1)^2} & t_1 < t \leq t_2 \\ 1 & t > t_2 \end{cases} \tag{5.2}$$

The bump-like function described in Equation 5.2 serves as a multiplier to the model-calibrated diagnosis rate, thus, being the diagnosis rate under the pandemic scenario $D(t) = d(t) * d_{\text{red}}(t)$ with $d_{\text{red}}(t) \neq 1$ only during the COVID-19 pandemic, and $d_{\text{red}}(t) = 1$ otherwise. In Table 5.1, the fitted values of each parameter involved in the bump-like description of the TB notification drops are reported.

Bump Parameters	
Country	$\Theta = \{h, t_1, t_2, k_1, k_2\}$
Indonesia	$\Theta = \{0.494,\ 0.391,\ 17.31,\ 6.226,\ 117.4\}$
Pakistan	$\Theta = \{0.398,\ 0.257,\ 18.04,\ 3095.3,\ 826.8\}$
Kenya	$\Theta = \{0.248,\ 0.859,\ 5.218,\ 0.905,\ 46.51\}$
India	$\Theta_1 = \{0.393,\ 0.272,\ 1.25,\ 134.7,\ 0.645\}$
	$\Theta_2 = \{0.594,\ 0.139,\ 1.069,\ 3.111,\ 114.12\}$

Table 5.1: Fitted parameters for diagnosis reduction in selected countries. The fitting procedure is a Levenberg-Marquardt Nonlinear Least-Squares using *minpack.lm* R's package[223], where Equation 5.2 is applied to the WHO data normalised by the 2019 mean. For Indonesia, Pakistan and Kenya, one bump is enough for reproducing the data, whereas in India two separate bumps need to be concatenated, and are denoted here as Θ_1 and Θ_2 respectively. h, k_1 and k_2 are dimensionless quantities, whereas t_1 and t_2 have units of year^{-1}.

Finally, during the period of recovery, we proposed the deployment of interventions that are aimed at compensating for the drop in diagnosis rates during the pandemic years. In this chapter, this is modelled by multiplying the diagnosis by a scale

parameter at some point after the end of the pandemic disruption. Once the recovery period is over, we assume that the diagnosis rate goes back to its original value as given by $d(t)$ up to the end of the simulation.

5.2.2 First-line treatment reduction

According to previous reports[76, 177], first-line TB treatment completion has dropped effectively as a consequence of the COVID-19 pandemic, with interruptions in the supply of drugs that delay the start of the treatment in those cases in which the remaining medical capabilities have been enough to diagnose the disease. This inconvenience could not only worsen the expected treatment outcome for the patient but also drive secondary infections even in diagnosed patients if they are not able to quarantine until the treatment can be carried out. This situation, in terms of the epidemiological model, is modelled by including a fraction of under-treatment pulmonary TB individuals (T_p) in the expression of the force of infection ($\lambda(t)$). On the baseline scenario and without disruptions, those T_p individuals are not able to contribute to $\lambda(t)$ as we assume that they are under control by the healthcare system, thus, being controlled and either under quarantine or, later on, medicated with TB drugs that greatly reduce their infectiousness. This means that, under normal circumstances, diagnosed individuals are expected not to be a risk for the rest of the population. However, when disruptions in the supply chain appear, a drop is observed in the first-line and second-line treatment completion [177], and then diagnosed individuals who are not able to either start the treatment or quarantine could become a risk. For this reason, we obtain an estimate of the fraction of T_p individuals that contribute to $\lambda(t)$, T_{inf}, from Cilloni et al. [177] as

$$T_{\text{inf}} = (1 - \eta)T_p \tag{5.3}$$

where $\eta = 0.788$. This value attempts to capture this kind of impact in countries like India and Kenya. It is based on expert opinion in the Stop TB Partnership and USAID about the side effects of the COVID-19 pandemic on TB treatment completion. We assume it to be a good proxy for the real value in the other countries included in this study.

5.3 TB burden under the pandemic disruption

To forecast the effect that disruptions in the diagnostic capabilities and the treatment completion have on TB incidence and mortality trends, we selected four different high-burden countries, 3 in Asia (India, Indonesia, Pakistan) and 1 in Africa (Kenya).

Then, we calibrated the mathematical model[135] using the current WHO estimates for TB incidence and mortality rates in those countries and produced forecasts in two separate scenarios. The baseline scenario assumes no disruption, whereas the perturbed scenario incorporates the effects of the pandemic on TB diagnosis and treatment adherence. In the different countries analysed, the duration of the disruptions has been of variable intensity and length, and while some countries experienced an almost complete return to pre-pandemic levels by June 2021 (India, Pakistan), other countries were still registering lower case notification rates by the end of 2021 compared to values before the COVID-19 irruption.

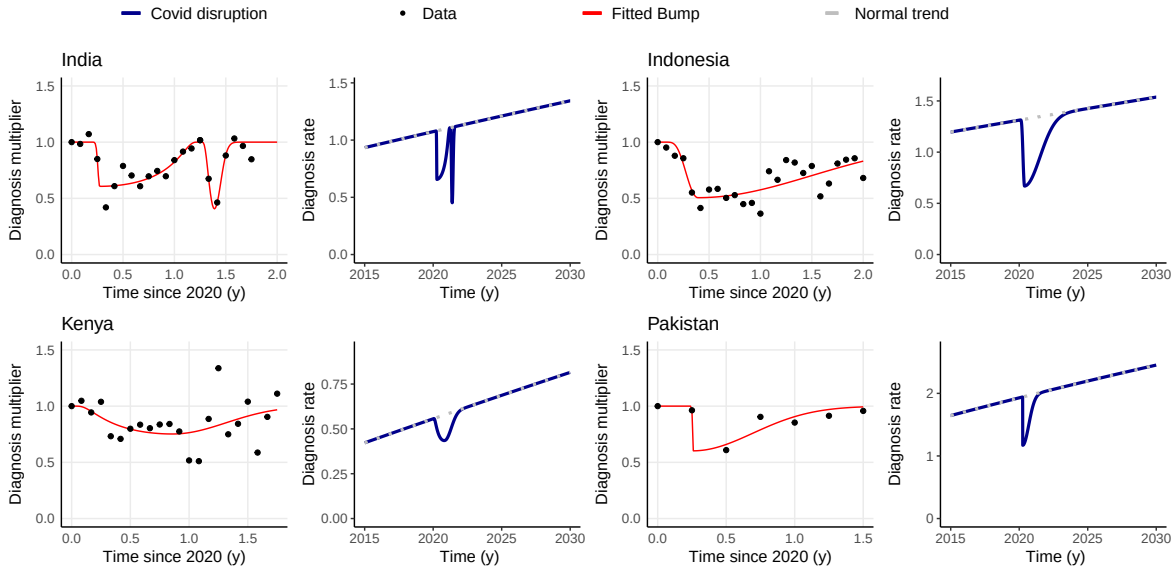

Figure 5.1: Changes in the diagnosis rate before, during, and after the pandemic period.
We present both the original data and the fitted bumps we use for modelling the disruption, along with the diagnosis rates in two scenarios: the baseline, with no disruption (dotted lines), and the pandemic scenario, where the drop in diagnosis happens and is followed by a return of the diagnosis rates to the baseline scenario. Diagnosis multipliers are obtained directly using the WHO data as the TB notifications in that period divided by the mean of TB notifications in the year 2019. The four countries considered are India, Indonesia, Kenya, and Pakistan

While treatment adherence is assumed to be reduced a 22% from the pre-pandemic values, according to Cilloni et al.[177], disruption is introduced based on available data. These were made publicly available by the WHO for Indonesia, Kenya, and Pakistan [224], and by the Nikshay governmental program for India[225] during the moths -or trimesters, for Pakistan- that followed the irruption of COVID-19. To incorporate those data into our model, we use a piece-wise bump-function $d_{\text{red}}(t)$ to model a transient continuous drop in the diagnosis rate trend $d(t)$ that was foreseen within our model upon its calibration on pre-pandemic data (see Methods, Equation 5.1). Proceeding

this way, the actual diagnosis rate in the COVID-19 scenario, $D(t)$, can be obtained as the product of the model-calibrated diagnosis rate and the fitted bump function capturing the disruption due to the COVID-19 pandemic, as shown in Equation 5.4 and Figure 5.1.

$$D(t) = d(t) * d_{\text{red}}(t) \ . \tag{5.4}$$

Figure 5.2 shows the estimated TB incidence per million inhabitants per year in the four countries considered, both in the baseline scenario and considering the negative impact of the COVID-19 pandemic. As observed, a transient surge of TB incidence starts in 2020, which is later foreseen to return to values close to the baseline trend. In the figure, the dotted line represents the baseline scenario, namely, what would have been the projected evolution of TB incidence without the disruptions of the pandemic. The size of the peak reflects the severity of the saturation of the healthcare system in each country which led to drops of different intensity in diagnosis. The results show that the estimated COVID-19 impact on TB incidence trends is larger in the three Asian countries analysed than in Kenya. This is a direct consequence of the less severe decays in TB case notifications that have been observed in Africa in comparison to other regions [76], which have been used to inform our mathematical model. These regional differences, in turn, may be due to a combination of factors. First, as stated by Haider et al.[226], some of those countries adopted early measures for facing the pandemic, secondly, COVID-19 has had a smaller effect in Africa, which can be due, in part, to a strong under-diagnosis and partially because its younger population.

Important enough, even if COVID-19 disruptions are assumed to happen only during the pandemic years, the long-term effects span for longer times, sometimes up to five years since the start of the COVID-19 pandemic. As observed in Figure 5.2, in the long term, TB incidence levels stabilise and recover to their baseline values approximately by the year 2030, resulting in a 10 year window of higher burden that makes the incidence go off the way of TB eradication stated in the End TB Strategy. Moreover, in the absence of any further intervention, the peak of TB incidence caused by the disruptions associated with the COVID-19 pandemic will produce not only new TB cases but also an increase in TB-related deaths all across the world. Specifically, by the end of the simulation period in the year 2035, our model predicts an increase in mortality as shown in Figure 5.3, where we have represented both the increment percentage and the total number of accumulated additional deaths between 2020 and 2035. Particularly, we forecast an increase in the number of deaths of 1.43%(1.01-1.84, 95%CI) in India, 3.14%(2.58-4.02, 95%CI) in Indonesia, 0.73%(0.65-0.86, 95%CI) in Kenya and 1.96%(1.29-2.62, 95%CI) in Pakistan. In absolute terms, the total number

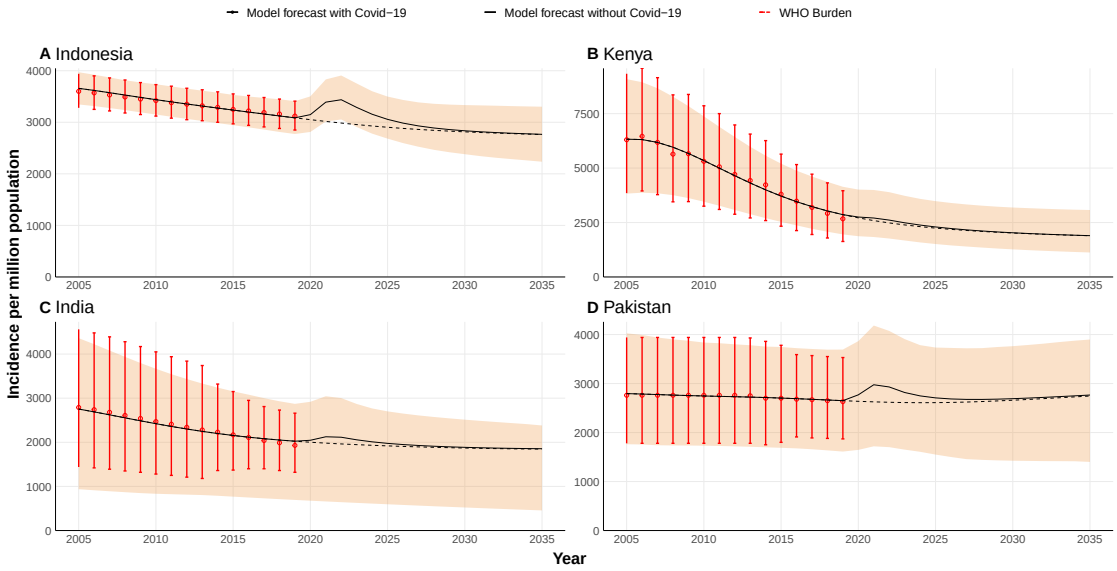

Figure 5.2: Projected annual TB incidence in four high-burden countries over the period 2005-2035.
The data-driven model is calibrated with WHO incidence data up to 2019[76]. The shaded area represents the 95%CI and the black line is the median of the model outcome for 500 independent runs of the disrupted scenario. The dotted black line is the model forecast for the scenario in which there was no Covid-19 pandemic. Red dots with error bars are the TB burden provided by the WHO[76] used for calibration. Projected incidence values are calculated at the end of the corresponding year on the x-axis. The impact of COVID-19 is modelled as a reduction in diagnosis rates and treatment completion for two years (2020 and 2021), see Fig. 5.1 and main text. The four countries considered are **A** Indonesia. **B** Kenya. **C** India. **D** Pakistan, which account for 42.1% of the total number of TB infections worldwide.

of excess deaths could be over 400000 individuals in these four countries alone (Figure 5.3B).

Finally, and given the characteristics of COVID-19 spreading, in which variants started spreading faster than the measures to control them, it was not clear if the pandemic was reaching an end soon. Even today, the risk of suffering another wave of COVID-19 is not zero. Under those circumstances, we decided to perform a sensitivity analysis in which we explore the hypothetical scenario of having an additional disruption in diagnosis similar to the one that already happened. Thus, we perform a new set of simulations in which we forecast both incidence and mortality when another bump equal to the fitted ones is introduced right after the end of the former. In Indonesia, Kenya, and Pakistan, this is trivial, as there is only one big bump in diagnosis reported, whereas, in India, there were two separate bumps, a first, big one, and a second, narrow one. In this situation, we analysed separately each case, studying the case of repeating either the first bump or the narrowest, second bump.

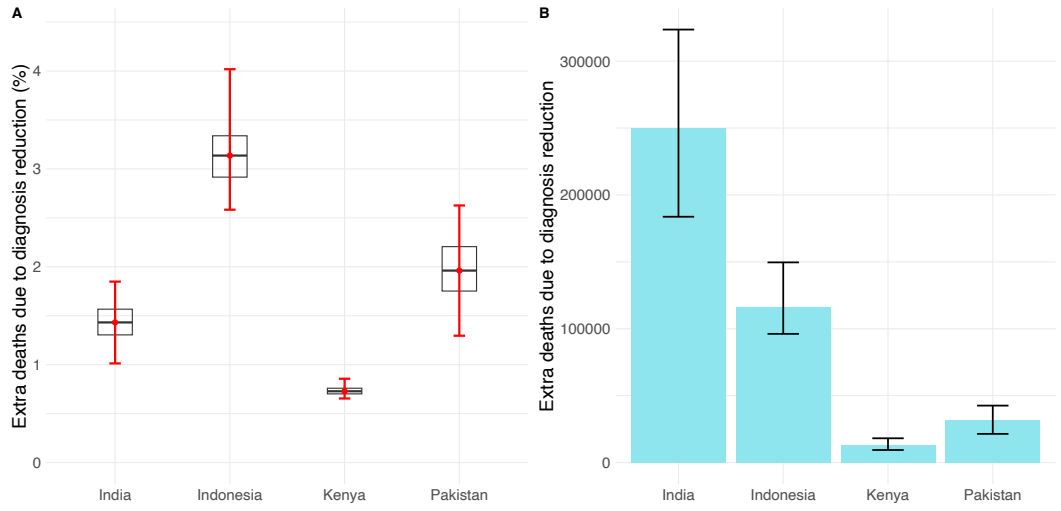

Figure 5.3: Model predictions of additional TB-related deaths due to COVID-19-related disruptions in healthcare systems.
In both panels, the error bars are the 95%CI of 500 independent runs of the model under the pandemic scenario. **A** Percentage of increase of mortality in comparison to the baseline scenario in 2035 for each of the four countries studied. Boxplots represent the inter-quartile range and the central values are the median values. **B** Cumulative number of excess deaths caused by the pandemic impact during the whole time window simulated (2020-2035) for each country under study as indicated in the x-axis. Central values are calculated as median values.

The results of this analysis are reported in Figure 5.4, where diagnosis rates, incidence temporal series, and mortality in 2035 are reported in each scenario.

We observed that, if another disruption is to happen, an even greater increase in mortality occurs in every country, which leads to more deaths associated with the diagnosis disruptions. Specifically, in India we expect an additional 146k (CI 110-117) deaths in the big secondary wave scenario and an additional 42k (CI 32-52) deaths even in the narrow secondary wave scenario, which translates into relative increases in mortality of 36.9% (CI 34.9-39.6) and 14.6% (CI 13.4-16.2) respectively concerning the already bad normal scenario with just a primary bump. In Indonesia, an additional 139k (CI 115-177) deaths are expected, which corresponds to a 54.5% (CI 53.3-55.5) relative increase, while in Kenya and Pakistan 9k (CI 6-13) and 15k (CI 10-18) additional deaths are expected, with relatives increases of mortality of 41.3% (CI 39.3-43.2) and 32.4% (CI 29.2-36.2) respectively. Moreover, incidence levels, especially in Indonesia, but happening in all countries, need more time to recover the levels of the baseline scenario, risking, even more, the END TB goals.

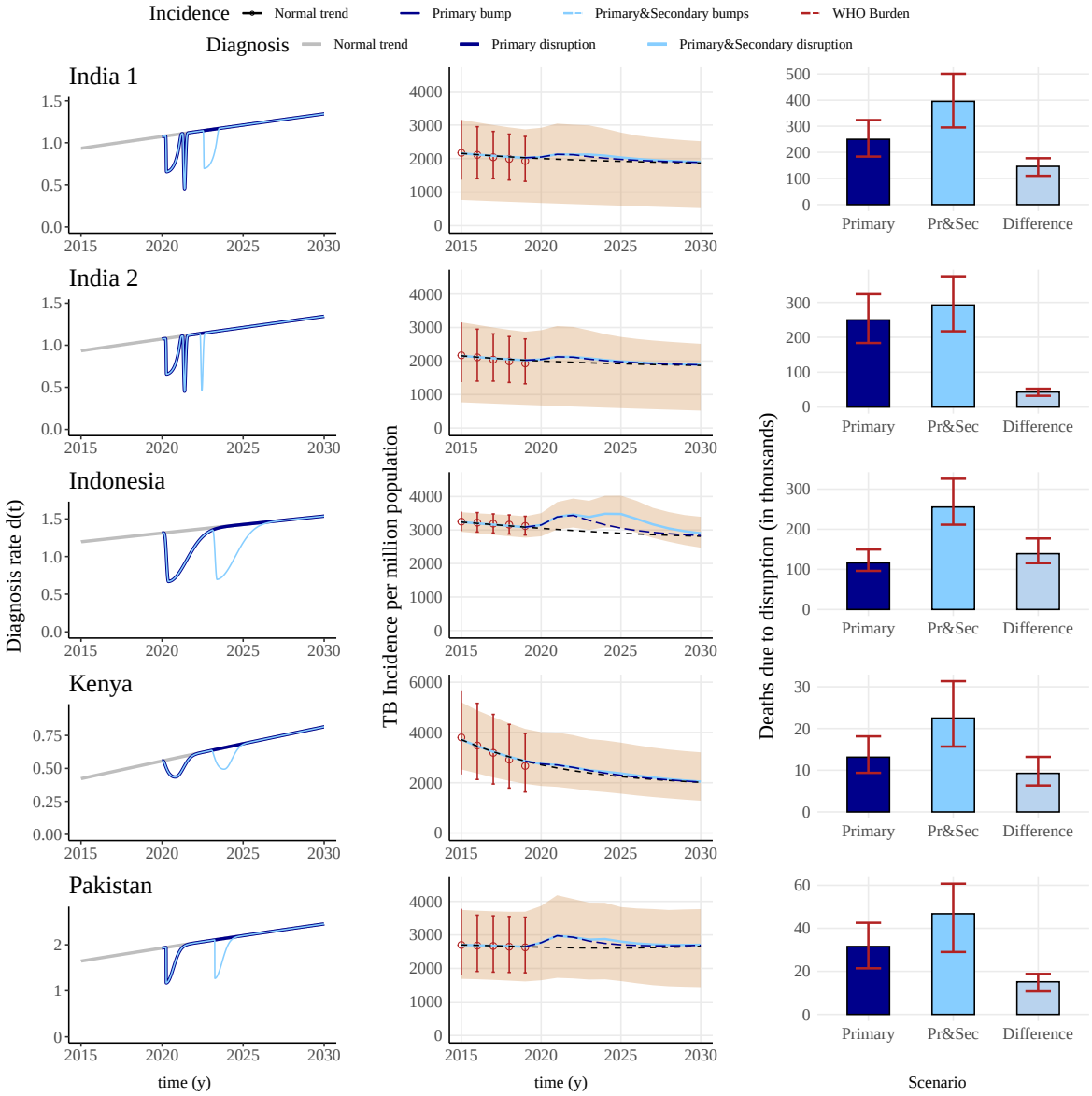

Figure 5.4: Diagnosis and TB burden in alternative scenarios. The first column reports the diagnosis rate $D(t)$, in each country, in the baseline scenario (grey dotted line) compared to the COVID-19 primary disruption and the hypothetical second disruption (blue lines). The second column reports TB incidence temporal series in each country in the same scenarios as before. If a secondary disruption is introduced, baseline incidence levels take more time to be reached. Finally, the third and last column reports the expected mortality in the year 2035 comparing the primary and primary plus secondary scenarios. In the latter, an increase in mortality leads to even more deaths caused by the pandemic disruption of TB care.

5.4 Boosting interventions in the recovery period

The pandemic circumstances will lead to notable increases in TB incidence and mortality. This represents a critical setback concerning the objective of eradicating TB disease within the next few decades, making it hardly achievable without a rapid and effective recovery strategy. More importantly, the disruptions will cause many preventable deaths. It is thus of utmost importance to elucidate whether new policies could be implemented to revert the negative impact of COVID-19 on TB disease. In this section, we explore the potential of interventions focused on compensating the decay in diagnosis rates observed during the biennium 2020-2021, through a compensatory boost in the next years, as sketched in figure 5.5.

Schematically, the previous formula yields a diagnosis curve that is increased to a fixed value for a given amount of time, as shown in Figure 5.5. In this Figure, the dotted line represents the baseline scenario, the red line captures the disruption in diagnosis due to the COVID-19 pandemic, and finally, the green line captures the proposed scenario where a boost in diagnosis is introduced.

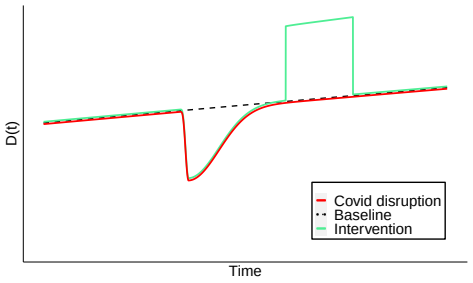

Figure 5.5: Schematic representation of the increase in diagnosis rate in the post-pandemic scenario. We consider a compensatory period during which the diagnosis rate is boosted up to $d(t) * d_{inc}$, with $d_{inc} > 0$.

While improvements in passive case-finding routine practice are unlikely to unlock sufficient increases in diagnosis rates, these, combined with the implementation of properly designed strategies of active case-finding would constitute the paradigmatic type of interventions capable of producing diagnosis improvements comparable to those here explored. The potential intervention over the diagnosis of TB cases is modelled using a piece-wise function that combines Equation 5.4 with an additional piece introduced after the pandemic disruption is over, and for a parameterised duration, $\mathrm{T}_{\mathrm{rec}}^{\mathrm{end}} - \mathrm{T}_{\mathrm{rec}}^{\mathrm{st}}$, to be determined. More specifically, we assume that over this new period, the pre-pandemic diagnosis rate is effectively increased by a factor $d_{\mathrm{inc}} \geq 1$. That is:

$$D(t) = \begin{cases} d(t) * d_{\mathrm{red}}(t) & \text{if} \quad t < \mathrm{T}_{\mathrm{rec}}^{\mathrm{st}} \\ d(t) * d_{\mathrm{red}}(t) * d_{\mathrm{inc}} & \text{if} \quad \mathrm{T}_{\mathrm{rec}}^{\mathrm{st}} \leq t < \mathrm{T}_{\mathrm{rec}}^{\mathrm{end}} \\ d(t) * d_{\mathrm{red}}(t) & \text{if} \quad t > \mathrm{T}_{\mathrm{rec}}^{\mathrm{end}} \end{cases} \tag{5.5}$$

The efficacy of such a compensatory period will in principle be proportional to the intensity and the duration of the intervention. We decided to analyse several

combinations of those parameters to explore if a region of the plane yields an eradication of the additional mortality introduced by the diagnosis disruption. Then, in Figure 5.6, we show the impact of considering different combinations of diagnosis boost and duration of the boost on the cumulative excess mortality in 2035.

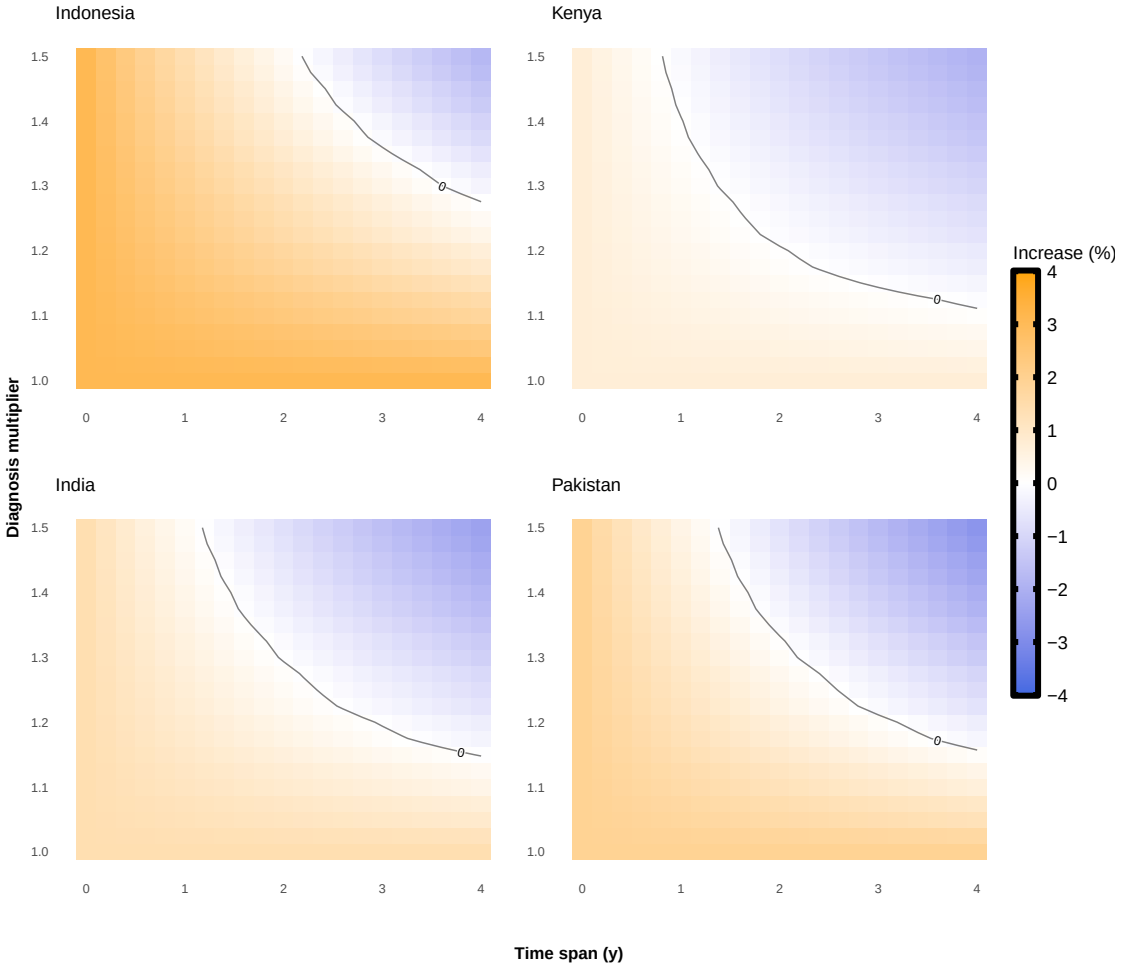

Figure 5.6: Relative increase of the expected number of deaths when an intervention is introduced in 2022 with respect to the projected impact of the COVID-19 pandemic. We assume that during the recovery period, whose duration is given by the parameter T_{rec} (the values of the X-axis), there is an increase in the diagnosis rate characterised by a factor $d_{inc} > 1$ (value of the Y-axis). Level (white) curves represent combinations of parameters that give the same excess deaths percentage, as indicated by the values over the curves. The four countries under study are Indonesia, Kenya, India, and Pakistan.

Clearly, the more intense and longer the additional effort is, the larger the number of averted deaths by the end of the simulation period. As can be seen, an increase in diagnosis rate during a certain amount of time could eventually revert the negative impact of COVID-19 in TB mortality measured in 2035. More specifically, for all four countries, there is a region in the parameter space for which the increase in mortality

in 2035 is close to zero (highlighted contour line of the different panels) if the diagnosis rate of new TB cases increases from 10% to 50% of its original value for a period that spans between 1 and 4 years. Importantly, this implies that the extra death toll that is expected from the effect of COVID-19 on TB diagnosis and treatment during the last two years could be fully mitigated if ambitious interventions focused on increasing case detection in the next few years are deployed. Focusing on selected cases, Table 5.2 reports the number of averted deaths in each country in 2035 when the additional effort is applied for two to four years and considering increases in the diagnosis rates of 15%, 30%, and 45%, starting right after the end of 2022.

Number of averted deaths (in thousands) by 2035							
Country	Diagnosis effort	T=2y		T=3y		T=4y	
Indonesia	1.15	39	(32-49)	55	(46-70)	70	(59-89)
	1.30	72	(60-91)	100	(84-126)	127	(107-158)
	1.45	100	(83-126)	138	(115-173)	172	(145-214)
Kenya	1.15	9	(6-13)	13	(9-19)	17	(12-25)
	1.30	18	(12-25)	25	(17-36)	32	(22-46)
	1.45	26	(18-36)	36	(25-51)	45	(31-64)
India	1.15	137	(59-170)	197	(88-244)	253	(114-312)
	1.30	256	(117-320)	361	(168-451)	457	(216-572)
	1.45	357	(165-454)	497	(235-632)	625	(302-791)
Pakistan	1.15	16	(11-20)	23	(17-29)	30	(22-37)
	1.30	29	(21-37)	42	(30-52)	54	(39-66)
	1.45	40	(29-50)	57	(41-70)	72	(53-89)

Table 5.2: Cumulative number of averted deaths (in thousands) in 2035 with a post COVID-19 intervention initiated in 2022 in each of the countries studied. The values in the table are computed by calculating the difference between the model forecast for mortality with the pandemic scenario and with non-pharmaceutical interventions of different intensities of diagnosis effort and duration of the recovery period. Values are the median of the outcome and figures in parentheses are the 95% CI of the model projections.

The reported values are obtained by comparing model forecasts for the estimated number of TB-related deaths in the pandemic scenario with the outcome obtained when the recovery strategy is adopted after the end of the COVID-19 disruptions. The model suggests that it is generally better to increase the diagnosis rate for shorter times than to increase the temporal span and have smaller increments of the diagnosis rate. This is because, in the former situation, more deaths are averted in the long term. Nonetheless, the ideal scenario is still the one in which both dimensions are boosted at the same time, as the longer the time the effort is maintained for a given multiplier, the lower the TB-related death toll caused by the pandemic. As noted before, we stress that for an effort ratio of 1.30 and a temporal span of 3 years, the number of averted deaths neglects the 100% of additional deaths expected due to the COVID-19 disruptions (see Figure 5.3), i.e., the pandemic impact on TB burden could be fully mitigated.

5.5 Alternative scenarios with disrupted TB transmission

A conceptually deep limitation of this chapter that needs to be stressed is that we only describe the effects of COVID-19-induced reductions in TB diagnosis rates and treatment adherence as the main drivers of the interaction between both processes. Admittedly, the effects of the COVID-19 crisis on TB dynamics are more complex than what is described here, and will most likely include alterations in transmission dynamics, effects mediated by economic impact, and long-term damages to healthcare quality standards beyond diagnosis rates; all these being aspects that lie out the scope of our study, mainly because the relevant data needed to describe the effects of them on TB dynamics are yet to be produced.

On top of that, trying to analyse the global effect of countermeasures on the transmission dynamics of TB is also difficult. Although some of the non-pharmaceutical interventions adopted worldwide have proven their efficacy in reducing COVID-19 spreading [227], their effectiveness highly depends upon general public adherence and proper knowledge about the pandemic risks. Whereas some studies [228, 229, 230, 231] show that the knowledge, attitude, and practice towards COVID-19 basic preventive strategies and conducts are in general positive, there is a great variation between communities and, for example, in India, between socioeconomic levels. Specifically, rural populations, as well as individuals with lower education, and unskilled occupations, are associated with lower scores of knowledge, attitude, and practice toward the basic preventive strategies against COVID-19, which would in turn be expected to contribute to halting TB transmission too[230]. This lack of adherence in the lower socioeconomic levels [232] suggests that it might be misleading to assume that the implementation of countermeasures induces a reduction in the TB force of infection.

Interestingly enough, if we observe the changes in mobility according to Google's data [233], along with the Covid-19 confirmed cases and the reduction in the TB notifications in India from Feb 2020 to Oct 2021[225], in Figure 5.7, we realise that during high-Covid-19 burden periods, where more strict measures are implemented, presence in households and Grocery & pharmacy places increases. Moreover, changes in mobility patterns suggest that, during several phases of the pandemic, measures forced individuals to interact in closed spaces.

On the other hand, the changes in mobility due to lockdowns and other restrictions indicate that most of the interactions happen in residential areas (e.g., households) while these interventions are in place. Admittedly, this could be at the root of

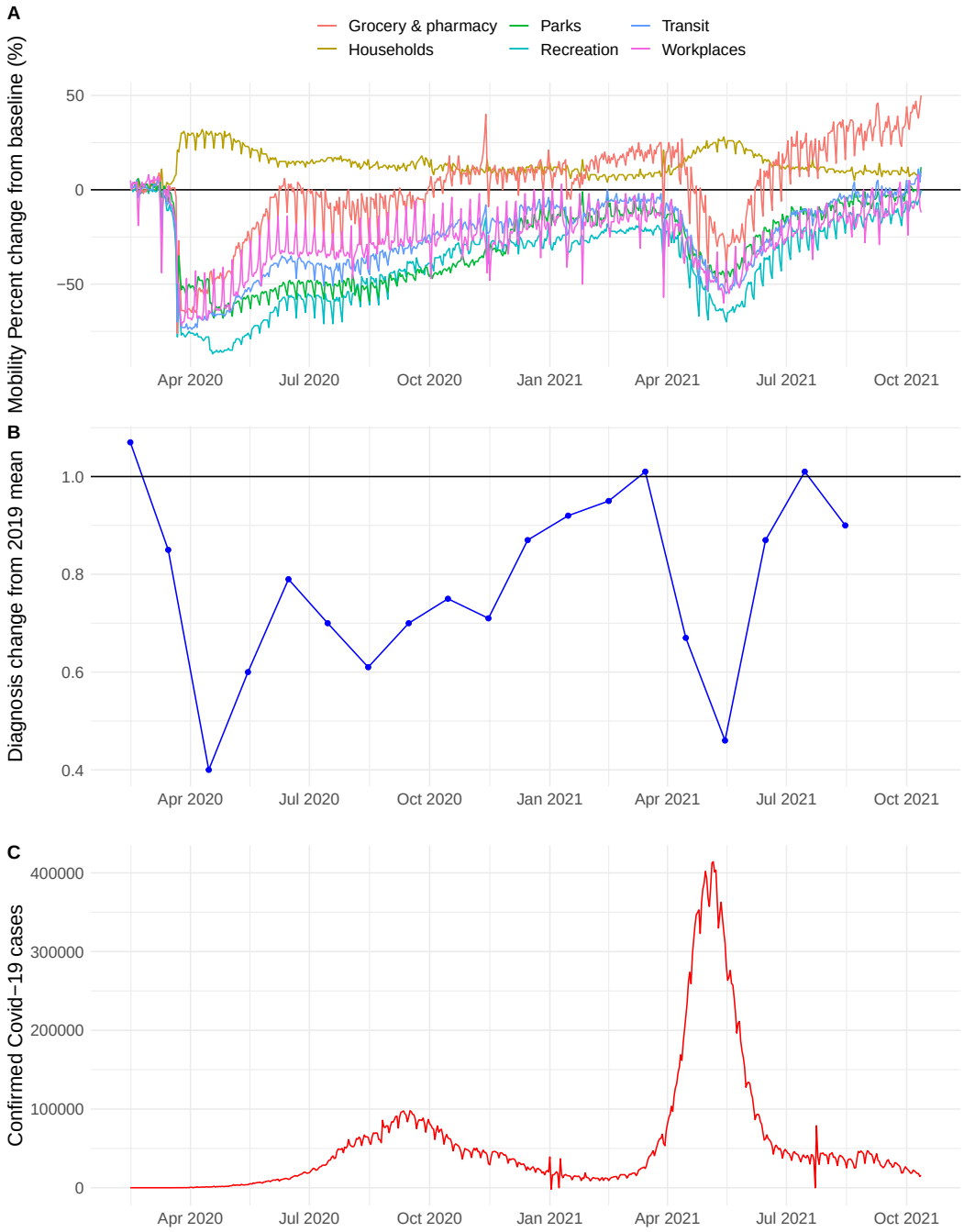

Figure 5.7: Comparison between the changes in mobility, the changes in TB notification cases, and the Covid-19 confirmed cases for the same period in India. **A** Percent change in mobility in selected environments when compared to the same period in 2019. **B** Per unit change in the TB notifications across public and private hospitals in India, according to Nikshay's data[225]. **C** Covid-19 Confirmed cases in India.

some recent observations that report that the number of children diagnosed with TB has increased and that non-pharmaceutical public health interventions likely reduced influenza transmission, but have a lesser effect on *Mycobacterium tuberculosis* transmission during 2020 [234, 235, 236]. From Figure 5.7 we also learned that during

those high-incidence COVID-19 periods, when mobility changes drastically, a match with periods of low TB notification when compared to the same period in 2019 is found. This suggests that neither arguing about rises nor decreases in transmission seems to have enough support from data.

Regardless of the lack of data, as facemasks and social distancing have been globally introduced as a countermeasure for avoiding COVID-19 transmission, some effect is expected over the transmission of other airborne diseases such as TB. Then, to contextualise our findings in broader scenarios where changes in TB transmission -either towards enhanced or reduced spreading- are considered, we show the results of the basic burden outcomes, incidence, and mortality, in each country, for scenarios in which the transmission is either reduced or enhanced.

In the model, the force of infection is calculated as:

$$\lambda(a,t) = \beta(t) \sum_{a'} M(a,a',t) \Upsilon(a',t) \tag{5.6}$$

where $\beta(t)$ is a half sigmoid calibrated by the model, $M(a,a',t)$ represents the relative contact frequency that an individual of age a has with individuals of age a' at time t, with respect to the overall average of contacts that an individual has per unit time with anyone else. $\Upsilon(a',t)$, on the other hand, represents the weighted density of all the infectious individuals within age group a' at time step t. All together build the force of infection, which represents the rate at which infection occurs at time step t for a susceptible individual in age-group a.

Given the information presented in Figure 5.7, it is difficult to quantify a variation in the force of infection, as mobility changes suggest that individuals left public spaces and frequented more private and closed spaces. At the same time, the non-pharmaceutical interventions implemented to halt COVID-19 transmission might have affected the transmission of TB. Early evidence shows that this is not the case and that the transmission of TB has remained constant or even has increased in certain contexts [235, 236]. Thus, we perform our sensitivity analysis introducing a multiplicative factor that comprises both increases and decreases evenly distributed around the base value in the range $\beta_r \in [0.85, 1.15]$, representing variations from -15% to 15% of the base value. The new value of the force of infection is thus obtained as:

$$\bar{\lambda}(a,t) = \beta_r \lambda(a,t) \tag{5.7}$$

In Figure 5.8 the results for the sensitivity over $\lambda(a,t)$ with a treatment completion scale factor of 0.788, and the results are, as expected, highly dependent upon the force of infection values.

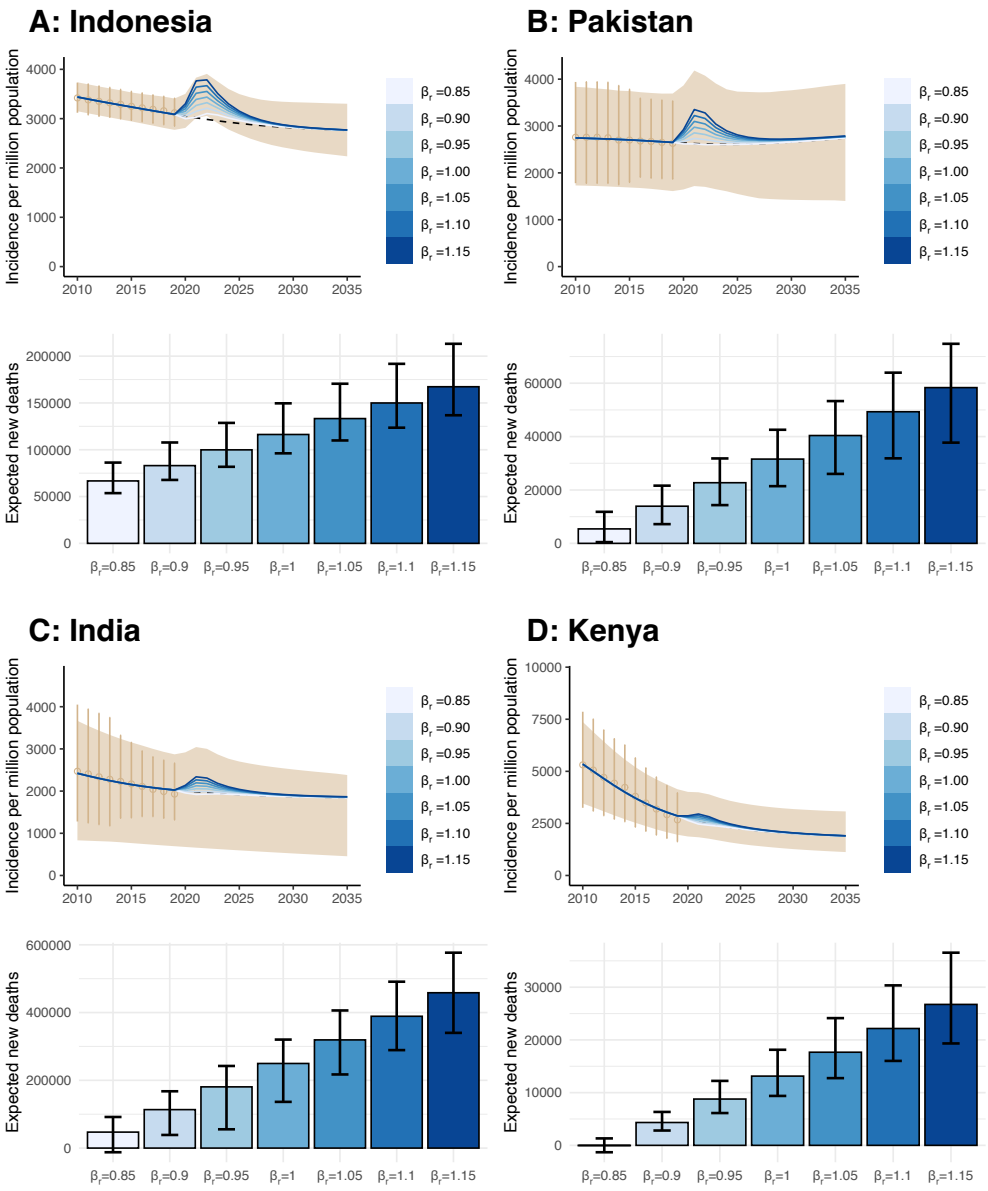

Figure 5.8: TB burden under alternative scenarios in selected countries for a fixed value of $\eta = 0.788$. In each country, the top figure shows the baseline changes in incidence per million population when β_r is introduced. The peak area changes with the value of β_r, either increasing ($\beta_r > 1$) or decreasing ($\beta_r < 1$) from the $\beta_r = 1$ standard scenario. The bottom figure shows the expected additional deaths measured in 2035 (thus, the integral of the peak) when compared to the forecast without Covid-19. The colours for each value of β_r are the same in both figures.

This is because the infections in the model are mainly driven through primary infections, i.e., those that occur upon susceptible individuals. Primary infections are highly dependent on $\lambda(a,t)$ too, as in the model they are calculated as the sum over all age groups a of the product $\lambda(a,t)S(a,t)$, thus, the fraction of susceptible individuals of age a that gets infected in time step t. Nevertheless, $\lambda(a,t)$ also affects reinfections, which ultimately leads to a high reduction of the expected burden if it decreases, along with an increment of incidence and mortality if it decreases.

Regarding the treatment completion, in the main results, a fixed value of $\eta = 0.788$ multiplicative factor is adopted, as literature findings support it. Here, we also decided to explore a more conservative case in which the multiplicative factor is raised to $\eta = 0.90$, which allows more patients to be treated quickly in the model. Then, we perform our simulations and produce forecasts for every alternative scenario. Figure 5.9 shows the forecasts with the alternative treatment completion value, and when the force of infection is modified accordingly to the multiplicative factor β_r.

Moreover, in Figure 5.9 we recover the same qualitative behaviour that in the previous case, but not quantitatively, as all future burdens are lower because we are allowing more sick individuals to be treated than in the previous scenario during the pandemic period. Interestingly, something that needs to be highlighted is that the results of the sensitivity over transmission show that, most of the time, even in cases with $\beta_r = 0.85$ (a hard reduction of 15%), we expect an increase in the death toll, being Kenya and Pakistan the exceptions in Figure 5.9. In both panels, in any other case, a significant, non-crossing zero value, is found for the increase in mortality, even with reduced transmission. This adds up to the necessity of a global response to minimise the damage dealt by the pandemic to the burden of TB.

5.6 Discussion

The COVID-19 pandemic impacted enormously our societies, and even today, much remains to be clarified about its impact on the − physical and mental − health of the general population. As of November 2023, the coronavirus SARS-CoV-2 had infected more than 687 million individuals, causing the death of more than 6.9 million people worldwide. Although the SARS-CoV-2 and its associated disease COVID-19 were first identified more than two years ago, the scientific community has already been able to describe many of the clinical characteristics and pathogenesis of COVID-19, especially during the acute phase [237, 238]. However, there are important features that remain less known, such as the long-term consequences of the disease [239, 240, 241] and the relation between comorbidities and their risks upon infection by SARS-CoV-2

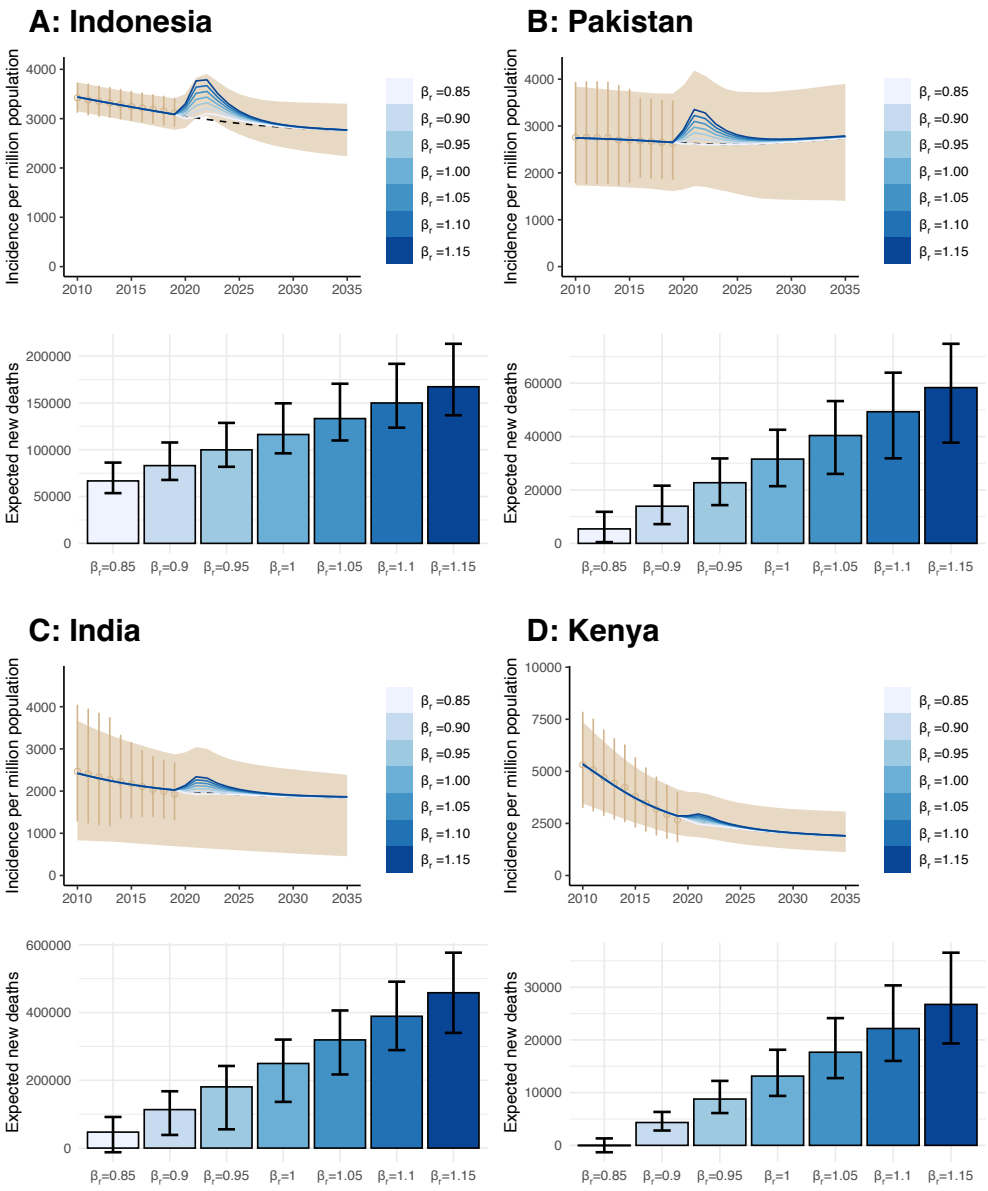

Figure 5.9: TB burden under alternative scenarios in selected countries for a fixed value of $\eta = 0.9$. In each country, the top figure shows the baseline changes in incidence per million population when β_r is introduced. The peak area changes with the value of β_r, either increasing ($\beta_r > 1$) or decreasing ($\beta_r < 1$) from the $\beta_r = 1$ standard scenario. The bottom figure shows the expected additional deaths measured in 2035 (thus, the integral of the peak) when compared to the forecast without Covid-19. The colors for each value of β_r are the same in both figures.

[242, 243]. Another important question that is not fully assessed concerns the indirect effects of the pandemic, and the NPIs adopted for its control and mitigation of other diseases.

In particular, the large number of healthy individuals that were infected in a very short period, producing the so-called epidemic waves, led to the saturation of many healthcare systems, which in turn induced the implementation of very restrictive measures such as lockdowns and curfews in those countries. These compulsory interventions have been argued to be at the root of important reductions in diagnosis rates of other deadly diseases[127, 128]. Yet, the long-term consequences are still to be determined. In this chapter, we have focused on the impact of the pandemic on the care of TB, since disruptions in health care of this disease could be dramatic [220, 177] given that even without a pandemic scenario, more than 1.5 million lives are lost every year because of the disease.

Using a data-driven epidemiological model [135], we have quantified the negative impact of COVID-19 on TB diagnosis and its long-term consequences. We have also shown that a rapid and intense post-pandemic intervention could eventually mitigate the expected increase in the incidence and mortality of TB. Countries enrolled in this work have been selected because of their high TB burden, contributing an important amount of cases to the annual TB incidence recorded by the WHO global report. Certainly, all four countries together accounted for a 42.1% of the global TB cases in the year 2019. Individually, India comprises 26.5%, Indonesia accounts for 8.47%, Kenya represents 1.40% and Pakistan is responsible for 5.71% of all cases globally. Additionally, for these countries, the reduction in TB case notification due to the COVID-19 pandemic has been well-documented [76, 224], and spans from milder (Kenya) to more severe magnitudes (Indonesia), which make them suitable case studies to estimate the pandemic negative impact and the design of corrective interventions.

Our results show that a drop in diagnosis rates and first-line treatment compliance statistics leads to a pronounced increase in TB incidence in comparison to the baseline scenario. In turn, the growth in TB burden leads to an upsurge in mortality, producing almost 400,000 excess deaths by 2035 in the four countries of the study combined. However, our study also shows that most of these deaths can still be prevented. In particular, our projections show that an increase in available diagnosis capabilities for some time has very positive effects on the long-term TB burden since the pandemic effect can be greatly contained. More specifically, if the intervention is powerful and maintained for enough time, the entirety of the expected excess deaths can be avoided. It is worth stressing that the intervention proposed here is aimed at increasing the rate of diagnosed individuals, thus bringing them to treatment as soon as possible. This

ultimately points towards cutting TB transmission to a point wherein pre-pandemic burden levels are recovered. As we have demonstrated here, one such intervention could be enough for full mitigation of the negative impact of the COVID-19 pandemic on TB incidence and mortality.

However, it is important to acknowledge that the specific interventions needed to achieve enhancements in the diagnosis rates such as the ones explored in this study -between 10% and 50% increase above basal values-, should most likely go beyond policies focused on reducing the diagnostic delay of patients seeking care after experiencing TB symptoms under passive case finding scenarios. Instead, active case finding strategies (ACF) constitute a robust family of interventions that can lead to reductions of both patients [244, 245], and health care system components [246, 247] of total TB diagnosis delays that are often compatible with case detection rate improvements similar to those explored here. Along these lines, several epidemiological studies published in the last decade report positive ACF experiences in diverse high-TB burden settings in both rural and urban areas in Africa and Asia alike. For example, in 2020, Vo et al. reported an increase of 15.9% of TB notifications (all-forms) in 6 districts of Ho-Chi Minh, Vietnam, concerning another 6 control districts in the same city [248]. Other studies conducted previously in broad administrative districts in northern Uganda in 2018 [249], and in Cambodia in 2016 [250] report results from even more successful ACF strategies, able to increase all-forms TB diagnosis rates up to 30.4% and 46%, respectively, in comparison to control districts. Similar examples also include ACF strategies targeting rural, and even nomad populations, in African countries such as Ethiopia ([251], 98.4% increase in all-forms of TB notification rates in 2013) or Nigeria, ([252], 24.5% of increase for all TB notifications among nomadic populations in Adamawa state, 2015). Finally, other studies have made use of mathematical modelling to stress that boosting diagnosis rates through ACF is not only feasible but also cost-effective in the mid to long term [253, 254]. These results, taken together, suggest that the implementation of ambitious nationwide strategies of ACF in countries such as the ones studied here could contribute significantly to reducing the TB burden to the extent of mitigating the detrimental effects that COVID-19 has had on the TB epidemics worldwide.

The results of this chapter are affected, as previously stated in other chapter, from limitations that affect TB transmission models. For instance, the outcome of our model depends on a series of epidemiological parameters and initial burden estimates that are subject to strong sources of uncertainty, thus propagating this uncertainty to the results. This means that future improvements in measuring the input data are expected to impact the quantitative outcomes of our mathematical model, in the same

way as it would affect any other model that leans on them. Moreover, in our work, we have only described the disruption caused by the COVID-19 pandemic on the TB care system via a reduction of diagnostic capabilities and treatment availability. Even if these are arguably the primary, and the first effects of the COVID-19 pandemic on TB transmission dynamics that have been characterised, there may be many other effects that are yet hard to parameterise, such as the effect on the transmission that non-pharmaceutical interventions had in the countries that carried them out.

On the one hand, it should be possible, shortly, to produce more detailed estimates on the disruptions of the pandemic on the complete TB cascade of care, based on the corresponding empiric data disclosed at a greater level of detail than the inputs used in this study. In fact, at the moment of writing this study, there is great heterogeneity in the available empirical data about the effects of the TB cascade of care, which points toward the urge to improve data availability for properly understanding the vast effects of COVID-19 on TB care[75]. Moreover, it is clear that other models, which provide a fine-grain structure capable of reproducing the full TB cascade of care, will be needed to take advantage of this kind of data, which is certainly unfeasible with the model used in this study. Furthermore, it is well known that the emerging pandemic has disrupted profoundly the age structure of social contacts in human populations worldwide through a combination of mobility restrictions, lockdowns, social distancing, and adaptive conducts driven by self-perceived risk, often associated with the stark variations in susceptibility to severe disease and death that have been extensively reported for COVID-19. All these effects combined have arguably re-wired age-dependent contact structures in a way that is not fully understood and may not be completely transient. On the other hand, geopolitical and economic shifts driven by the pandemic will certainly exert differential effects on TB transmission dynamics between countries.

While the TB modelling community should commit to characterising these phenomena in depth and incorporating them into model forecasts, these are all questions that remain beyond the scope of this study. Be it as it may, the model projections reported here point towards a worrying scenario about the effects of the current pandemic on TB burden evolution shortly, regardless of the detailed implementation of the disruptions. As more data on the possibly disparate effects of the COVID-19 pandemic on TB is reported [76, 224], updated modelling scenarios can be considered. Similarly, while the duration of the pandemic has been selected to be the length of the fitted bumps (which is directly related to available data) for all countries under study, the longer this data is reported, the better quantitative outcomes can be forecasted. Similarly, precise measures of how the pandemic affects the model

parameters, such as updated mortality risks or transmission rates, would also increase the quality of the forecasts.

In summary, our work in this chapter shows that implementing a strategy aimed at boosting TB diagnosis rates after the pandemic holds the promise of mitigating, if not fully reverting, the negative impact of the COVID-19 pandemic on TB excess incidence and mortality, even if that period of boosted diagnosis is transient. While the importance of early diagnosis to arrest TB transmission is well known in TB epidemiology [255, 256], we describe here how pushing that aspect of global TB management strategies in the early post-covid time has the potential of reverting a large fraction of the negative impact caused by the pandemic on the global TB-epidemics. Interventions such as chronic cough screenings among people seeking healthcare, or even active screening of TB cases among non-symptomatic individuals, along with protocols targeting specifically pre-clinical and/or smear-negative TB cases do all hold the potential of boosting early diagnosis rates in a way that may well be compatible with the scenarios modelled in this study [255, 256, 257, 258]. To prevent the COVID-19 pandemic from destroying all the progress achieved during the last years in global TB control, it is time to prioritise such interventions.

Chapter 6

The end of the journey

> A hard beginning maketh a good ending.
>
> John Heywood

ALONG the journey taken in this Ph.D. thesis, novel research results in the field of Tuberculosis (TB) epidemiology have been obtained through different research ideas. As stated multiple times, TB is a persistent infectious disease whose eradication, for now, is still a dream that requires international cooperation, reducing global inequity, and new and better tools to combat spreading and halt TB transmission. To help in the eradication effort, we have focused our research on exploring the interaction between perturbations and the basal TB trends that came from a complex mathematical model for TB spreading, which we use as the base model. In this sense, the primal objective of reducing the bias in the forecast of TB trends when perturbations that interact with the disease dynamics hit has always been in mind, and the main results are related, precisely, to the study of the introduction of either positive perturbations (vaccines) or negative ones (the interaction of TB and COVID-19). The original idea has evolved into a workable framework that provides a better understanding of the interaction of those perturbations and how ignoring them may bias our predictions. The research result is presented in 3 different chapters, with Chapter 3 and Chapter 4 focused on the interplay between novel TB vaccines and the model-based forecasts, and Chapter 5 focused on the interplay between the COVID-19 pandemic and the TB dynamics.

In Chapter 3, and for the first time in the literature, we have unraveled a problem that arises when dealing with TB vaccines whose efficacy has been addressed in a real clinical trial. The complex natural history of the disease makes it possible to model vaccines in different ways according to the mechanisms it has to provide protection, i.e., in terms of the interaction between the vaccine and the natural history. This is key to introducing the vaccines into models to address the impact in the long term. However,

so far the specific combination of mechanisms that confer protection is not measured in the trials but is usually theorised by the modeller when the vaccine impact is forecasted with the mathematical model. Our results highlight the difficulty that compromises the ability to model vaccines whose efficacy has been measured with distinct trial designs, and how the different descriptions of the mechanistic effect of the vaccines lead to a significant variation in the impact outcomes. This holds particular significance in the context of TB due to the critical role that Randomised Control Trials (RCTs) play in assessing vaccine efficacy, further compounded by the absence of clear correlates of protection[115], as for this lack of reliable correlates, TB vaccine efficacy is harder to foresee before phases 2b/3 of the development pipeline than for other diseases. In this sense, the methods that are introduced in this thesis target precisely those RCTs to provide a better way of comparing vaccines that have been tested using different architectures, which is not possible in simpler analyses.

To mitigate the uncertainty and reduce the need to make modelling assumptions, our research has introduced two distinct methodologies tailored to the unique trial structures for cohorts with IGRA-negative and IGRA-positive results at the start of the trial, as those are the two more recent architectures used in clinical trials for testing PoD in preventive TB vaccines. The first method, for the first kind of trials, measures the distribution of times between IGRA conversion and active disease to independently estimate the effect of the vaccine over the progression to disease for fast progressors. This estimation, added to a derived mathematical constraint that couples all the possible mechanisms of protection that the vaccine can act through, gives the full characterisation of the vaccine in a way that can be later introduced in mathematical models. However, for IGRA-positive designs, the first method is not employable, and we have derived a second methodology that works in those trials. It is based on a combination of *in-silico* RCT simulations and statistical analyses and allows us to measure the compatibility of vaccine descriptions -adapted to the trial design- and the observed trial results. The resulting compatibility metrics, which are Bayesian posteriors, enable the generation of more robust vaccine impact forecasts that do not require assumptions in the mechanistic effect anymore, although it is still hypothesised that the vaccine works as an AoN.

Despite having limitations in both methodologies, they offer, for the first time, a practical framework that can be adapted and expanded to future TB vaccine trials, and highlights a problem that so far has not been addressed. This is a significant step forward in the quest to define specific profiles of vaccine protection for real vaccines, which reduces the bias in the model-based evaluation of TB vaccines.

Then, in Chapter 4, we have explored the impacts of simulated, hypothetical new

TB vaccines in a country undergoing a fast ageing process such as China. Those impacts are obtained conditioned to the modelling approach used to capture, precisely, the effects of these sudden demographic changes and their interaction with vaccine profiles, and age of targetted populations. Our research highlights that the promising immunisation campaigns targeting older age groups in those countries are indeed hopeful, but also shows that to reduce TB incidence and mortality, the vaccine should be able to target the routes to disease that contribute the most to the pool of new cases in the vaccinated age-group. Furthermore, the results also highlight that vaccines targeting different routes to disease show mixed levels of impact depending on their interaction with the immunological status of the targeted population.

Regarding the coupling with ageing, the results capture the relevance of implementing comprehensive ways of describing the demographic change and its effect on the contact networks. Specifically, we recover that models should preserve the intrinsic connectivity of contact networks while evolving the matrices according to the demographic change, so the new contact patterns capture the expected contact network matching this demography and not the one in which it was measured. The impact of this modelling decision on the vaccine impact forecast also varies heavily depending on the age group being targeted, and those implications should be considered when producing model-based estimations to avoid yielding biased results.

Finally, the results in Chapter 5 measure the impact of the COVID-19 pandemic on the control of TB in high-burden settings. Many aspects of COVID-19's impact on our society remain poorly understood, including the indirect effects of pandemic control measures, such as lockdowns and curfews on the contact distributions, or the healthcare saturation on the diagnosis and treatment of other diseases. This is a cause for concern, particularly when it comes to TB care, as there are direct and negative consequences of having disruptions in TB care such as not diagnosing infectious individuals, or not treating them properly. Having in mind the previous considerations, our results have allowed us to quantify the negative effects of COVID-19 on TB mortality, which is expected to rise as a consequence, but also bring hope as they suggest that an appropriate post-pandemic intervention can mitigate the long-term effects. Moreover, our results emphasise the importance of enhancing TB diagnosis rates, possibly through active case-finding strategies, to counteract the pandemic's detrimental effects on TB incidence and mortality, but also to the overall control of the disease.

It is, though, necessary to remark that, although we have obtained several novel key results, they must also be taken with care, for the model-based outcomes carry limitations that affect all TB transmission models. To be fair, any model-based outcome inherits a great uncertainty as a consequence of the epidemiological

parameters, and initial burden estimates -or other calibration data- are subject to strong uncertainties, which are propagated to the results. Any future improvements in measuring the input data, even small reductions in its uncertainty should impact the quantitative outcomes of our -or any other- mathematical model. Improvements in the model itself, such as better calibration procedures, or even more complete descriptions of the natural history, are also expected to impact the outcomes, and if any advancement is done in this regard, it should be incorporated. In any case, for the research tasks performed in this thesis, the mathematical model in use is essentially an adequate tool, that incorporates detailed descriptions of key processes, such as the coupling between the TB dynamics and demographic evolution.

It is also worth noting that, in our methods to address the mechanistic descriptions of the vaccines that are more suitable to describe empiric data, we have been forced to model vaccines as either all-or-nothing, or leaky, and without further evidence, the adoption of one framework above the other may be biasing the results too. Concerning the interaction with COVID-19, we have only described the disruption of the TB care system via a reduction of diagnostic capabilities and treatment availability. Although these are arguably the more relevant effects of the COVID-19 pandemic on TB transmission that have been characterised, there may be many other effects that are yet hard to parameterise, such as the effect on the transmission that non-pharmaceutical interventions had in the countries that carried them out, or even biological changes in susceptibility as a consequence of the Sars-Cov-2 infection.

In summary, the research goals that were proposed in the first chapter have been accomplished, and the contents of this thesis offer a workable modelling framework that combines real data, compartmental models, and statistical methods, to provide solutions to some of the challenges in the TB literature. Along the way we have described the effect in the model-based TB trends after a perturbation happens in a way which is focused on the interplay between the perturbation and the natural history of the disease and the disease dynamics. Moreover, this thesis highlights the importance of tailored immunisation strategies informed by mathematical models, integrating vaccine attributes, population demographics, and the underlying TB characteristics for effective TB control.

6.1 What remains to be done.

Although the path taken in this thesis has been long, and the research presented in this book has taken one step further in several key aspects of TB modelling, especially regarding the characterisation of novel TB vaccines, there is still much to be done as

the field continues to grow. There are multiple ways in which the results discussed here can be extended, either to improve our understanding of the interaction between perturbations and TB dynamics or to improve the quality of the quantitative results. Some of those ideas may become projects and lead to new and interesting results shortly.

On the one hand, the spreading model that has been used in this thesis could use some enhancements that, as the world is becoming more and more connected, will help to tackle more nuanced questions that require the integration on additional data into our modeling frameworks. In this sense, the inclusion in the model of different routes of treatment associated with the prevalence of different strains of TB, especially focused on dealing with multi-drug-resistant strains, will also allow the application of our model to address questions regarding the problematic emergence of antibiotic resistances in TB. In the same spirit, the addition of internal and external migratory fluxes into the model may improve its usability, capturing a contribution to disease transmission which now is hindered by design. The introduction of those fluxes will allow for the evaluation of the impact of local measures at the global level, and will contribute to address the cost that the lack of international cooperation has on TB control. However, for implementing any of those elements in the model, high-quality data should be gathered, which may not be available in all settings. To end with the model improvements, it will also benefit, if data is available, the introduction of different populations that are mixed, but that present different levels of genetic susceptibility to the disease, as some populations appear to bear more risk than others. Should this aspect be included in this -or another - TB transmission model, although the complexity will increase, so will the versatility and utility of the model.

On the other hand, regarding the most important topics discussed in this thesis, some aspects may be polished to extend the usability of methods. First, to improve some of the presented results, one needs to reduce the uncertainty associated with the model inputs, so the uncertainty in model outcomes decreases too. To this end, as more and more data is collected each year -on almost every topic-, exploring new data sources and studies should allow finding better inputs to feed the model, as there is plenty of literature that may have remained shadowed. This, in principle, will propagate to the results and produce less uncertain outcomes.

Second, concerning the characterisation of the mechanistic effect of vaccines to plug them into spreading models rationally, the integration of methodologies presented in this thesis into the trial's designs might produced enhanced results, or, at least, more complete descriptions of the vaccines at play. In this sense, having access to anonymised micro data from trials directly will allow for building the trial models more accurately,

and will make the vaccine characterisation more precise. Moreover, the extension of the methods to more architectures -if applicable- and to other vaccines, as long as they start to finish their respective clinical trials will help to address the power -and the limitations- of them, and will serve as a starting point to develop more powerful frameworks for precise vaccine characterisation.

Finally, the introduction of big perturbations such as COVID-19 must be done to produce flexible forecasts, granting us the ability to adapt the outcomes of our models tu the description of situations (such as wars, pandemics, or natural disasters) that are essentially impossible to predict. This is important as one of the main goals of those models is to serve as policy-making tools, and, for instance, if there is a long-term effect of the perturbation that may interact with the tested intervention, such as a vaccine, it should be considered. In this regard, a future line of work that we have in the making is precisely to characterise if the COVID-19 pandemic has compromised the impact of a hypothetical TB vaccine, which could be further extended to study the effect over other public health interventions. In summary, there are still plenty of things to do, and taking as a starting point the results of this thesis, the border of knowledge could be pushed further once again.

Chapter 7

Bibliography

[1] Anurag Bhargava, Madhavi Bhargava, Ajay Meher, Andrea Benedetti, Banurekha Velayutham, G Sai Teja, Basilea Watson, Ganesh Barik, Rajeev Ranjan Pathak, Ranjit Prasad, et al. Nutritional supplementation to prevent tuberculosis incidence in household contacts of patients with pulmonary tuberculosis in india (rations): a field-based, open-label, cluster-randomised, controlled trial. *The Lancet*, 402(10402):627–640, 2023.

[2] Emile Littré et al. *Oeuvres complètes d'Hippocrate*, volume 6. JB Baillière, 1849.

[3] Paul MV Martin and Estelle Martin-Granel. 2,500-year evolution of the term epidemic. *Emerging infectious diseases*, 12(6):976, 2006.

[4] Emil F Frey. The earliest medical texts. In *Clio Medica. Acta Academiae Internationalis Historiae Medicinae. Vol. 20*, pages 79–90. Brill, 1986.

[5] Nicole Elizabeth Smith. *The paleoepidemiology of malaria in the Ancient Near East*. University of Arkansas, 2015.

[6] Vivian Nutton. The reception of fracastoro's theory of contagion: the seed that fell among thorns? *Osiris*, 6:196–234, 1990.

[7] Henry Connor. John graunt frs (1620-74): The founding father of human demography, epidemiology and vital statistics. *Journal of medical biography*, page 09677720221079826, 2022.

[8] Alexandra J Stewart and Phillip M Devlin. The history of the smallpox vaccine. *Journal of infection*, 52(5):329–334, 2006.

[9] SWB Newsom. Pioneers in infection control: John snow, henry whitehead, the broad street pump, and the beginnings of geographical epidemiology. *Journal of Hospital Infection*, 64(3):210–216, 2006.

[10] Agnes Ullmann. Pasteur-koch: Distinctive ways of thinking about infectious diseases. *Microbe-American Society for Microbiology*, 2(8):383, 2007.

[11] Robert Koch. Die aetiologie der tuberkulose. 2010.

[12] Stella R Quah. *International encyclopedia of public health*. Academic press, 2016.

[13] Stephen Feinstein. *Louis Pasteur: The father of microbiology*. Enslow Publishers, Inc., 2008.

[14] SY Tan and E Berman. Robert koch (1843-1910): father of microbiology and nobel laureate. *Singapore medical journal*, 49(11):854–855, 2008.

[15] Joan W Bennett and King-Thom Chung. Alexander fleming and the discovery of penicillin. 2001.

[16] Kathrin I Mohr. History of antibiotics research. *How to Overcome the Antibiotic Crisis: Facts, Challenges, Technologies and Future Perspectives*, pages 237–272, 2016.

[17] Fred Brauer, Carlos Castillo-Chavez, and Carlos Castillo-Chavez. *Mathematical models in population biology and epidemiology*, volume 2. Springer, 2012.

[18] David Held, Anthony McGrew, David Goldblatt, and Jonathan Perraton. Global transformations: Politics, economics and culture. In *Politics at the Edge: The PSA Yearbook 1999*, pages 14–28. Springer, 1999.

[19] Pierre-Yves Donzé and Paloma Fernández Pérez. Health industries in the twentieth century, 2019.

[20] Stanley Plotkin. History of vaccination. *Proceedings of the National Academy of Sciences*, 111(34):12283–12287, 2014.

[21] David M Morens, Gregory K Folkers, and Anthony S Fauci. The challenge of emerging and re-emerging infectious diseases. *Nature*, 430(6996):242–249, 2004.

[22] Klaus Dietz and JAP Heesterbeek. Bernoulli was ahead of modern epidemiology. *Nature*, 408(6812):513–514, 2000.

[23] William O Kermack and Anderson G McKendrick. Contributions to the mathematical theory of epidemics–i. 1927. *Bulletin of mathematical biology*, 53(1-2):33–55, 1991.

[24] William O Kermack and Anderson G McKendrick. Contributions to the mathematical theory of epidemics—ii. the problem of endemicity. *Bulletin of mathematical biology*, 53(1-2):57–87, 1991.

[25] WO Kermack and AG McKendrick. Contributions to the mathematical theory of epidemics—iii. further studies of the problem of endemicity. *Bulletin of mathematical biology*, 53(1-2):89–118, 1991.

[26] Roy M Anderson. The role of mathematical models in the study of hiv transmission and the epidemiology of aids. *Journal of Acquired Immune Deficiency Syndromes*, 1(3):241–256, 1988.

[27] Valerie Isham. Mathematical modelling of the transmission dynamics of hiv infection and aids: a review. *Journal of the Royal Statistical Society Series A: Statistics in Society*, 151(1):5–30, 1988.

[28] Joël Mossong, Niel Hens, Mark Jit, Philippe Beutels, Kari Auranen, Rafael Mikolajczyk, Marco Massari, Stefania Salmaso, Gianpaolo Scalia Tomba, Jacco Wallinga, et al. Social contacts and mixing patterns relevant to the spread of infectious diseases. *PLoS medicine*, 5(3):e74, 2008.

[29] Suhail Ahmad. Pathogenesis, immunology, and diagnosis of latent mycobacterium tuberculosis infection. *Clinical and Developmental Immunology*, 2011, 2011.

[30] Jakko van Ingen, Zeaur Rahim, Arnout Mulder, Martin J Boeree, Roxane Simeone, Roland Brosch, and Dick Van Soolingen. Characterization of mycobacterium orygis as m. tuberculosis complex subspecies. *Emerging infectious diseases*, 18(4):653, 2012.

[31] LF Ayvazian. History of tuberculosis. *Lung biology in health and disease*, 66:1–20, 1993.

[32] Albert R Zink, Erika Molnár, N Motamedi, György Pálfy, Antónia Marcsik, and Andreas G Nerlich. Molecular history of tuberculosis from ancient mummies and skeletons. *International Journal of Osteoarchaeology*, 17(4):380–391, 2007.

[33] Qingyun Liu, Aijing Ma, Lanhai Wei, Yu Pang, Beibei Wu, Tao Luo, Yang Zhou, Hong-Xiang Zheng, Qi Jiang, Mingyu Gan, et al. China's tuberculosis epidemic stems from historical expansion of four strains of mycobacterium tuberculosis. *Nature ecology & evolution*, 2(12):1982–1992, 2018.

[34] Jared J Eddy. The ancient city of rome, its empire, and the spread of tuberculosis in europe. *Tuberculosis*, 95:S23–S28, 2015.

[35] Helen D Donoghue, Antónia Marcsik, Carney Matheson, Kim Vernon, Emilia Nuorala, Joseph E Molto, Charles L Greenblatt, and Mark Spigelman. Co–infection of mycobacterium tuberculosis and mycobacterium leprae in human archaeological samples: a possible explanation for the historical decline of leprosy. *Proceedings of the Royal Society B: Biological Sciences*, 272(1561):389–394, 2005.

[36] Romy Müller, Charlotte A Roberts, and Terence A Brown. Biomolecular identification of ancient mycobacterium tuberculosis complex dna in human remains from britain and continental europe. *American journal of physical anthropology*, 153(2):178–189, 2014.

[37] Gundula Müldner, Carolyn Chenery, and Hella Eckardt. The 'headless romans': multi-isotope investigations of an unusual burial ground from roman britain. *Journal of Archaeological Science*, 38(2):280–290, 2011.

[38] Neville Morley. Cities and economic development in the roman empire. *Settlement, urbanization, and population*, pages 143–160, 2011.

[39] P Bennike. Facts or myths? a re-evaluation of cases of diagnosed tuberculosis in the past in denmark. *Tuberculosis past and present*, pages 561–573, 1999.

[40] DG Rokhlin. Diseases of ancient men (bones of the men of various epochs–normal and pathological changed). *Moscow-Leningrad: Publishing House" Nauka*, 1965.

[41] R Jankauskas. Tuberculosis in lithuania: paleopathological and historical correlations, 1999.

[42] Anne C Stone, Alicia K Wilbur, Jane E Buikstra, and Charlotte A Roberts. Tuberculosis and leprosy in perspective. *American journal of physical anthropology*, 140(S49):66–94, 2009.

[43] Marvin J Allison, Enrique Gerszten, Juan Munizaga, Calogero Santoro, and Daniel Mendoza. Tuberculosis in pre-columbian andean populations. *Prehistoric tuberculosis in the Americas*, pages 49–61, 1981.

[44] Takao Suzuki and Takao Inoue. Earliest evidence of spinal tuberculosis from the aneolithic yayoi period in japan. *International Journal of Osteoarchaeology*, 17(4):392–402, 2007.

[45] H Herzog, Basel. History of tuberculosis. *Respiration*, 65(1):5–15, 1998.

[46] John F Murray, Hans L Rieder, and Annette Finley-Croswhite. The king's evil and the royal touch: the medical history of scrofula. *The International Journal of Tuberculosis and Lung Disease*, 20(6):713–716, 2016.

[47] Michele A Riva. From milk to rifampicin and back again: history of failures and successes in the treatment for tuberculosis. *The Journal of Antibiotics*, 67(9):661–665, 2014.

[48] René Jules Dubos and Jean Dubos. *The white plague: tuberculosis, man, and society*. Rutgers University Press, 1987.

[49] Jared Diamond. The arrow of disease. *Discover*, 13(10):64–73, 1992.

[50] John Frith. History of tuberculosis. part 1-phthisis, consumption and the white plague. *Journal of Military and Veterans Health*, 22(2):29–35, 2014.

[51] Foziyah Zakir, Farah Islam, Aamena Jabeen, and Sivakumar Sivagurunathan Moni. Vaccine development: a historical perspective. *Biomedical Research*, 30(3):452–455, 2019.

[52] John F Murray, Dean E Schraufnagel, and Philip C Hopewell. Treatment of tuberculosis. a historical perspective. *Annals of the American Thoracic Society*, 12(12):1749–1759, 2015.

[53] Giovanni Battista Migliori, Jean-Pierre Zellweger, Ibrahim Abubakar, E Ibraim, José A Caminero, Gerard De Vries, Lia D'Ambrosio, Rosella Centis, Giovanni Sotgiu, Olivia Menegale, et al. European union standards for tuberculosis care, 2012.

[54] L Trnka, D Daňková, and E Švandová. Six years' experience with the discontinuation of bcg vaccination: 1. risk of tuberculosis infection and disease. *Tubercle and Lung Disease*, 74(3):167–172, 1993.

[55] L Trnka, D Dankova, J Zitova, L Cimprichova, Giovanni Battista Migliori, L Clancy, and JP Zellweger. Survey of bcg vaccination policy in europe: 1994-96. *Bulletin of the World Health Organization*, 76(1):85, 1998.

[56] Andrea Infuso, D Falzon, et al. European survey of bcg vaccination policies and surveillance in children, 2005. *eurosurveillance*, 11(3):5–6, 2006.

[57] Marc Daniels. Tuberculosis in europe during and after the second world war.—i. *British medical journal*, 2(4636):1065, 1949.

[58] Innocent K Paul, Goodluck Nchasi, Deusdedith B Bulimbe, Meshack K Mollel, George G Msafiri, Alex Mbogo, Mayunga B Mswanzari, Msengi Joseph, Ashraf Mahmoud, and Anastasiia Volkova. Public health concerns about tuberculosis caused by russia/ukraine conflict. *Health Science Reports*, 6(4):e1218, 2023.

[59] Clark Lawlor. *Consumption and literature: The making of the romantic disease*. Springer, 2006.

[60] Kristin J Cummings. Tuberculosis control: challenges of an ancient and ongoing epidemic. *Public Health Reports*, 122(5):683–692, 2007.

[61] Charles L Daley, Peter M Small, Gisela F Schecter, Gary K Schoolnik, Ruth A McAdam, William R Jacobs Jr, and Philip C Hopewell. An outbreak of tuberculosis with accelerated progression among persons infected with the human immunodeficiency virus: an analysis using restriction-fragment—length polymorphisms. *New England journal of medicine*, 326(4):231–235, 1992.

[62] Gargi Thakur, Shalvi Thakur, and Harshad Thakur. Status and challenges for tuberculosis control in india–stakeholders' perspective. *Indian Journal of Tuberculosis*, 68(3):334–339, 2021.

[63] Lixia Wang, Hui Zhang, Yunzhou Ruan, Daniel P Chin, Yinyin Xia, Shiming Cheng, Mingting Chen, Yanlin Zhao, Shiwen Jiang, Xin Du, et al. Tuberculosis prevalence in china, 1990–2010; a longitudinal analysis of national survey data. *The Lancet*, 383(9934):2057–2064, 2014.

[64] D Falzon, A Infuso, and F Aït-Belghiti. In the european union, tb patients from former soviet countries have a high risk of multidrug resistance. *The International Journal of Tuberculosis and Lung Disease*, 10(9):954–958, 2006.

[65] Mukund Uplekar, Diana Weil, Knut Lonnroth, Ernesto Jaramillo, Christian Lienhardt, Hannah Monica Dias, Dennis Falzon, Katherine Floyd, Giuliano Gargioni, Haileyesus Getahun, et al. Who's new end tb strategy. *The Lancet*, 385(9979):1799–1801, 2015.

[66] Ben J Marais and Alimuddin Zumla. History of tuberculosis and drug resistance. *New Engl J Med*, 368(1):88–90, 2013.

[67] WHO Stop TB. an expanded dots framework for effective tuberculosis control (who/cds/tb/2002.297). *Geneva: World Health Organization*, 2002.

[68] Rein MGJ Houben and Peter J Dodd. The global burden of latent tuberculosis infection: a re-estimation using mathematical modelling. *PLoS medicine*, 13(10):e1002152, 2016.

[69] Marcel A Behr, Paul H Edelstein, and Lalita Ramakrishnan. Revisiting the timetable of tuberculosis. *Bmj*, 362, 2018.

[70] Hawult Taye, Kassahun Alemu, Adane Mihret, James LN Wood, Ziv Shkedy, Stefan Berg, and Abraham Aseffa. Global prevalence of mycobacterium bovis infections among human tuberculosis cases: Systematic review and meta-analysis. *Zoonoses and Public Health*, 68(7):704–718, 2021.

[71] Anoushiravan Kazemnejad, Shahram Arsang Jang, Firouz Amani, and Alireza Omidi. Global epidemic trend of tuberculosis during 1990-2010: using segmented regression model. *Journal of research in health sciences*, 14(2):115–121, 2014.

[72] World Health Organization et al. Global tuberculosis report 2022. geneva: Who; 2022, 2022.

[73] Unidad de Investigación en Tuberculosis de Barcelona. The covid-19 pandemic remains getting worse the tuberculosis control, November 2021. [Online; posted November-2021].

[74] Amyn A Malik, Nauman Safdar, Subhash Chandir, Uzma Khan, Saira Khowaja, Najam Riaz, Rabia Maniar, Maria Jaswal, Aamir J Khan, and Hamidah Hussain. Tuberculosis control and care in the era of covid-19. *Health policy and planning*, 35(8):1130–1132, 2020.

[75] C Finn McQuaid, Anna Vassall, Ted Cohen, Kathy Fiekert, RG White, et al. The impact of covid-19 on tb: a review of the data. *The International Journal of Tuberculosis and Lung Disease*, 25(6):436–446, 2021.

[76] World Health Organization. Global tuberculosis report 2021, 2021.

[77] M Berry and OM Kon. Multidrug-and extensively drug-resistant tuberculosis: an emerging threat. *European Respiratory Review*, 18(114):195–197, 2009.

[78] Christoph Lange, Dumitru Chesov, Jan Heyckendorf, Chi C Leung, Zarir Udwadia, and Keertan Dheda. Drug-resistant tuberculosis: an update on disease burden, diagnosis and treatment. *Respirology*, 23(7):656–673, 2018.

[79] Paul EM Fine. Bcg: the challenge continues. *Scandinavian journal of infectious diseases*, 33(1):58–60, 2001.

[80] TuBerculosis vaccine iniciative. Pipeline of vaccines, 2023.

[81] David P Spence, Jason Hotchkiss, Christianna S Williams, and Peter D Davies. Tuberculosis and poverty. *British Medical Journal*, 307(6907):759–761, 1993.

[82] Paul Farmer, Simon Robin, St-L Ramilus, and Jim Yong Kim. Tuberculosis, poverty, and" compliance": lessons from rural haiti. In *Seminars in respiratory infections*, volume 6, pages 254–260, 1991.

[83] Sukhan Jackson, AC Sleigh, GJ Wang, and XL Liu. Poverty and the economic effects of tb in rural china. *The International Journal of Tuberculosis and Lung Disease*, 10(10):1104–1110, 2006.

[84] E Drucker, P Alcabes, B Sckell, and W Bosworth. Childhood tuberculosis in the bronx, new york. *The Lancet*, 343(8911):1482–1485, 1994.

[85] V Singh, A Jaiswal, JDH Porter, JA Ogden, R Sarin, PP Sharma, VK Arora, and RC Jain. Tb control, poverty, and vulnerability in delhi, india. *Tropical Medicine & International Health*, 7(8):693–700, 2002.

[86] Daniel Gerszon Mahler, Nishant Yonzan, and Christoph Lakner. The impact of covid-19 on global inequality and poverty. 2022.

[87] Priya Venkatesan. Worrying lack of funding for tuberculosis. *The Lancet Infectious Diseases*, 22(3):318, 2022.

[88] Tom A Yates, Palwasha Y Khan, Gwenan M Knight, Jonathon G Taylor, Timothy D McHugh, Marc Lipman, Richard G White, Ted Cohen, Frank G Cobelens, Robin Wood, et al. The transmission of mycobacterium tuberculosis in high burden settings. *The Lancet infectious diseases*, 16(2):227–238, 2016.

[89] Lauren A Lambert, Lori R Armstrong, Mark N Lobato, Christine Ho, Anne Marie France, and Maryam B Haddad. Tuberculosis in jails and prisons: United states, 2002- 2013. *American journal of public health*, 106(12):2231–2237, 2016.

[90] CB Beggs, CJ Noakes, PA Sleigh, LA Fletcher, and K Siddiqi. The transmission of tuberculosis in confined spaces: an analytical review of alternative epidemiological models. *The international journal of tuberculosis and lung disease*, 7(11):1015–1026, 2003.

[91] Edward A Nardell. Transmission and institutional infection control of tuberculosis. *Cold Spring Harbor perspectives in medicine*, 6(2):a018192, 2016.

[92] George W Comstock. Epidemiology of tuberculosis. *American Review of Respiratory Disease*, 125(3P2):8–15, 1982.

[93] American Thoracic Society et al. Targeted tuberculin testing and treatment of latent tuberculosis infection. *American Journal of Respiratory and Critical Care Medicine*, 161(supplement_3):S221–S247, 2000.

[94] C Robert Horsburgh Jr and Eric J Rubin. Latent tuberculosis infection in the united states. *New England Journal of Medicine*, 364(15):1441–1448, 2011.

[95] Rosa Sloot, Maarten F Schim van der Loeff, Peter M Kouw, and Martien W Borgdorff. Risk of tuberculosis after recent exposure. a 10-year follow-up study of contacts in amsterdam. *American journal of respiratory and critical care medicine*, 190(9):1044–1052, 2014.

[96] Jason R Andrews, Farzad Noubary, Rochelle P Walensky, Rodrigo Cerda, Elena Losina, and C Robert Horsburgh. Risk of progression to active tuberculosis following reinfection with mycobacterium tuberculosis. *Clinical infectious diseases*, 54(6):784–791, 2012.

[97] L Aaron, D Saadoun, I Calatroni, O Launay, N Memain, V Vincent, G Marchal, B Dupont, O Bouchaud, D Valeyre, et al. Tuberculosis in hiv-infected patients: a comprehensive review. *Clinical microbiology and infection*, 10(5):388–398, 2004.

[98] PDO Davies, WW Yew, D Ganguly, AL Davidow, LB Reichman, K Dheda, and GA Rook. Smoking and tuberculosis: the epidemiological association and immunopathogenesis. *Transactions of the Royal Society of Tropical Medicine and Hygiene*, 100(4):291–298, 2006.

[99] Chi C Leung, Wing W Yew, Chi K Chan, Kwok C Chang, Wing S Law, Shuk N Lee, Lai B Tai, Eric CC Leung, Ronald KF Au, Shan S Huang, et al. Smoking adversely affects treatment response, outcome and relapse in tuberculosis. *European respiratory journal*, 45(3):738–745, 2015.

[100] Neus Altet, Irene Latorre, María Ángeles Jiménez-Fuentes, José Maldonado, Israel Molina, Yoel González-Díaz, Celia Milà, Esther García-García, Beatriz Muriel, Raquel Villar-Hernández, et al. Assessment of the influence of direct tobacco smoke on infection and active tb management. *PloS one*, 12(8):e0182998, 2017.

[101] Christie Y Jeon and Megan B Murray. Diabetes mellitus increases the risk of active tuberculosis: a systematic review of 13 observational studies. *PLoS medicine*, 5(7):e152, 2008.

[102] Kamila Romanowski, Edward G Clark, Adeera Levin, Victoria J Cook, and James C Johnston. Tuberculosis and chronic kidney disease: an emerging global syndemic. *Kidney international*, 90(1):34–40, 2016.

[103] Jing-Wen Ai, Qiao-Ling Ruan, Qi-Hui Liu, and Wen-Hong Zhang. Updates on the risk factors for latent tuberculosis reactivation and their managements. *Emerging microbes & infections*, 5(1):1–8, 2016.

[104] FT Hakim and RE Gress. Immunosenescence: deficits in adaptive immunity in the elderly. *Tissue antigens*, 70(3):179–189, 2007.

[105] Pere-Joan Cardona. Reactivation or reinfection in adult tuberculosis: Is that the question? *International journal of mycobacteriology*, 5(4):400–407, 2016.

[106] E Vynnycky and PEM Fine. The natural history of tuberculosis: the implications of age-dependent risks of disease and the role of reinfection. *Epidemiology & Infection*, 119(2):183–201, 1997.

[107] Asim K Dutt and William W Stead. Smear-negative pulmonary tuberculosis. In *Seminars in respiratory infections*, volume 9, pages 113–119, 1994.

[108] SALVADOR Alvarez and WILLIAM R McCABE. Extrapulmonary tuberculosis revisited: a review of experience at boston city and other hospitals. *Medicine*, 63(1):25–55, 1984.

[109] Matthew R Weir and George F Thornton. Extrapulmonary tuberculosis. experience of a community hospital and review of the literature. *The American journal of medicine*, 79(4):467–478, 1985.

[110] Edine W Tiemersma, Marieke J van der Werf, Martien W Borgdorff, Brian G Williams, and Nico JD Nagelkerke. Natural history of tuberculosis: duration and fatality of untreated pulmonary tuberculosis in hiv negative patients: a systematic review. *PloS one*, 6(4):e17601, 2011.

[111] JE Golub, S Bur, WA Cronin, S Gange, N Baruch, GW Comstock, and RE Chaisson. Delayed tuberculosis diagnosis and tuberculosis transmission. *The international journal of tuberculosis and lung disease*, 10(1):24–30, 2006.

[112] Alvin Kuo Jing Teo, Shweta R Singh, Kiesha Prem, Li Yang Hsu, and Siyan Yi. Duration and determinants of delayed tuberculosis diagnosis and treatment in high-burden countries: a mixed-methods systematic review and meta-analysis. *Respiratory research*, 22(1):1–28, 2021.

[113] Marie-Laurence Lambert, Epco Hasker, Armand Van Deun, Dominique Roberfroid, Marleen Boelaert, and Patrick Van der Stuyft. Recurrence in tuberculosis: relapse or reinfection? *The Lancet infectious diseases*, 3(5):282–287, 2003.

[114] Carlos Martin, Nacho Aguilo, Dessislava Marinova, and Jesus Gonzalo-Asensio. Update on tb vaccine pipeline. *Applied Sciences*, 10(7):2632, 2020.

[115] Kamlesh Bhatt, Sheetal Verma, Jerrold J Ellner, and Padmini Salgame. Quest for correlates of protection against tuberculosis. *Clinical and Vaccine Immunology*, 22(3):258–266, 2015.

[116] Iman Satti and Helen McShane. Current approaches toward identifying a correlate of immune protection from tuberculosis. *Expert review of vaccines*, 18(1):43–59, 2019.

[117] Mario Tovar, Sergio Arregui, Dessislava Marinova, Carlos Martín, Joaquín Sanz, and Yamir Moreno. Bridging the gap between efficacy trials and model-based impact evaluation for new tuberculosis vaccines. *Nature communications*, 10(1):5457, 2019.

[118] Mario Tovar, Yamir Moreno, and Joaquín Sanz. Addressing mechanism bias in model-based impact forecasts of new tuberculosis vaccines. *Nature communications*, 14(1):5312, 2023.

[119] Christopher da Costa, Philip Onyebujoh, Georges Thiry, and Alimuddin Zumla. Advances in development of new tuberculosis vaccines. *Current Opinion in Pulmonary Medicine*, 29(3):143–148, 2023.

[120] Cynthia H Cassell, Pratima L Raghunathan, Olga Henao, Katina A Pappas-DeLuca, Whitney L Rémy, Emily Kainne Dokubo, Rebecca D Merrill, and Barbara J Marston. Global responses to the covid-19 pandemic. *Emerging Infectious Diseases*, 28(Suppl 1):S4, 2022.

[121] Imen Ayouni, Jihen Maatoug, Wafa Dhouib, Nawel Zammit, Sihem Ben Fredj, Rim Ghammam, and Hassen Ghannem. Effective public health measures to mitigate the spread of covid-19: a systematic review. *BMC public health*, 21(1):1–14, 2021.

[122] Shahul H Ebrahim and Ziad A Memish. Covid-19–the role of mass gatherings. *Travel medicine and infectious disease*, 34:101617, 2020.

[123] Sara Stevano, Tobias Franz, Yannis Dafermos, and Elisa Van Waeyenberge. Covid-19 and crises of capitalism: intensifying inequalities and global responses. *Canadian Journal of Development Studies/Revue canadienne d'études du développement*, 42(1-2):1–17, 2021.

[124] Jessica A Gold. Covid-19: adverse mental health outcomes for healthcare workers, 2020.

[125] Yuxin Chen, Xin Tong, Jian Wang, Weijin Huang, Shengxia Yin, Rui Huang, Hailong Yang, Yong Chen, Aijun Huang, Yong Liu, et al. High sars-cov-2 antibody prevalence among healthcare workers exposed to covid-19 patients. *Journal of Infection*, 81(3):420–426, 2020.

[126] FM Fusco, M Pisaturo, V Iodice, R Bellopede, O Tambaro, G Parrella, G Di Flumeri, R Viglietti, R Pisapia, MA Carleo, et al. Covid-19 among healthcare workers in a specialist infectious diseases setting in naples, southern italy: results of a cross-sectional surveillance study. *Journal of Hospital Infection*, 105(4):596–600, 2020.

[127] Mike Richards, Michael Anderson, Paul Carter, Benjamin L Ebert, and Elias Mossialos. The impact of the covid-19 pandemic on cancer care. *Nature Cancer*, 1(6):565–567, 2020.

[128] Rashid Ansumana, Osman Sankoh, and Alimuddin Zumla. Effects of disruption from covid-19 on antimalarial strategies. *Nature Medicine*, 26(9):1334–1336, 2020.

[129] C Finn McQuaid, Nicky McCreesh, Jonathan M Read, Tom Sumner, Rein MGJ Houben, Richard G White, Rebecca C Harris, CMMID COVID-19 Working Group, et al. The potential impact of covid-19-related disruption on tuberculosis burden. *European Respiratory Journal*, 56(2), 2020.

[130] World Health Organization et al. Global tuberculosis report 2023. geneva: Who; 2023, 2023.

[131] Dongmei Chen. Modeling the spread of infectious diseases: A review. *Analyzing and modeling spatial and temporal dynamics of infectious diseases*, pages 19–42, 2014.

[132] Glenn Marion, Liza Hadley, Valerie Isham, Denis Mollison, Jasmina Panovska-Griffiths, Lorenzo Pellis, Gianpaolo Scalia Tomba, Francesca Scarabel, Ben Swallow, Pieter Trapman, et al. Modelling: understanding pandemics and how to control them. *Epidemics*, 39:100588, 2022.

[133] Alfonso de Miguel Arribas, Alberto Aleta, and Yamir Moreno. Assessing the effectiveness of perimeter lockdowns as a response to epidemics at the urban scale. *Scientific Reports*, 13(1):4474, 2023.

[134] Jamie Bedson, Laura A Skrip, Danielle Pedi, Sharon Abramowitz, Simone Carter, Mohamed F Jalloh, Sebastian Funk, Nina Gobat, Tamara Giles-Vernick, Gerardo Chowell, et al. A review and agenda for integrated disease models including social and behavioural factors. *Nature human behaviour*, 5(7):834–846, 2021.

[135] Sergio Arregui, María José Iglesias, Sofía Samper, Dessislava Marinova, Carlos Martin, Joaquín Sanz, and Yamir Moreno. Data-driven model for the assessment of mycobacterium tuberculosis transmission in evolving demographic structures. *Proceedings of the National Academy of Sciences*, 115(14):E3238–E3245, 2018.

[136] Sergio Arregui, Alberto Aleta, Joaquín Sanz, and Yamir Moreno. Projecting social contact matrices to different demographic structures. *PLoS computational biology*, 14(12):e1006638, 2018.

[137] Laith J Abu-Raddad, Lorenzo Sabatelli, Jerusha T Achterberg, Jonathan D Sugimoto, Ira M Longini Jr, Christopher Dye, and M Elizabeth Halloran. Epidemiological benefits of more-effective tuberculosis vaccines, drugs, and diagnostics. *Proceedings of the National Academy of Sciences*, 106(33):13980–13985, 2009.

[138] Chathika Krishan Weerasuriya, Rebecca Claire Harris, Matthew Quaife, Christopher Finn McQuaid, Richard G White, and Gabriela B Gomez. Affordability of adult tuberculosis vaccination in india and china: a dynamic transmission model-based analysis. *Vaccines*, 9(3):245, 2021.

[139] Rebecca C Harris, Tom Sumner, Gwenan M Knight, Hui Zhang, and Richard G White. Potential impact of tuberculosis vaccines in china, south africa, and india. *Science Translational Medicine*, 12(564):eaax4607, 2020.

[140] Han Fu, Joseph A Lewnard, Isabel Frost, Ramanan Laxminarayan, and Nimalan Arinaminpathy. Modelling the global burden of drug-resistant tuberculosis avertable by a post-exposure vaccine. *Nature communications*, 12(1):1–9, 2021.

[141] Rebecca C Harris, Matthew Quaife, Chathika Weerasuriya, Gabriela B Gomez, Tom Sumner, Fiammetta Bozzani, and Richard G White. Cost-effectiveness of routine adolescent vaccination with an m72/as01e-like tuberculosis vaccine in south africa and india. *Nature communications*, 13(1):1–8, 2022.

[142] Christopher JL Murray and Joshua A Salomon. Modeling the impact of global tuberculosis control strategies. *Proceedings of the National Academy of Sciences*, 95(23):13881–13886, 1998.

[143] Christopher Dye and Brian G Williams. Eliminating human tuberculosis in the twenty-first century. *Journal of the Royal Society Interface*, 5(23):653–662, 2008.

[144] Laith J Abu-Raddad, Lorenzo Sabatelli, Jerusha T Achterberg, Jonathan D Sugimoto, Ira M Longini, Christopher Dye, and M Elizabeth Halloran. Epidemiological benefits of more-effective tuberculosis vaccines, drugs, and diagnostics. *Prod Nat Acad Sci USA*, **106**(**33**):13980–5, 2009.

[145] Eline L Korenromp, Fabio Scano, Brian G Williams, Christopher Dye, and Paul Nunn. Effects of human immunodeficiency virus infection on recurrence of tuberculosis after rifampin-based treatment: an analytical review. *Clin Infect Dis*, **37**(**1**):101–12, 2003.

[146] BJ Marais, RP Gie, HS Schaaf, AC Hesseling, CC Obihara, JJ Starke, DA Enarson, PR Donald, and N Beyers. The natural history of childhood intra-thoracic tuberculosis: a critical review of literature from the pre-chemotherapy era [state of the art]. *The International Journal of Tuberculosis and Lung Disease*, 8(4):392–402, 2004.

[147] Christopher Dye, Geoffrey P Garnett, Karen Sleeman, and Brian G Williams. Prospects for worldwide tuberculosis control under the who dots strategy. *Lancet*, **352**(**9144**):1886–91, 1998.

[148] Pedro Dornelles Picon, Sergio Luiz Bassanesi, Maria Luiza Avancini Caramori, Roberto Luiz Targa Ferreira, Carla Adriane Jarczewski, and Patrícia Rodrigues Vieira. Risk factors for recurrence of tuberculosis. *J Bras Pneum*, **33**(**5**):572–8, 2007.

[149] T Pillay, M Khan, J Moodley, M Adhikari, and H Coovadia. Perinatal tuberculosis and hiv-1: considerations for resource-limited settings. *Lancet Inf Dis*, **4**(**3**):155–65, 2004.

[150] UN. Population division database. *https://population.un.org/wpp/*, 2022.

[151] Moses Chapa Kiti, Timothy Muiruri Kinyanjui, Dorothy Chelagat Koech, Patrick Kiio Munywoki, Graham Francis Medley, and David James Nokes. Quantifying age-related rates of social contact using diaries in a rural coastal population of kenya. *PloS one*, 9(8):e104786, 2014.

[152] Alessia Melegaro, Emanuele Del Fava, Piero Poletti, Stefano Merler, Constance Nyamukapa, John Williams, Simon Gregson, and Piero Manfredi. Social contact structures and time use patterns in the manicaland province of zimbabwe. *PloS one*, 12(1):e0170459, 2017.

[153] O le Polain de Waroux, Sandra Cohuet, Donny Ndazima, AJ Kucharski, Aitana Juan-Giner, Stefan Flasche, Elioda Tumwesigye, Rinah Arinaitwe, Juliet Mwanga-Amumpaire, Yap Boum, et al. Characteristics of human encounters and social mixing patterns relevant to infectious diseases spread by close contact: a survey in southwest uganda. *BMC infectious diseases*, 18(1):1–12, 2018.

[154] Deus Thindwa, Kondwani C Jambo, John Ojal, Peter MacPherson, Mphatso Dennis Phiri, Amy Pinsent, McEwen Khundi, Lingstone Chiume, Katherine E Gallagher, Robert S Heyderman, et al. Social mixing patterns relevant to infectious diseases spread by close contact in urban blantyre, malawi. *Epidemics*, 40:100590, 2022.

[155] Jonathan M Read, Justin Lessler, Steven Riley, Shuying Wang, Li Jiu Tan, Kin On Kwok, Yi Guan, Chao Qiang Jiang, and Derek AT Cummings. Social mixing patterns in rural and urban areas of southern china. *Proceedings of the Royal Society B: Biological Sciences*, 281(1785):20140268, 2014.

[156] Yoko Ibuka, Yasushi Ohkusa, Tamie Sugawara, Gretchen B Chapman, Dan Yamin, Katherine E Atkins, Kiyosu Taniguchi, Nobuhiko Okabe, and Alison P Galvani. Social contacts, vaccination decisions and influenza in japan. *J Epidemiol Community Health*, 70(2):162–167, 2016.

[157] Supriya Kumar, Mudita Gosain, Hanspria Sharma, Eric Swetts, Ritvik Amarchand, Rakesh Kumar, Kathryn E Lafond, Fatimah S Dawood, Seema Jain, Marc-Alain Widdowson, et al. Who interacts with whom? social mixing insights from a rural population in india. *PLoS One*, 13(12):e0209039, 2018.

[158] Mario Tovar, Alberto Aleta, Joaquín Sanz, and Yamir Moreno. Modeling the impact of covid-19 on future tuberculosis burden. *Communications medicine*, 2(1):1–10, 2022.

[159] Stephen J Millen, Pieter W Uys, John Hargrove, Paul D Van Helden, and Brian G Williams. The effect of diagnostic delays on the drop-out rate and the total delay to diagnosis of tuberculosis. *PLoS One*, **3**(**4**):e1933, 2008.

[160] Timur V Elzhov, Katharine M Mullen, Andrej-Nikolai Spiess, Ben Bolker, Maintainer Katharine M Mullen, and MASS Suggests. Package 'minpack. lm'. *Title R Interface Levenberg-Marquardt Nonlinear Least-Sq. Algorithm Found MINPACK Plus Support Bounds*, 2016.

[161] T Lietman and SM Blower. Potential impact of tuberculosis vaccines as epidemic control agents. *Clinical Infectious Diseases*, 30(Supplement_3):S316–S322, 2000.

[162] Rebecca C Harris, Tom Sumner, Gwenan M Knight, Tom Evans, Vicky Cardenas, Chen Chen, and Richard G White. Age-targeted tuberculosis vaccination in china and implications for vaccine development: a modelling study. *The Lancet Global Health*, 7(2):e209–e218, 2019.

[163] Chathika K Weerasuriya, Rebecca C Harris, C Finn McQuaid, Fiammetta Bozzani, Yunzhou Ruan, Renzhong Li, Tao Li, Kirankumar Rade, Raghuram Rao, Ann M Ginsberg, et al. The epidemiologic impact and cost-effectiveness of new tuberculosis vaccines on multidrug-resistant tuberculosis in india and china. *BMC medicine*, 19(1):1–13, 2021.

[164] Gwenan M Knight, Ulla K Griffiths, Tom Sumner, Yoko V Laurence, Adrian Gheorghe, Anna Vassall, Philippe Glaziou, and Richard G White. Impact and cost-effectiveness of new tuberculosis vaccines in low-and middle-income countries. *Proceedings of the National Academy of Sciences*, 111(43):15520–15525, 2014.

[165] Chia-Lin Tseng, Olivia Oxlade, Dick Menzies, Anne Aspler, and Kevin Schwartzman. Cost-effectiveness of novel vaccines for tuberculosis control: a decision analysis study. *BMC Public Health*, 11(1):1–16, 2011.

[166] Elad Ziv, Charles L Daley, and Sally Blower. Potential public health impact of new tuberculosis vaccines. *Emerging infectious diseases*, 10(9):1529–1535, 2004.

[167] CP Bhunu, W Garira, Z Mukandavire, and G Magombedze. Modelling the effects of pre-exposure and post-exposure vaccines in tuberculosis control. *Journal of theoretical biology*, 254(3):633–649, 2008.

[168] Susanne F Awad, Julia A Critchley, and Laith J Abu-Raddad. Epidemiological impact of targeted interventions for people with diabetes mellitus on tuberculosis transmission in india: Modelling based predictions. *Epidemics*, 30:100381, 2020.

[169] Sourya Shrestha, Violet Chihota, Richard G White, Alison D Grant, Gavin J Churchyard, and David W Dowdy. Impact of targeted tuberculosis vaccination among a mining population in south africa: a model-based study. *American journal of epidemiology*, 186(12):1362–1369, 2017.

[170] Siyu Liu, Yong Li, Yingjie Bi, and Qingdao Huang. Mixed vaccination strategy for the control of tuberculosis: A case study in china. *Mathematical Biosciences & Engineering*, 14(3):695, 2017.

[171] Sourya Shrestha, Susmita Chatterjee, Krishna D Rao, and David W Dowdy. Potential impact of spatially targeted adult tuberculosis vaccine in gujarat, india. *Journal of The Royal Society Interface*, 13(116):20151016, 2016.

[172] Marissa Renardy and Denise E Kirschner. Evaluating vaccination strategies for tuberculosis in endemic and non-endemic settings. *Journal of theoretical biology*, 469:1–11, 2019.

[173] Ted Cohen, Caroline Colijn, and Megan Murray. Modeling the effects of strain diversity and mechanisms of strain competition on the potential performance of new tuberculosis vaccines. *Proceedings of the National Academy of Sciences*, 105(42):16302–16307, 2008.

[174] Douglas Young and Christopher Dye. The development and impact of tuberculosis vaccines. *Cell*, 124(4):683–687, 2006.

[175] Eunha Shim and Alison P Galvani. Distinguishing vaccine efficacy and effectiveness. *Vaccine*, 30(47):6700–6705, 2012.

[176] Lucien Le Cam. Maximum likelihood: an introduction. *International Statistical Review/Revue Internationale de Statistique*, pages 153–171, 1990.

[177] Lucia Cilloni, Han Fu, Juan F Vesga, David Dowdy, Carel Pretorius, Sevim Ahmedov, Sreenivas A Nair, Andrei Mosneaga, Enos Masini, Suvanand Sahu, et al. The potential impact of the covid-19 pandemic on the tuberculosis epidemic a modelling analysis. *EClinicalMedicine*, 28, 2020.

[178] Lewis K Schrager, Rebecca C Harris, and Johan Vekemans. Research and development of new tuberculosis vaccines: A review. *F1000Research*, 7, 2018.

[179] Michele D Tameris, Mark Hatherill, Bernard S Landry, Thomas J Scriba, Margaret Ann Snowden, Stephen Lockhart, Jacqueline E Shea, J Bruce McClain, Gregory D Hussey, Willem A Hanekom, et al. Safety and efficacy of mva85a, a new tuberculosis vaccine, in infants previously vaccinated with bcg: a randomised, placebo-controlled phase 2b trial. *The Lancet*, 381(9871):1021–1028, 2013.

[180] Olivier Van Der Meeren, Mark Hatherill, Videlis Nduba, Robert J Wilkinson, Monde Muyoyeta, Elana Van Brakel, Helen M Ayles, German Henostroza, Friedrich Thienemann, Thomas J Scriba, et al. Phase 2b controlled trial of m72/as01e vaccine to prevent tuberculosis. *New England Journal of Medicine*, 379(17):1621–1634, 2018.

[181] Dereck R Tait, Mark Hatherill, Olivier Van Der Meeren, Ann M Ginsberg, Elana Van Brakel, Bruno Salaun, Thomas J Scriba, Elaine J Akite, Helen M Ayles, Anne Bollaerts, et al. Final analysis of a trial of m72/as01e vaccine to prevent tuberculosis. *New England Journal of Medicine*, 381(25):2429–2439, 2019.

[182] Helen McShane. Insights and challenges in tuberculosis vaccine development. *The Lancet Respiratory Medicine*, 7(9):810–819, 2019.

[183] Elisa Nemes, Hennie Geldenhuys, Virginie Rozot, Kathryn T Rutkowski, Frances Ratangee, Nicole Bilek, Simbarashe Mabwe, Lebohang Makhethe, Mzwandile Erasmus, Asma Toefy, et al. Prevention of m. tuberculosis infection with h4: Ic31 vaccine or bcg revaccination. *New England Journal of Medicine*, 379(2):138–149, 2018.

[184] Madhukar Pai, Claudia M Denkinger, Sandra V Kik, Molebogeng X Rangaka, Alice Zwerling, Olivia Oxlade, John Z Metcalfe, Adithya Cattamanchi, David W Dowdy, Keertan Dheda, et al. Gamma interferon release assays for detection of mycobacterium tuberculosis infection. *Clinical microbiology reviews*, 27(1):3–20, 2014.

[185] RD Ellis, M Hatherill, D Tait, M Snowden, G Churchyard, W Hanekom, T Evans, and AM Ginsberg. Innovative clinical trial designs to rationalize tb vaccine development. *Tuberculosis*, 95(3):352–357, 2015.

[186] Mike Frick et al. 2016 report on tuberculosis research funding trends, 2005–2015: no time to lose. *Treatment Action Group*, 2016.

[187] Iñaki Comas and Sebastien Gagneux. The past and future of tuberculosis research. *PLoS pathogens*, 5(10):e1000600, 2009.

[188] Gerald Voss, Danilo Casimiro, Olivier Neyrolles, Ann Williams, Stefan HE Kaufmann, Helen McShane, Mark Hatherill, and Helen A Fletcher. Progress and challenges in tb vaccine development. *F1000Research*, 7, 2018.

[189] Pai M, Behr M A, Dowdy D, Dheda K, Divangahi M, Boehme C C, Ginsberg A, Swaminathan S, Spigelman M, Getahun H, Menzies D, and Raviglione M. Tuberculosis. *Nature reviews. Disease primers*, 2(16076), 2016.

[190] Helen A Fletcher. Correlates of immune protection from tuberculosis. *Current molecular medicine*, 7(3):319–325, 2007.

[191] Anne O'Garra, Paul S Redford, Finlay W McNab, Chloe I Bloom, Robert J Wilkinson, and Matthew PR Berry. The immune response in tuberculosis. *Annual review of immunology*, 31:475–527, 2013.

[192] Nicolas A Menzies, Emory Wolf, David Connors, Meghan Bellerose, Alyssa N Sbarra, Ted Cohen, Andrew N Hill, Reza Yaesoubi, Kara Galer, Peter J White, et al. Progression from latent infection to active disease in dynamic tuberculosis transmission models: a systematic review of the validity of modelling assumptions. *The Lancet Infectious Diseases*, 18(8):e228–e238, 2018.

[193] Peter R Cox. *Life tables*. Wiley Online Library, 1972.

[194] David Diez. Survival analysis in r. *OpenIntro. org*, 2013.

[195] David Schoenfeld. Partial residuals for the proportional hazards regression model. *Biometrika*, 69(1):239–241, 1982.

[196] Herbert W Hethcote. The mathematics of infectious diseases. *SIAM review*, 42(4):599–653, 2000.

[197] Christopher Dye, Geoffrey P Garnett, Karen Sleeman, and Brian G Williams. Prospects for worldwide tuberculosis control under the who dots strategy. *The Lancet*, 352(9144):1886–1891, 1998.

[198] Ben Bolker et al. bbmle: Tools for general maximum likelihood estimation, 2010.

[199] Troels Lillebaek, Asger Dirksen, Inga Baess, Benedicte Strunge, Vibeke Ø Thomsen, and Åse B Andersen. Molecular evidence of endogenous reactivation of mycobacterium tuberculosis after 33 years of latent infection. *The Journal of infectious diseases*, 185(3):401–404, 2002.

[200] M Elizabeth Halloran, Kari Auranen, Sarah Baird, Nicole E Basta, Steven E Bellan, Ron Brookmeyer, Ben S Cooper, Victor DeGruttola, James P Hughes, Justin Lessler, et al. Simulations for designing and interpreting intervention trials in infectious diseases. *BMC medicine*, 15(1):1–8, 2017.

[201] Philana Ling Lin and JoAnne L Flynn. The end of the binary era: revisiting the spectrum of tuberculosis. *The Journal of Immunology*, 201(9):2541–2548, 2018.

[202] Lewis Schrager, Padmapriyadarsini Chandrasekaran, Bernard Fritzell, Mark Hatherill, P Lambert, Helen McShane, Nadia Tornieporth, and Johan Vekemans. Who preferred product characteristics for new vaccines against tuberculosis. *Lancet Infectious Diseases*, 18(8), 2018.

[203] Sam Abbott, Hannah Christensen, Maeve K Lalor, Dominik Zenner, Colin Campbell, Mary E Ramsay, and Ellen Brooks-Pollock. Exploring the effects of bcg vaccination in patients diagnosed with tuberculosis: Observational study using the enhanced tuberculosis surveillance system. *Vaccine*, 37(35):5067–5072, 2019.

[204] CK Weerasuriya, RA Clark, RG White, and RC Harris. New tuberculosis vaccines: advances in clinical development and modelling. *Journal of internal medicine*, 288(6):661–681, 2020.

[205] PG Smith, LC Rodrigues, and PEM Fine. Assessment of the protective efficacy of vaccines against common diseases using case-control and cohort studies. *International journal of epidemiology*, 13(1):87–93, 1984.

[206] M Gabriela M Gomes, Marc Lipsitch, Andrew R Wargo, Gael Kurath, Carlota Rebelo, Graham F Medley, and Antonio Coutinho. A missing dimension in measures of vaccination impacts. *PLoS pathogens*, 10(3):e1003849, 2014.

[207] Ian Sutherland, Eva Švandová, and S Radhakrishna. The development of clinical tuberculosis following infection with tubercle bacilli: 1. a theoretical model for the development of clinical tuberculosis following infection, linking from data on the risk of tuberculous infection and the incidence of clinical tuberculosis in the netherlands. *Tubercle*, 63(4):255–268, 1982.

[208] Brian M Murphy, Benjamin H Singer, Shoana Anderson, and Denise Kirschner. Comparing epidemic tuberculosis in demographically distinct heterogeneous populations. *Mathematical biosciences*, 180(1-2):161–185, 2002.

[209] Brian M Murphy, Benjamin H Singer, and Denise Kirschner. On treatment of tuberculosis in heterogeneous populations. *Journal of theoretical biology*, 223(4):391–404, 2003.

[210] Katie D Dale, Malancha Karmakar, Kathryn J Snow, Dick Menzies, James M Trauer, and Justin T Denholm. Quantifying the rates of late reactivation tuberculosis: a systematic review. *The Lancet Infectious Diseases*, 21(10):e303–e317, 2021.

[211] David W Dowdy and Marcel A Behr. Are we underestimating the annual risk of infection with mycobacterium tuberculosis in high-burden settings? *The Lancet Infectious Diseases*, 22(9):e271–e278, 2022.

[212] Cheleka AM Mpande, Munyaradzi Musvosvi, Virginie Rozot, Boitumelo Mosito, Timothy D Reid, Constance Schreuder, Tessa Lloyd, Nicole Bilek, Huang Huang, Gerlinde Obermoser, et al. Antigen-specific t-cell activation distinguishes between recent and remote tuberculosis infection. *American Journal of Respiratory and Critical Care Medicine*, 203(12):1556–1565, 2021.

[213] Stephen Eubank, Hasan Guclu, VS Anil Kumar, Madhav V Marathe, Aravind Srinivasan, Zoltan Toroczkai, and Nan Wang. Modelling disease outbreaks in realistic urban social networks. *Nature*, 429(6988):180–184, 2004.

[214] Jacco Wallinga, Peter Teunis, and Mirjam Kretzschmar. Using data on social contacts to estimate age-specific transmission parameters for respiratory-spread infectious agents. *American journal of epidemiology*, 164(10):936–944, 2006.

[215] Jonathan M Read, Ken TD Eames, and W John Edmunds. Dynamic social networks and the implications for the spread of infectious disease. *Journal of The Royal Society Interface*, 5(26):1001–1007, 2008.

[216] Colin J Worby, Sandra S Chaves, Jacco Wallinga, Marc Lipsitch, Lyn Finelli, and Edward Goldstein. On the relative role of different age groups in influenza epidemics. *Epidemics*, 13:10–16, 2015.

[217] S Kiazyk and TB Ball. Tuberculosis (tb): Latent tuberculosis infection: An overview. *Canada Communicable Disease Report*, 43(3-4):62, 2017.

[218] Christian Lienhardt, Philippe Glaziou, Mukund Uplekar, Knut Lönnroth, Haileyesus Getahun, and Mario Raviglione. Global tuberculosis control: lessons learnt and future prospects. *Nature Reviews Microbiology*, 10(6):407–416, 2012.

[219] WHO Regional Office for Europe. Rapid communication on the role of the gen-expert Ò platform for rapid molecular testing for sars-cov-2 in the who european region, 2020.

[220] Paul Adepoju. Tuberculosis and hiv responses threatened by covid-19. *The Lancet HIV*, 7(5):e319–e320, 2020.

[221] Tovar.M. A data-driven tb spreading model that includes coupling with covid-19, 2022.

[222] Stephen J Millen, Pieter W Uys, John Hargrove, Paul D Van Helden, and Brian G Williams. The effect of diagnostic delays on the drop-out rate and the total delay to diagnosis of tuberculosis. *PloS one*, 3(4):e1933, 2008.

[223] Timur V. Elzhov, Katharine M. Mullen, Andrej-Nikolai Spiess, and Ben Bolker. *minpack.lm: R Interface to the Levenberg-Marquardt Nonlinear Least-Squares Algorithm Found in MINPACK*, 2016. R package version 1.2.

[224] WHO. Provisional number of people with new or relapse episodes of tb notified per month, 2022 (accessed Jan 30, 2022).

[225] Government of India. Nikshay online tool for monitoring tb control programme, 2021.

[226] Najmul Haider, Abdinasir Yusuf Osman, Audrey Gadzekpo, George O Akipede, Danny Asogun, Rashid Ansumana, Richard John Lessells, Palwasha Khan, Muzamil Mahdi Abdel Hamid, Dorothy Yeboah-Manu, et al. Lockdown measures in response to covid-19 in nine sub-saharan african countries. *BMJ Global health*, 5(10):e003319, 2020.

[227] Yacong Bo, Cui Guo, Changqing Lin, Yiqian Zeng, Hao Bi Li, Yumiao Zhang, Md Shakhaoat Hossain, Jimmy WM Chan, David W Yeung, Kin On Kwok, et al. Effectiveness of non-pharmaceutical interventions on covid-19 transmission in 190 countries from 23 january to 13 april 2020. *International Journal of Infectious Diseases*, 102:247–253, 2021.

[228] Goruntla Narayana, Bhupalam Pradeepkumar, Jinka Dasaratha Ramaiah, Thummala Jayasree, Dasari Laluprasad Yadav, and Bonala Kranthi Kumar. Knowledge, perception, and practices towards covid-19 pandemic among general public of india: a cross-sectional online survey. *Current medicine research and practice*, 10(4):153–159, 2020.

[229] Mohammad Ali, Zakir Uddin, Palash Chandra Banik, Fatema A Hegazy, Shamita Zaman, Abu Sleh Mohammed Ambia, Md Kaoser Bin Siddique, Rezoana Islam, Fatema Khanam, Sayed Mohammad Bahalul, et al. Knowledge, attitude, practice and fear of covid-19: A cross-cultural study. *medRxiv*, 2020.

[230] Balvir Singh Tomar, Pratima Singh, Deepak Nathiya, Supriya Suman, Preeti Raj, Sandeep Tripathi, Dushyant Singh Chauhan, et al. Indian community's knowledge, attitude, and practice toward covid-19. *Indian Journal of Social Psychiatry*, 37(1):48, 2021.

[231] Alak Paul, Dwaipayan Sikdar, Mohammad Mosharraf Hossain, Md Robed Amin, Farah Deeba, Janardan Mahanta, Md Akib Jabed, Mohammad Mohaiminul Islam, Sharifa Jahan Noon, and Tapan Kumar Nath. Knowledge, attitudes, and practices toward the novel coronavirus among bangladeshis: Implications for mitigation measures. *PloS one*, 15(9):e0238492, 2020.

[232] Anurag Bhargava and Hemant Deepak Shewade. The potential impact of the covid-19 response related lockdown on tb incidence and mortality in india. *Indian Journal of Tuberculosis*, 2020.

[233] Google. Covid-19 community mobility reports, 2021.

[234] Leonardo Martinez, Ye Shen, Ezekiel Mupere, Allan Kizza, Philip C Hill, and Christopher C Whalen. Transmission of mycobacterium tuberculosis in households and the community: a systematic review and meta-analysis. *American journal of epidemiology*, 185(12):1327–1339, 2017.

[235] ML Aznar, J Espinosa-Pereiro, N Saborit, N Jové, F Sánchez Martinez, S Pérez-Recio, A Vitoria, S Sanjoaquin, E Gallardo, J Llenas-García, et al. Impact of the covid-19 pandemic on tuberculosis management in spain. *International Journal of Infectious Diseases*, 2021.

[236] Yiman Geng, Gang Li, and Leiliang Zhang. The impact of covid-19 interventions on influenza and mycobacterium tuberculosis infection. *Frontiers in Public Health*, 9, 2021.

[237] W Joost Wiersinga, Andrew Rhodes, Allen C Cheng, Sharon J Peacock, and Hallie C Prescott. Pathophysiology, transmission, diagnosis, and treatment of coronavirus disease 2019 (covid-19): a review. *Jama*, 324(8):782–793, 2020.

[238] Muge Cevik, Krutika Kuppalli, Jason Kindrachuk, and Malik Peiris. Virology, transmission, and pathogenesis of sars-cov-2. *bmj*, 371, 2020.

[239] Michael Marshall. The four most urgent questions about long covid. *Nature*, 594(7862):168–170, 2021.

[240] Chaolin Huang, Lixue Huang, Yeming Wang, Xia Li, Lili Ren, Xiaoying Gu, Liang Kang, Li Guo, Min Liu, Xing Zhou, et al. 6-month consequences of covid-19 in patients discharged from hospital: a cohort study. *The Lancet*, 397(10270):220–232, 2021.

[241] Carole H Sudre, Benjamin Murray, Thomas Varsavsky, Mark S Graham, Rose S Penfold, Ruth C Bowyer, Joan Capdevila Pujol, Kerstin Klaser, Michela Antonelli, Liane S Canas, et al. Attributes and predictors of long covid. *Nature medicine*, 27(4):626–631, 2021.

[242] Adekunle Sanyaolu, Chuku Okorie, Aleksandra Marinkovic, Risha Patidar, Kokab Younis, Priyank Desai, Zaheeda Hosein, Inderbir Padda, Jasmine Mangat, and Mohsin Altaf. Comorbidity and its impact on patients with covid-19. *SN comprehensive clinical medicine*, pages 1–8, 2020.

[243] Bolin Wang, Ruobao Li, Zhong Lu, and Yan Huang. Does comorbidity increase the risk of patients with covid-19: evidence from meta-analysis. *Aging (Albany NY)*, 12(7):6049, 2020.

[244] Jin-Ou Chen, Yu-Bing Qiu, Zulma Vanessa Rueda, Jing-Long Hou, Kun-Yun Lu, Liu-Ping Chen, Wei-Wei Su, Li Huang, Fei Zhao, Tao Li, et al. Role of community-based active case finding in screening tuberculosis in yunnan province of china. *Infectious diseases of poverty*, 8(1):1–12, 2019.

[245] Vladimir N Kuznetsov, Andrej M Grjibovski, Andrey O Mariandyshev, Eva Johansson, and Gunnar A Bjune. A comparison between passive and active case finding in tb control in the arkhangelsk region. *International journal of circumpolar health*, 73(1):23515, 2014.

[246] Natalie Lorent, Kimcheng Choun, Sopheak Thai, Tharin Kim, Sopheaktra Huy, Reaksmey Pe, Johan van Griensven, Jozefien Buyze, Robert Colebunders, Leen Rigouts, et al. Community-based active tuberculosis case finding in poor urban settlements of phnom penh, cambodia: a feasible and effective strategy. *PloS one*, 9(3):e92754, 2014.

[247] Hemant Deepak Shewade, Vivek Gupta, Srinath Satyanarayana, Prabhat Pandey, UN Bajpai, Jaya Prasad Tripathy, Soundappan Kathirvel, Sripriya Pandurangan, Subrat Mohanty, Vaibhav Haribhau Ghule, et al. Patient characteristics, health seeking and delays among new sputum smear positive tb patients identified through active case finding when compared to passive case finding in india. *PloS one*, 14(3):e0213345, 2019.

[248] Luan Nguyen Quang Vo, Rachel Jeanette Forse, Andrew James Codlin, Thanh Nguyen Vu, Giang Truong Le, Giang Chau Do, Vinh Van Truong, Ha Minh Dang, Lan Huu Nguyen, Hoa Binh Nguyen, et al. A comparative impact evaluation of two human resource models for community-based active tuberculosis case finding in ho chi minh city, viet nam. *BMC Public Health*, 20(1):1–12, 2020.

[249] Esther Karamagi, Simon Sensalire, Martin Muhire, Herbert Kisamba, John Byabagambi, Mirwais Rahimzai, Frank Mugabe, Upenytho George, Jacqueline Calnan, Dejene Seyoum, et al. Improving tb case notification in northern uganda: evidence of a quality improvement-guided active case finding intervention. *BMC health services research*, 18(1):1–12, 2018.

[250] Fukushi Morishita, Mao Tan Eang, Nobuyuki Nishikiori, and Rajendra-Prasad Yadav. Increased case notification through active case finding of tuberculosis among household and neighbourhood contacts in cambodia. *PloS one*, 11(3):e0150405, 2016.

[251] Mohammed A Yassin, Daniel G Datiko, Olivia Tulloch, Paulos Markos, Melkamsew Aschalew, Estifanos B Shargie, Mesay H Dangisso, Ryuichi Komatsu, Suvanand Sahu, Lucie Blok, et al. Innovative community-based approaches doubled tuberculosis case notification and improve treatment outcome in southern ethiopia. *PloS one*, 8(5):e63174, 2013.

[252] S John, M Gidado, T Dahiru, A Fanning, AJ Codlin, and J Creswell. Tuberculosis among nomads in adamawa, nigeria: outcomes from two years of active case finding. *The International Journal of Tuberculosis and Lung Disease*, 19(4):463–468, 2015.

[253] E Mupere, NK Schiltz, E Mulogo, A Katamba, J Nabbuye-Sekandi, and ME Singer. Effectiveness of active case-finding strategies in tuberculosis control in kampala, uganda. *The International journal of tuberculosis and lung disease*, 17(2):207–213, 2013.

[254] Andrew S Azman, Jonathan E Golub, and David W Dowdy. How much is tuberculosis screening worth? estimating the value of active case finding for tuberculosis in south africa, china, and india. *BMC medicine*, 12(1):1–9, 2014.

[255] Peter M. Small and Madhukar Pai. Tuberculosis Diagnosis — Time for a Game Change. *New England Journal of Medicine*, 363(11):1070–1071, September 2010. Publisher: Massachusetts Medical Society _eprint: https://doi.org/10.1056/NEJMe1008496.

[256] Knut Lönnroth, Kenneth G Castro, Jeremiah Muhwa Chakaya, Lakhbir Singh Chauhan, Katherine Floyd, Philippe Glaziou, and Mario C Raviglione. Tuberculosis control and elimination 2010–50: cure, care, and social development. *The Lancet*, 375(9728):1814–1829, May 2010.

[257] Andrew S. Azman, Jonathan E. Golub, and David W. Dowdy. How much is tuberculosis screening worth? Estimating the value of active case finding for tuberculosis in South Africa, China, and India. *BMC Medicine*, 12(1):216, October 2014.

[258] J. N. Sekandi, D. Neuhauser, K. Smyth, and C. C. Whalen. Active case finding of undetected tuberculosis among chronic coughers in a slum setting in Kampala, Uganda. *The International Journal of Tuberculosis and Lung Disease*, 13(4):508–513, April 2009.

List of Figures

List of Tables

Resumen en español

La larga sombra de la Tuberculosis (TB) ha atormentado a la humanidad desde hace milenios, diezmando lenta, pero constantemente, a distintas civilizaciones humanas. Esta plaga -así llamada durante siglos- que nos acompaña desde hace tanto tiempo, es causada por los agentes del *Mycobacterium tuberculosis* complex, y ha estado presente en todos los territorios del planeta, segando la vida de millones. La respuesta real contra sus estragos no fue posible hasta el descubrimiento de los primeros antibióticos, el desarrollo de políticas de salud pública y de control, que permitieron obtener resultados esperanzadores en el control de la misma.

En la actualidad, aunque existen medicamentos eficaces, vacuna, y un mayor grado de conocimiento y de adherencia a las políticas de control, la TB persiste en todos los continentes, matando alrededor de 1,3 millones de personas solo en 2022. La necesidad de erradicarla ha ganado impulso en este siglo dada su prevalencia, y la preocupación por la irrupción de cepas multirresistentes. Por ello, distintos organismos junto a la comunidad científica están invirtiendo tiempo y financiación en desarrollar de nuevas herramientas que hagan plausible un mundo sin TB.

Por sus características complejas, la epidemiología de TB se beneficia del uso de modelos matemáticos de propagación que puedan utilizarse como herramientas para evaluar el impacto potencial de intervenciones de salud pública. Sin embargo, describir la propagación de la TB requiere modelos complejos que puedan cerrar la brecha entre modelo y datos, cuya implementación no es una tarea sencilla. Además, la existencia de diferentes perturbaciones externas que interactúan con la dinámica de la TB significa que deben tenerse en cuenta e incluirse en los modelos si se quiere estimar correctamente el impacto de las diferentes intervenciones.

En esta tesis, para contribuir al esfuerzo de investigación, me he centrado en explorar la interacción entre la dinámica de propagación de la TB e intervenciones de salud pública, como son las vacunas, y también las consecuencias de la pandemia de COVID-19 sobre el control de la TB, todo ello en el marco de un modelo matemático complejo. Los métodos que se proponen en este texto están desarrollados para crear un marco de trabajo en el que tanto las intervenciones de salud pública como la perturbación del COVID-19 se introducen en el modelo considerando el acoplamiento entre éste y la historia natural de la enfermedad, que es la que gobierna la dinámica. Trabajar con este enfoque ayuda a reducir el sesgo en las estimaciones y, modelo

mediante, podamos proporcionar resultados que puedan ayudar en el esfuerzo global de erradicación.

Entrando en materia, en el Capítulo 1 se realiza una introducción a conceptos básicos que contextualizan el resto de la tesis, partiendo de una breve historia de la epidemiología y el término epidemia, y pasando a conceptos específicos de la TB. Para ello, se explora su historia, sus características, y también su situación en el siglo XXI, puesto que lejos de dejar de ser una amenaza, la TB sigue activa en todos los continentes con gran fuerza. Seguidamente, en el Capítulo 2 se introducen los métodos que se van a emplear durante la tesis, con objeto de dotar al texto de todo el corpus de conocimiento que garantice reproducibilidad de los resultados mostrados. Específicamente, se describe completamente el modelo matemático que se usa sus fuentes de datos, y su funcionamiento, además de las características de su implementación en código.

Tras contextualizar la tesis e introducir los métodos globales que empleamos, en el Capítulo 3 se presentan algunos de los resultados más relevantes de este texto. Tras explorar la literatura respecto a la estimación de impacto de vacunas, se encuentra una fuerte discrepancia entre los resultados de eficacia que se miden en ensayos clínicos reales y su traducción a los modelos matemáticos, que requieren una interpretación mecanística de la vacuna en cuestión. Tomando esto como punto de partida, desarrollé sendos métodos matemáticos que, dados los resultados de 2 ensayos reales, con diferentes vacunas cuyas características diferían, permiten obtener esta descripción matemática. Esto permite, además, eliminar la necesidad de hacer conjeturas sobre el efecto mecanístico cuando se simula la introducción de la vacuna, pudiendo obtener resultados de impacto menos sesgados y, en general, obtener mejores caracterizaciones de las vacunas que están bajo desarrollo.

En el Capítulo 4, partiendo del conocimiento anterior, se explora un escenario en el que, de forma particular, se presumía que en China, una vacuna de eficacia comparable a la M72/AS01$_E$ produciría un alto impacto. Los resultados permiten explorar las diferencias de impacto cuando la descripción de la vacuna en el modelo es diferente, sometidos, además, a distintas formas de considerar el efecto de la demografía en el modelos, relevante en un país con un proceso de envejecimiento rápido como China. En general, los resultados de este trabajo lanzan un mensaje de cautela cuando se realizan las estimaciones de impacto, pues, de no hacerse correctamente, se pueden obtener resultados sesgados.

Finalmente, en el Capítulo 5 se abandona la exploración de impactos de vacunas para realizar un ejercicio centrado en una perturbación negativa, derivada de las consecuencias de la pandemia de COVID-19 durante sus años de mayor actividad.

Una de las consecuencias de esta pandemia fue la saturación de los hospitales y de los sistemas de diagnóstico, lo que afectó al control de otras enfermedades como la TB, pero también cáncer o malaria. Explorando datos reales sobre reducciones de diagnóstico y de escasez de tratamiento para la TB, los resultados muestran el impacto en muertes estimado que se espera en los próximos años debido a esta reducción en diagnóstico y al aumento de la incidencia, y también muestran que con una rápida respuesta que incremente las detecciones de casos, dicho impacto podría reducirse notablemente.

Para finalizar, en el Capítulo 6 se incluyen las conclusiones globales a las que ha llevado la investigación realizada para la creación de este documento, y que ha dado lugar a 4 artículos de investigación. Además, se incluye una brevísima disertación sobre las direcciones futuras a las cuales se puede apuntar partiendo de este documento, a su fecha de publicación. De forma resumida, no sin dificultad, en esta tesis he explorado la frontera de las interacciones de vacunas y perturbaciones con los modelos de propagación de TB, aportando soluciones que reducen el sesgo inherente a las predicciones basadas en modelos, principalmente, en las predicciones de impacto de vacunas y en las de la situación epidemiológica con o sin intervenciones.

Conclusiones en español

Durante el transcurso de esta tesis doctoral hemos obtenido multiples resultados novedosos en el campo de la epidemiología de Tuberculosis (TB) a través de diferentes proyectos de investigación. Como se ha mencionado e varias ocasiones en este documento, la TB es una enfermedad infecciosa persistente cuya erradicación, por el momento, no es más que un sueño que requeriría de cooperación internacional, reducir la desigualdad económica y social a nivel global, y nuevas y mejores herramientas para frenar la propagación de la enfermedad. Para contribuir en el esfuerzo científico para la erradicación, nuestra investigación se ha centrado en explorar las interacciones entre diferentes perturbaciones y la evolución de la TB que se predice empleando un modelo matemático complejo de propagación de la misma. En este sentido, el objetivo primario de la tesis ha sido siempre reducir el sesgo en las predicciones hechas con los modelos cuando aparecen estas perturbaciones, y los resultados principales están por ello relacionados con el estudio de la introducción de perturbaciones positivas (vacunas) o negativas (la interacción con el COVID-19). La idea original ha evolucionado hasta convertirse en un marco de trabajo que nos ha permitido entender mejor estas interacciones, y cómo ignorarlas sesgaba las predicciones obtenidas con los modelos. Los resultados obtenidos se encuentran distribuidos en los Capítulos 3, 4 y 5, estando los 2 primeros destinados al estudio de vacunas y el último al efecto del COVID-19 en el control de la TB.

En el Capítulo 3, y por primera vez en la literatura de TB, hemos mostrado un problema que aparece al tratar con vacunas contra la TB cuya eficacia se ha medido en ensayos clínicos reales. La interacción entre las vacunas y los modelos matemáticos es compleja, debido al la naturaleza compleja de la TB y del desarrollo de vacunas, lo que impone la necesidad de describir éstas de una manera que sea compatible con los modelos. Esto es, describir la vacuna en términos de su interacción con la historia natural de la enfermedad, pues hasta ahora, la combinación específica de mecanismos que confieren protección no se mide en los ensayos, sino que generalmente es el investigador el que asume una combinación específica. Nuestros resultados destacan esta dificultad que pone en riesgo la capacidad de modelar correctamente vacunas cuya eficacia ha sido medida en ensayos clínicos reales, y cómo las diferentes descripciones del efecto de las vacunas a nivel mecanístico conducen a una variación significativa en los resultados de impacto que se obtienen. Esto es de particular importancia en el contexto

de la TB debido al papel crítico que desempeñan los Ensayos de Control Aleatorizados (RCTs, por sus siglas en inglés) en la evaluación de la eficacia de las vacunas, agravado aún más por el desconocimiento actual de correlatos de protección[115]. Esta falta de correlatos hace que la eficacia estimada de las vacunas de TB sea más difícil de estimar a priori en la TB que en otras enfermedades. Por esta razón, los métodos que se introducen en esta tesis son relevantes, ya que permiten comparar, a posteriori, la eficacia de vacunas que han sido caracterizadas con RCTs diferentes, algo que no es posible con análisis más simples.

Para mitigar la incertidumbre y reducir la necesidad de tomar decisiones de modelización, nuestra investigación ha permitido desarrollar dos metodologías adaptadas a arquitecturas de ensayos específicas para cohortes con resultado IGRA-negativo, o IGRA-positivo, al principio del ensayo, pues éstas son las dos arquitecturas más recientes utilizadas en ensayos clínicos reales para medir PoD en vacunas de TB. El primer método, para el primer tipo de ensayo, se base en medir la distribución de tiempos entre la conversión IGRA y la enfermedad activa, para estimar de manera independiente el efecto de la vacuna sobre la progression a enfermedad en individuos que progresan rápido a enfermedad. Esto, unido a la derivación de una restricción matemática que acopla el efecto de los diferentes mecanismos de protección que puede activar la vacuna, proporciona una caracterización completa de forma que posteriormente puede ser introducida en modelos matemáticos. Sin embargo, para los diseños IGRA-positivos, el primer método no puede emplearse, por lo que hemos desarrollado otra metodología compatible con la arquitectura de estos ensayos. Esta se basa en el uso de simulaciones *in-silico* de ensayos y en análisis estadísticos, y permite medir la compatibilidad entre diferentes descripciones de la vacuna adaptadas al tipo de ensayo y los datos reales observados en el ensayo. Las métricas de compatibilidad resultantes, que son probabilidades Bayesianas a posteriori, permiten además, generar predicciones de impacto de vacunas que son agnósticas a la descripción empleada, y que ya no requieren tomar decisiones a priori sobre el efecto mecanicista de las mismas. No obstante, todavía quedan algunas hipótesis a priori como el funcionamiento AoN de las vacunas.

A pesar de tener limitaciones en ambas metodologías, éstas ofrecen, por primera vez, un marco práctico que puede ser adaptado y ampliado para futuros ensayos de vacunas contra la TB, y pone de manifiesto un problema que hasta ahora no se había considerado. Esto representa un avance significativo para definir los perfiles específicos de protección a nivel de mecanismos en vacunas reales, lo que reduce el sesgo en la evaluación posterior basada en modelos matemáticos.

A continuación, en el Capítulo 4, hemos explorado los impactos de hipotéticas

nuevas vacunas para TB en países que experimentan un proceso de envejecimiento poblacional rápido, como es el caso de China. Este impacto lo hemos estudiado, además condicionado al enfoque utilizado para modelar y capturar, de manera precisa, los efectos de estos cambios demográficos repentinos y sus interacciones con los perfiles de las vacunas y la edad de la población que se vacuna. Nuestra investigación muestra que las campañas de inmunización dirigidas a grupos de edad avanzada en estos países es, realmente, prometedora, pero también que para reducir la incidencia y mortalidad de la TB, la vacuna debe ser capaz de frenar a las rutas a enfermedad que más contribuyen a los nuevos casos en el grupo de edad vacunado. Además, los resultados también muestran que las vacunas que apuntan a diferentes rutas a enfermedad tienen niveles de impacto mixtos dependiendo de su interacción con el estado inmunológico de la población objetivo.

En cuanto a la conexión con el envejecimiento, los resultados capturan la importancia de implementar formas coherentes de describir el cambio demográfico y su efecto en las redes de contacto, ya éstas cambian sustancialmente debido a este cambio demográfico. Particularmente, encontramos que los modelos deben preservar la conectividad intrínseca de las redes de contacto mientras las matrices se adaptan de acuerdo con el cambio demográfico, de modo que los nuevos patrones de contacto reflejen la red de contactos esperada en la nueva demografía y no en la que se midió originalmente. El impacto de la forma de modelar el acoplamiento demografía-enfermedad en la predicción de impacto de las vacunas también varía considerablemente según el grupo de edad que se vacuna, y estas implicaciones deben tenerse en cuenta cuando se presentan resultados de impacto para evitar dar resultados sesgados.

Posteriormente, en el Capítulo 5, los resultados que hemos obtenido nos han permitido medir el impacto de la pandemia de COVID-19 en el control de la TB en entornos con alta carga tuberculosa. Muchos aspectos del impacto de esta pandemia en nuestra sociedad aún no se han caracterizado completamente, lo que incluye los efectos indirectos de las medidas de control como los confinamientos y toques de queda en las distribuciones de contactos, o los efectos de la saturación de los sistemas de salud en el diagnóstico y tratamiento de otras enfermedades. Esto es un motivo de preocupación, especialmente en lo que respecta al control de TB, ya que hay consecuencias negativas para su control y para los pacientes si se interrumpe el diagnóstico de personas infectadas o no se les trata adecuadamente. Teniendo en cuenta esta situación, nuestros resultados nos han permitido cuantificar los efectos negativos de la pandemia COVID-19 en la mortalidad por TB, la cual se espera que aumente como consecuencia, pero también nos han permitido traer algo de esperanza al

demostrar que una intervención posterior apropiada sería capaz de mitigar los efectos a largo plazo. Además, nuestros resultados enfatizan la importancia de mejorar el ritmo de diagnóstico de TB, posiblemente a través de la introducción de estrategias de búsqueda activa de casos, para contrarrestar los efectos perjudiciales de la pandemia en la incidencia y mortalidad de la TB, y también para el control general de la enfermedad.

No obstante, es necesario señalar que, aunque hemos obtenido varios resultados muy relevantes, deben ser tomados con precaución, ya que derivan de un modelo matemático que tiene limitaciones, como todos los modelos de transmisión de TB. Para ser justos, cualquier resultado basado en modelos arrastra una gran incertidumbre debido a los parámetros epidemiológicos y los datos de incidencia y mortalidad, u otros datos de calibración, están sujetos a fuertes incertidumbres que acaban propagadas a los resultados. Por ello, cualquier mejora en la medición de los datos, incluso siendo pequeñas reducciones en su incertidumbre, debería afectar a los resultados cuantitativos del modelo. También se espera que las mejoras en el propio modelo, como procedimientos de calibración más eficientes o descripciones más completas de la historia natural, afecten a los resultados, y de haber cualquier avance en este sentido, debería ser incorporado. En cualquier caso, para las tareas de investigación realizadas en esta tesis, el modelo matemático en uso es esencialmente una buena herramienta, ya que integra descripciones detalladas del acoplamiento entre la dinámica de la TB y la evolución demográfica.

También es importante señalar que, en nuestros métodos para abordar las descripciones de las vacunas que son más compatibles para describir datos empíricos, nos hemos visto obligados a modelar las vacunas como *all-or-nothing*, o como *leaky*, y sin tener más evidencia, la adopción de un enfoque sobre el otro puede sesgar los resultados. En lo que respecta a la interacción con el COVID-19, solo hemos descrito la interrupción del sistema sanitario de atención frente a TB a través de una reducción de las capacidades de diagnóstico y de la disponibilidad de tratamiento. Aunque estos son, sin duda, los efectos más relevantes de la pandemia de COVID-19 en la transmisión de la TB que se han caracterizado, puede haber muchos otros efectos que aún son difíciles de parametrizar, como el efecto de las intervenciones no farmacéuticas en los países que las llevaron a cabo, o incluso cambios biológicos en la susceptibilidad como consecuencia de la infección por Sars-Cov-2.

Recapitulando, los objetivos de investigación propuestos en el primer capítulo han sido alcanzados durante el desarrollo de la tesis, y el contenido aquí presentado ofrece un marco de trabajo que combina datos reales, modelos compartimentales y métodos estadísticos para desarrollar soluciones a algunos de los desafíos que existían en la literatura de TB. En el proceso hemos descrito el efecto que tiene en la situación

epidemiológica de la TB la ocurrencia de una perturbación, centrándonos en la interacción de ésta con la historia natural de la enfermedad y su dinámica. Además, esta tesis destaca la importancia de tener estrategias de inmunización personalizadas e informadas por modelos matemáticos que integran, no solo atributos de vacunas, sino también consideran la demografía de la población y las características especiales de la TB para desarrollar estrategias de control efectivas contra la enfermedad.

Lo que falta por hacer

Aunque el camino recorrido en esta tesis ha sido largo y la investigación que se presenta ha permitido dar un un paso hacia adelante en varios aspectos clave de la modelización de TB, principalmente en la caracterización de nuevas vacunas contra la TB, todavía queda mucho por hacer en este campo. Existen varias formas en las que se podrían ampliar los resultados discutidos en este documento, ya sea para mejorar nuestra comprensión de la interacción entre perturbaciones y la dinámica enfermedad, o para mejorar la calidad de los resultados cuantitativos que se han presentado. Algunas de esas ideas podrían convertirse en proyectos y conducir a resultados nuevos e interesantes en un futuro cercano.

Por un lado, el modelo de propagación que se ha utilizado en esta tesis podría beneficiarse de algunas mejoras que, dado que el mundo está cada vez más conectado, ayudarían a responder preguntas que requieran de la integración de más datos en los modelos. En este sentido, la inclusión en el modelo de diferentes rutas de tratamiento asociadas a las diferentes cepas de TB, pesando específicamente en aquellas multirresistentes, debería permitir la aplicación del modelo para responder preguntas abiertas sobre el problema de la emergencia de cepas resistentes a antibióticos. Siguiendo esta filosofía, la adición de flujos migratorios internos y externos al modelo mejoraría la aplicabilidad del mismo, ya que podríamos capturar una contribución a la transmisión que ahora mismo no existe por diseño. La introducción de estos flujos permitiría medir el impacto que tienen medidas locales a nivel global, y también caracterizar el coste que tiene la falta de cooperación internacional en el control de la enfermedad. Sin embargo, para poder implementar cualquiera de estos elementos, se requiere disponer de datos de calidad, que actualmente pueden no estar disponible en todos los lugares de interés. Para finalizar las posibles mejoras al modelo, éste podría beneficiarse además de considerar distintos tipos de poblaciones con diferente susceptibilidad genética, si hubiera datos, puesto que algunas de éstas poblaciones pueden estar sometidas a mayor riesgo de contraer la TB. La inclusión de estos aspectos en el modelo incrementaría su complejidad, pero también la versatilidad y utilidad del

mismo.

Por otro lado, respecto a los temas más relevantes discutidos en esta tesis, algunos aspectos podrían pulirse todavía un poco más para extender las capacidades de los métodos. Primero, para mejorar los resultados, deberíamos ser capaces de reducir la incertidumbre asociada con los datos de entrada del modelo, pues esta se propaga a los resultados. Para ello, como cada vez hay más datos -de prácticamente todo-, explorar nuevas bases de datos y nuevos trabajos debería permitir encontrar datos de mayor calidad para introducir al modelo, puesto que hay mucha literatura que por ahora ha podido quedar en las sombras. Esto, en principio, debería propagarse a los resultados y reducir su incertidumbre.

Segundo, respecto a la caracterización de los efectos mecanísticos de las vacunas para su introducción en modelos matemáticos de forma racional, la integración en los ensayos de las metodologías propuestas en esta tesis permitiría alcanzar resultados más concluyentes. En este sentido, si tuviésemos acceso a datos anonimizados micro sobre los participantes de los ensayos, la caracterización de los efectos de las vacunas sería más precisa. Además, la extensión de los métodos a otras arquitecturas, y a ensayos de otras vacunas conforme acaben los ensayos que están realizándose, servirá para determinar su alcance -y sus limitaciones- y puede ser un comienzo para desarrollar métodos todavía mejores para la caracterización.

Finalmente, la introducción de grandes perturbaciones como el COVID-19 debe llevarse a cabo para generar predicciones flexibles, dotando a los modelos de la capacidad de describir situaciones (como guerras, pandemias, o desastres naturales) que son esencialmente imposibles de predecir. Esto es relevante ya que uno de los principales objetivos de estos modelos es servir como herramientas para la toma de decisiones en materia de salud pública, y, por ejemplo, si existe un efecto a largo plazo de la perturbación que podría interactuar con la intervención que se quiere introducir, como puede ser una una vacuna, ello debe ser considerado. En este sentido, una línea de trabajo que tenemos en desarrollo es precisamente caracterizar si la pandemia de COVID-19 ha afectado significativamente el impacto de una hipotética vacuna contra la TB, y que queremos extender a otras posibles intervenciones de salud pública. En resumen, todavía quedan muchas cosas por hacer, pero tomando como punto de partida los resultados presentados esta tesis, el límite del conocimiento puede ser desplazado hacia adelante una vez más.